2015

The design and synthesis of novel michellamine B analogues targeting HIV

Yueting Lu
University of Wollongong

THE DESIGN AND SYNTHESIS OF NOVEL MICHELLAMINE B ANALOGUES TARGETING HIV

A thesis submitted in fulfilment of the requirements for the award of the degree of

DOCTOR OF PHILOSOPHY

from

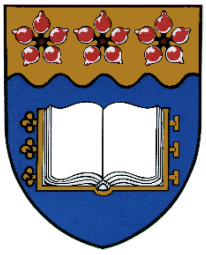

UNIVERSITY OF WOLLONGONG

by

Yueting Lu
B.Sc. (Appl. Chem.)
M.Eng. (Appl. Chem.)

Supervisor:
Prof. Paul A. Keller

SCHOOL OF CHEMISTRY

March 2015

Certification

I, Yueting Lu, declare that this thesis, submitted in fulfilment of the requirements for the award of Doctor of Philosophy, in the School of Chemistry, University of Wollongong, is wholly my own work unless otherwise referenced or acknowledged. This document has not been submitted for qualifications at any other academic institution.

Yueting Lu

March 2015

Publication

Lu, Y.; Hendra, R.; Oakley, A.; Keller, P. A. Efficient synthesis and antioxidant activity of coelenterazine derivatives *Tetrahedron Lett.* **2014**, *55*, 6212-6215.

Table of Contents

Acknowledgements

Paul Keller for his insight, direction, encouragement and friendship throughout my PhD study.

Aaron Okaley for the ideas and knowledge he provided in regards to the work done on coelenterazine project.

All the past and present members of the Keller Research Group, Sreenu, Ali, Ashraf, Alex, Adel, Josh, Phoung, Mohammed, Andrew T., Steven W., Stephen B., Aaron, Ari, Nick, Jamie, Mel, Akash, etc, for their help and friendship over the years. A special thanks to Rudi for the biological testing.

Anthony Willis for the X-ray structure determinations, Rachada Haritakun for the anti-malaria and anti-cancer testing and Alysha Elliott for the anti-bacterial testing.

Glennys O'Brien for her support, friendship and demonstrating and tutoring opportunities.

The staffs (M. Kelso, C. Hyland, E. Manning, etc) and students of chemistry for making the department a comfortable place to work. A special thanks to Wilford Lie for the NMR support.

My families for the love and support provided over the past 29 years.

My wife Jiajia for her continuous support, for her love, for sharing the best and the worst times with me. And my little son Jacob for his arrival to our little world.

Abstract

The dimeric naphthylisoquinoline alkaloid michellamine B, with its moderate anti-HIV activity, has gained significant interest as a potential lead compound. Herein, both monomeric and dimeric analogues with novel isoquinoline units were synthesized to evaluate the importance of this isoquinoline unit for HIV RT inhibitory activity.

The synthesis started from the preparation of key precursors of naphthylboronic acid/ester and halogenated dihydroisoquinolines. The naphthylboronic acid **37** was synthesized by a Diels-Alder method over 8 steps proceeding in 37% overall yield from commercially available 3,3-dimethylacrylic acid **59**. The naphthylboronic ester **38**, with an ethyl ester substituent in the naphthyl ring, was prepared by a Wittig method over 7 steps with an overall yield of 43%. Halogenated 3,4-dihydroisoquinolines (**39-41**) featuring methoxy groups and double bonds between C1 and N were obtained from a four-step synthesis proceeding in 39-48% overall yields from commercially available benzaldehydes. Brominated 3,4-dihydroisoquinolin-1(2*H*)-ones **42** with a carbonyl group were successfully prepared over 4 steps with an overall yield of 18%.

Three monomeric naphthylisoquinolines (**96-98**) with an ethyl ester substituent in the naphthyl ring were prepared from the naphthylboronic ester (**38**) and halogenated isoquinolines (**39-42**) *via* Pd-catalyzed Suzuki cross-coupling, while three monomeric naphthylisoquinolines (**43**, **99-100**) with methyl substituent in the naphthyl ring were prepared from the naphthyl boronic acid (**37**) and halogenated isoquinolines (**39-42**). In order to activate the ArC3 position for the subsequent dimerization, three phenolic monomeric naphthylisoquinolines (**44**, **107** and **109**) were obtained *via* debenzylation

reactions using Pd/C/H_2 reduction system. Two dimeric naphthylisoquinolines (**112** and **113**), as michellamine B analogues, were successfully synthesized from the phenolic monomeric naphthylisoquinolines (**44** and **107**) *via* a Ag_2O-induced oxidative dimerization strategy.

The synthesized monomeric and dimeric naphthylisoquinolines were tested *in vitro* against the HIV-1 RT enzyme showing weak to mild inhibitory activities with IC_{50} values up to 61.3 μM. Five monomeric naphthylisoquinolines (**99**, **43**, **97**, **109** and **44**) exhibited moderate activity against *Plasmodium falciparum* (2.66-4.34 μg/mL), while all the monomeric naphthylisoquinolines showed high cytotoxicity (1.95-30.09 μg/mL). All the monomeric naphthylisoquinolines exhibited moderate to low activities against the three cell lines KB (oral cavity cancer), MCF-7 (breast cancer) and NCI-H187 (small cell lung cancer). All the monomeric naphthylisoquinolines showed no activities against *Escherichia coli*, *Klebsiella pneumoniae*, *Acinetobacter baumannii* and *Pseudomonas aeruginosa*, while three compounds (**99**, **43** and **109**) exhibited low activity against *Staphylococcus aureus* with MIC values from 16 μg/mL to 32 μg/mL.

Coelenterazine-like imidazo[1,2-*a*]pyridines, as inhibitors of bioluminescent luciferase for the study of its enzymatic kinetics, were synthesized *via* a highly convergent and adaptable synthesis route. This simple synthesis involves 11 steps in total with only six linear steps, proceeding in respectable 33-44% overall yields from commercially available 2-aminonicotinic acid. The antioxidant abilities of four new coelenterazine analogues (**121**, **123-125**) were evaluated, showing moderate activities with IC_{50} values from 58.7 μM to 72.8 μM. Their optical properties, including UV absorption, fluorescent emission, Stocks shift and quantum yields, were also studied.

Abbreviations

^{13}C NMR	carbon nuclear magnetic resonance spectroscopy
^{1}H NMR	proton nuclear magnetic resonance spectroscopy
°C	degrees Celsius
AIDS	acquired immune deficiency syndrome
ABTS	2,2'-azino-bis(3-ethylbenzothiazoline-6-sulphonic acid)
Ac	acetate
ACN	acetonitrile
APT	attached proton test (^{13}C NMR)
Ar	aryl
ArC	aromatic carbon
ArH	aromatic proton
Bn	benzyl
bs	broad singlet
δ	chemical shift (NMR)
d	doublet (NMR)
dba	dibenzylideneacetone
dd	doublet of doublets (NMR)
ddd	doublet of doublet of doublets (NMR)
DNA	deoxyribonucleic acid
DMF	*N*,*N*-dimethylformamide
DMSO	dimethylsulfoxide
DPPH	2,2-diphenyl-1-picrylhydrazyl

EC_{50}	median effective concentration
EDC	1-ethyl-3-(3-dimethylaminopropyl)carbodiimide
e.g.	*exempli gratia* (“for example”)
EI	electron impact
eq.	equivalent
ESI	electrospray ionisation
g	gram(s)
gHMBC	gradient heteronuclear multiple bond correlation
gHSQC	gradient heteronuclear single quantum coherence
h	hour(s)
HAART	highly active antiretroviral therapy
HBTU	*N*,*N*,*N*′,*N*′-tetramethyl-*O*- (1*H*-benzotriazol-1-yl)uronium hexafluorophosphate
HIV	human immunodeficiency syndrome
HOBt	1-hydroxybenzotriazole hydrate
HPLC	high performance liquid chromatography
HRMS	high resolution mass spectrometry
Hz	hertz
IC_{50}	median inhibitory concentration (50%)
IR	infrared
J	coupling constant
μ	micro
m	multiplet (NMR)
m	medium (IR)
M	molar

M^+	molecular ion
MeOH	methanol
mg	milligram
MHz	megahertz
MIC	minimal inhibitory concentration
min	minutes
mL	millilitre(s)
mmol	millimole(s)
mol	mole(s)
Mp.	melting point
MS	mass spectrometry
m/z	mass to charge ratio
NBS	*N*-bromosuccinimide
2D NOESY	two dimensional nuclear overhauser effect spectroscopy
nm	nanometre(s)
NMR	nuclear magnetic resonance
NRTIs	nucleoside reverse transcriptase inhibitors
NNRTIs	non-nucleoside reverse transcriptase inhibitors
Ph	phenyl
ppm	parts per million
Piv	pivaloyl
PyBOP	benzotriazol-1-yl-oxytripyrrolidinophosphonium hexafluorophosphate
q	quartet (NMR)
RNA	ribonucleic acid
RT	reverse transcriptase

s	singlet (NMR)
s	strong (IR)
t	triplet (NMR)
TFA	trifluoroacetic acid
Tf	triflate
THF	tetrahydrofuran
TLC	thin layer chromatography
TOCSY	total correlation spectroscopy
TMS	tetramethylsilane
U.N.	United Nations
UV/Vis	ultraviolet/visible
w	weak (IR)

Chapter 1: Introduction

1.1 Human immunodeficiency virus (HIV)

1.1.1 The background of HIV

Acquired immune deficiency syndrome (AIDS) is a disease caused by HIV.[1,2] HIV infects vital cells such as CD_4^+ T cells which play essential roles in the human immune system.[3] Once the CD_4^+ T cell numbers drop to 500 cells/mm^3,[4] cell immunity is gradually lost and the body becomes more susceptible to life-threatening infections, including opportunistic infections and tumors which do not usually affect people who have fully functional immune systems.

The first case of HIV infection was reported in early 1980s,[5,6] and it then spread rapidly around the world. HIV is transmitted primarily *via* unprotected sex, contaminated blood transfusions, hypodermic needles, and mother to child transmission. It is estimated that there were 35 million people living with HIV at the end of 2013 and a reported 1.5 million individuals dying of the disease including 190,000 children (younger than 15 years old) over the year 2013.[7] There is no cure or vaccine for AIDS; however, antiretroviral treatment can slow the course of the disease. AIDS has had a great impact both on society and economic, and it has become a common issue of the world.

Two types of HIV have been characterized: HIV-1 and HIV-2. HIV-1 is the virus that was initially discovered and is associated with stronger virulence and infectivity,[8] and is therefore the cause of the majority of HIV infections globally. In this thesis, any reference to HIV refers to HIV-1 unless otherwise stated.

1.1.2 HIV lifecycle and RT enzyme

Upon entry into the target cell in human body, the HIV retrovirus uses three key enzymes to complete its life cycle: reverse transcriptase (RT), integrase (IN) and protease (PR). Reverse transcription is catalyzed by the retroviral enzyme RT. RT reverse transcribes a single-stranded genomic RNA molecule into double-stranded DNA, which can subsequently be integrated into host cell DNA, depending on the retroviral enzyme IN as well as host cellular cofactors. After the successful addition of viral DNA to the host genome, the virus can replicate.[9] RT has two enzymatic activities: a polymerase that can copy either RNA or DNA and an RNase H that degrades the RNA strand of RNA-DNA intermediates formed during viral DNA synthesis, thus RT present a crucial target for inhibition of HIV replication.

1.1.3 Nucleoside reverse transcriptase inhibitors (NRTIs), non-nucleoside reverse transcriptase inhibitors (NNRTIs) and highly active antiretroviral therapy (HAART)

The RT can be inhibited by two classes of drugs: NRTIs and NNRTIs. **Table 1.1** summarizes the characteristics of the two classes of HIV RT inhibitors, and highlights the differences between NRTIs and NNRTIs.[10]

Table 1.1 Characteristics of HIV RT inhibitors: NRTIs and NNRTIs.

Characteristic	NRTIs[11-13]	NNRTIs[14,15]
Chemical structure	Analogues of the natural substrates, i.e. nucleosides	Chemically diverse, non-nucleoside
Active from	Metabolic conversion to 5′-triphosphates by host-cell enzymes	No metabolic conversion
Mechanism of action	Incorporate into growing DNA chain, terminate chain synthesis	Induce conformational changes in RT, reducing catalytic activities
Type of inhibition	Competitive with the natural substrates	Non-competitive or uncompetitive
Binding site	Catalytic site	Hydrophobic pocket
Spectrum	Broad spectrum antiretrovirals	HIV specific RT inhibitors
Selectivity	Low to moderate	Very high

The first RT inhibitors approved zidovudine[13] (**Figure 1.1**) were the NRTIs which compete as triphosphates with normal nucleoside substrates for incorporation into the viral genome, thus behaving as chain terminators. NNRTIs with a wide range of chemically diverse structures, have gained a definitive and important place in clinical use based on their unique antiviral potency with generally low toxicity and favourable pharmacokinetic properties.[16-18] Unlike nucleoside analogues, NNRTIs bind in specific pockets of the HIV RT, which will alter its reverse replication without interfering with the human cell cycle or mitochondrial DNA synthesis because of their different structures from the nucleoside analogues. NNRTIs were found have a more potential than the NRTIs, and have gained the greatest importance due to their specificity and low

cytotoxicity.[10]

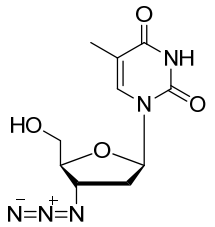

Figure 1.1 First RT inhibitor zidovudine.

HIV undergoes dramatic genetic variation due to the rapid replication of the virus in human body, which further complicates the development of effective agents and vaccines.[19] Since 1996, a combination of different inhibitors called HAART, has provided an effective way to treat AIDS patients by dramatic reduction in viral loads and restoration of the immune system.[20] As NNRTIs represent the most potent anti-HIV drugs due to their unique antiviral potency, high specificity and low cytotoxicity, they have become indispensable components of HAART regimen. However, the rapid emergence of drug resistance and serious side effects from the long-term drug use has become a new issue. Therefore, it is essential to design and develop new anti-HIV drugs, especially new NNRTIs.

1.1.3.1 Currently marketed NNRTIs

The era of NNRTIs started with the independent discovery of two series of compounds: 1-(2-hydroxyethoxymethyl)-6-(phenylthio)thymine (HEPT) (**1**) derivatives[21,22] and 4,5,6,7-tetrahydroimidazo[4,5,1-*jk*][1,4]benzodiazepin-2(1*H*)-one (TIBO) (**2**) derivatives (**Figure 1.2**).[23,24] Both HEPT (**1**) and TIBO derivative (**2**) are highly active compounds against HIV by interacting with an allosteric site of RT.

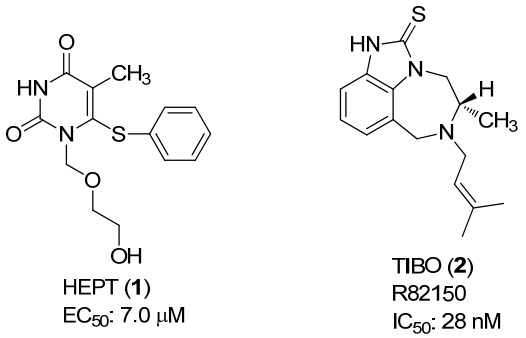

Figure 1.2 The structure of the early NNRTIs: HEPT and TIBO derivative R82150.

Following the discovery of HEPT (**1**) and TIBO (**2**), three other compounds were identified as first-generation NNRTIs, including nevirapine (**3**), delavirdine (**4**), efavirenz (**5**) (**Figure 1.3**). nevirapine (**3**), a dipyridodiazepinone, which was first approved by the FDA for clinical use in 1996, is a highly specific inhibitor of HIV-1 reverse transcriptase (RT) and exhibits an IC_{50} of 84 nM in enzyme assays and an IC_{50} of 40 nM against HIV-1 replication in cell culture.[25] The following year, delavirdine (**4**), a bis(heteroary1)piperazine (BHAP) analogue with 98% inhibition and an IC_{50} value of 1.1 μM, entered the market.[26] In 1998, the 1,4-dihydro-2*H*-3,1-benzoxazin-2-ones analogue efavirenz (**5**), which exhibited a 95% inhibitory concentration of 1.5 nM for the inhibition of HIV-1 replicative spread in cell culture, was approved by the FDA as a NNRTI for clinical use.[27]

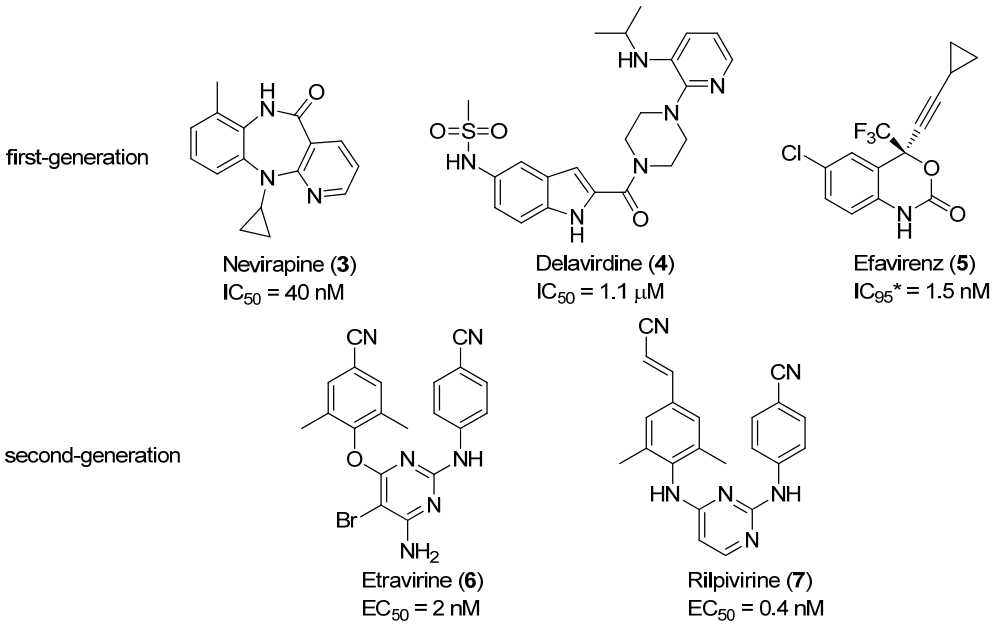

Figure 1.3 Currently marketed first-generation and second-generation NNRTIs and their biological activities against HIV in cell culture. * The IC_{95} was the concentration of test compound that inhibited virus expression by at least 95% relative to virus expression in untreated control samples.

Second-generation NNRTIs include etravirine (**6**), and rilpivirine (**7**) (**Figure 1.3**), which are the analogues of diarylpyrimidine (DAPY) compounds. Compared to the first-generation NNRTIs, these flexible antiretroviral drugs display a higher genetic barrier to resistance. Structural studies showed that DAPY analogues can bind the enzyme RT in multiple conformations and adapt to changes in the NNRTI-binding pocket, which helps it escape the effects of drug-resistance mutations.[28] Etravirine (**6**) and rilpivirine (**7**) were introduced to the market in 2008 and 2011 respectively, and both drugs show superior activity profiles against wild-type and mutant HIV-1 strains compared to all currently approved NNRTIs.[29] The high potency, minimal adverse effects, easy synthesis and formulation make them the best NNRTIs in the market.

All five marketed NNRTIs are generally safe and well tolerated, although central nervous system side effects are associated with the use of efavirenz (**5**),[30] whereas

nevirapine (**3**) causes hepatotoxicity and a severe rash.[31]

1.1.3.2 Next generation NNRTIs

The need for new therapeutic agents that are able to overcome resistance and safety problems prompted the development of new NNRTIs. At present, the next generation of NNRTIs are undergoing clinical development (**Figure 1.4**).

3-Cyanophenoxypyrazole lersivirine (**8**)[32] and aryl phosphinate-indole GSK 2248761 (**9**)[33] had been undergo phase IIb trials. However, on 10 February 2011, the FDA put a hold on development of GSK 2248761 (**9**) due to four reports of seizures as part of a clinical trial involving treatment-experienced patients, and on 5 February 2013, ViiV Healthcare announced that the company has decided to stop the development of lersivirine (**8**) as it was determined that the compound would not provide an improvement over existing medicines in the NNRTI class.

There are two NNRTIs undergoing phase IIa trials, the triazole analogue RDEA806 (**10**)[34] and the dipyridodiazepinone BILR 355 BS (**11**).[35] They have been demonstrated to be safe, well tolerated and potent in antiretroviral activity studies.

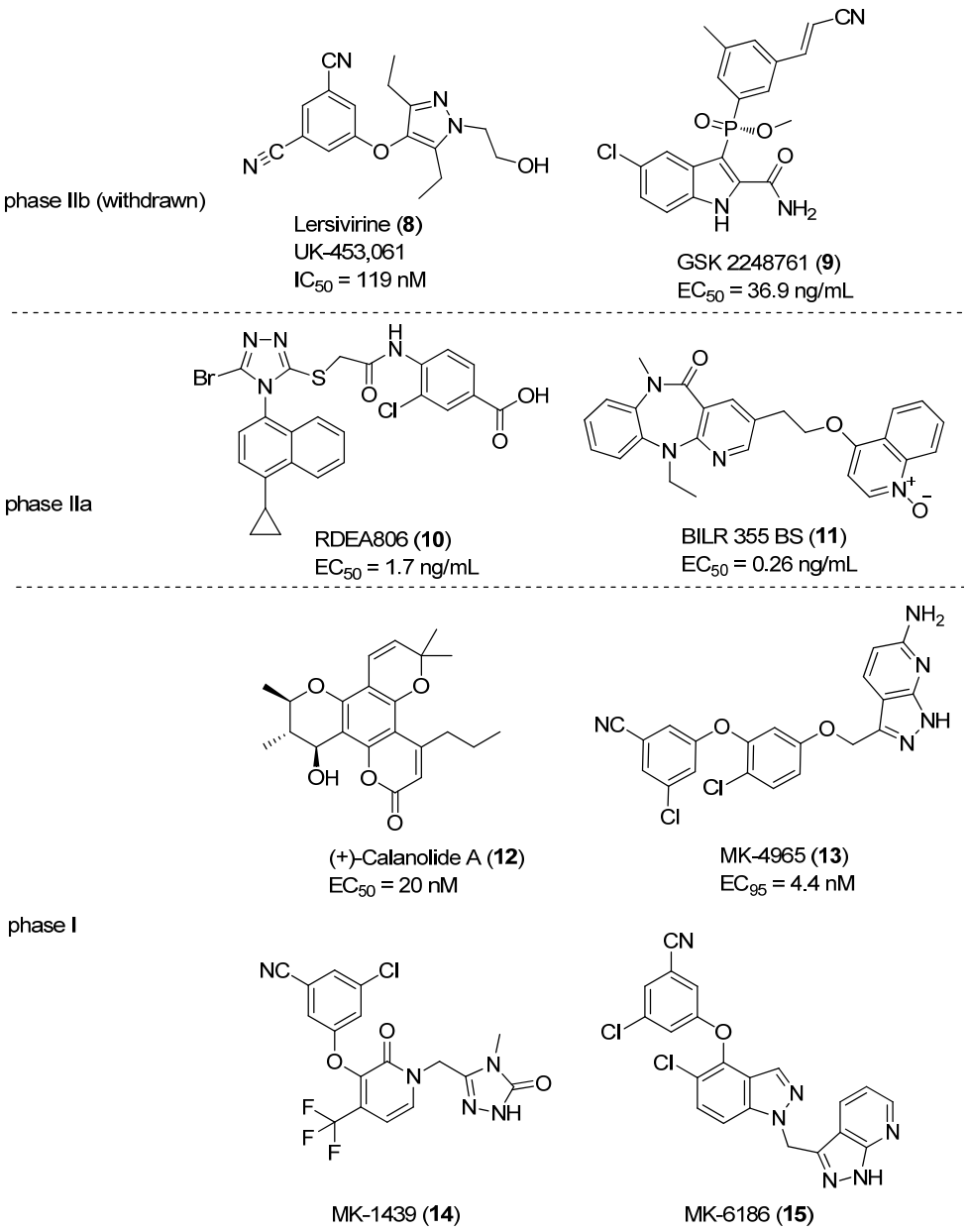

Figure 1.4 Chemical structures of the next-generation NNRTIs and their biological activities against HIV in cell culture.

The other four NNRTIs including the natural substrate (+)-calanolide A (**12**),[36] and three biaryl ether moiety compounds MK-4965 (**13**),[37] MK-1439 (**14**)[38] and MK-6186 (**15**),[39] showed promising anti-HIV properties and are currently undergoing Phase I clinical trials. While none of these drugs have currently been approved by the FDA for use as anti-HIV treatments, the current stage of development and companies responsible for

each drug are showed in **Table 1.2**.[40]

Table 1.2 Current statuses of the clinical trials of next-generation NNRTIs.

Research code	Sponsor	Status
UK-453,061	ViiV Healthcare	Phase IIb (withdrawn)
GSK 2248761	ViiV Healthcare	Phase IIb (withdrawn)
RDEA806	Ardea Bioscience	Phase IIa
RILR 355 BS	Boehringer Ingelheim Pharmaceuticals	Phase IIa
(+)-Calanolide A	Sarawak MediChem Pharmaceuticals	Phase I
MK-4965	Merck Research Laboratories	Phase I
MK-1439	Merck Research Laboratories	Phase I
MK-6186	Merck Research Laboratories	Phase I

1.2 Michellamine analogues

1.2.1 Background of the michellamines

The continuous worldwide threat due to the AIDS epidemic has stimulated huge efforts in developing medical drugs or vaccines against this rapidly spreading disease, and the steps of screening natural substrates for new class drugs have always continued. In the course of a broad screening program on a large number of natural sources by the Boyd laboratory at the National Cancer Institute in US, the michellamines (**Figure 1.5**) were discovered from the leaves of the tropical plant *Ancistrocladus korupensis* in Cameroon.[41] A more extensive testing showed that michellamines B (**17**) exhibited EC_{50} values (inhibition of viral cell killing or noncytopathic infections) between 1 and 88 μM, and IC_{50} values of cytotoxicity from 42 to greater than 240 μM against a remarkable

diversity of strains of both HIV-1 and HIV-2 in a wide spectrum of cell types.[42] Subsequent studies to uncover the mechanism of the action of michellamine B have indicated that it does not block the initial binding of HIV to target cells; rather it inhibits cellular fusion and syncytium formation, and is a non-competitive inhibitor of HIV RT.[43]

The michellamines (**16-18**) are not only of biological and pharmaceutical significance in the search for novel anti-HIV agents, but also represented three new members in a novel class of naturally occurring dimeric naphthylisoquinoline alkaloids. They are each composed of four aromatic systems: two naphthyl and two tetrahydroisoquinoline systems (**Figure 1.4**). These unique structures contain rare C5-C8′ and C5‴-C8″ biaryl linkages as well as six phenolic OH and two secondary amino groups which result in the exceptionally high polarity.

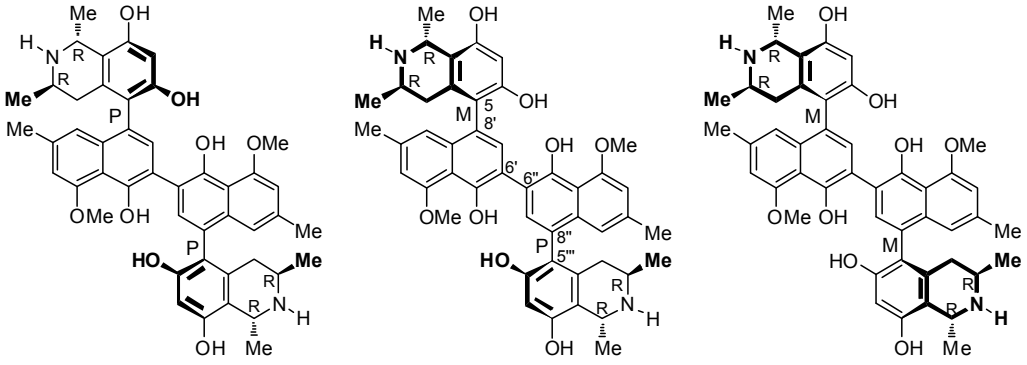

Figure 1.5. Chemical structures of michellamine A-C and their biological activities against HIV (RF Strain) in cell culture.

Moreover, four new monomeric alkaloids korupensamines A-D (**19-22**) (**Figure 1.6**) were isolated from the *A. korupensis* at a later date. These biosynthetic precursors of michellamine showed no anti-HIV activity, but were found to have antimalarial activity

against *Plasmodium falciparum* and *Plasmodium berghei*. The IC_{50} values for Korupensamine A (**19**) were 0.31 and 0.56 μg/mL against *P. falciparum* and *P. berghei*, respectively, and 0.18 and 0.41 μg/mL for korupensamine B (**20**). Conversely the michellamines (**16-18**) showed only weak activity against both of the malarial parasite species, with IC_{50} values ranging from 20 to greater than 50 μg/mL.[44]

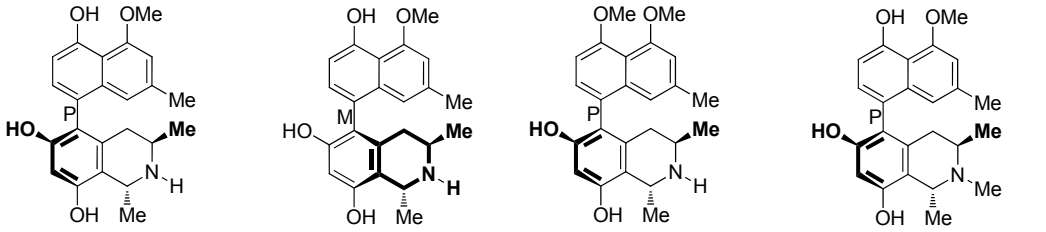

Figure 1.6 Chemical structures of korupensamines A-D.

1.2.2 Previous synthetic strategy for preparing michellamine B

Due to the promising anti-HIV properties of the michellamines and the demonstrated need of large quantities for further pharmaceutical studies, several research groups developed syntheses of michellamines A-C (**16-18**).[45-51] The strategies towards the synthesis of the michellamine skeleton mainly followed two pathways (**Scheme 1.1**). Both routes required the initial synthesis of the naphthyl unit and isoquinoline unit. In route A, a naphthylisoquinoline was formed first *via* a cross coupling before the dimerization reaction. Pd-catalyzed Suzuki reactions and Stille reactions were applied to achieve the cross coupling, and in some case, the "lactone methodology" as a different strategy to build the naphthylisoquinoline alkaloid, was also used.[52,53] While in route B, a binaphthyl core was first prepared, followed by a di-coupling with isoquinoline unit. In some reports, instead of starting from a naphthyl unit, biphenol was used to prepare the binaphthyl core.[54,55]

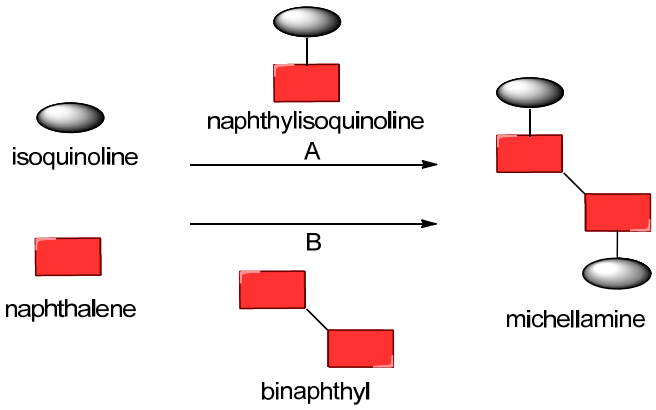

Scheme 1.1 Two pathways for synthesis of michellamine. A: forming naphthylisoquinoline before dimerization; B: forming binaphthyl core before coupling isoquinoline.

Besides these two main pathways, in a recent report of stereo-selective synthesis of michellamine B (**17**), axial chirality was installed by asymmetric Suzuki-Miyaura coupling reactions before the isoquinoline was constructed in the monomeric biaryl compound.[56]

1.2.3 Analogues of michellamine B

Michellamine B (**17**), as a novel class of natural products that feature promising bioactivities against HIV, has captured the attention of scientists. Although elegant pathways have been developed for the stereoselective total synthesis of michellamine B (**17**), there is an urgent demand for the design and synthesis of even more active and less toxic analogues with more simple structures.

1.2.3.1 Michellamine B analogues based on the modification of the isoquinoline and binaphthyl units

In order to assess the importance of the methoxy and isoquinoline substituents to anti-HIV activity and simplify the synthetic sequence, simplified analogues of michellamine B lacking the two methoxy and methyl groups on central binaphthyl core

(**23**) or lacking a second tetrahydroisoquinoline group (**24**) were synthesized (**Figure 1.7**).[57] The RT inhibition activities of **23** and **24** were obtained with IC_{50} values of 62 μM and 1000 μM, respectively, while the IC_{50} value of michellamine B was 33 μM. However, these two simplified analogues exhibited more activity (IC_{50} values of 36 μM and 30 μM, respectively) in inhibiting phosphorylation of histones by rat brain protein kinase C (IC_{50} = 130 μM) (**Table 1.3**).

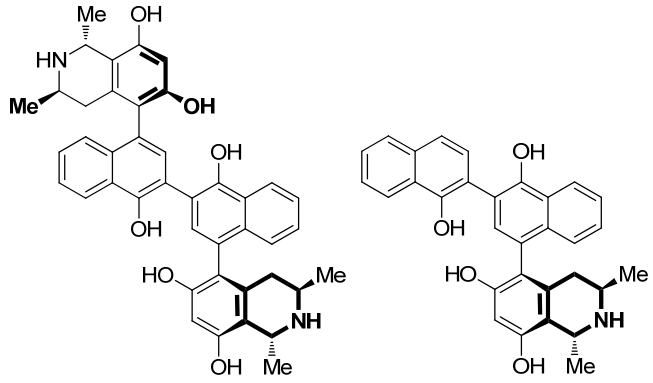

Figure 1.7 Simplified analogues of michellamine B.

Table 1.3 Inhibitory activities of michellamine B and the analogues **23** and **24**.[57]

Compound	HIV RT IC_{50} (μM)	Protein kinase C IC_{50} (μM)
michellamine B (**17**)	33	130
23	62	36
24	1000	30

The importance of the isoquinoline unit in michellamine B to anti-HIV activity was evaluated by a series of structural analogues, in which the tetrahydroisoquinoline rings

were exchanged with a variety of simple aromatic rings and the R unit was tested as either H, Me or OMe (**Figure 1.8**).[58] All the analogues (**25-27**) showed no activities for anti-HIV, which indicated that the tetrahydroisoquinoline ring is an essential part for desired biological activity. Moreover, **25ie**, **26iie** and **27iiie** bearing the dihydroxyphenyl substitution exhibited elicited toxicity in the CEM-SS cytoprotection assay,[59] which suggested that the 2,4-dihydroxy substitution may play a significant role in the cellar toxicities.

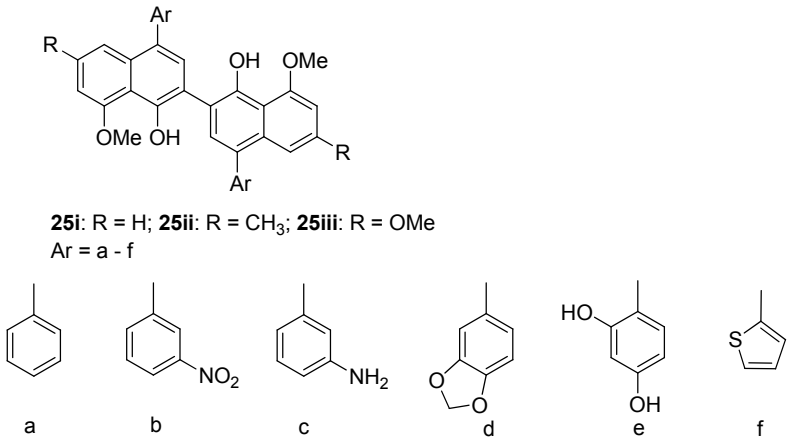

Figure 1.8 Michellamine B analogues in which isoquinoline units were replaced by different aromatic rings.

Similar work from our group also indicate that the isoquinoline unit is essential to the anti-HIV activity (**Figure 1.9**).[60] In this work, the central binaphthyl core of the michellamine B analogues was selectively attached with ethyl ester group instead of the original methyl group in some scaffolds, and aromatic ring units like phenyl or naphthyl were used to replace the isoquinoline unit. From the assays of activity against HIV-RT, all the analogues only showed weak inhibitory activities with a maximum 28% RT inhibition (**26ia**). The poor inhibition may be considered evidence for the importance of isoquinoline unit for anti-HIV properties.

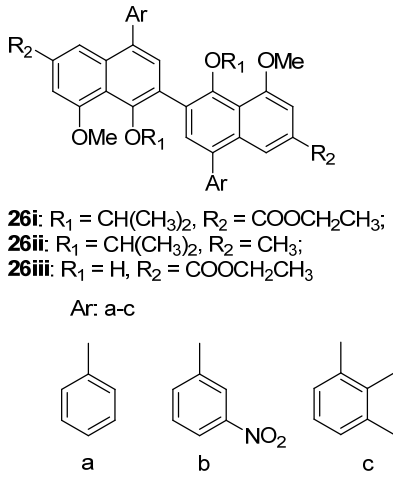

Figure 1.9 Michellamine B analogues in which isoquinoline units were replaced by different aromatic rings.

Another report from our group has shown that binaphthyl derivative gossypol (**27**) (**Figure 1.10**) is a weak reverse transcriptase inhibitor and this pharmacophore based study was also supported by HIV RT testing.[61]

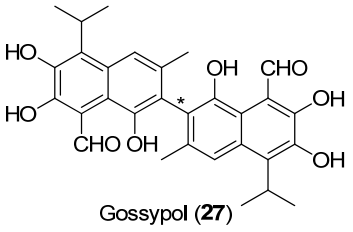

Figure 1.10 Chemical structure of gossypol.

1.2.3.2 Biaryl analogues inspired by michellamine B

Since michellamine B (**17**) is a large lead compound with a molecular weight of 757 g/mol, analogues with a smaller core unit replacing the binaphthyl core unit were designed and synthesized. During the last few years, our group was interested in the synthesis of biaryl scaffolds based on michellamine B (**17**) as a novel class of NNRTIs.

The design of new michellamine B analogues was primarily based on decreasing the size of the molecules while maintaining the hydrophobic nature of the binaphthyl core. This can be done through the replacement of this core by smaller biaryl or biheterocyle scaffolds, including biindole (**28**), biphenyl (**29**), bipyrimidine (**30**), biaryl compound containing pyridine and uracil (**31**), biaryl compound containing pyridine and pyrimidine (**32-33**) (**Figure 1.11**). However, all the compounds only show weak to medium inhibitory activities against HIV RT, with a maximum 68.1% RT inhibition.

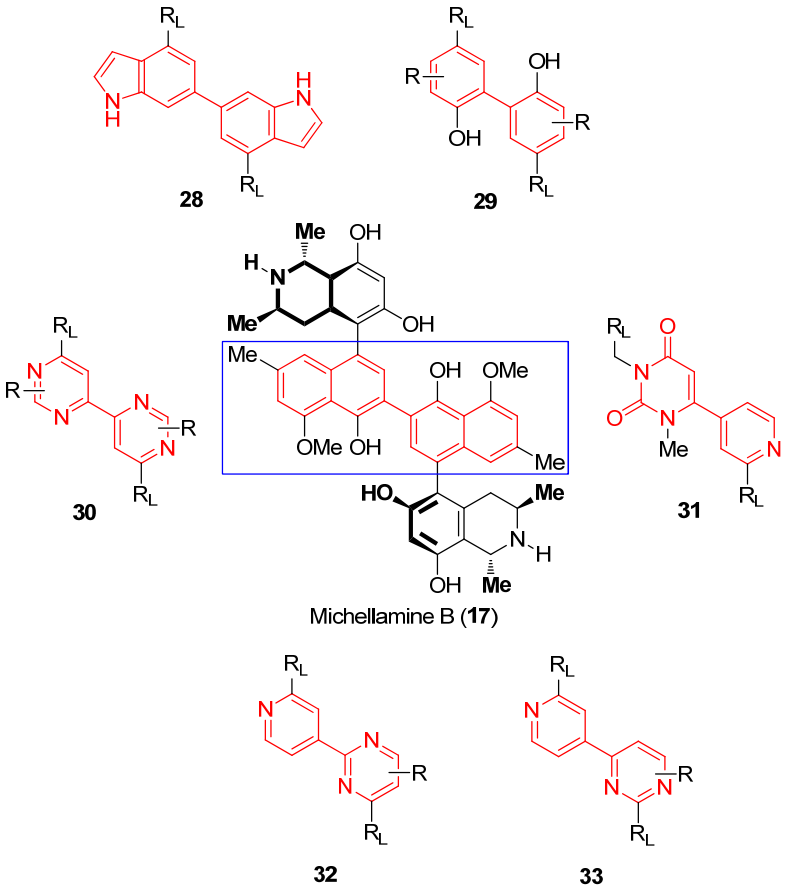

Figure 1.11 Biaryl substitutions of the binaphthyl core of the michellamine B.

1.2.3.3 Michellamine B analogues from or based on natural substrates

Apart from the simplifying the structures of the michellamine B, efforts have been made to search for structural analogues of this promising anti-HIV lead with better

pharmacological properties, either by isolation of further representatives from the plants or by synthetic procedures based on the obtained natural substrates.

Jozimine A (**35**), as a first non-natural dimer of natural substrate dioncophylline A (**34**) which isolated from *Triphyophyllum peltatum*, was synthesized and evaluated for biological activity (**Figure 1.12**).[62] Although, regrettably, it did not show a particular antiviral activity comparable to that of michellamine B (**17**), it surprisingly displayed a high antimalarial activity against *P. falciparum*, with an IC_{50} value of 0.075 µg/mL. On the other hand, michellamines are inactive towards *P. falciparum* and the monomeric alkaloid dioncophylline A (**34**) only showed a moderate activity with IC_{50} value of 1.44 µg/ml (**Table 1.4**). These results provide impetus to design, synthesize, and test further related and non-related unnatural dimers of naturally occurring or artificial monomeric naphthylisoquinoline alkaloids.

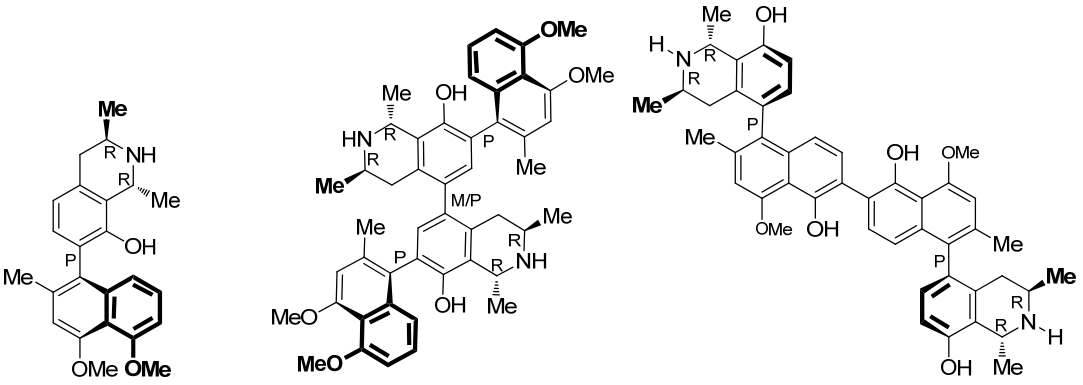

Figure 1.12 Chemical structure of dioncophylline A, jozimine A and C.

A number of dimeric naphthylisoquinoline alkaloids[a] were synthesized or isolated in the past few years, including pindikamine A,[63] jozimine C (**36**),[64] jozipeltine A,[65] ancistrogriffithine A,[66] shuangancistrotectorines A-E,[67] jozimine A_2[68] and

[a] *The structures of these dimeric naphthylisoquinoline alkaloids are showed in Appendix 1.*

mbandakamines A and B.[69] Similar to jozimine A (**35**), these structural analogues of michellamine B all exhibit good anti-malarial activities. Only jozimine C (**36**) which has a close structural relationship to the michellamines showed comparable anti-HIV activity (EC_{50} = 27 μg/mL) to that of michellamine B (**17**) (EC_{50} = 14 μg/mL) (**Table 1.4**).

Table 1.4 Bioactivities against HIV RT and *P. falciparum*.*

Compounds	IC_{50} (μg/mL)	
	HIV RT	*P. falciparum*
michellamine B[64]	14	NA
jozimine A[62]	NA	0.075
pindikamine A[63]	NA	1.23
jozimine C[64]	27	0.445
jozipeltine A[65]	NA	0.875~2.53
ancistrogriffithine A[66]	NA	0.035
shuangancistrotectorines A-E[67]	NA	0.052~1.05
jozimine A_2[68]	NA	0.0014 μM
mbandakamines A and B[69]	NA	0.043~0.148 μM

*The data are collected from different reported papers and the biological test conditions used may be different.

1.3 Aims

Since the discovery of the michellamine B as a potential anti-HIV drug, a great range of its analogues were designed and synthesized for the evaluation of bioactivities. From

the previous reports,[58,60,70] the isoquinoline unit has proven to play an essential part for bioactivity against HIV RT. Although, numerous works have been performed based on michellamine B, there is no systematic study of the isoquinoline analogues for anti-HIV properties.

Therefore, the aims of this project are:

1) To synthesis naphthyl boronic acid (**37**) or ester (**38**) as the core of the michellamine B analogues for subsequent Suzuki cross-coupling (discussed in **Chapter 2**).

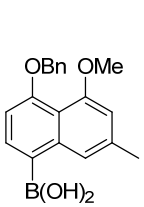

37

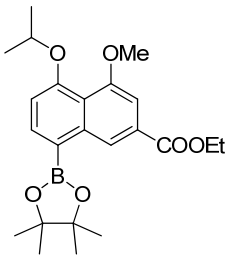

38

2) To design and synthesize novel halogenated isoquinolines (**39-42**) as the subunits of the michellamines B analogues for the subsequent Suzuki cross-coupling with naphthyl boronic acid (discussed in **Chapter 2**).

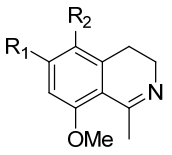

39: R_1 = H, R_2 = Br;
40: R_1 = OMe, R_2 = Br;
41: R_1 = OMe, R_2 = I

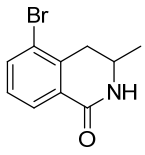

42

3) To establish a robust Pd-catalyzed Suzuki cross coupling between the naphthyl boronic acid/ester (**37**, **38**) and halogenated isoquinolines (**39-42**) leading to the monomeric naphthylisoquinolines. For example, **43** can be obtained from the Suzuki cross-coupling between **37** and **40**. (discussed in **Chapter 3**).

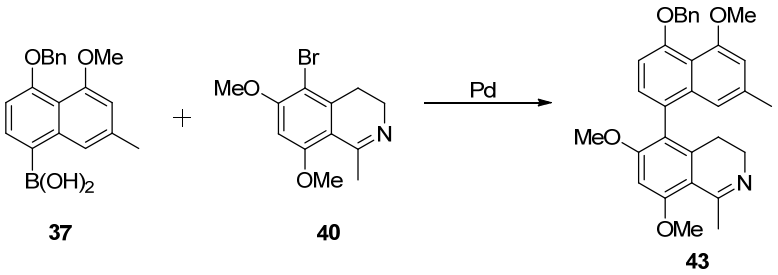

37 **40** **43**

4) To synthesize the target dimeric michellamine B analogues *via* Ag_2O-mediated oxidative dimerization of unprotected monomeric naphthylisoquinolines. For example, michellamine B analogue **45** can be obtained from the dimerization reaction of unprotected monomeric naphthylisoquinoline **44** (discussed in **Chapter 3**).

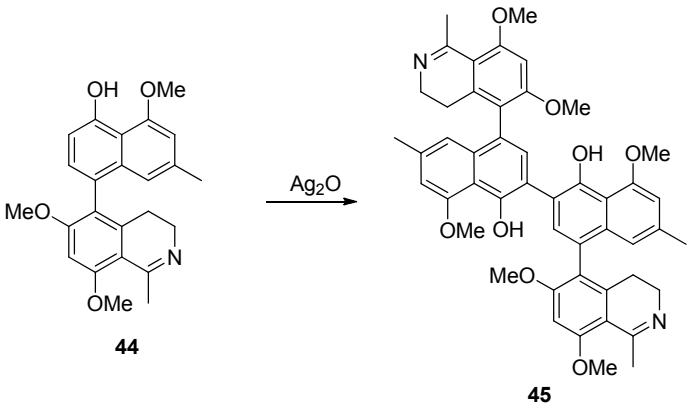

44 **45**

5) To test the obtained michellamine B analogues and all the monomeric intermediates for their inhibition activity against HIV RT and to obtain information of structure-activity relationship (SAR). To test all the monomeric naphthylisoquinolines for their anti-malaria activity (discussed in **Chapter 4**).

Chapter 2: Synthesis of Precursors

2.1 The synthetic strategy

Michellamine B, with its moderate anti-HIV activity, has gained significant interest, and various methods for constructing this unique dimeric naphthylisoquinoline alkaloid have been achieved.[42,46,48,50] One of the most popular strategies is building this dimeric compound from active anti-malarial monomeric naphthylisoquinolines. In this strategy, naphthylisoquinoline is first synthesized from naphthylboronic acid/ester and brominated isoquinoline *via* a palladium-catalyzed Suzuki cross-coupling.[48,50,56,71]

In this project, a similar strategy will be adopted to complete the synthesis of the michellamine B analogues. In order to prepare the monomeric naphthylisoquinoline, a naphthylboronic acid/ester and halogenated isoquinoline unit will be first prepared as precursors for the subsequent Suzuki cross-coupling. For example, the synthesis of **45** can be achieved from monomeric naphthylisoquinoline **43** which requires two precursors **37** and **40** for the synthesis (**Scheme 2.1**).

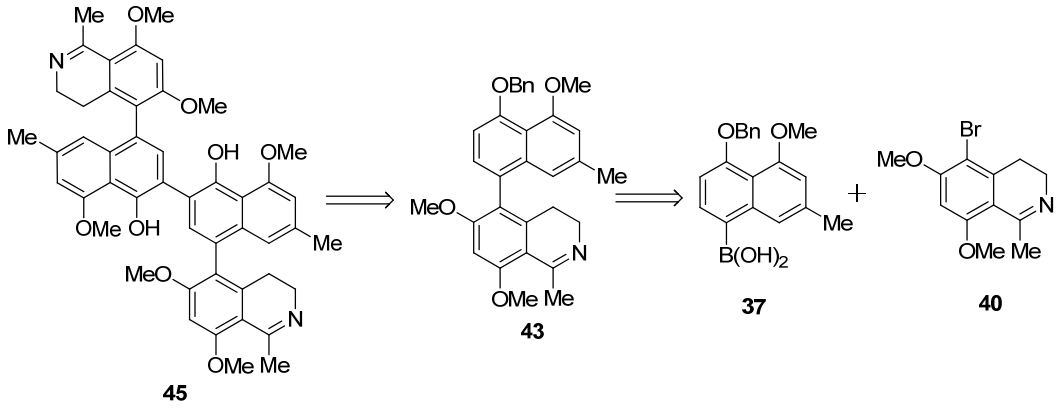

Scheme 2.1 The synthetic strategy towards the michellamine B analogue **45**.

2.2 Synthesis of naphthylboronic acid/ester

2.2.1 The designed synthetic routes of naphthylboronic acid/ester

The naphthylboronic acid/ester, as a major intermediate in the synthesis of michellamine B analogues, will be used for the subsequent Suzuki cross-coupling with isoquinoline units. There are currently two methodologies for the synthesis of this key intermediate.[56,71] In this project, both methodologies were applied to obtain the target naphthylboronic acid/ester (**37**, **38**).

The first strategy starts from commercially available 3-hydroxybenzaldehyde **46**, followed by a bromination reaction to give intermediate **47**. A Wittig reaction will be applied to afford **48**, then the naphthyl ring **49** can be obtained from the cyclization reaction. Finally a Miyaura borylation reaction will give the naphthylboronic ester **38** (**Scheme 2.2**).[71] This method was first established for the synthesis of the korupensamines, and the subsequent biomimetic synthesis of the michellamines.[71]

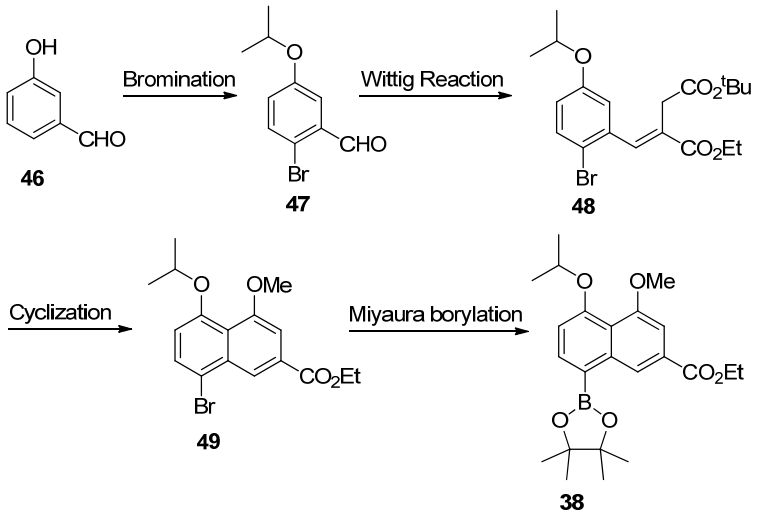

Scheme 2.2 The synthetic strategy for naphthylboronic ester **38**.

The ethyl ester group at the 2-position in the naphthyl ring of **38** served as possible

variable, which is structurally different compared to the methyl group in the naphthyl moiety of michellamine B. It allows for possible transformations, such as to the carboxylic acid or the methyl alcohol, allowing for the impact of this variable in HIV inhibition to be assessed. The bromo substituent at the C8 position served as a good handle for the subsequent borylation reaction or direct Suzuki cross-coupling with boronic acids/esters.

The second strategy is a recently developed methodology to build the naphthyl ring.[56] Starting from the commercially available 3,3-dimethylacrylic acid **50**, an esterification and addition reaction will give diene **51**. Then, a Diels-Alder reaction with 1,4-benzoquinone will be employed to afford the dione **52**. After 5 steps (reduction, protection, deprotection, triflation and Miyaura borylation), the naphthylboronic acid **37** can be obtained for the subsequent Suzuki cross-coupling reaction (**Scheme 2.3**).

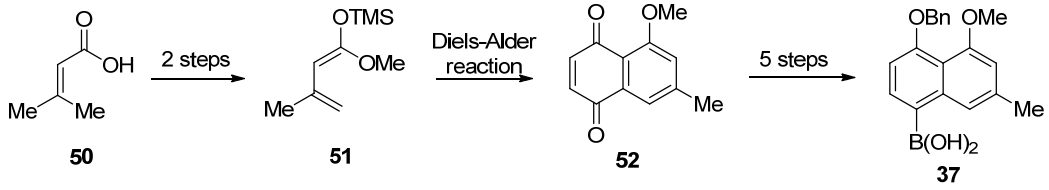

50 **51** **52** **37**

Scheme 2.3 The synthetic strategy of naphthylboronic acid **37**.

2.2.2 Naphthylboronic ester synthesized by the Wittig method

2.2.2.1 Synthesis of brominated naphthyl 49

The precursor ylide **54** was first prepared from triethyl phosphonoacetate and *tert*-butyl bromoacetate in quantitative yield using the Arbuzov reaction and was purified *via* bulb-to-bulb distillation. The hydroxyl group in the commercially available benzaldehyde **46** was protected using 2-bromopropane, followed by a bromination reaction on the phenyl ring to afford **47**, both in 87% yield. A

Horner-Wadsworth-Emmons reaction was then applied using the prepared ylide **54** to afford the intermediate **48** in 71% yield. A one-pot, three-step (hydrolysis, cyclisation and hydrolysis) ring closure gave naphthyl **56** with free phenol group in a 98% yield. Methylation of **56** gave the brominated naphthyl **49** in 92% (**Scheme 2.4**).

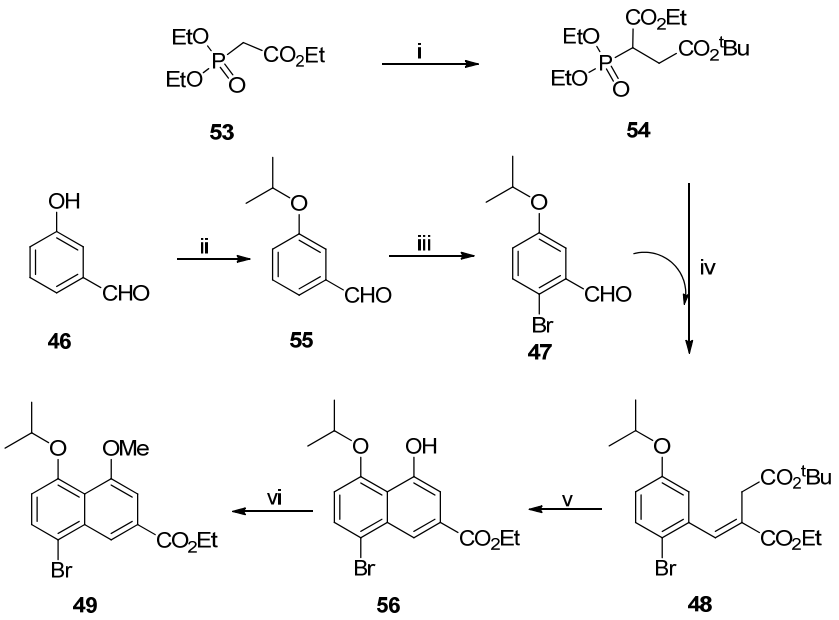

Scheme 2.4 Reagents and conditions: (i) *tert*-butyl bromoacetate, NaH, THF, 0 ^{o}C, 15 h, 96%; (ii) 2-bromopropane, K_2CO_3, DMF, 18 h, 87%; (iii) Br_2, NaOAc, DMF, rt, 18 h, 87%; (iv) NaH, THF, 0 ^{o}C, 18 h, 71%; (v) 1) TFA, rt, 15 h; 2) acetic anhydride, 5 h; 3) NaOEt, rt, 4 h; 98%; (vi) K_2CO_3, acetone, 15 h, 92%.

Analysis of the EI mass spectrum of **49** showed a peak at *m/z* 366 assigned as molecular ion. The protons of the C4 methoxy group were assigned to the singlet at δ 4.00 ppm in the ^{1}H NMR spectrum, while the ethyl ester protons were assigned to the coupled triplet and quartet at δ 1.45 ppm and δ 4.45 ppm respectively. The isopropyl methyl groups were equivalent, assigned to the doublet at δ 1.40 ppm. The naphthyl ArH1 and ArH3 were assigned to the doublets at δ 8.56 ppm and δ 7.46 ppm respectively with a coupling constant of 1.2 Hz, while the ArH6 and ArH7 were assigned to the doublets at δ 6.87 ppm and δ 7.70 ppm respectively with a coupling constant of J = 7.8 Hz.

This six-step synthesis proceeded in 47% overall yield and all the compounds synthesized were spectroscopically identical to those reported.[70]

2.2.2.2 Attempted reduction of the ethyl ester group in 49

In order to be consistent with the structure of michellamine B, the ethyl ester group in **49** required conversion into the methyl group *via* reduction (**57**), bromination (**58**) followed by another reduction reaction (**59**) (**Scheme 2.5**). However, attempts at the initial reduction of the bromine handle at C8 position using $LiAlH_4$ at 0 ^oC resulted in the naphthyl **60** in 76% yield, despite a high yield being reported for the same reaction.[71] As the ester group in the naphthyl ring could impact anti-HIV activity of michellamine B analogues, and hence be important for the SAR studies in this project, it remained in our scaffolds. An alternative methodology will be used to achieve the desired naphthylboronic acid with the methyl substituent **37** (discussed in next section **2.2.3**).

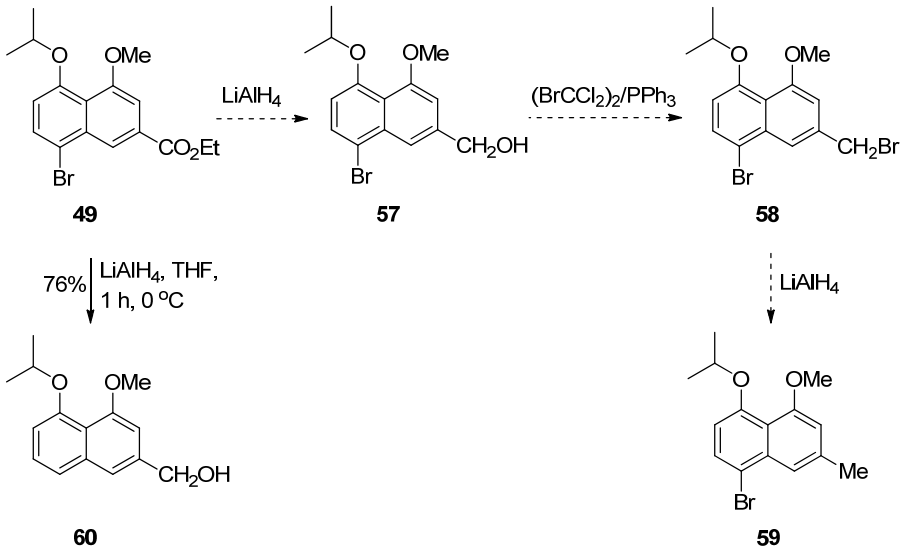

Scheme 2.5 Attempted reduction of ethyl ester group in **49**.

2.2.2.3 Borylation of the brominated naphthyl 49

The preparation of boronic esters *via* a palladium catalyzed cross-coupling reaction of bis(pinacolato)diboron and aryl halides were described for the first time in 1995.[72] Before that, arylboronic acids were traditionally synthesized using Grignard or lithium reagents.[73,74] For this project, borylation was attempted using activated aryl halides and the critical base, potassium acetate.

The boronic ester **38** was prepared using the Miyaura borylation conditions (**Scheme 2.6**). A solution of brominated naphthyl **49**, bis(pinacolato)diboron (**61**), potassium acetate and $PdCl_2$(dppf) in THF was heated at reflux for 18 h to give the naphthylboronic ester **38** in 91% yield. Analysis of the ^{1}H NMR spectrum of **38** indicated a new strong singlet peak located at δ 1.26 ppm assigned to the tetramethyl groups (2×C(CH_3)$_2$) in the boronic ester. From the ^{13}C NMR spectrum of **38**, the peaks at δ 83.6 and δ 83.7 ppm were assigned to the two quaternary carbons and the tetramethyl groups were assigned to the peaks at δ 25.1 and δ 25.0 ppm. The peak in the MS (EI) spectrum at *m/z* 414 was assigned as the molecular ion of the boronated naphthyl **38**. The boronated naphthyl **38** was spectroscopically identical to that reported in the literature.[60]

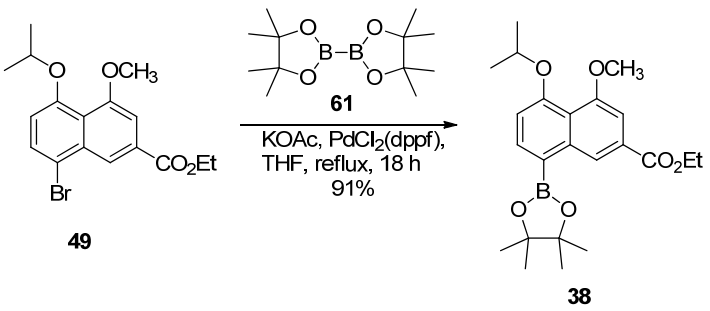

Scheme 2.6 Borylation of the brominated naphthyl **53**.

Scheme 2.7 illustrates the proposed catalytic cycle[75] of the Miyaura borylation to produce the boronated naphthyl **38**. It proceeds *via* oxidative addition of the aryl halide to the palladium complex. Then, the halogen of the arylpalladium(II) halide is replaced by an acetate ion, followed by a transmetalation between bis(pinacolato)diboron and this acetate arylpalladium(II) intermediate species. Finally, reductive elimination generates the borylated compound**.**

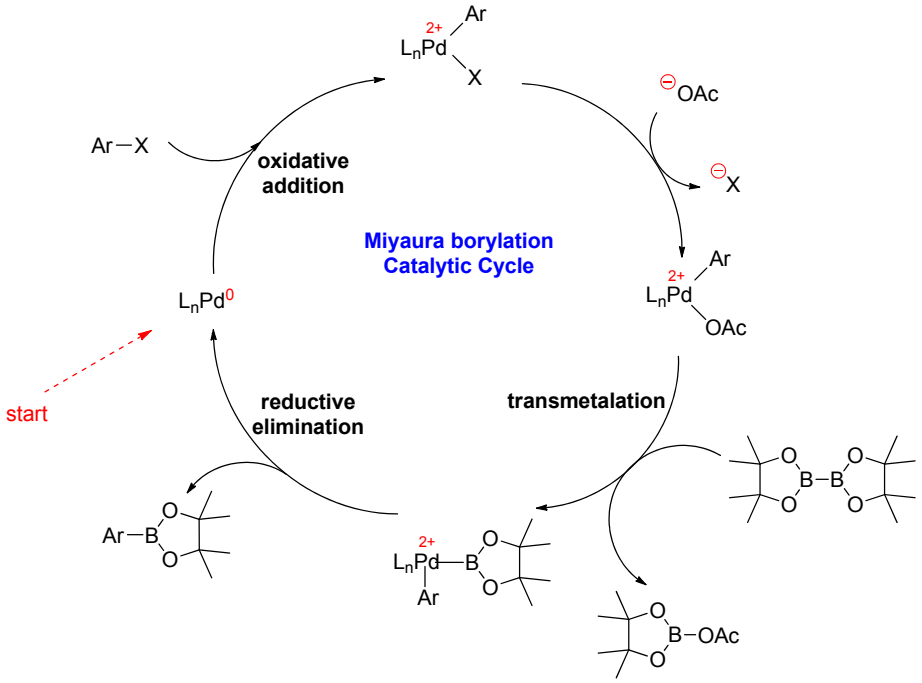

Scheme 2.7 Suggested catalytic cycle for the Miyaura borylation.

2.2.3 Naphthylboronic acid prepared by the Diels-Alder method

Due to the failure of the reduction reaction from ethyl ester group to the methyl in the naphthyl unit **49**, an alternative methodology was employed. This recently reported strategy developed boronic acid **37** from the commercially available carbocyclic acid **50** in a concise synthesis with high yields.[56] Key steps include a Diels-Alder reaction, a selective protection of phenol, and a Miyaura borylation.

Starting from commercially available 3,3-dimethylacrylic acid **50**, esterification with excess methanol catalyzed by concentrated H_2SO_4 provided the ester **62** as a colourless oil in 83% yield after purification by a reduced pressure distillation (**Scheme 2.8**).

Commercial LDA reagent and TMSCl was first used to react with **62** to prepare the desired diene **51**, however, a low yield (37%) was obtained. This was attributed to the deactivation of the LDA reagent. Therefore, the LDA was freshly prepared before reaction from diisopropylamine and *n*-BuLi,[76] and the desired diene **51** was obtained as a light yellow liquid in a quantitative yield (98%) and used for next step without further purification.

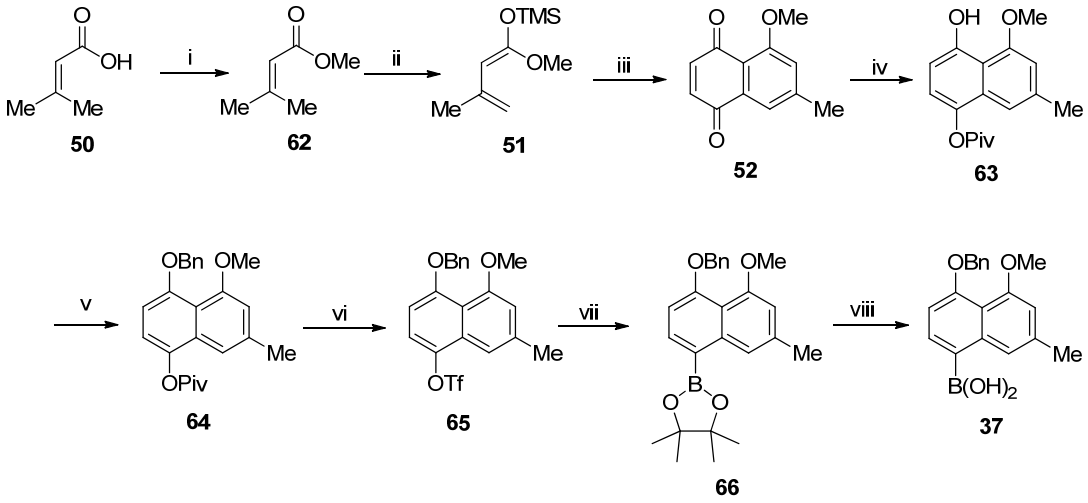

Scheme 2.8 Reagents and conditions: (i) MeOH, conc. H_2SO_4, reflux, 16 h, 83%; (ii) 1) diisopropylamine, *n*-BuLi, THF, −78 °C to rt, 2 h; 2) TMSCl, −78 °C to rt, 3 h, 98%; (iii) benzoquinone, CH_2Cl_2, AcOH, rt, 24 h, 84%; (iv) 1) $Na_2S_2O_4$, CH_2Cl_2, H_2O, rt, 1 h; 2) PivCl, Et_3N, CH_2Cl_2, 0 °C, 2.5 h, 87%; (v) BnBr, NaH, DMF, 0 °C to rt, 1 h, 93%; (vi) 1) conc. KOH, MeOH, H_2O, 50 °C, 3 h; 2) Tf_2O, Et_3N, −78 °C, 0.5 h, 89% (vii) $Pd(dppf)Cl_2$, dppf, bis(pinacolato)diboron, dioxane, 100 °C, 7 h, 92 %; (viii) $NaIO_4$, conc. HCl, THF, H_2O, rt, 12 h, 82%.

A Diels-Alder reaction between diene **51** and 1,4-benzoquinone afforded dione **52** in 84% yield as yellow crystals after recrystallization from methanol. $Na_2S_2O_4$ was used to

reduce the dione **52** to a diphenol intermediate, followed by a selective substitution of the phenolic substituent. The phenol not protected by H-bonding is more reactive and was substituted by the pivaloyl chloride, affording **63** as a white solid in 87% yield over two steps. Benzyl bromide was used to protect the other phenol group giving **64** in 93% yield. The pivaloyl group in **64** was then removed using KOH and then the deprotected intermediate was reacted with triflic anhydride to afford the triflate compound **65** in 89% yield.

The boronic ester **66** was prepared in 92% yield *via* a Miyaura borylation reaction using Pd(dppf)Cl_2 and bis(pinacolato)diboron (**61**). In order to improve the yield of the subsequent Suzuki coupling, a more active boronic acid **37** was prepared from **66** in 82% yield using $NaIO_4$ in an acidic aqueous condition (**Scheme 2.8**).

The structure of boronic acid **37** was initially identified from the peak at *m/z* 322 in the MS (EI) spectrum assigned as the molecular ion. A comparison of the ^{1}H NMR spectra of boronic ester **66** with the boronic acid **37** showed that the highfield singlet peak at δ 1.40 ppm assigned to tetramethyl groups in the spectrum of **66** could not be observed in the spectrum of **37**, indicating the boronic ester had been removed. The signals of ArH3 and ArH6 in the spectrum of **37** were shifted downfield to δ 6.95 ppm and δ 6.80 ppm compared to δ 6.84 ppm and δ 6.70 ppm in **66**, the peaks assigned to the methyl group in the spectrum of **37** were shifted highfield to δ 2.46 ppm compared to δ 2.49 ppm in **66**, while the peak assigned to the methoxy stayed the same at δ 3.92 ppm in both **66** and **37**. Notably, the carbon directly attached to the boron atom in both **66** and **37** didn't show any signal in the ^{13}C NMR spectra, even after a 12 h scan in high concentration. The naphthylboronic acid **37** was spectroscopically identical to that reported in the literature.[56]

2.3 Synthesis of 3,4-dihydroisoquinolines

2.3.1 Design of dihydroisoquinoline units

There have been limited studies on the importance of the tetrahydroisoquinoline unit of michellamine B for anti-HIV activity. There is only one report mentioning that the tetrahydroisoquinoline unit plays an essential role in its activity.[58] In this report, the tetrahydroisoquinoline unit in michellamine B was replaced by different aromatic substituents, and most of the tested derivatives showed little or no activity against HIV.[58] Similar work from our group concurred with this result.[60,70]

However, in these studies none of the substituents have structural similarity to the tetrahydroisoquinoline unit. Therefore, investigation towards tetrahydroisoquinoline analogues, such as dihydroisoquinoline and dihydroisoquinolin-1(2*H*)-one, in michellamine B derivatives is of great significance, and will also provide information for SAR study.

The design of these dihydroisoquinoline units (**39-42, Figure 2.1**) was based on:

1) An introduction of double bound between C1 and N to afford the 3,4-dihydroisoquinoline system, which removes one chiral element in the tetrahydroisoquinoline and shortens the synthetic procedure.

2) A removal or replacement of OH groups on C6 and C8 by OMe groups due to the reported toxicity associated with phenolic groups.[58]

3) The introduction of a carbonyl group on C1 to increase the hydrophilicity of the molecule.

4) An introduction of halogen handles (Br or I) at C5 for subsequent Suzuki coupling

reaction to afford the monomeric naphthylisoquinoline alkaloid.

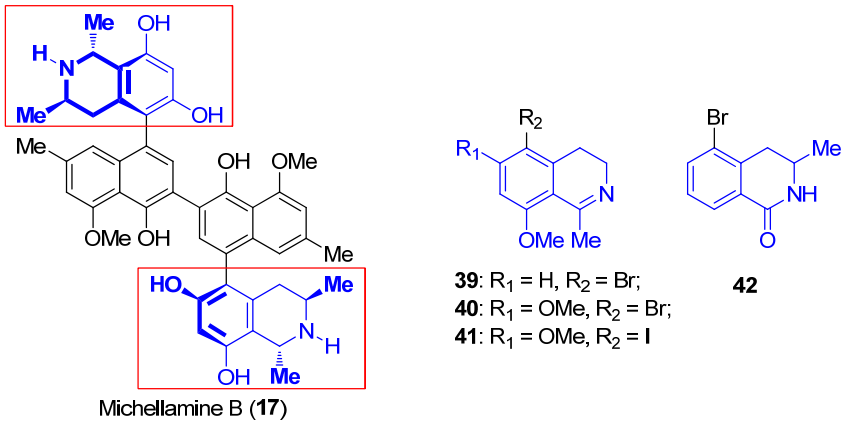

Figure 2.1 Structure of michellamine B and the designed 3,4-dihydroisoquinoline derivatives.

2.3.2 Synthetic strategy

There are many synthetic strategies developed for the synthesis of 1,2,3,4-tetra- and 3,4-dihydroisoquinoline derivatives and most of them contains a key step – a cyclisation reaction of phenylethylamine derivatives which can be achieved under the Bischler-Napieralski conditions. It is reported that electron donating aryl substituents such as hydroxyl and methoxy groups are required to allow such ring closures to occur.[77-79]

The synthesis of the designed 3,4-dihydroisoquinoline derivative **72** was proposed in **Scheme 2.9**. The first step involves the condensation between the appropriate aldehyde and nitromethane which would afford the nitrostyrene **68**. Reduction of nitrostyrene would produce the phenylethylamine derivative **69**, which can then be converted to the key acetamide intermediate **70** by acetylation. Bromination at C2 would afford the intermediate **71** which can be cyclized at C5 position under Bischler-Napieralski conditions to produce the desired dihydroisoquinoline derivatives **72**.

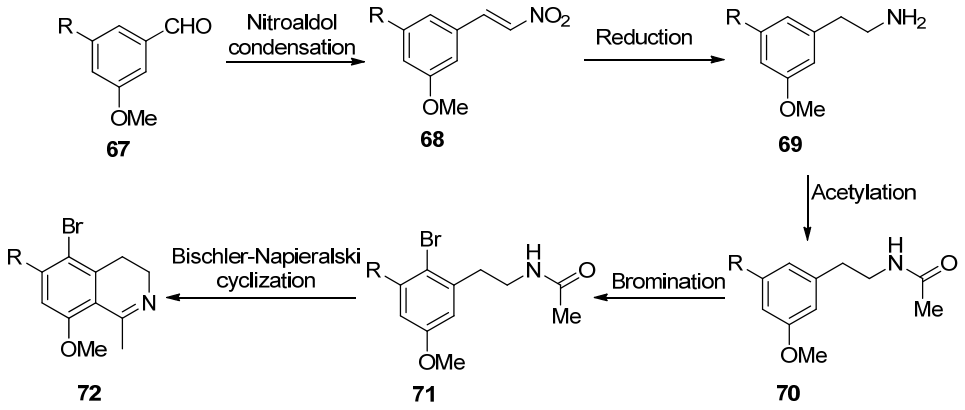

Scheme 2.9 Proposed synthesis of brominated 3,4-dihydroisoquinoline **72**.

In order to introduce the carbonyl group in the isoquinoline unit to increase the hydrophilicity of the molecule, 3,4-dihydroisoquinolin-1(2*H*)-one is designed and the synthesis of this scaffold involves a key electrophile intermediate isocyanatoalkylbenzene (**Scheme 2.10**). This isocyanate intermediate also allows the ring closure to occur in intermediate **75**, as a normal Bischler-Napieralski reaction requires electron donating aryl substituents such as hydroxyl and methoxy groups for such ring closures; groups lacking in **75**.

In this proposed synthetic strategy for 3,4-dihydroisoquinolin-1(2*H*)-one, a nitroaldol condensation reaction with commercially available 2-bromobenzyaldehyde will first give nitrostyrene intermediate **74**, followed by a reduction reaction to afford phenylethylamine derivative **75**. An isocyanate formation reaction of **75** will then give the key intermediate isocyanatoalkylbenzene **76**. A Friedel-Crafts type cyclisation reaction will finally furnish the 3,4-dihydroisoquinolin-1(2*H*)-one **42** (**Scheme 2.10**).

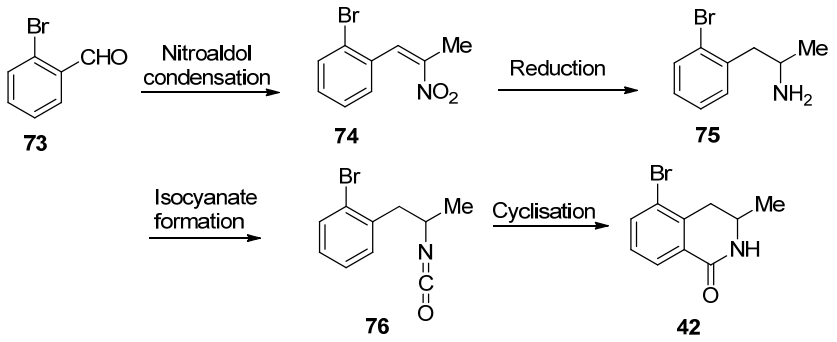

Scheme 2.10 Proposed synthesis of 3,4-dihydroisoquinolin-1(2*H*)-one.

2.3.3 Synthesis of 3,4-dihydroisoquinolines 39-42

2.3.3.1 Synthesis of 3,4-dihydroisoquinolines 39-41

Starting from commercially available benzaldehyde **77** and **78**, a nitroaldol reaction using nitromethane catalysed by ammonium acetate produced the desired nitrostyrenes **79** (91%) and **80** (96%) in high yields after purification by recrystallization from methanol.

The nitrostyrenes were then reduced by $LiAlH_4$ to afford the corresponding phenylethylamine intermediates which were directly acetylated using acetyl chloride to afford *N*-phenethylacetamide **81** (56%) and **82** (63%). *N*-acetyl-*N*-phenethylacetamides were also obtained as side products from these reactions. The purification of the phenylethylamine intermediates were also attempted and lower yields of acetamide **81** (38%) and **82** (45%) were eventually obtained. These may be attributed to the loss of phenylethylamines during the column chromatography.

The bromination reaction using Br_2 gave the brominated amides **83** (87%) and **84** (89%). Finally, a Bischler-Napieralski cyclisation with $POCl_3$ furnished the brominated 3,4-dihydroisoquinolines **39** and **40** as brown solids in 88% and 90% yields,

respectively (**Scheme 2.11**).

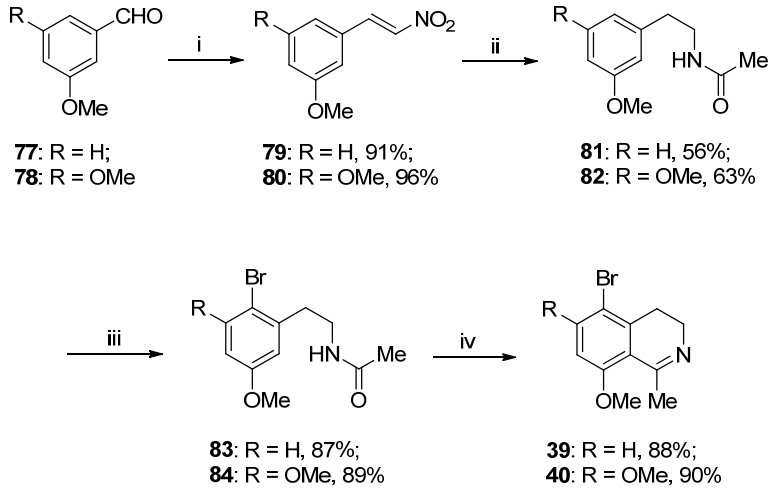

Scheme 2.11 Reagents and conditions: (i) CH_3NO_2, CH_3COONH_4, AcOH, reflux, 5 h; (ii) a. $LiAlH_4$, THF, 0 ^oC to reflux, 5 h; b. CH_3COCl, Et_3N, THF, 0 ^oC, 15 min; (iii) Br_2, CH_2Cl_2, 0 ^oC to rt, 2 h; (iv) P_2O_5, $POCl_3$, CH_3CN, reflux, 6 h.

Analysis of the mass spectrum (EI) of **39** showed isotopic peaks for the monobrominated derivative at *m/z* 253 and *m/z* 255 assigned to the molecular ion peak. Analysis of the ^1H NMR spectrum for **39** revealed two *ortho*-split doublets at δ 7.87 ppm and δ 7.00 ppm, each with a relative integration of one, were assigned to the aromatic protons H6 and H7 respectively, with the corresponding carbons assigned to the peaks at δ 141.5 ppm (C6) and δ 113.2 ppm (C7) in the ^{13}C NMR spectrum.

Analysis of the mass spectrum (EI) of **40** showed isotopic peaks for the monobrominated derivative at *m/z* 283 and *m/z* 285 assigned to the molecular ion peak. The ^1H NMR spectrum for **40** showed only one singlet proton in the aromatic region at δ 6.81 ppm assigned to the aromatic proton H7 with the corresponding carbon assigned to a resonance at δ 96.9 ppm (C7) in the ^{13}C NMR spectrum. The NMR and MS spectra of both **39** and **40** were consistent with the reported data.[80]

The mechanism for the cyclization of phenylethylamides under Bischler-Napieralski conditions has been studied by Fodor and Nagubandi.[81] The reaction involves an initial dehydration step of the amide, mediated by the condensing agent, followed by cyclization (**Scheme 2.12**). The dehydration step starts by the nucleophilic attack of the carbonyl group on the phosphorus atom of $POCl_3$, forming species **85**. Deprotonation of **85** leads to the formation of the imidoyl phosphate species **86** in which the loss of the phosphate as a good leaving group affords the imidoyl salt **87**. At elevated temperatures, the benzene ring affects the new ring closure through the nucleophilic attack at acetyleynic carbon forming the intermediate **88** which deprotonates rapidly under the influence of aromaticity to afford the 3,4-dihydroisoquinoline derivative **72**.

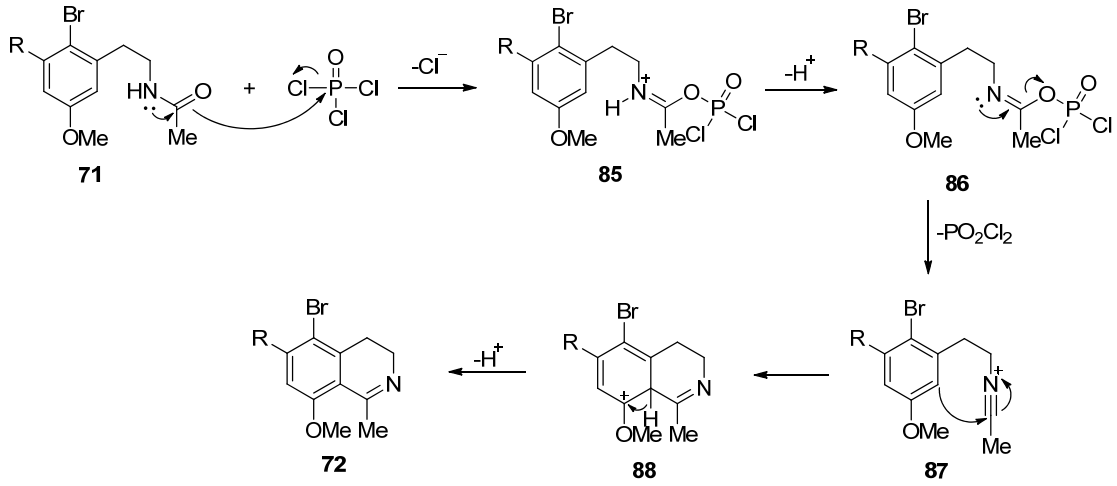

Scheme 2.12 Mechanism of the Bischler-Napieralski cyclization**.**

Later experiments (see **Chapter 3.1.2**) illustrated that a more active handle on the isoquinoline with methoxy on C6 was required. Therefore, iodo 3,4-dihydroisoquinoline **41** was prepared. From the acetamide **89**, iodination using I_2 and Ag_2SO_4 furnished the iodo acetamide intermediate **90** as a white solid in 87% yield. Iodo 3,4-dihydroisoquinoline **41** was then obtained as a yellow solid in 86% yield *via* a

Bischler-Napieralski cyclisation of **90** with $POCl_3$ (**Scheme 2.13**).

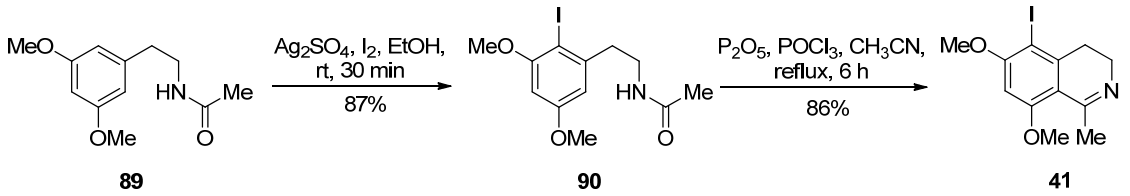

Scheme 2.13 Synthesis of iodo-3,4-dihydroisoquinoline **41**.

Analysis of the mass spectrum (EI) of **41** showed a peak at *m/z* 331 assigned to the molecular ion. The ^{1}H NMR spectrum of **41** showed only one singlet proton in the aromatic region at δ 6.76 ppm assigned to the aromatic proton H7, with the corresponding carbon assigned to a resonance at δ 96.0 ppm (C7) in the ^{13}C NMR spectrum. Two triplets at δ 3.71 ppm and δ 3.19 ppm were assigned to the H3 and H4 protons respectively. The most downfield peak located at δ 176.1 ppm was assigned to C1 in the ^{13}C NMR spectrum. Two close peaks located at δ 167.7 ppm and δ 166.7 ppm were assigned to the C8 and C6 attached with methoxy group.

2.3.3.2 Synthesis of 3,4-dihydroisoquinolin-1(2*H*)-one 42

The synthesis of 3,4-dihydroisoquinolin-1(2*H*)-one[82] started from commercially available 2-bromobenzaldehyde **73**. Nitroaldol condensation of **73** was first carried out using nitroethane and resulted in the synthesis of nitrostyrene **74** in 96% yield. The compound **74** was then reduced to the primary amine **75** using $LiAlH_4$ in 87% yield. The isocyanate **76** was obtained in 71% from the reaction between primary amine **75** and triphosgene. The final cyclisation reaction of **76** with $AlCl_3$ and tetrachloroethylene gave the desired 3,4-dihydroisoquinolin-1(2*H*)-one **42** in 31% yield (**Scheme 2.14**).

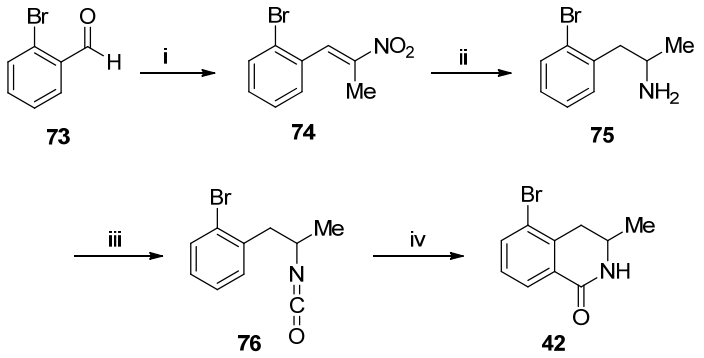

Scheme 2.14 Reagents and conditions: (i) $CH_3CH_2NO_2$, CH_3COONH_4, AcOH, reflux, 2 h, 96%; (ii) $LiAlH_4$, H_2SO_4, THF, 0 ^oC to rt, 18 h, 87%; (iii) triphosgene, toluene, reflux, 3 h, 71%; (iv) $AlCl_3$, tetrachloroethylene, 80 ^oC, 3 h, 31%.

Analysis of the EI mass spectrum of **42** showed isotopic peaks for the monobrominated derivative at *m/z* 241 and *m/z* 239 assigned to the molecular ion. The ^1H NMR spectrum of **42** showed two doublets at δ 8.00 ppm and δ 7.72 ppm assigned to the aromatic proton H8 and H6 respectively, with the corresponding carbons assigned to the peaks at δ 127.3 ppm (C8) and δ 135.9 ppm (C6) in the ^{13}C NMR spectrum. A triplet (J = 8.0 Hz) at δ 7.28 ppm was assigned to the aromatic proton H7, with the corresponding carbon assigned to the peak at δ 128.4 ppm in the ^{13}C NMR spectrum. The peak at δ 164.6 ppm in the ^{13}C NMR spectrum was assigned to the carbonyl carbon C1. The 3,4-dihydroisoquinolin-1(2*H*)-one **42** was spectroscopically identical to that reported in the literature.[82]

The ring closure in this reaction is based on the 1:1 complex formation of aluminum chloride and the corresponding isocyanate. Upon the formation of the intermediate **91** an intramolecular nucleophilic attack at the electrophilic carbon leads to ring closure (species **92**). Rearomatisation and protonation of the oxygen atom give rise to intermediate **93** and subsequent keto-enol tautomerism affords the 3,4-dihydroisoquinolin-1(2*H*)-one **42** (**Scheme 2.15**).

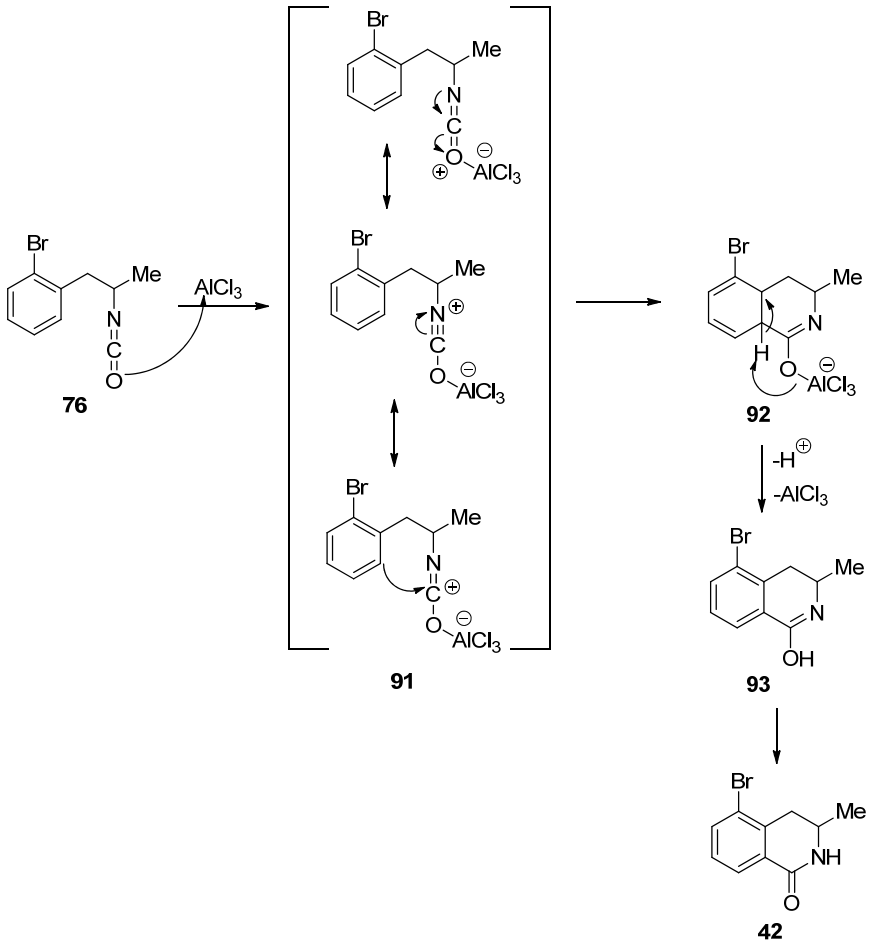

Scheme 2.15 Proposed mechanism of the cyclization reaction of isocyanate (**69**) to afford 3,4-dihydroisoquinolin-1(2*H*)-one (**42**).

2.4 Conclusions

The naphthylboronic acid/ester (**37**-**38**) and halogenated isoquinolines (**39**-**42**) were synthesized as precursors for the subsequent Suzuki cross-coupling to afford the monomeric naphthylisoquinoline alkaloids.

The naphthylboronic acid **37** was synthesized by a Diels-Alder method over 8 steps proceeding in 37% overall yield from commercially available 3,3-dimethylacrylic acid **50**. The naphthylboronic ester **38**, with an ethyl ester substituent in the naphthyl ring, was prepared by a Wittig method over 7 steps with an overall yield of 43%.

Halogenated 3,4-dihydroisoquinolines (**39**-**41**) featuring methoxy groups and double bonds between C1 and N were obtained from a four-step synthesis proceeding in 39-48% overall yields from commercially available benzaldehydes. Brominated 3,4-dihydroisoquinolin-1(2*H*)-one **42** with a carbonyl group was successfully prepared over 4 steps with an overall yield of 18%.

Chapter 3: Synthesis of Michellamine B Analogues

3.1 Preparation of monomeric naphthylisoquinoline alkaloids *via* Suzuki coupling

3.1.1 Background of the Suzuki coupling

There are many synthetic routes for the construction of aryl-alkyl bonds in modern synthetic chemistry and palladium-catalyzed reactions have a prominent place among these methods.[83,84] These reactions are widespread in the synthesis of active/functional molecules in life sciences and material sciences. Palladium-catalyzed Suzuki–Miyaura cross-coupling, which was first reported in 1979,[85] has contributed with a great impact on organic synthesis due to the easy preparation of the precursors, high yield and the low toxicity of by-products.[86] This reaction is widely used to build the biaryl linkage in the synthesis of michellamine B analogues.[46,51,56,71] The 2010 Nobel Prize in Chemistry was awarded jointly to Richard F. Heck, Ei-ichi Negishi and Akira Suzuki for their work on Pd-catalyzed cross-coupling synthesis.[87-89]

In the Suzuki reaction, the coupling of arylboronic acids/esters with aryl halides has been widely explored and these reactions are generally catalyzed by palladium complexes with various ligands. The general scheme for the Suzuki reaction is shown below where a carbon-carbon single bond is formed by coupling an organoborane with a halide using a palladium catalyst and a base (**Scheme 3.1**).

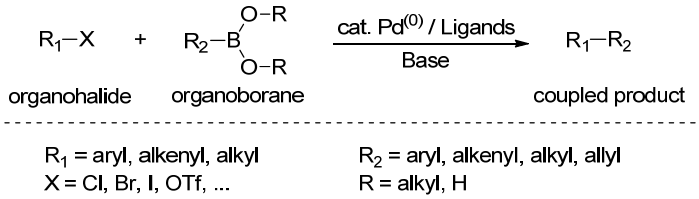

Scheme 3.1 Palladium-catalyzed Suzuki-Miyaura cross-coupling reaction.

The reaction rate of Suzuki coupling is determined by the relative reactivity of the aryl halide decreasing depending on the halogen substituent in order of I > OTf > Br > Cl. Moreover, aryl halides with electron-withdrawing groups are more reactive compared to electron rich aryl halides.[74,90]

3.1.2 Synthetic strategy towards towards monomeric naphthylisoquinoline alkaloids

The monomeric naphthylisoquinoline alkaloids, which showed good anti-malarial activity, are the precursors of the michellamine B analogues. They can be synthesized by a coupling reaction between the corresponding naphthyl unit and isoquinoline unit. Herein, naphthylboronic ester **38** and naphthylboronic acid **37** will be used to react with halogenated isoquinoline **39-42** separately *via* Pd-catalyzed Suzuki cross-coupling to synthesize the monomeric naphthylisoquinoline alkaloids **94** and **95**.

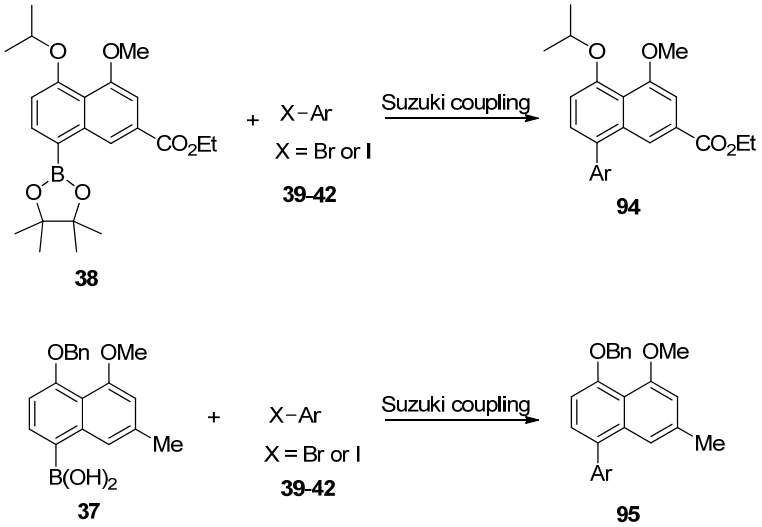

Scheme 3.2 Synthetic strategy towards towards monomeric naphthylisoquinoline *via* Suzuki cross-coupling.

3.1.3 Suzuki coupling using naphthylboronic ester 38 towards monomeric naphthylisoquinoline alkaloids

The initial attempt at this Suzuki cross-coupling was based on the method developed in the previous synthesis of biaryl scaffolds in our group.[80] In this reaction, a catalyst system of $Pd(dba)_3$, Buchwald's ligands[91-93] and K_3PO_4 were used to give the naphthylisoquinoline alkaloid **96** (Entry 1, **Table 3.1**). However, the reaction in the presence of this powerful catalyst afforded the desired product **96** in only 11% yield. Other separated products from the reaction mixture included the de-brominated derivative, starting material, and homo-coupled product, as evidenced by mass spectroscopy (ESI) analysis. Compound **96** obtained relative good solubility in most polar solvents such as CH_2Cl_2 and methanol, and a triethylamine deactivated column chromatography (hexane/ethyl acetate: 50/50) was used to purify this compound.

Analysis of the ^{1}H NMR spectrum of **96** showed two *ortho*-split doublets (J = 8.5 Hz) at δ 7.28 ppm and δ 6.97 ppm assigned to the aromatic protons H6 and H7 in the isoquinoline unit, with the corresponding carbons assigned to the peaks at δ 133.7 ppm (C6) and δ 109.9 ppm (C7) in the ^{13}C NMR spectrum. The two *meta*-split doublets (J = 1.0 Hz) at δ 7.78 ppm and δ 7.39 ppm in ^{1}H NMR spectrum were assigned to the aromatic protons ArH1 and ArH3 in the naphthyl ring with the corresponding carbons assigned to the peaks at δ 121.8 ppm (ArC1) and δ 105.1 ppm (ArC3) in the ^{13}C NMR spectrum. 2D NMR spectroscopy (gCOSY, gHSQC and gHMBC) was used to assign the two methoxy groups Ar4-OCH_3 (δ 4.02 ppm) and 8-OCH_3 (δ 3.95 ppm), corresponding to the peaks at δ 56.5 ppm and δ 55.6 ppm in the ^{13}C NMR spectrum, respectively. The peak at lowest downfield (δ 166.8 ppm) in ^{13}C NMR spectrum was

assigned to the carbonyl carbon in the ester group and the following peak (δ 164.9 ppm) was assigned to C1 in the isoquinoline unit. The peak at *m/z* 461 in the MS (EI) spectrum was assigned as the molecular ion of the naphthylisoquinoline alkaloid **96**.

Table 3.1 Trial coupling reactions to give naphthylisoquinoline alkaloid **96**.

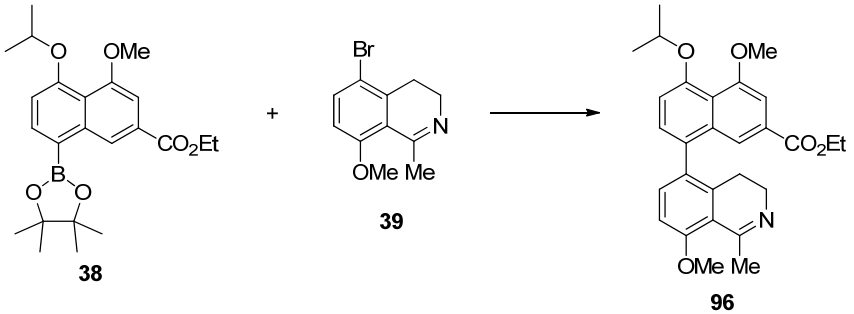

Entry	Catalyst	Base	Solvent	Reflux hours	Yield

1	$Pd(dba)_3$*	K_3PO_4	dioxane/H_2O	18 h	11%
2	$Pd(dppf)Cl_2$	K_2CO_3	dioxane/H_2O	18 h	39%
3	$Pd(PPh_3)_4$	K_3PO_4	dioxane/H_2O	18 h	58%
4	$Pd(PPh_3)_4$	K_3PO_4	DME/H_2O	18 h	57%
5	$Pd(PPh_3)_4$	$Ba(OH)_2$	DME/H_2O	18 h	40%
6	$Pd(PPh_3)_4$	$NaHCO_3$	DME/H_2O	18 h	trace
7	$Pd(PPh_3)_4$	Na_2CO_3	DME/H_2O	18 h	42%
8	$Pd(PPh_3)_4$	Na_2CO_3	toluene/H_2O	18 h	44%
9	$Pd(PPh_3)_4$	K_3PO_4	toluene/H_2O	18 h	57%

**Buchwald's ligands were used in this reaction.*

The optimisation of this reaction involved the use of different palladium catalysts, bases and solvents, and is summarised in **Table 3.1**. The first attempt (Entry 1) using a catalytic system of $Pd(dba)_3$ and Buchwald's ligands afforded the coupled product **96** only 11% yield. After replacing the catalyst with $Pd(dppf)Cl_2/K_2CO_3$ (Entry 2), a moderate yield of 39% was obtained and a lower amount of the de-brominated product was detected by TLC and MS spectrum. Probing the reaction conditions using $Pd(PPh_3)_4$ as the palladium catalyst while keeping the base with K_3PO_4 and solvent dioxane significantly increased the yield of **96** (58%, Entry 3), even with a half load of the catalyst. All the $Pd(PPh_3)_4$ used in the coupling reactions are prepared from $PdCl_2$ and triphenylphosphine in our laboratory.

The screening of different bases indicated that K_3PO_4 was more efficiently applied in palladium catalytic systems containing $Pd(PPh_3)_4$, although the choice of base is still empirical and no general rule for their selection has been established. Specifically, the

strong base of $Ba(OH)_2$ gave a decreased yield of 40% (Entry 5), the weak Na_2CO_3 resulted in a comparable yields (42% in DME and 44% in toluene, Entry 7 and Entry 8), while the weakest base $NaHCO_3$ obtained the worst results and only trace amount of **96** was produced in this reaction (Entry 6). All the bases used were dissolved in distilled water with a concentration of 5 M.

The use of different solvents indicated that the solvent had only small impact to the yield of the coupling reaction. The reaction involves the solvent dioxane (Entry 3) gave the best yield of 58%, while the reactions with the other two solvents (DME and toluene, Entry 4 and Entry 9) produced slightly less compound, both with the yield of 57%.

The reaction time of this Suzuki cross-coupling hasn't been systematically studied. The only information obtained from the experiments illustrated that the reaction with a longer time (24 h) resulted in the same yield (58%) under the catalytic system of $Pd(PPh_3)_4/K_3PO_4$/dioxane.

The catalytic cycle[74] of this Suzuki cross-coupling reaction starts with oxidative addition, followed by transmetalation and then reductive elimination (**Scheme 3.3**). The first step is the oxidative addition of the organohalide to the Pd(0) to form a Pd(II) complex. A molecule of the hydroxide or alkoxide base then replaces the halide on the palladium complex, while another adds to the organoborane to form a borate reagent making its R_2 group more nucleophilic. In the transmetalation step, the R_2 group from the borate replaces the halide anion on the palladium complex. Reductive elimination then gives the final coupled product, regenerates the palladium catalyst, and the catalytic cycle can begin again.

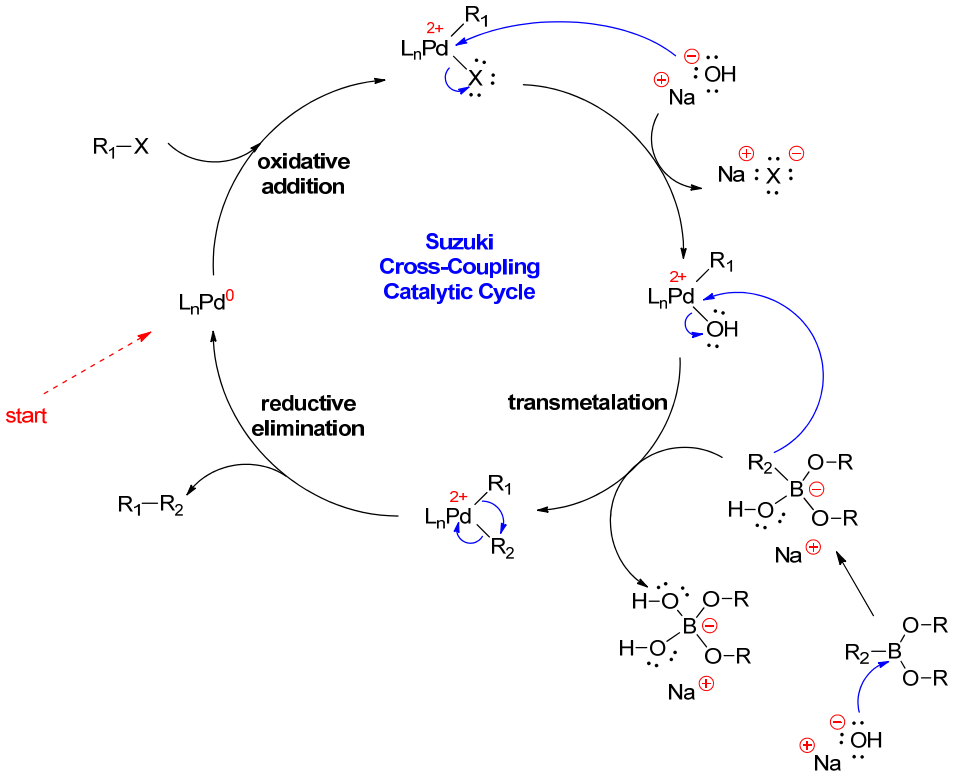

Scheme 3.3 Palladium-catalyzed Suzuki-Miyaura cross-coupling catalytic cycle.[74]

Based on the above trial reactions, a catalytic system of $Pd(PPh_3)_4/K_3PO_4$/dioxane was selected to conduct the Suzuki coupling reactions with an additional two isoquinoline units (**Table 3.2**). The reaction of boronic ester **38** with brominated isoquinoline **40** was then attempted under these conditions, giving the desired **97** in trace amount only (**Table 3.2**, Entry 1). The low yield obtained was attributed to the decreased reactivity of the aryl halide caused by the electron rich methoxy group attached in C6 position.[74,94,95] Instead of searching a more efficient catalytic system, a more reactive substituent in the isoquinoline unit such as iodo or OTf groups was evaluated to optimize the yield of **97**. This concept was also supported by previous report.[96] A novel isoquinoline scaffold **41** with a iodide handle was then prepared and used for the Suzuki coupling reaction. To be expected, **97** was obtained in a much better yield of 44% under the same reaction conditions (Entry 2) after purification by a triethylamine deactivated

flash silica gel column chromatography (hexane/ethyl acetate: 50/50). The problem associated with steric hindrance at C5 position in the isoquinoline unit made this moderate yield satisfactory for the purpose of this project.

Analysis of the ^{1}H NMR spectrum of **97** showed a singlet at δ 6.52 ppm assigned to the aromatic proton in the isoquinoline unit with the corresponding carbon assigned to a resonance at δ 94.1 ppm in the ^{13}C NMR spectrum. Two *ortho*-split doublets (J = 7.8 Hz) at δ 7.20 ppm and δ 7.06 ppm were assigned to the aromatic protons ArH7 and ArH6 in the naphthyl ring with the corresponding carbons assigned to the peaks at δ 129.6 ppm (ArC7) and δ 114.1 ppm (ArC6) in the ^{13}C NMR spectrum. Two singlets located at δ 7.71 ppm and δ 7.37 ppm in the aromatic range of ^{1}H NMR spectrum were assigned to the aromatic protons ArH1 and ArH3 in the naphthyl ring with the corresponding carbons assigned to the peaks at δ 121.7 ppm and δ 105.2 ppm in the ^{13}C NMR spectrum. 2D NMR spectroscopy (gCOSY, gHSQC and gHMBC) was used to assign the three methoxy groups Ar4-OCH_3 (δ 4.01 ppm), 8-OCH_3 (δ 3.97 ppm) and 6-OCH_3 (δ 3.68 ppm), corresponding to the peaks at δ 56.6 ppm, δ 55.8 ppm and δ 55.6 ppm in the ^{13}C NMR spectrum, respectively. The peak in the MS (EI) spectrum at *m/z* 491 was assigned as the molecular ion of the naphthylisoquinoline alkaloid **97**.

Table 3.2 Suzuki coupling reaction to synthesize naphthylisoquinoline alkaloid **97-98**.

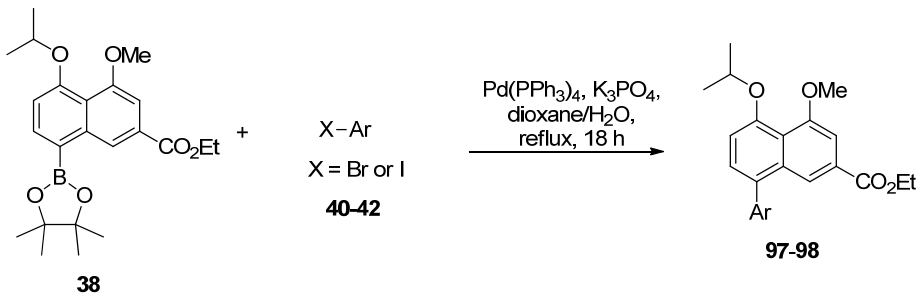

Entry	Ar	X	Isoquinoline	Product	Yield
1	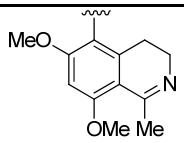	Br	**40**	**97**	trace
2	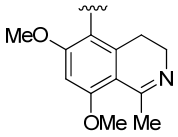	I	**41**	**97**	44%
3	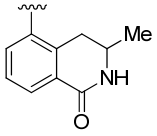	Br	**42**	**98**	54%

The same catalytic system of $Pd(PPh_3)_4/K_3PO_4$/dioxane was applied to the coupling reaction between naphthylboronic ester **38** and brominated 3,4-dihydroisoquinolin-1(2*H*)-ones **42** (**Table 3.2**, Entry 3). Naphthylisoquinoline alkaloid **98** was obtained as a brown solid in 54% yield and was purified by a triethylamine deactivated flash silica gel column chromatography (hexane/ethyl acetate: 50/50).

X-ray quality crystals of **98** were obtained by recrystallization from a mixture of CH_2Cl_2 and hexane. The X-ray structure[b] of compound **98** (see **Appendix 2.1** for X-ray crystallographic data) showed that the naphthyl ring and isoquinoline ring are not in the same plane but distributed as vertical to each other, which significantly reduces the steric hindrance of C5 position in the isoquinoline unit, allowing the Suzuki reaction to occur. The ethyl ester substituent in the naphthyl ring and the methyl group in the

[b] *All the X-ray crystallographic structures in this thesis were solved by Dr. Anthony Willis from Australian National University.*

isoquinoline unit stop the axis between C10 and C11 from freely rotation, making compound **98** feature an axial chirality (**Figure 3.1**).

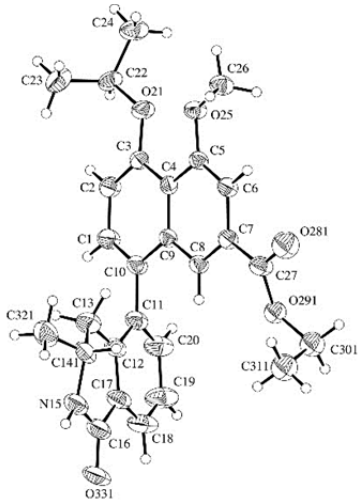

Figure 3.1 The crystal structure of naphthylisoquinoline alkaloid **98**.

Diastereomerism of **98**, caused by axial chirality, can be observed from the ^{1}H NMR spectrum. Two singlets located at δ 7.78 ppm and δ 7.60 ppm, each with a relative integration of half proton, were assigned to the aromatic proton ArH1 in the naphthyl ring. Similarly, the peaks located at δ 7.28 ppm and δ 7.23 ppm, each with a relative integration of half proton, were assigned to the aromatic proton ArH7.

Comparing the four Suzuki cross-coupling reactions between naphthylboronic ester **38** and four different isoquinoline units (**39**-**41**), reaction involving **39** gave the best coupling yield (58%), while the brominated isoquinoline **40** with a methoxy group in C6 position were inactive in the coupling reaction. The X-ray quality crystal of naphthylisoquinoline alkaloid **98** can be obtained, which may be attributed to the introduction of carbonyl group in the isoquinoline unit favouring the formation of H-bonds.

3.1.4 Suzuki coupling using naphthylboronic acid 37 towards monomeric naphthylisoquinoline alkaloids

The Suzuki cross-coupling reactions between naphthylboronic acid **37** and halogenated isoquinolines **39-42** were performed using the catalyst system of $Pd(PPh_3)_4/Na_2CO_3$/dioxane (**Table 3.3**).

Table 3.3 Suzuki coupling reaction to synthesize naphthylisoquinoline alkaloid **43**, **99-100**.

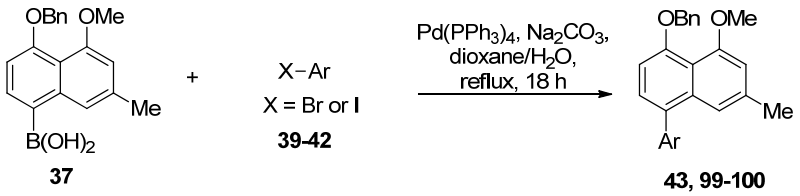

Entry	Ar	X	Isoquinoline	Product	Yield

1	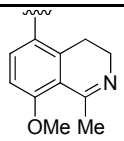	Br	**39**	**99**	57%
2	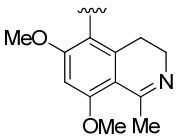	Br	**40**	**43**	trace
3	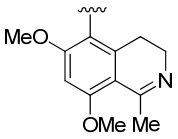	I	**41**	**43**	51%
4	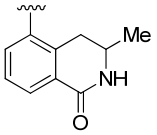	Br	**42**	**100**	75%

Naphthylisoquinoline **99** was obtained as a light brown solid in 57% (Entry 1) after purification by a triethylamine deactivated flash silica gel column chromatography (hexane/ethyl acetate: 60/40). Analysis of the ^{1}H NMR spectrum of **99** showed peaks located at the range of δ 7.66-7.33 ppm and δ 5.23 ppm which were assigned to the aromatic protons and the methylene protons respectively of the benzyl protecting group. Two *ortho*-split doublets (J = 8.5 Hz) at δ 7.27 ppm and δ 6.95 ppm were assigned to the aromatic protons H6 and H7 in the isoquinoline unit with the corresponding carbons assigned to the peaks at δ 133.6 ppm (C6) and δ 109.8 ppm (C7) in the ^{13}C NMR spectrum. The other two *ortho*-split doublets (J = 7.9 Hz) at δ 7.14 ppm and δ 6.89 ppm were assigned to the aromatic protons ArH2 and ArH3 in the naphthyl ring with the corresponding carbons assigned to the peaks at δ 128.2 ppm (ArC2) and δ 107.2 ppm (ArC3) in the ^{13}C NMR spectrum. 2D NMR spectroscopy (gCOSY, gHSQC and gHMBC) were used to assign the two methoxy groups and two methyl groups:

Ar-OCH_3 (δ 3.95 ppm) and 8-OCH_3 (δ 3.94 ppm), 1-CH_3 (δ 2.55 ppm) and Ar-CH_3 (δ 2.34 ppm). Analysis of EI mass spectrum of **99** showed a peak at *m/z* 451, assigned as the molecular ion, further confirming the presence of the compound **99**.

Similar to the reaction between **38** and **40** described in section **3.1.3**, the Suzuki coupling reaction involving less reactive brominated isoquinoline **40** gave the desired **43** in trace amount only (Entry 2). The more reactive iodo isoquinoline **41** afforded the desired naphthylisoquinoline **43** in a much better yield of 51% (Entry 3). By the same reaction sequence, naphthylboronic acid **37** and brominated isoquinoline **42** gave naphthylisoquinoline **99** as a light brown solid in 75% (Entry 4).

X-ray quality crystals of **99** and **100** were developed by a slow recrystallization from a mixture of CH_2Cl_2 and hexane. The X-ray structures of naphthylisoquinoline alkaloid **99** and **100** are shown in **Figure 3.5** (see **Appendix 2.2** and **2.3** for X-ray crystallographic data). Both structures show the naphthyl ring and isoquinoline unit are distributed vertically to each other, which significantly reduced the steric hindrance of C5 position in the isoquinoline unit during the Suzuki cross-coupling reactions.

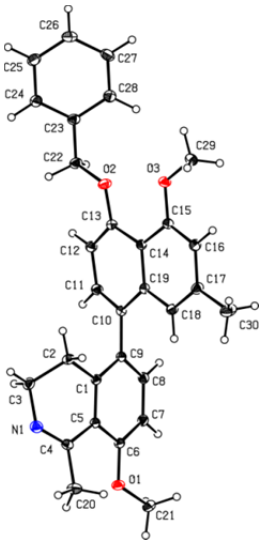

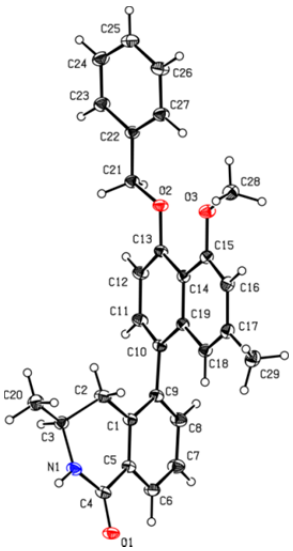

Figure 3.2 The crystal structures of naphthylisoquinoline alkaloid **99** (left) and **100** (right).

Comparing the four Suzuki cross-coupling reactions between naphthylboronic acid **37** and four different isoquinoline units (**39-41**), the reaction involving **42** gave the best coupling yield (75%), while the brominated isoquinoline **40** with a methoxy group in C6 position were inactive in the coupling reaction. Boronic acid **37** showed more reactivity in the Suzuki coupling comparing to boronic ester **38** (**Table 3.2** and **Table 3.3**).

3.2 Preparation of michellamine B analogues *via* oxidative dimerization

3.2.1 Oxidative dimerization background

There are a vast number of biaryl natural products with great structural divergence in nature. These biaryl molecules, with a broad range of biological activities including anti-HIV, anti-malaria, anti-cancer and anti-bacterial activities, are of great importance in medicinal chemistry. Numerous synthetic methods have been developed for introducing the biaryl linkage into organic compounds.[97,98] The popular Suzuki reaction and related organometallic methods employ specific functionality directly to the sites of reaction.[74] Oxidative coupling methods are also well known, where biaryl bonds are formed directly at unsubstituted aryl sites, which have been activated either by the aryl units themselves or by ring substituents. Compared to organometallic methods, oxidative coupling has a clear advantage for the formation of biaryl dimers, as it requires no prior functionalisation of the aromatic reaction sites.[97,98]

A great number of biaryl compounds have been prepared *via* oxidative dimerization, utilizing a broad variety of oxidizing agents including $Tl(CF_3CO_2)_3$,[99] di-*tert*-butyl peroxide,[100] $Pb(OAc)_4$[101] and Ag_2O.[45] As a necessary precondition for oxidative

coupling reactions, the aromatic portions have to be electron rich (ideally phenolic). Multiple products can be obtained from the presence of more than one reactive site in the phenolic precursor, depending on the steric and electronic demands.

The good activities against HIV of the dimeric naphthylisoquinolines michellamines have triggered numerous efforts to synthesize these complicated compounds. The initial strategy for preparing the dimeric naphthylisoquinolines from monomeric precursors is *via* a Suzuki-Miyaura coupling.[56] This multiple step synthesis involved five different types of reactions including bromination, borylation, cross coupling, protection and deprotection (**Scheme 3.4**).

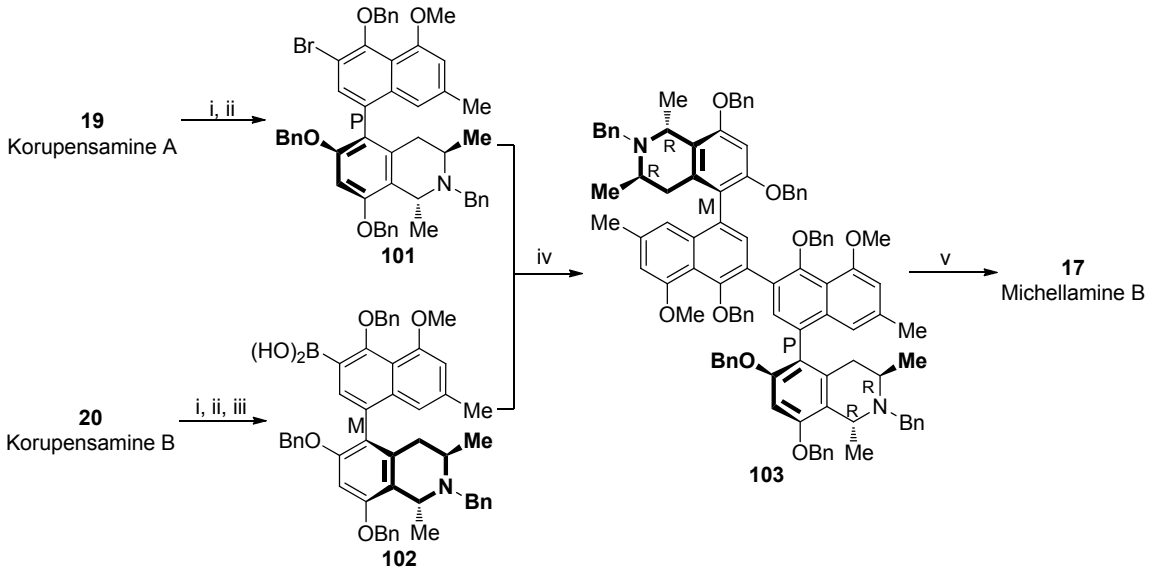

Scheme 3.4 Preparation of michellamine B *via* Suzuki-Miyaura coupling strategy. Reactions involved (i: protection; ii: bromination; iii: borylation; iv: Suzuki coupling; v: deprotection).

The introduction of oxidative dimerization strategy reduced the number of the reaction steps from five down to only one.[102] In this strategy, the phenolic monomeric naphthylisoquinoline can be directly transformed to the dimer in one step under the oxidative reagent such as $Pb(OAc)_4$. This simple reaction involved a deeply

violet-coloured intermediate diketone **104** (**Figure 3.3**) which can be reduced into desired dimer compound by column chromatography with dichloromethane/methanol as the eluent in good yield (**Scheme 3.5**).

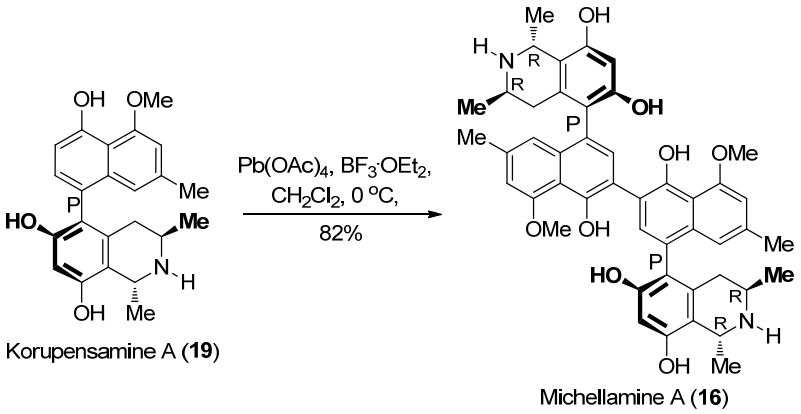

Scheme 3.5 Preparation of michellamine A *via* one-step oxidative dimerization strategy.[102]

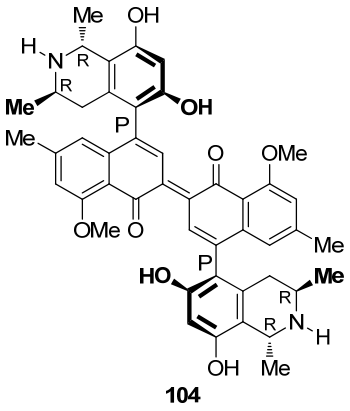

Figure 3.3 Structure of the intermediate diketone **104**.

3.2.2 Synthetic strategy towards the dimeric naphthylisoquinoline alkaloids

A two-step synthetic strategy towards the dimeric naphthylisoquinoline alkaloids is outlined in **Scheme 3.6**. The first deprotection reaction will afford the phenolic intermediate **105**. This electron rich phenolic group will significantly activate the

adjacent ArC3 position, allowing the subsequent dimerization reaction to occur. The following step is the direct dimerization reaction from the monomeric naphthylisoquinoline alkaloid **105** to afford dimeric product **106**.

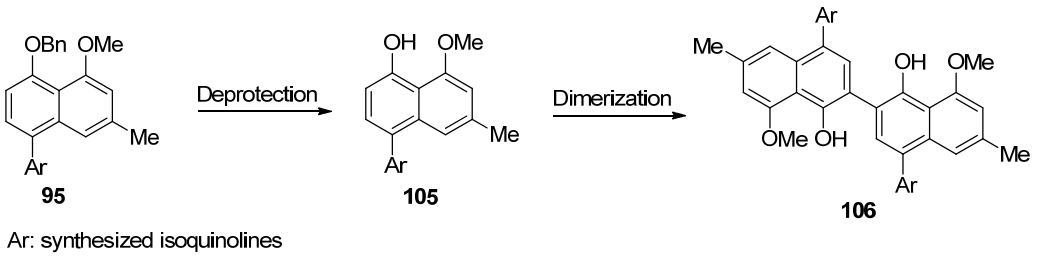

Scheme 3.6 Synthetic strategy towards dimeric naphthylisoquinoline alkaloids.

All the monomeric and dimeric naphthylisoquinoline alkaloids obtained in this strategy will be racemic and directly used for the biological activity testing without further separation. The active racemic compound can be further separated by chiral HPLC, leading to the active chiral dimeric naphthylisoquinoline. This strategy will significantly reduce the synthetic steps for michellamine B analogues compared to the Suzuki coupling strategy, as well as avoid synthesizing inactive compounds from the multiple-step synthesis.

3.2.3 Debenzylation of monomeric naphthylisoquinoline alkaloid

As oxidative coupling reactions required electron rich phenolic protons, debenzylation reactions of the monomeric naphthylisoquinoline alkaloids were performed. An efficient reduction system of $Pd/C/H_2$ in MeOH/ CH_2Cl_2 was utilised and the results of the deprotection reactions of the three monomeric naphthylisoquinoline alkaloids **43**, **100** and **99** under these conditions are summarized in **Table 3.4**.

Table 3.4 Preparation of unprotected naphthylisoquinolines.

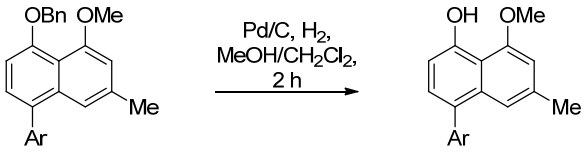

43, 99-100 **44, 107-108**

Entry	Ar	Reactant	Product	Yield
1	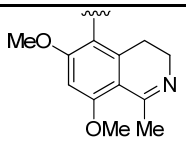	**43**	**44**	95%
2	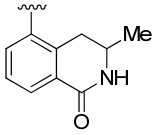	**100**	**107**	94%
3	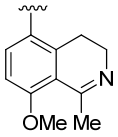	**99**	**108**	0

The debenzylation reaction was carried out under Pd/C/H_2 in MeOH/ CH_2Cl_2. After 2 h, TLC analysis indicated the completion of the reaction. Unprotected naphthylisoquinoline **44** was obtained as a brown solid in 95% yield (Entry 1) after a short flash silica gel column chromatography. In the ^{1}H NMR spectrum of **44**, the typical benzyl signals shown in reactant **43** located at the range of δ 7.32-7.62 ppm (aromatic ring) and δ 5.22 ppm ($ArCH_2$) cannot be observed, while a new peak located at δ 9.48 ppm, with a relative integration of one proton, was assigned to the generated phenolic hydroxyl group of **44**. The two *ortho*-split doublets (J = 7.8 Hz) at δ 7.04 ppm and δ 6.86 ppm were assigned to the aromatic protons ArH3 and ArH2 in the naphthyl ring with the corresponding carbons assigned to the peaks at δ 109.4 ppm (ArC2) and δ

129.9 ppm (ArC3) in the ^{13}C NMR spectrum. Analysis of EI mass spectrum of **44** showed a peak at *m/z* 451 assigned as the molecular ion, further confirming the completion of the reaction.

Applying the same conditions, the scaffold **100** produced the phenolic naphthylisoquinoline **107** as a brown solid in a high yield (94%) (Entry 2). The high resolution mass spectrum (ESI) for **107** showed a peak at *m/z* 348.1594 assigned as the molecular formula ($C_{22}H_{22}NO_3$, calcd. 348.1600). Analysis of the ^1H NMR spectrum showed a singlet located at δ 9.44 ppm assigned to the phenolic hydroxyl group, indicating that the benzyl protecting group was removed.

The same reaction conditions were applied to the reaction of **99**, however, no compound **108** was obtained from this reaction (Entry 3). Monitoring of MS spectra during the reaction indicated that the reduction of the C, N double bond occurred, leading to the compound **109** (**Scheme 3.7**), before the debenzylation reaction. Phenolic naphthylisoquinoline **109**, with a free amine group in the isoquinoline unit, was obtained in 92% yield. As the impact of this free amine group for biological activity of michellamine B analogues could be important information for the SAR study of this project, no other alternative debenzylation method was attempted.

The high resolution mass spectrum (ESI) for **109** showed a peak at *m/z* 364.1926 assigned as the molecular formula ($C_{23}H_{26}NO_3$, calcd. 364.1913), confirming the presence of **109**. As this phenolic naphthylisoquinoline with a free amine group (**109**) obtained relative low solubility in deuterated chloroform, deuterated methanol was used in NMR analysis and as expected no signal of phenol hydroxyl or amine can be observed in the ^1H NMR spectrum of **109**. The absence of the typical benzyl signals

shown in reactant **99** located at the range of δ 7.33-7.62 ppm (aromatic ring) and δ 5.23 ppm ($ArCH_2$) indicated that the benzyl protecting group was removed.

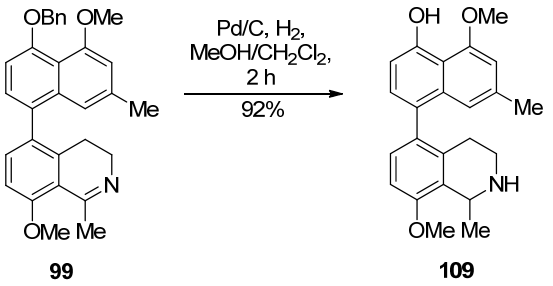

Scheme 3.7 The debenzylation reaction of naphthylisoquinoline **99**.

3.2.4 Synthesis of michellamine B analogues

In order to prepare the dimeric michellamine B analogues by the oxidative coupling method, a trial reaction using phenolic naphthyl **63** was first attempted. Treatment of phenolic naphthyl **63** in CH_2Cl_2 containing 0.2% NEt_3 with excessive Ag_2O gave the deep-violet coloured reaction mixture, due to the formation of diphenoquinone intermediate **110**. After 18 h stirring in air, the purple coloured diphenoquinone **110** was purified from a short silica gel column chromatography (CH_2Cl_2/methanol: 10/1), and then reduced using Pd/C/H_2, affording the dimeric compound **111** as a brown solid in 42% over two steps (**Scheme 3.8**).

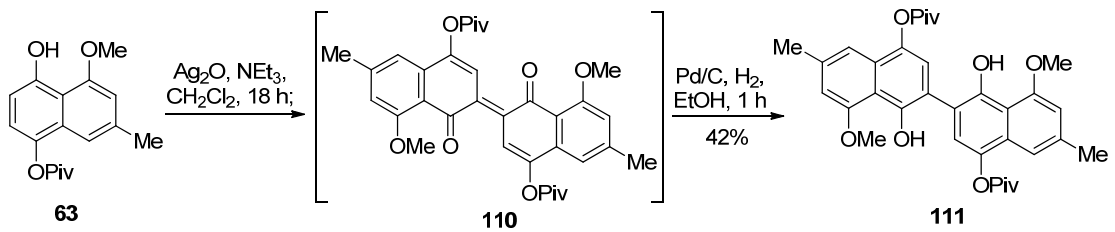

Scheme 3.8 Preparation of **111** by oxidative dimerization strategy.

Analysis of the ^{1}H NMR spectrum of **111** showed a singlet located at δ 9.59 ppm assigned to the phenolic hydroxyl groups. Three sets of singlets (δ 7.21 ppm, δ 7.13 ppm and δ 6.64 ppm) in the aromatic range were assigned to the six aromatic protons (ArH3 and ArH3′, ArH5 and ArH5′, ArH7 and ArH7′) respectively, indicating the completion of the dimerization. The high resolution mass spectrum (ESI) for **111** showed a peak at *m/z* 575.2647 assigned as the molecular formula ($C_{34}H_{39}O_8$, calcd. 575.2645), confirming the synthesis of the desired dimer product.

Besides Ag_2O, other oxidants were also attempted in the oxidative dimerization reaction of **63**, leading to either complete decomposition ($Pd(OAc)_4$) or no reaction ($Tl(CF_3COO)_3$).

The oxidative dimerization reactions of the phenolic naphthylisoquinolines (**44**, **107** and **109**) towards michellamine B analogues were performed using Ag_2O as oxidants and the results were summarized in **Table 3.5**.

Dimeric naphthylisoquinoline **112** (Entry 1) was obtained as a brown solid in 31% coupling yield from its corresponding phenolic monomer **44** after purified by flash silica gel column chromatography (CH_2Cl_2/methanol: 10/1). As this michellamine B analogue (**112**) was obtained relative low solubility in deuterated chloroform, deuterated methanol was used in NMR analysis and as a result no signal of phenolic hydroxyl could be observed in the ^{1}H NMR spectrum of **112**. Four sets of singlets located at δ 7.25 ppm, δ 6.84 ppm, δ 6.83 ppm and δ 6.65 ppm were assigned to the aromatic protons (ArH3 and ArH3′, ArH7 and ArH7′, H7 and H7′, ArH5 and ArH5′) in naphthyl rings and isoquinolines respectively, indicating the formation of dimer compound. gHMBC was used to assign three methoxy singlets δ 4.14 ppm (Ar8-OCH_3 and

Ar8′-OCH_3), δ 4.09 ppm (8-OCH_3 and 8′-OCH_3) and δ 3.85 ppm (6-OCH_3 and 6′-OCH_3). ^{13}C NMR spectrum analysis illustrated 24 peaks, consistent with the structure of **112**. The high resolution mass spectrum (ESI) of **112** showed peaks at *m/z* 781.3528 assigned as the molecular formula ($C_{48}H_{48}N_2O_8$, calcd. 781.3489), further confirming the presence of desired compound.

Table 3.5 Oxidative dimerization reaction to synthesize michellamine B analogues.

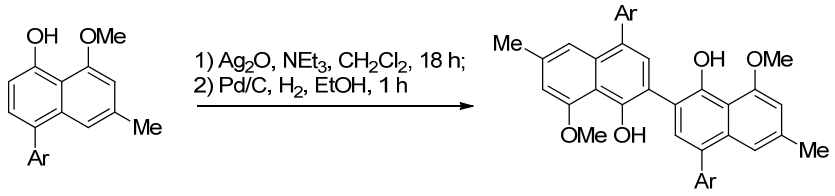

44, **107**, **109** **112-114**

Entry	Ar	Reactant	Product	Yield
1	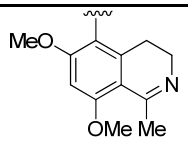	**44**	**112**	31%
2	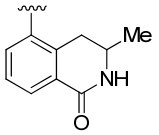	**107**	**113**	35%
3	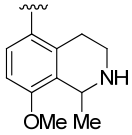	**109**	**114**	0

The dimeric compound **113** was obtained as a brown solid in 35% yield from monomeric naphthylisoquinoline **107** (Entry 2). The high resolution mass spectrum (ESI) of **113** showed peaks at *m/z* 693.2996 assigned as the molecular formula ($C_{44}H_{41}N_2O_6$, calcd. 693.2965), indicating the presence of desired compound.

Unfortunately, the direct oxidative coupling of phenolic naphthylisoquinoline **109** with free amine didn't succeed for the synthesis of **114**, leading to complex reaction mixtures instead (Entry 3). The dimerization reaction using $Pd(OAc)_4$ as an oxidising reagent was also attempted, since a high coupling yield was reported for the monomer containing free amine group using this oxidising system.[101] However, no desired compound was obtained again. The reason behind the unsuccessful formation was not clear and may be attributed to the free amine in the isoquinoline unit. Due to time constraints and insufficient material, the protection of amine in **109** and the following dimerization reaction could not be conducted.

A proposed mechanism for the oxidative dimerization of monomeric naphthylisoquinoline **105** is outlined in **Scheme 3.9**. The deprotonation of **105** by base first gives phenolate anion **115**. The one electron oxidation of **115** by oxidant then affords phenoxy radical **116** which can transform the radical to the *ortho* position, leading to **117**. The coupling between two phenoxy radical **117** generates intermediate **118** and subsequent keto-enol tautomerism affords the desired dimeric naphthylisoquinoline **119**. Over oxidization of **119** leads to diphenoquinone intermediate **106** which can be reduced back to **106** under appropriate condition.

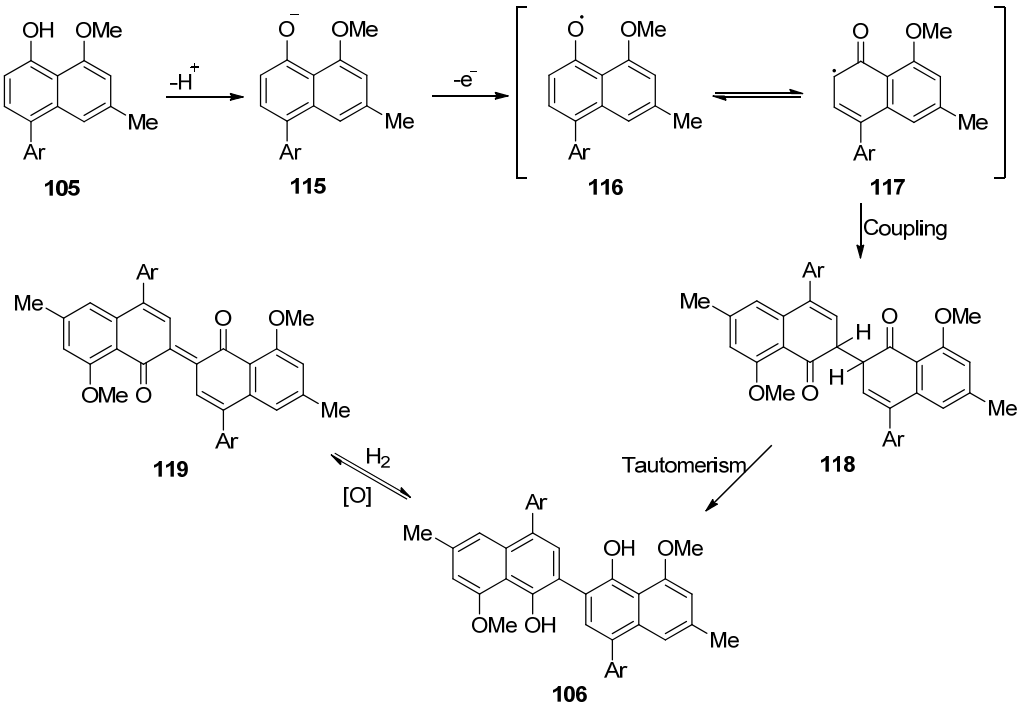

Scheme 3.9 Proposed mechanism of the oxidative dimerization reaction to prepare michellamine B analogues.

3.3 Conclusions

Three monomeric naphthylisoquinolines (**96-98**) with an ethyl ester substituent in the naphthyl ring were prepared in 44%-58% from the naphthylboronic ester (**38**) and halogenated isoquinolines (**39-42**) *via* Pd-catalyzed Suzuki cross-coupling, while three monomeric naphthylisoquinolines (**43**, **99-100**) with methyl substituent in the naphthyl ring were prepared 51%-75% from the naphthyl boronic acid (**37**) and halogenated isoquinolines (**39-42**). Iodo isoquinoline **41** proved to be more reactive in the Suzuki reaction comparing to the brominated isoquinoline **40**.

In order to activate the ArC3 position for the subsequent dimerization, three phenolic monomeric naphthylisoquinolines (**44**, **107** and **109**) were obtained 92%-95% *via* debenzylation reactions using Pd/C/H_2 reduction system, though the double bond

between C and N in the isoquinoline unit of **99** was reduced during the reaction, leading to **109** with free amine.

Two dimeric naphthylisoquinolines (**112** and **113**), as michellamine B analogues, were synthesized in 31%-35% from the phenolic monomeric naphthylisoquinolines (**44** and **107**) *via* a Ag_2O-induced oxidative dimerization strategy, while this oxidative coupling of naphthylisoquinoline **109** with free amine was unsuccessful for the corresponding dimer.

Chapter 4: Biological Activities Testing

4.1 General information

The synthesized monomeric and dimeric naphthylisoquinolines were evaluated against HIV-1 reverse transcriptase through *in vitro* screening using a Roche colorimetric RT assay kit (see **Chapter 7**). This assay was performed at University of Wollongong by the candidate.

The monomeric naphthylisoquinolines were also screened for their activity against the human cancer cell lines NCI-H187 (small cell lung cancer), KB (oral cavity cancer) and MCF-7 (breast cancer) as well as malaria (*Plasmodium falciparum*, K1 strain) and Vero cell (cytotoxicity). These assays were conducted by Dr. Rachada Haritakun at the National Center for Genetic Engineering and Biotechnology (BIOTEC), Thailand.

The monomeric naphthylisoquinolines were also tested for bacterial growth inhibition activity against a primary panel including *Escherichia coli*, *Klebsiella pneumoniae*, *Acinetobacter baumannii*, *Pseudomonas aeruginosa* and *Staphylococcus aureus* (MRSA). The biological testing was conducted by Dr. Alysha Elliott in the Worldwide Antibiotic Discovery Initiative (WADI), Brisbane.

4.2 HIV RT testing

4.2.1 Testing methods and principle

A colorimetric Reverse Transcriptase assay was used to quantitatively determine retroviral reverse transcriptase activity. The testing takes advantage of the ability of reverse transcriptase to synthesize DNA using the hybrid poly (A) × oligo $(dT)_{15}$ as a

template and primer. Digoxigenin- and biotin-labeled nucleotides in an optimized ratio are incorporated into the same DNA molecule by the RT activity. The detection and quantification of the synthesized DNA as a parameter for RT activity follows a sandwich ELISA protocol: biotin-labeled DNA binds to the surface of streptavidin-coated microplate modules. In the next step, an antibody to digoxigenin, conjugated to peroxidase (anti-DIG-POD), is added and bound to the digoxigenin-labeled nucleotides. In the final step, the peroxidase substrate ABTS is added. The peroxidase enzyme catalyzes the cleavage of the substrate to produce a coloured reaction product. The absorbance of the samples is determined using a microplate reader, and is directly correlated to the level of RT activity in the sample (**Figure 4.1**).[103]

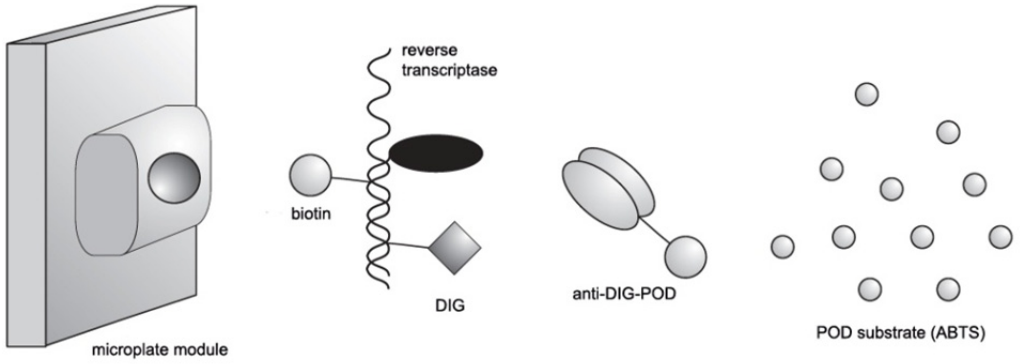

Figure 4.1 The testing principle of the colorimetric RT assay (modified from reference 103).

The percentage inhibition of RT is calculated by subtracting the absorbance value of negative control (sample that does not contain RT, *n*) from absorbance of Sample (v_i) and compared to the value from absorbance of positive control (sample that does not contain an inhibitor, *p*) subtracting absorbance of negative control (**Formula 4.1**).[103]

$$\%Inhibition = 100\% - (\frac{v_i - n}{p - n} \times 100\%)$$

Formula 4.1 The calculation of the percentage inhibition of RT in the colorimetric assay.

4.2.2 Testing results

The percentage inhibition of all compounds was obtained at the potential inhibitory concentrations of 50.0 μM and 10.0 μM. Subsequently, the six most promising compounds were selected and their inhibitory activity was obtained at additional four concentrations (100.0 μM, 75.0 μM, 25 μM and 5 μM).

IC_{50} values of these promising inhibitors were determined using linear regression via Excel software. Concentrations (X) and inhibitions (Y) were plotted and a straight line (linear regression) was fitted the data. IC_{50} value is then estimated using the fitted line, *i.e.*,

$$Y = a * X + b,$$

$$IC_{50} = (0.5 - b)/a.$$

The percentage inhibition of each sample was measured in duplicate experiments and the average values are reported in **Table 4.1.**

Table 4.1. The HIV-RT inhibitory results for the monomeric naphthylisoquinolines and dimeric naphthylisoquinolines.

Entry	Compound	#	% RT inhibition (μM)*						IC_{50}
			100	**75**	**50**	**25**	**10**	**5**	**(μM)**
1	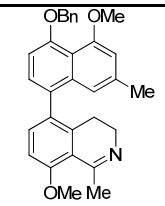	**99**	-	-	1.8	-	3.6	-	-
2	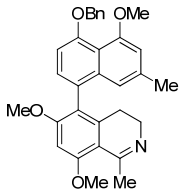	**43**	71.2	30.2	35.6	28.1	10.2	23.5	80.8
3	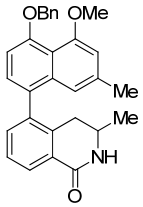	**100**	44.6	28.3	26.0	27.4	36.6	13.0	164.6
4	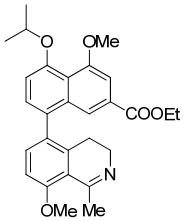	**96**	49.1	30.0	22.7	25.1	18.8	0	113.1
5	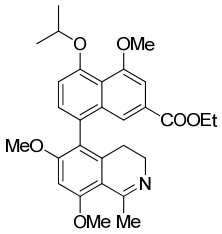	**97**	-	-	0	-	14.7	-	

Entry	Compound	#	% RT inhibition (μM)*						IC_{50}
			100	75	50	25	10	5	(μM)
6	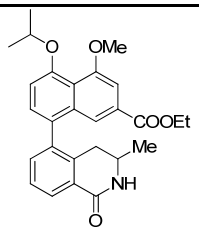	**98**	40.8	36.9	28.8	34.0	23.7	1.1	121.6
7	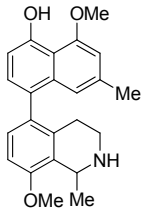	**108**	-	-	0	-	0	-	-
8	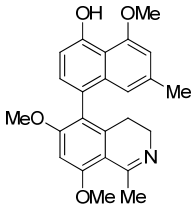	**44**	50.5	42.8	34.6	41.5	36.8	18.6	101.8
9	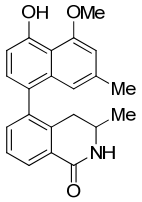	**107**	69.8	63.9	23.3	47.9	13.3	35.4	61.3
10	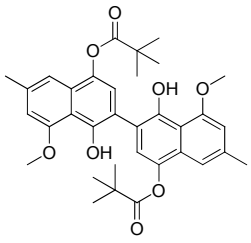	**111**	-	-	0	-	12.2	-	-

Entry	Compound	#	% RT inhibition (μM)*						IC_{50}
			100	75	50	25	10	5	(μM)
11	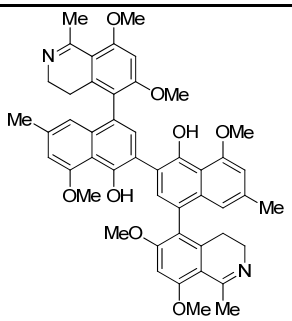	112	-	-	2.6	-	8.1	-	-
12	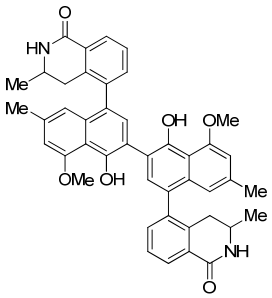	113	-	-	7.3	-	6.9	-	-

*Shown is the average % inhibition of duplicate experiments.

Analysis of the RT inhibition results for monomeric naphthylisoquinolines (Entries 1-9) revealed weak to mild activities against the enzyme with a percentage inhibition from 1.1% to 71.2%. The only exception was compound **108** (Entry 7) featuring both a phenol hydroxyl group and a free amine group which showed no activity against the enzyme. The activities of these monomeric naphthylisoquinolines (Entries 1-6, 8-9) are significantly higher than the inhibition activities reported for korupensamine analogues (**Figure 4.2**), while the korupensamines obtaining three phenol hydroxyl groups and a free amine group showed no anti-HIV activity.[44] The inactivity of **109** may be attributed to the structural similarity to korupensamines.

The introduction of carbonyl group in the isoquinoline unit increased the activity

significantly and all the monomeric naphthylisoquinolines obtaining this group (**100**, **98** and **107**) showed mild activities with IC_{50} values from 61.3 μM to 164.4 μM (Entry 3, 6 and 9). Compound **107** (Entry 9) featuring the phenol hydroxyl group and carbonyl group gave the best IC_{50} value (61.3 μM) among all the testing compounds.

Compound **43** (Entry 2) with benzyl protecting group and two methoxy groups in the isoquinoline unit obtained the highest inhibition (71.2%) at the concentration of 100 μM among all the testing compounds. Its deprotected product **44** (Entry 8) with phenol hydroxyl group exhibited slightly weaker activity with an IC_{50} of 101.8 μM reduced from 80.8 μM of **43**. These results showed that the removal of phenol hydroxyl groups both in the naphthyl ring and isoquinoline unit can increase the anti-HIV activity of the monomeric naphthylisoquinolines.

The impact of the ester group in the naphthyl ring to the activity was still unclear from the testing results. The activity increased dramatically from compound **99** (Entry 1) with methyl substituent to compound **96** (Entry 4) with ethyl ester substituent, whereas decreasing trends were observed from the other two pairs (**43** and **97**, Entry 2 and 5, **100** and **98**, Entry 3 and 6).

Weak inhibitory activity was observed for the dimeric naphthylisoquinolines (**112** and **113**, Entry 11 and 12) with a maximum inhibition of only 8.1% at the concentration of 10 μM, which is dramatically weaker compared to the reported EC_{50} value (10 μM) of michellamine B.[42] Comparing the structure of **112** and michellamine B (**Figure 4.2**), the only difference is the isoquinoline units. There are two hydroxyl groups and a free amine in the isoquinoline unit of the michellamine B, there are two methoxy groups and a C, N double bond in the isoquinoline unit of **112**, while there is a carbonyl group but

no other substituents in the isoquinoline unit of **113**. The introduction of carbonyl group in the isoquinoline unit of **113** showed no increase in the inhibition against the RT. The absence of hydroxyl groups and free amine in the isoquinoline unit decrease the activity against RT significantly comparing to the activity (EC_{50}: 10 μM) of michellamine B reported. These groups might be essential to bind with the enzyme as well as keep the hydrophilicity of the molecules.

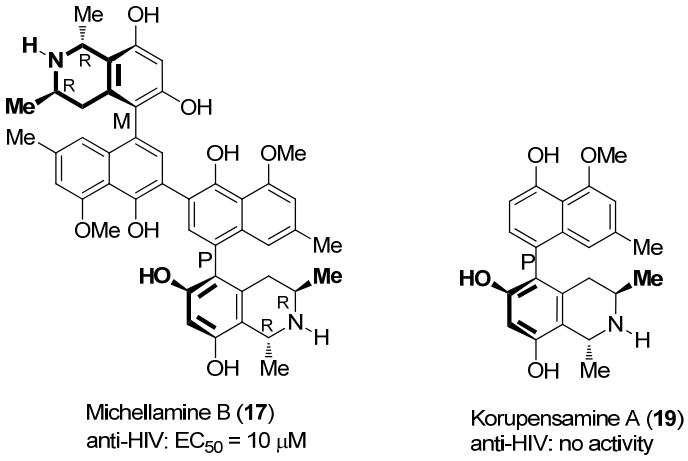

Figure 4.2 Chemical structures of michellamine B and korupensamine A.

The RT inhibitory activities of these testing compounds can be summarised in the following SAR points:

- Monomeric naphthylisoquinoline derivative with similar structure as korupensamines are not active against RT enzyme.

- The introduction of carbonyl group in the isoquinoline unit in monomeric naphthylisoquinolines increased the activity against HIV RT but decrease the activity of dimeric naphthylisoquinolines.

- The removal of phenol hydroxyl groups in isoquinoline unit can increase the

anti-HIV activity of monomeric naphthylisoquinolines but decrease the activity of dimeric naphthylisoquinolines.

- The ethyl ester group in the naphthyl ring of monomeric naphthylisoquinolines has impact in the activity, but the pattern was unclear.

4.3 Anti-malarial and cytotoxicity testing

The testing results of the monomeric naphthylisoquinolines against malaria (*Plasmodium falciparum*) and Vero cell (cytotoxicity) are summarized in **Table 4.2**.

Table 4.2 The IC_{50} values of the monomeric naphthylisoquinolines against *Plasmodium falciparum* and Vero cell.

Entry	Compound	#	***Plasmodium falciparum*** **(malaria, K1 Strain)** **IC_{50} (μg/mL)***	**Vero cell Cytotoxicity IC_{50} (μg/mL)[§]**
1	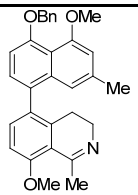	**99**	4.34	3.27
2	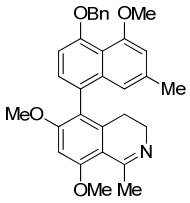	**43**	2.94	1.95
3	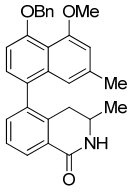	**100**	inactive	16.08

Entry	Compound	#	*Plasmodium falciparum* (malaria, K1 Strain) IC_{50} (μg/mL)*	Vero cell Cytotoxicity IC_{50} (μg/mL)[§]
4	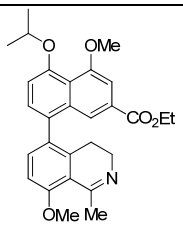	**96**	inactive	9.14
5	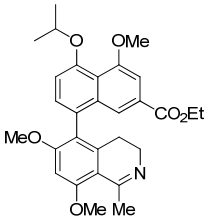	**97**	2.83	3.08
6	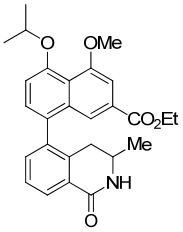	**98**	inactive	15.56
7	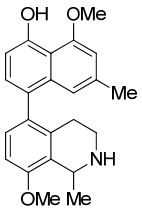	**109**	2.66	2.22
8	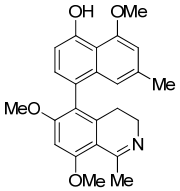	**44**	3.13	7.33
9	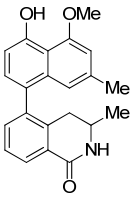	**107**	inactive	30.09

*IC_{50} of positive control: Dihydroartemisinine = 2.52 nM, Mafloquine= 0.0290 μM

§IC_{50} of positive control: Ellipticine = 1.83 mg/mL

From **Table 4.2**, monomeric naphthylisoquinolines (**99**, **43**, **97**, **109** and **44**) exhibited weak activity against *Plasmodium falciparum* (2.66-4.34 μg/mL) in comparison to the positive controls Dihydroartemisinine (2.52 nM) and Mafloquine (0.0290 μM), while compound **100**, **96**, **98** and **107** didn't show any activity. Analysis of the chemical structures of these inactive compounds revealed that all the compounds containing carbonyl group in the isoquinoline unit are inactive against *P. falciparum*.

Compound **109** (Entry 7), featuring a phenol hydroxyl group in the naphthyl ring and a free amine group in the isoquinoline unit, obtained the best anti-malaria activity with an IC_{50} value of 2.66 μg/mL. However, this result is still significantly weaker than the reported activity of korupensamine B (0.18 μg/mL, **Figure 4.3**) tested under similar conditions. Analysis of these two structures indicated that the absence of two phenol hydroxyl groups in the isoquinoline unit may decrease the activity of compound **109**.

All the testing compounds showed high cytotoxicity (1.95-30.09 μg/mL) compared with the positive control Ellipticine (1.83 mg/mL). The compounds with carbonyl group in the isoquinoline unit (**100**, **98** and **107**) exhibited less cytotoxicity with IC_{50} values up to 30.09 μg/mL (**107**, Entry 9) compared to the other tested compounds.

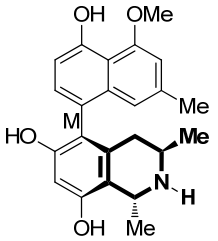

Korupensamine B (**20**)
0.18 μg/mL against *P. falciparum*

Figure 4.3 Chemical structure and anti-malaria activity of korupensamine B.

The anti-malaria and cytotoxicity activities of these derivatives can be summarised in the following SAR points:

- Monomeric naphthylisoquinolines containing a carbonyl group in the isoquinoline unit are inactive against *P. falciparum*, but have less cytotoxicity in Vero cell compared to the other tested compounds.

- The absence of phenol hydroxyl group in the isoquinoline unit may decrease the activity against *P. falciparum*.

- The introduction of C, N double bond in the isoquinoline unit decrease the anti-malaria activity.

4.4 Anti-cancer testing

A random screening testing of the monomeric naphthylisoquinolines were conducted and these compounds were tested against the three cell lines KB (oral cavity cancer), MCF-7 (breast cancer) and NCI-H187 (small cell lung cancer). All the compounds showed cell growth inhibition in micromolar concentrations. The testing results are summarised in **Table 4.3**.

Table 4.3 The IC_{50} values of the monomeric naphthylisoquinolines against three cancer cell lines KB (oral cavity cancer), MCF-7 (breast cancer) and NCI-H187 (small cell lung cancer).

Entry	Compound	#	KB (oral cavity cancer) IC_{50} (µg/mL)*	MCF-7 (breast cancer) IC_{50} (µg/mL)[§]	NCI-H187 (small cell lung cancer) IC_{50} (µg/mL)[£]
1	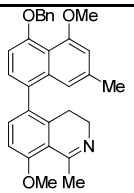	**99**	14.44	14.99	5.71
2	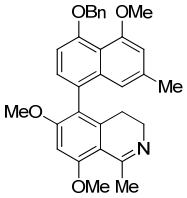	**43**	4.99	6.41	5.54
3	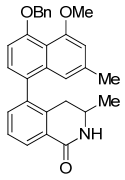	**100**	11.7	34.28	16.85
4	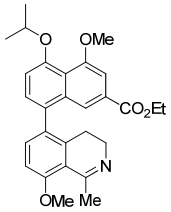	**96**	29.08	35.29	7.03
5	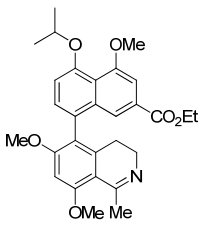	**97**	12.84	15.71	6.15

Entry	Compound	#	KB (oral cavity cancer) IC_{50} (μg/mL)*	MCF-7 (breast cancer) IC_{50} (μg/mL)[§]	NCI-H187 (small cell lung cancer) IC_{50} (μg/mL)[£]
6	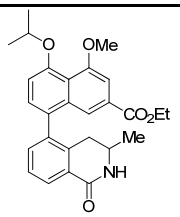	**98**	17.67	30.27	17.11
7	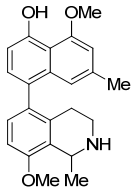	**109**	7.44	8.51	6.23
8	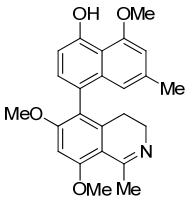	**44**	37.95	45.62	10.55
9	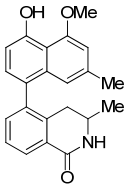	**107**	17.2	17.5	18.03

*IC_{50} of positive control: Ellipticine = 1.47 μg/mL, Doxorubicin = 0.600 μg/mL

[§]IC_{50} of positive control: Tamoxifen = 6.13 μg/mL, Doxorubicin = 7.51 μg/mL

[£]IC_{50} of positive control: Ellipticine = 2.47 μg/mL, Doxorubicin = 0.064 μg/mL

From **Table 4.3**, all the monomeric naphthylisoquinolines exhibited moderate to low activities against the three cell lines KB (oral cavity cancer), MCF-7 (breast cancer) and NCI-H187 (small cell lung cancer). Compound **43** (Entry 2) with two methoxy groups and a C, N double bond in the isoquinoline unit showed best activity against breast cancer among all the testing compounds with an IC_{50} value of 6.41 μg/mL which is slightly better than that of positive control Doxorubicin (7.51 μg/mL). The activities

against oral cavity cancer and small cell lung cancer of **43** (Entry 2) are also superior to those of other compounds with IC_{50} values of 4.99 μg/mL and 6.41 μg/mL respectively, which are both in the same order of magnitude as corresponding positive controls.

Compound **99** (Entry 1) with a methoxy group and a C, N double bond in the isoquinoline unit showed decreased activity in all three cell lines KB (14.44 μg/mL), MCF-7 (14.99 μg/mL) and NCI-H187 (5.71 μg/mL) comparing to **43** due to the absence of one methoxy group in isoquinoline unit.

Compound **109** (Entry 7) obtaining unprotected phenol and amine groups also exhibited moderate activities against all three cell lines, with an IC_{50} value of 7.44 μg/mL against oral cavity cancer, an IC_{50} value of 8.51 μg/mL against breast cancer and an IC_{50} value of 6.23 μg/mL against small cell lung cancer.

4.4 Anti-microbial testing

A high throughput screening testing for anti-bacterial activity of the monomeric naphthylisoquinolines were conducted. These compounds were tested for bacterial growth inhibition activity against a primary panel including *Escherichia coli*, *Klebsiella pneumoniae*, *Acinetobacter baumannii*, *Pseudomonas aeruginosa* and *Staphylococcus aureus* (MRSA). The MIC (Minimum Inhibitory Concentration) values of all the testing compounds were summarised in **Table 4.4**.

Table 4.4 Antimicrobial activity results of the monomeric naphthylisoquinolines.

Entry	Compound	#	GN_001 *E. coli* ATCC 25922	GN_003 *K. pneumoniae* ATCC 700603	GN_034 *A. buamanii* ATCC 19606	GN_042 *P. aeruginosa* ATCC 27853	GP_020 *S. aureus* ATCC 43300 (MRSA)
			MIC (µg/mL)				
1	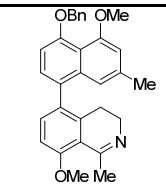	**99**	>32	>32	>32	>32	32
2	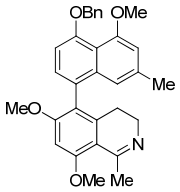	**43**	>32	>32	>32	>32	16
3	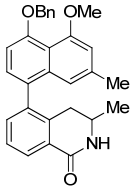	**100**	>32	>32	>32	>32	>32
4	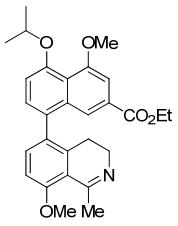	**96**	>32	>32	>32	>32	>32
5	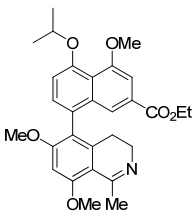	**97**	>32	>32	>32	>32	>32

Entry	Compound	#	GN_001 *E. coli* ATCC 25922	GN_003 *K. pneumoniae* ATCC 700603	GN_034 *A. buamanii* ATCC 19606	GN_042 *P. aeruginosa* ATCC 27853	GP_020 *S. aureus* ATCC 43300 (MRSA)
			MIC (µg/mL)				
6	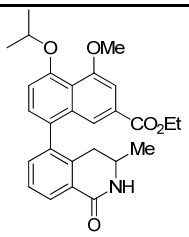	**98**	>32	>32	>32	>32	>32
7	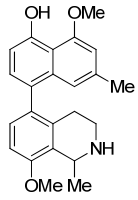	**109**	>32	>32	>32	>32	32
8	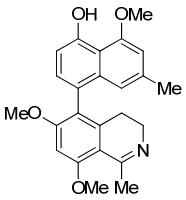	**44**	>32	>32	>32	>32	>32
9	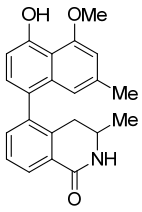	**107**	>32	>32	>32	>32	>32
10	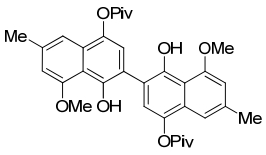	**92**	>32	>32	>32	>32	>32

Table 4.5 MIC values of postive controls.

Entry	Compound	**GN_001** ***E. coli*** **ATCC 25922**	**GN_003** ***K. pneumoniae*** **ATCC 700603**	**GN_034** ***A. buamanii*** **ATCC 19606**	**GN_042** ***P. aeruginosa*** **ATCC 27853**	**GP_020** ***S. aureus*** **ATCC 43300 (MRSA)**
		MIC (μg/mL)				
1	Colistin	0.06	≤0.015-0.03	0.03	≤0.25	-
2	Polymyxin B	0.03	≤0.015	≤0.015	≤0.25	-
3	Vancomycin	-	-	-	-	0.5-1
4	Daptomycin	-	-	-	-	1

From **Table 4.4**, all the monomeric naphthylisoquinolines showed no activities against *Escherichia coli*, *Klebsiella pneumoniae*, *Acinetobacter baumannii* and *Pseudomonas aeruginosa*, while three compounds (**99**, **43** and **109,** Entry 1, 2 and 7) without carbonyl group and ester group exhibited low activity against *Staphylococcus aureus* with MIC values from 16 to 32 μg/mL (Entry 1, 2 and 7).

4.5 Conclusions

The synthesized monomeric and dimeric naphthylisoquinolines were tested *in vitro* against the HIV-1 RT enzyme showing weak to moderate inhibitory activities. The monomeric naphthylisoquinolines exhibited better anti-HIV activity than korupensamines with percentage inhibition from 1.1% to 71.2%. Compound **107** obtaining phenol and carbonyl group demonstrated best activity with an IC_{50} value of

61.3 μM, while **43** with benzyl protecting group obtained the highest inhibition (71.2%) at the concentration of 100 μM among all the testing compounds. Mild inhibitory activity was observed for the dimeric naphthylisoquinolines (**112** and **113**) with a maximum inhibition of only 8.1% at the concentration of 10 μM.

Five monomeric naphthylisoquinolines (**99**, **43**, **97**, **109** and **44**) exhibited moderate activity against *Plasmodium falciparum* (2.66-4.34 μg/mL). Compound **97**, featuring two methoxy groups in the isoquinoline unit and an ester group in naphthyl ring, obtained best anti-malaria activity with an IC_{50} value of 5.76 μM. All the testing compounds showed high cytotoxicity (1.95-30.09 μg/mL).

All the monomeric naphthylisoquinolines exhibited moderate to low activities against the three cell lines KB (oral cavity cancer), MCF-7 (breast cancer) and NCI-H187 (small cell lung cancer). Moderate activity against small cell lung cancer was obtained for **99** (IC_{50} = 5.71 μg/mL), whereas compound **43** with two methoxy groups in the isoquinoline unit showed best activity against breast cancer among all the testing compounds with an IC_{50} value of 6.41 μg/mL.

All the monomeric naphthylisoquinolines showed no activities against *Escherichia coli*, *Klebsiella pneumoniae*, *Acinetobacter baumannii* and *Pseudomonas aeruginosa*, while three compounds (**99**, **43** and **109**) exhibited low activity against *Staphylococcus aureus* with MIC values from 16 μg/mL to 32 μg/mL.

Chapter 5: Design and Synthesis of Analogues of Marine Bioluminescent Substrate Coelenterazine

In a separate project, analogues of marine bioluminescent substrate coelenterazine were designed, synthesized and used as the inhibitors to bind with the bioluminescent coelenterazine-utilizing luciferase. As the exact bioluminescent enzymatic mechanism has yet to be uncovered due to the instability of coelenterazine, to elucidate the enzymatic mechanism, it is of significant importance to obtain structural information of the luciferases binding with either the substrate, or an inhibitor that closely resembles the substrate. Herein, these synthesized coelenterazine-like inhibitors will be used for future crystallography work and for the study of the luciferase's enzymatic kinetics.

5.1 Background of coelenterazine and its analogues

5.1.1 Coelenterazine and its properties

Bioluminescence, a beautiful light emission phenomenon from living organisms, has captured the attention of scientists, leading to the discovery of the natural substrate coelenterazine (**120**, **Figure 5.1**) in the jellyfish *Aequorea victoria*, amongst others.[104,105] This imidazo[1,2-*a*]pyrazine-based chromophore was isolated and its structure was determined in 1974.[106]

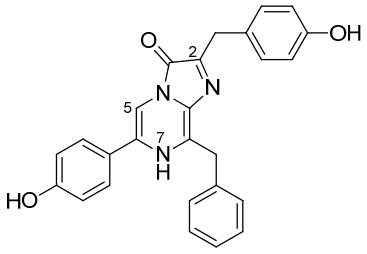

Coelenterazine (**120**)

Figure 5.1 Chemical structure of coelenterazine.

Coelenterazine (**120**) plays a key role in bioluminescence by binding covalently to luciferase which is activated to bioluminescence by reaction with calcium ions.[107] This sensitive system has been used for the detection of calcium ions in cells.[107] Luciferase is also widely employed in molecular biology as a reporter gene in cell culture experiments and small animal imaging due to its ability to emit light.[108]

Apart from its light-emitting property, further interest in this heterocyclic compound has arisen due to discovery of its potent antioxidant properties[109] with reports of chemical reactivity assays with singlet oxygen,[110] radical anion superoxide[111] and the inhibition of lipid peroxidation.[112,113] These results show that the imidazo[1,2-*a*]pyrazine-based coelenterazine derivatives are a new family of antioxidants.[114-117] These diverse applications make coelenterazine a useful molecule for both medical and molecular biological use.

5.1.2 Synthesis of coelenterazine

Coelenterazine (**120**) was synthesized in 1989[118] by a condensation between an α-oxo aldehyde and a fully substituted 2-aminopyrazine; the pyrazine was prepared by another condensation reaction between an α-amino nitrile and an α-nitroso ketone.[118] On the basis of this pioneering work, improvements to this strategy using organometallic coupling developed a more flexible and convergent preparation.[119-123] Another attractive synthetic approach towards coelenterazine is *via* a biomimetic and modular peptide synthesis method, which is based on a double intermolecular dehydration.[124]

5.1.3 Coelenterazine-like imidazo[1,2-*a*]pyridine-based inhibitor

Coelenterazine (**120**) is not stable and reacts with O_2 to emit light catalysed by luciferase.[125] In this reaction, the substrate coelenterazine firstly binds reversibly to the

enzyme, forming the enzyme-substrate complex (Michaelis complex). The enzyme then catalyzes the chemical step and releases the product. In order to characterize the luciferase bioluminescent mechanism, it is essential to obtain the crystal structure of Michaelis complex in this transition state. However, the instability of coelenterazine and the rapid catalytic rate of this bioluminescence reaction has made it extremely difficult to observe and characterize the Michaelis complex.

An enzyme inhibitor is a molecule that binds to an enzyme and prevents it from working in the normal manner. An ideal inhibitor will closely resemble enzyme substrate in structure and be chemically stable. Due to the structural similarity, such an inhibitor can bind to the enzyme leading to inhibitor-enzyme Michaelis complex without transforming to the product, giving the chance to observe the bindings in the active sites of the enzyme.[126]

The acidic proton in N7 position in the pyrazine ring of coelenterazine (**120**, **Figure 5.1**) enable this structure transform to several resonant structures, and the proposed first step in the mechanism of the bioluminescent reaction of coelenterazine is the deprotonation of this acidic proton.[127] Therefore, in order to trap the Michaelis complex from transforming to the products, the design of the potential inhibitor should remove this acidic proton in N7 position. Eligible scaffolds, such as imidazopyridine, imidazooxazine and imidazopyridazine, became the candidates of the inhibitors (**Figure 5.2**).

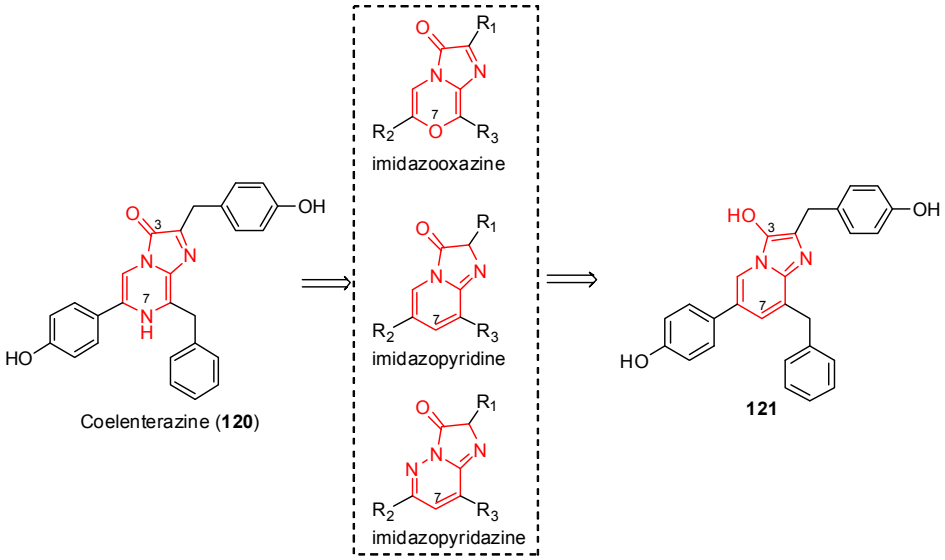

Figure 5.2 Structural analogues of the coelenterazine.

The imidazo[1,2-*a*]pyridine ring system was first introduced by Tschitschibabin[128] in 1925. The pharmacological properties of this skeleton are currently the object of renewed interest as illustrated by the number of patents containing this scaffold.[129] The synthesis of 3-hydroxyimidazo[1,2-*a*]pyridine derivatives was first achieved *via* a condensation of 2-aminopyridine 1-oxide and phenacyl bromides,[130] before a more efficient methodology using 2-aminopyridine and phenylglyoxals for the condensation was developed.[131-133] The imidazo[1,2-*a*]pyridine analogue **121** was selected as the potential inhibitor target in this project after the evaluation of the synthetic feasibility.

5.2 Synthetic strategy towards imidazo[1,2-*a*]pyridine-based inhibitor 121

The synthesis of coelenterazine-like inhibitor **121** involves a key step to prepare the central aromatic ring 3-hydroxyimidazo[1,2-*a*]pyridine **123** (**Figure 5.3**). It is reported that the structurally similar ring imidazo[1,2-*a*]pyrazine **122** (**Figure 5.3**) can be synthesized from a condensation between 2-aminopyrazine and benzylglyoxal. Compared to the extensively studied imidazo[1,2-*a*]pyrazine (**122**), the

imidazo[1,2-*a*]pyridine heterocycle is still poorly investigated, especially the 3-hydroxyimidazo[1,2-*a*]pyridine variation (**123**). There is no report about the condensation between 2-aminopyridine and benzylglyoxals, but this strategy will be adopted towards the synthesis of 3-hydroxyimidazo[1,2-*a*]pyridine derivatives in this project.

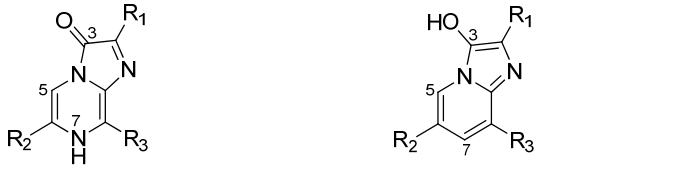

imidazo[1,2-*a*]pyrazine (**122**) 3-hydroxylimidazo[1,2-*a*]pyridine (**123**)

Figure 5.3 Structures of imidazo[1,2-*a*]pyrazine and imidazo[1,2-*a*]pyridine.

The proposed synthesis of imidazo[1,2-*a*]pyridine-based inhibitor **121** is illustrated in **Scheme 5.1**. Two key precursors, 2-aminopyridine **126** and benzylglyoxal **129**, are required for the final condensation to prepare **121**. The synthesis of **126** will start from the commercially available 2-aminonicotinic acid **124**. Bromination followed by a two-step Weinreb ketone synthesis, should produce intermediate **125**. With a subsequent Suzuki coupling and Wolff-Kishner reduction will give the 2-aminopyridine **126**. Synthesis of benzylglyoxal **129** will require a bromination and oxidation from the commercially available 1-(4-hydroxyphenyl)propan-2-one (**127**). The final condensation between 2-aminopyridine and benzylglyoxal will afford the desired imidazo[1,2-*a*]pyridine **121**.

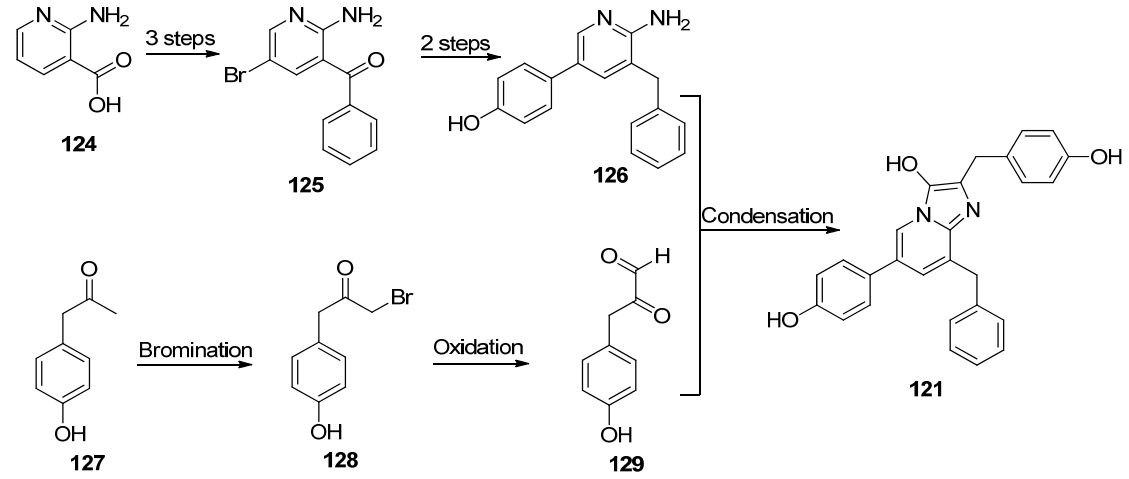

Scheme 5.1 Synthetic strategy towards imidazo[1,2-*a*]pyridine **121**.

Imidazo[1,2-*a*]pyridine **121** will be used to bind with luciferase for the study of its bioluminescent catalytic mechanism. The potential antioxidant activity of this coelenterazine-like compound (**121**) will also be evaluated.

5.3 Synthesis of coelenterazine analogues

5.3.1 Synthesis of 2-aminopyridine derivative 126

Starting from commercially available 2-aminonicotinic acid (**124)**, bromination with Br_2 in glacial acetic acid provided **130** as a white crystalline needle in 97% yield after recrystallized from methanol (**Scheme 5.2**).[134] Analysis of ^{1}H NMR of **130** showed two *meta*-split doublets (J = 2.5 Hz) at δ 8.44 ppm and δ 8.33 ppm assigned to the aromatic protons ArH4 and ArH6, confirming that the bromination had occurred in ArC5 position.

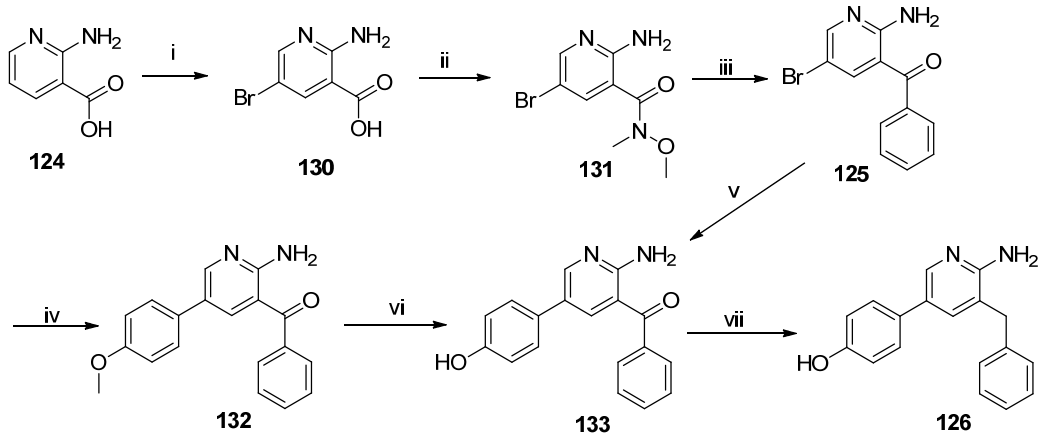

Scheme 5.2 Reagents and conditions: (i) Br_2, HOAc, rt, 20 h, 97%; (ii) $CH_3NHOCH_3 \cdot HCl$, HBTU, HOBt, DMF, rt, 5 h, 74%; (iii) C_6H_5MgBr, −50 °C, THF, 5 h, 95%; (iv) 4-methoxyphenylboronic acid, $Pd(dppf)Cl_2$, $NaHCO_3$, toluene, reflux, 12 h, 85%; (v) EtSH, NaH, DMF, 100 °C, 15 h, 82%; (vi) 4-hydroxyphenylboronic acid, $PdCl_2(PPh_3)_2$, Na_2CO_3, 1,4-dioxane, reflux, 20 h, 91%; (vii) $NH_2NH_2 \cdot H_2O$, KOH, ethanediol, 240 °C, 3 h, 86%.

Conversion of this compound into the desired phenylmethanone **125** required a two-step Weinreb ketone synthesis involving the preparation of Weinreb amide **131** and a subsequent Grignard reaction. Three different coupling reactions were attempted to obtain 2-amino-5-bromo-*N*-methoxy-*N*-methylnicotinamide (**131)**. Reaction of 1-ethyl-3-(3-dimethylaminopropyl)carbodiimide hydrochloride (EDC·HCl) with 1-hydroxybenzotriazole hydrate (HOBt) resulted in a 24% yield of **131**. The use of benzotriazol-1-yl-oxytripyrrolidinophosphonium hexafluorophosphate (PyBOP) gave a better yield of 46%, while HOBt and *N*,*N*,*N*′,*N*′-tetramethyl-*O*-(1*H*-benzotriazol-1-yl)uronium hexafluorophosphate (HBTU) provided the best outcome of 74% (**Table 5.1**).

Table 5.1 Attempted reaction conditions for coupling reaction.

	Coupling reagents	Solvent	Yield
1	EDC·HCl, HOBt, *N,N*-diisopropylethylamine	DMF	24%
2	PyBOP, *N*-methylmorpholine	CH_2Cl_2	46%
3	HOBt, HBTU, *N,N*-diisopropylethylamine	DMF	74%

The reaction of **131** with phenylmagnesium bromide afforded the ketone **125** as a yellow crystalline solid in 95% yield.[134] Analysis of the ^{13}C NMR spectrum of **125** showed absence of methyl (δ 33.4 ppm) and methoxy peaks (δ 61.5 ppm), indicating the synthesis of the desired **125**.

In order to obtain the novel biaryl intermediate **133**, a direct Suzuki coupling of **125** with 4-methoxyphenylboronic acid using $Pd(dppf)Cl_2$ as a catalyst gave the novel biaryl intermediate **132** in 85% yield, followed by a demethylation with sodium ethanethiolate which provided **133** as a pale yellow solid in 82% yield. However, the more direct Suzuki coupling of **125** with 4-hydroxyphenylboronic acid to give compound **133** was also investigated. Comparing to the two-step synthesis above, a higher yield of 91% was achieved group during this Suzuki reaction involving active phenol hydroxyl group. This improved method not only avoided the use of the unpleasant reagent ethanethiol, but also reduced one synthetic step and increased overall yield from 70% (with two steps) to 91%.

Analysis of the EI mass spectrum of **133** showed a peak at *m/z* 290 assigned as the molecular ion of **133**. In the ^1H NMR spectrum, a singlet at δ 9.46 ppm, with the relative integration of one, was assigned to the phenol hydroxyl proton. Two singlets at

δ 8.50 ppm and δ 7.60 ppm were assigned to the aromatic protons ArH4 and ArH6 in the pyridine ring respectively. Analysis of the ^{1}H NMR spectrum of **133** showed peaks located at δ 7.30 ppm and δ 6.79 ppm which were assigned to the aromatic protons of phenol.

Finally, Wolff-Kishner reduction of **133** using hydrazine hydrate and KOH furnished the new aminopyridine derivative **126** as a white solid in 86% yield after separation using flash silica gel column chromatography (hexane/ethyl acetate: 50/50) (**Scheme 5.2**). Analysis of ^{1}H NMR spectrum of **126** showed a peak at δ 4.02 ppm assigned to the methylene ($ArCH_2$) generated from the reduction, with the corresponding carbon assigned to the peak at δ 34.5 ppm in the ^{13}C NMR spectrum, indicating the completion of the reaction. Analysis of the EI mass spectrum of **126** showed a peak at *m/z* 276 and was assigned as the molecular ion.

5.3.2 Synthesis of benzylglyoxal

5.3.2.1 Attempted reactions towards α-bromoketone intermediate

The synthesis of benzylglyoxal requires a key α-bromoketone intermediate and there are three different reported methods to prepare it.[120,122,135]

The direct bromination from 1-(4-((*tert*-butyldimethylsilyl)oxy)phenyl)propan-2-one (**134**) was first attempted to afford the target intermediate **137**, as a similar reaction was reported (**Scheme 5.3**).[135] However, a mixture of dibrominated (**136**) and two monobrominated (**135** and **137**) products was obtained, as identified by EI mass spectrometry and ^{1}H NMR spectral analysis. TLC analysis of the reaction mixture showed only a single spot due to the similar polarity, indicating that compound **137** is not able to be separated from the mixture with the other two species.

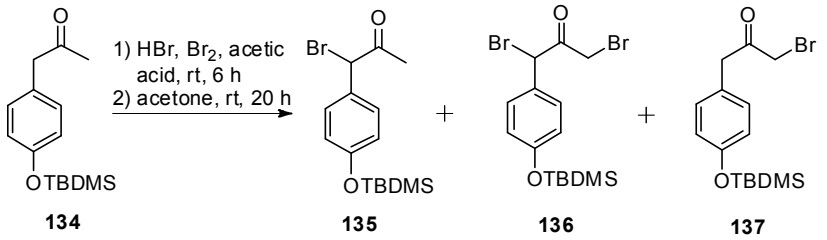

Scheme 5.3 Attempted direct bromination of phenylpropan-2-one **134**.

The second reported method for the synthesis of **140** was an organozinc method[122] and was then attempted (**Scheme 5.4**). The addition of 4-(chloromethyl)phenyl acetate **138** to commercial Zn dust in the presence of LiCl at 25 °C afforded the organozinc complex within 24 h. Trapping with bromoacetyl chloride after transmetalation with CuCN·2LiCl furnished the desired α-bromoketone intermediate **140**. However, a low yield (12%) was obtained for **140** from this reaction. A homo-coupling occurred during the reaction producing the side product **139** in 75%.

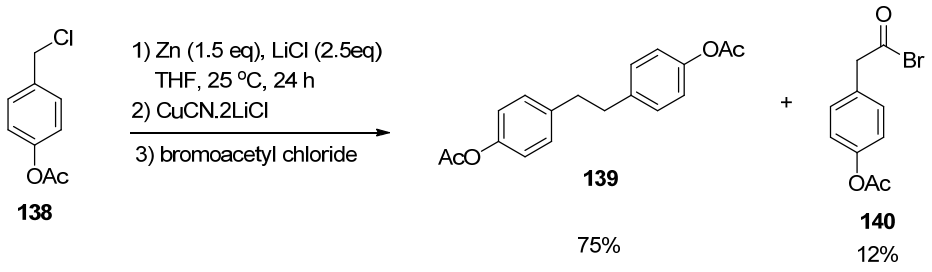

Scheme 5.4 Attempted organozinc reaction towards the α-bromoketone intermediate **140**.

The third reported method[120] required use of the sensitive and explosive diazomethane and was not attempted, as a simpler, more practical synthetic route, involving a ring-opening reaction of epichlorohydrin, was designed – this is discussed in the following section.

5.3.2.2 Synthesis of benzylglyoxal *via* an epichlorohydrin ring-opening strategy

This designed synthetic route (**Scheme 5.5**) has not previously been used to synthesize the benzylglyoxal fragment required, however, all the proposed methodologies involved are reliable.

A grignard reagent was firstly prepared from the *tert*-butyldimethylsilyl protected 4-bromophenol **141**, followed by a ring-opening reaction of commercially available epichlorohydrin to afford **143** (80%).[136] Dess-Martin periodinate oxidation of the alcohol **143** gave the ketone **145** (91%),[137] which was then treated with LiBr in acetone yielding α-bromoketones **137**.[138] The reactive α-bromoketone **137** was treated with $AgNO_3$ in acetonitrile overnight, which gave the nitrate ester **148** as a yellow oil in 89% yield. The esterification reaction from **145** directly to nitrate ester **148** was also attempted under the same condition described above, however no reaction was observed. Finally, reaction of **148** with NaOAc in DMSO at room temperature for one hour furnished the novel 4-hydroxylbenzylglyoxal **129** as a colourless solid in 87% yield (**Scheme 5.5**).[122]

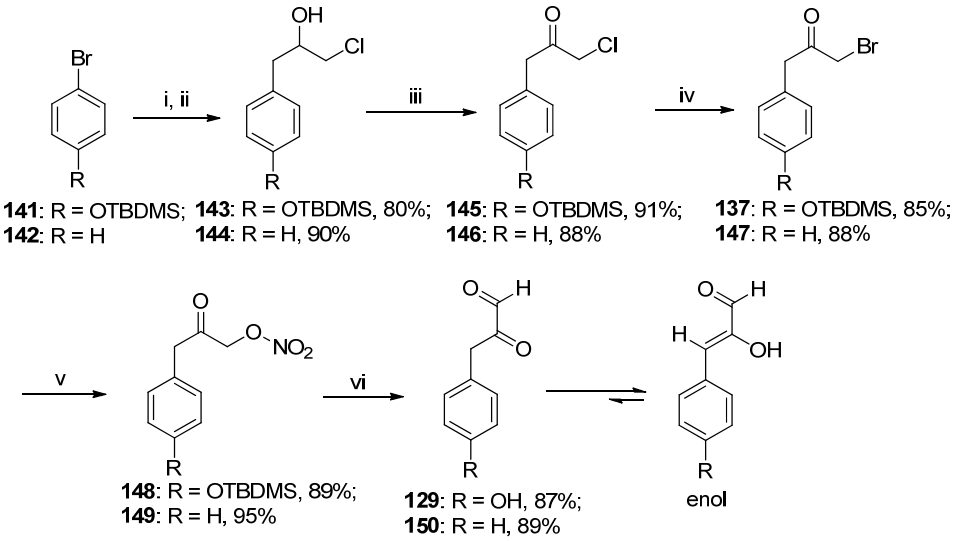

Scheme 5.5 (i) Mg, THF, rt, 2 h; (ii) epichlorohydrin, THF, 0 ^{o}C, 8 h; (iii) Dess-Martin reagent, CH_2Cl_2, rt, 12 h; (iv) LiBr, acetone, rt, 24 h; (v) $AgNO_3$, MeCN, rt, 18 h; (vi) NaOAc, DMSO, rt, 1 h.

The ^{1}H NMR spectrum of **129** displayed a broad singlet at δ 9.45 ppm assigned to the alkene hydroxyl group with the corresponding carbon assigned to a resonance at the relatively low shift of δ 149.2 ppm in the ^{13}C NMR spectrum, clearly indicating that **129** existed entirely in the enol form.

By the same reaction sequence, benzylglyoxal **150**, without the phenolic hydroxyl group, was prepared with an overall yield of 59%. Benzylglyoxal **150** was spectroscopically identical to that reported in the literature.[122]

5.3.3 Condensation reaction between 2-aminopyridines and benzylglyoxals

The key condensation reaction between the 2-aminopyridines and benzylglyoxals has not been previously reported. Therefore, the condensation of aminopyridine **126** and benzylglyoxals **129** was initially attempted using 1,4-dioxane as the solvent with a catalytic amount of hydrochloric acid at room temperature under an N_2 atmosphere, however no reaction was observed. Increasing the temperature to reflux gave a new,

highly fluorescent compound as indicated by TLC analysis (UV light visualisation at 365 nm). Upon reaction quenching with water, the resulting brown precipitate was filtered and recrystallization from methanol/ether afforded the imidazo[1,2-*a*]pyridine **121** as a yellow solid in 62% yield (**Scheme 5.6**). Coelenterazine analogue **121** were both air- and light-sensitive, and had low solubility even in methanol.

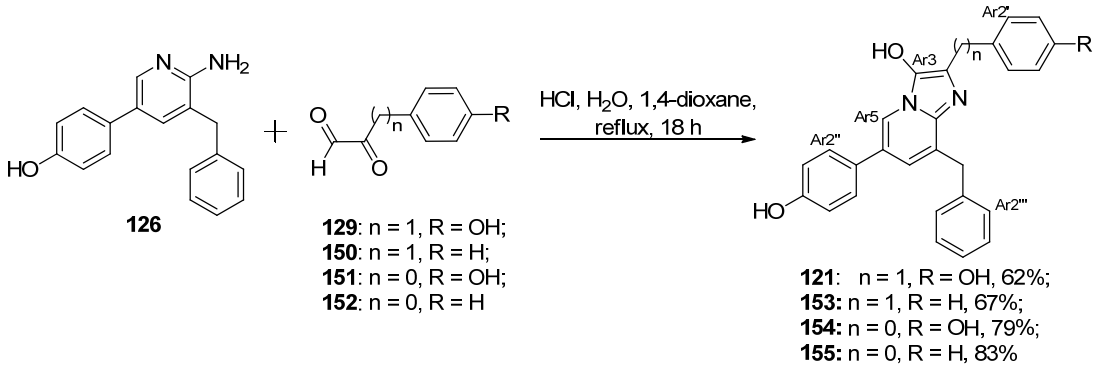

Scheme 5.6 Condensation of aminopyridine and arylglyoxals to produce the imidazo[1,2-*a*]pyridine-based coelenterazine derivatives.

The high resolution mass spectrum (ESI) for **121** showed a peak at *m/z* 423.1706 assigned as the molecule formula ($C_{27}H_{23}N_2O_3$, calcd. 423.1709), indicating the presence of **121**. Analysis of the ^{1}H NMR spectrum of **121** (**Figure 5.4**) showed two singlets at δ 4.21 ppm and δ 4.02 ppm, assigned to the two sets of benzyl methylene protons $ArCH_2$. The aromatic doublets at δ 7.07 ppm and δ 6.69 ppm associated with typical phenyl *ortho*-coupling (J = 8.0 Hz) were assigned to the protons (ArH2′ and ArH6′, ArH3′ and ArH5′) in the benzyl substituent with phenolic group. The two *ortho*-coupling peaks (J = 8.1 Hz) at δ 7.40 ppm and δ 6.86 ppm were assigned to the protons (ArH2″ and ArH6″, ArH3″ and ArH5″) in the phenol substituent. The singlet at δ 8.31 ppm was assigned to the aromatic proton ArH5 next to nitrogen atom in the pyridine ring. No signals of the three phenolic hydroxyl protons can be observed as

deuterated methanol was used as solvent for ^{1}H NMR analysis. No ^{13}C NMR spectrum of **121** was obtained due to the low solubility and poor stability.

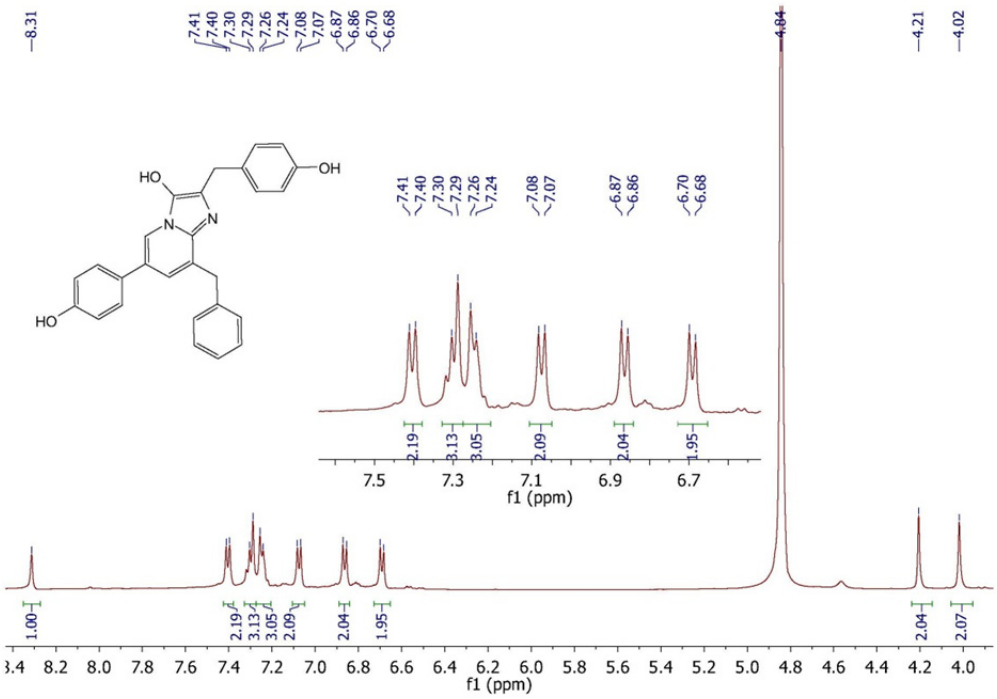

Figure 5.4 ^{1}H NMR spectrum (500 MHz, CD_3OD) of **121**.

Under the same condensation conditions, commercially available 4-hydroxylphenylglyoxal (**151**) and phenylglyoxal (**152**) were synthesized, as well as the synthesized benzylglyoxal **150**, and were used to react with aminopyridine **126**, affording the imidazo[1,2-*a*]pyridine analogues **153**-**155** as yellow solids in the yields of 67-83% (**Scheme 5.6**).

The proposed mechanism of condensation between aminopyridine **126** and benzylglyoxal **129** has been outlined in **Scheme 5.7**. The lone pair electrons of the amine in **126** first attack the aldehyde giving the intermediate **156** which then takes place a Chapman-like rearrangement, leading to intermediate **157**. A cyclization of **156** affords the **158** which eventually leads to imidazo[1,2-*a*]pyridine **121** after dehydration.

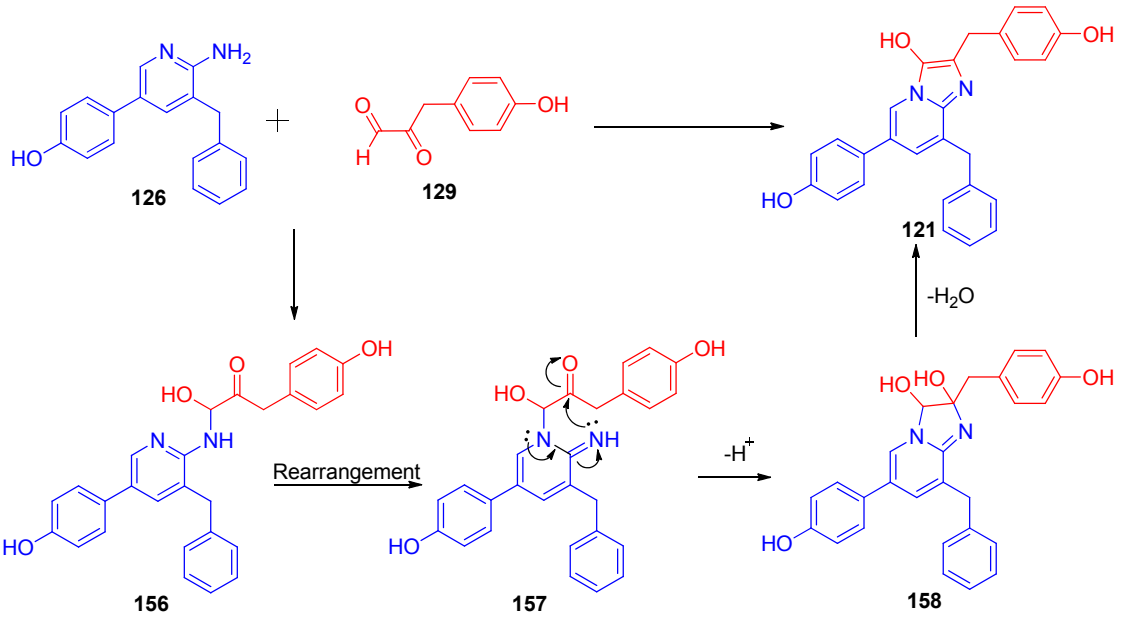

Scheme 5.7 Proposed mechanism of condensation to prepare imidazo[1,2-*a*]pyridine **121**.

Four new coelenterazine analogues (**121**, **153-155**) based on the 3-hydroxyimidazo[1,2-*a*]pyridine scaffold were eventually prepared in 33%-44% yield over 6 linear steps and will be used for the biological activity testing.

5.4 Optical properties of imidazo[1,2-*a*]pyridines

The UV absorption maxima, fluorescent emission maxima, Stokes shift and quantum yields were measured for imidazo[1,2-*a*]pyridines (**121**, **153-155**) in methanol solution and the data are summarized in **Table 5.2**.

The compounds (**154-155**), with phenyl substituent in the C2 position of the imidazo[1,2-*a*]pyridine ring, exhibited slightly larger UV absorption maxima (277 nm) compared to the compounds (**121**, **153**) with corresponding benzyl substituents (276 nm, **Figure 5.5**). Compounds (**121**, **154**) possessing phenolic hydroxyl group in Ar′ substituent ring showed higher UV absorbance than the compounds without such group

(**153**, **155**), with decadic molar attenuation coefficients (lgε) 5.3 $L \cdot mol^{-1} \cdot cm^{-1}$ and 5.4 $L \cdot mol^{-1} \cdot cm^{-1}$ respectively.

Table 5.2 Absorption and emission data of imidazo[1,2-*a*]pyridines in methanol solution.

Compound	λ_{max} (abs) (nm)	lgε ($L \cdot mol^{-1} \cdot cm^{-1}$)	λ_{max} (em) (nm)	Stokes shift (nm)	ϕ*
121	276	5.3	392	116	0.25
153	276	5.0	388	112	0.075
154	277	5.4	390	113	0.19
155	277	5.2	393	116	0.042

* Values were obtained by the peak height and tryptophan was used as standard.

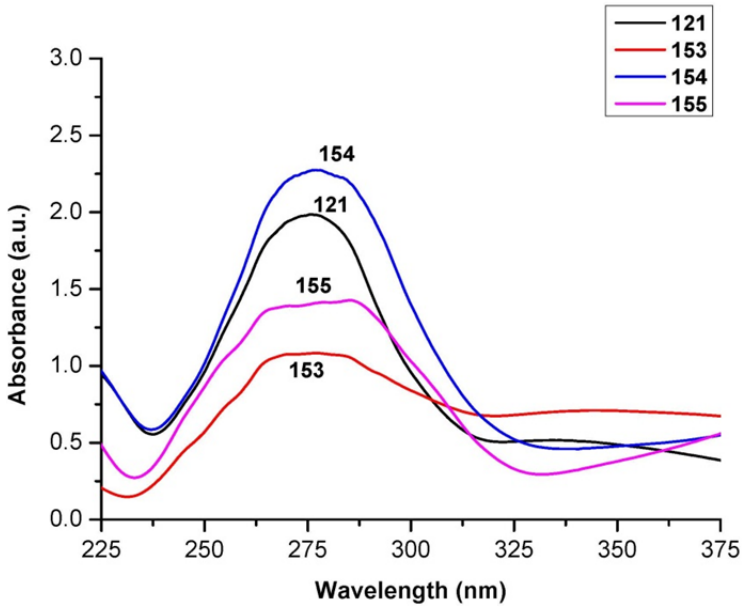

Figure 5.5 UV absorption spectra of imidazo[1,2-*a*]pyridines (**121**, **153-155**) in CH_3OH ($c = 1.0 \times 10^5$ mol/L).

The fluorescent emission spectra, exited by the wavelength of corresponding absorption maxima, are showed in **Figure 5.6**. The Stocks shifts, calculated from subtracting

emission maxima and absorption maxima, ranged from 112 nm (**153**) to 116 nm (**121**, **155**). The quantum yields, measured in methanol solution and using tryptophan as a standard, ranged from 0.042 (**155**) to 0.25 (**121**). The results indicated that compound **121**, with a moderate quantum yield of 0.25, is potential fluorescent material.

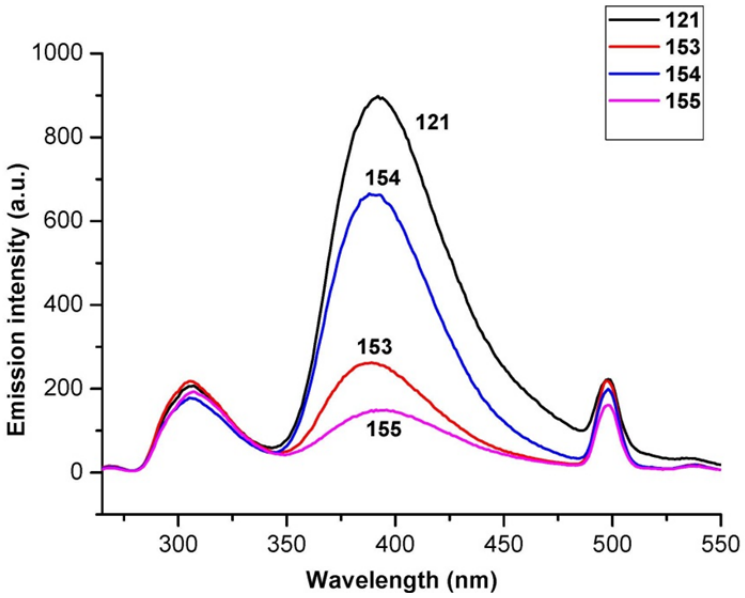

Figure 5.6 Fluorescent emission spectra of imidazo[1,2-*a*]pyridines (**121**, **153**-**155**) in CH_3OH ($c = 1.0\times10^5$ mol/L).

5.5 Antioxidant activities

It is reported that the imidazo[1,2-*a*]pyrazine-based coelenterazine possessed potent antioxidant properties.[109] Due to the structural similarity of imidazo[1,2-*a*]pyridine and imidazo[1,2-*a*]pyrazine, impetus was provided to test the prepared coelenterazine-like imidazo[1,2-*a*]pyridines for their antioxidant activity.

The *in vitro* antioxidant abilities of the imidazo[1,2-*a*]pyridines (**121**, **153**-**155**) and the two intermediate aminopyridines **132** and **126** were analysed using 2,2-diphenyl-1-picrylhydrazyl (DPPH) assays[139] with the moderate antioxidant reagent

L-ascorbic acid as a standard.[c] Their abilities to scavenge DPPH radicals were studied both on reaction rates and inhibition. The reaction of DPPH with compounds **121**, **154** and **155** were fast, reaching peaks within 20 minutes, whereas compounds **6**, **126** and **153** were relatively slow in comparison (**Figure 5.4**). Compounds **121**, **154** and **155** demonstrated a higher percentage of inhibition compared to **132**, **126** and **153** at 30 min, while the value is similar with the standard L-ascorbic acid (**Figure 5.5**). **Table 5.2** illustrates that imidazo[1,2-*a*]pyridine **155** had the highest inhibition of 97% in 30 minutes, which was higher than that of the standard. The IC_{50} values of **121**, **154** and **155** ranged from 58.7 μM to 72.8 μM, indicating that these three imidazo[1,2-*a*]pyridines possessed moderate antioxidant abilities. The IC_{50} values of the imidazo[1,2-*a*]pyridines were in the same order of magnitude as that of the standard L-ascorbic acid and therefore are potential antioxidant candidates.

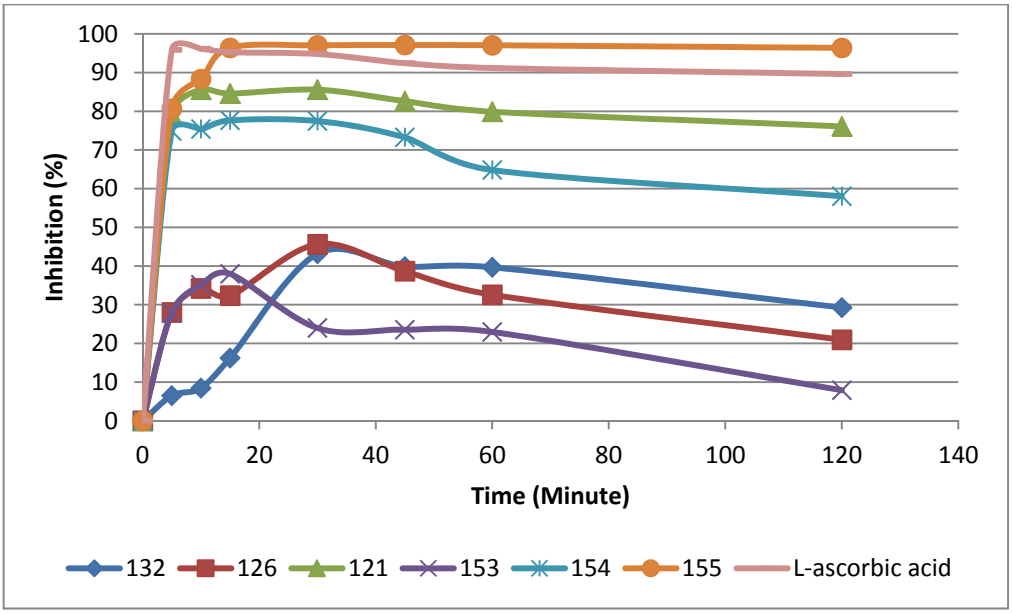

Figure 5.4 Time course of scavenging DPPH radicals by compounds **132**, **126**, **121**, **153**, **154**, **155** and L-ascorbic acid. The reaction mixture (200 μL) in methanol contained DPPH (37.5 μM) in the presence of the target antioxidant (25 μM). The absorbance was measured at 515 nm.

[c] *This assay was performed at University of Wollongong by the candidate.*

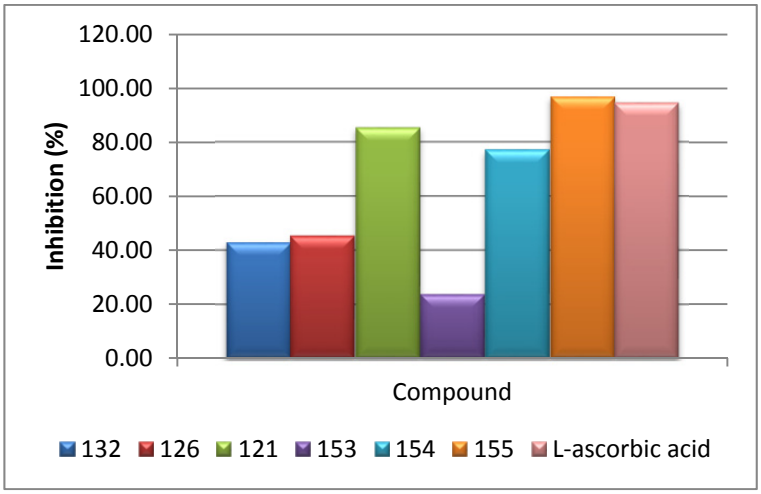

Figure 5.5 Inhibition percentages at 30 min in the concentration of 100 μM. The reaction mixture (200 μL) in methanol contained DPPH (37.5 μM) in the presence of **132** (25 μM), **126** (25 μM), **121** (25 μM), **153** (25 μM), **154** (25 μM), **155** (25 μM) or L-ascorbic acid (25 μM). The reaction mixtures were kept at 30 °C for 30 minutes and the absorbance was measured at 515 nm.

Table 5.2 Inhibition percentage and IC_{50} values of **132**, **126**, **121**, **153**, **154**, **155** and L-ascorbic acid.[a]

Compound	Inhibition (%)	IC_{50} (μM)
132	43	>100
126	46	>100
121	86	58.7
153	24	>100
154	77	72.8
154	97	60.6
L-ascorbic acid	95	36.6

[a]The reaction mixture (200 μL) in methanol contained DPPH (37.5 μM) in the presence of the target antioxidant (25 μM). The reaction mixtures were kept at 30 °C for 30 min and then the absorbance was measured at 515 nm.

5.5 Conclusions

Coelenterazine-like imidazo[1,2-*a*]pyridines, as inhibitors of bioluminescent luciferase for the study of its enzymatic kinetics, were synthesized *via* a highly convergent and adaptable synthesis route. This simple synthesis involves 11 steps in total with only six linear steps, proceeding in respectable 33-44% overall yields from commercially available 2-aminonicotinic acid. The antioxidant abilities of four new coelenterazine analogues (**121**, **153-155**) were evaluated, showing moderate activities with IC_{50} values from 58.7 μM to 72.8 μM. Their optical properties, including UV absorption, fluorescent emission, Stocks shift and quantum yields, were also studied.

Chapter 6: Conclusions and Future Directions

6.1 Preparation of as precursors for subsequent Suzuki cross-coupling

6.1.1 Synthesis of naphthylboronic acid 37 and naphthylboronic ester 38

Naphthylboronic acid **37** was prepared *via* a Diels-Alder method starting from commercially available 3,3-dimethylacrylic acid **59**. Key steps include a Diels-Alder reaction between prepared diene **51** and 1,4-benzoquinone (84%), a selective protection of phenol group in a diphenol intermediate (87%) and a Miyaura borylation reaction to give the boronic ester **66** (92%). This developed strategy gave naphthylboronic acid **37** in 37% over 8 steps and allowed scalable access to these precursors in a time-efficient and inexpensive manner.

Naphthylboronic ester **38** with an ethyl ester substituent was successfully synthesized by a Wittig method over 7 steps with an overall yield of 43%. Key steps include a Wittig reaction to prepare intermediate **48** (71%), a cyclisation to give naphthyl ring **56** (98%) and a Miyaura borylation reaction to give the boronic ester **38** (91%).

Both naphthylboronic acid **37** and naphthylboronic ester **38** were used for the subsequent Suzuki cross-coupling to prepare the monomeric naphthylisoquinolines.

6.1.2 Synthesis of halogenated 3,4-dihydroisoquinolines (39-42)

The synthesis of four dihydroisoquinolines **39-42** was achieved in four or five steps starting from the appropriate benzaldehyde derivative. The challenging step was the cyclization of the halogenated phenylethyl acetamide intermediates (**83-84**, **90**) which were achieved using a mixture of P_2O_5 and $POCl_3$ affording the dihydroisoquinoline

derivatives (**39-41**) in 86%-90% yields. On the other hand, the synthesis of 3,4-dihydroisoquinolin-1(2*H*)-one **42** was achieved through the cyclisation of key intermediate isocyanate **69** (31%).

All these dihydroisoquinolines **39-42** were used for the subsequent Suzuki cross-coupling for the preparation of a variety of monomeric naphthylisoquinoline alkaloids derivatives.

6.1.3 Suggested synthesis of halogenated isoquinolines

The HIV RT testing result indicated that the phenol hydroxyl group and carbonyl group in the isoquinoline unit gave a significant impact to activity against enzyme. In order to further explore the importance of these two groups in the isoquinoline unit for the biological activity of michellamine B analogues, a series of isoquinoline derivatives can be designed (**Figure 6.1**) and used for the subsequent Suzuki cross-coupling to prepare the michellamine B analogues. The designed units aim to investigate the role that may be played for the RT inhibition activity.

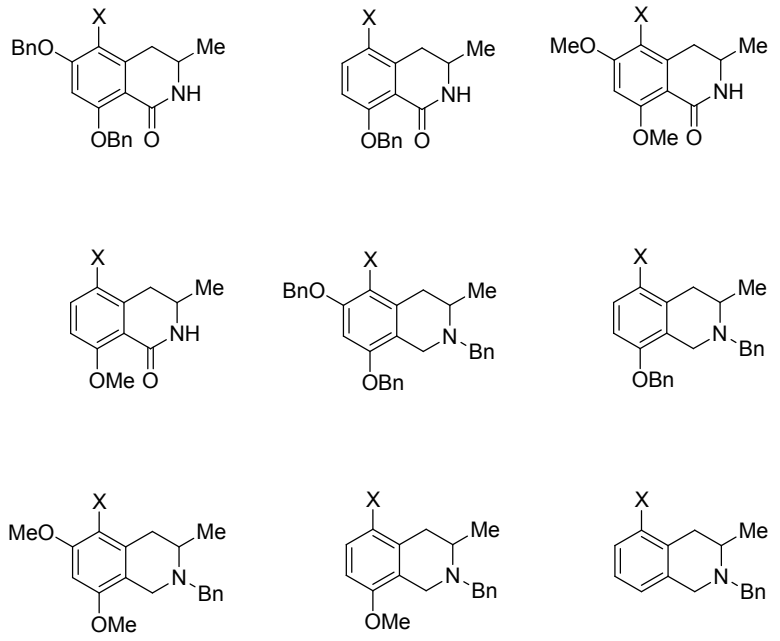

Figure 6.1 Examples for isoquinoline units that may be incorporated into the synthesis of michellamine B analogues. X refers to a suitable handle, such as Br, I and OTf.

The synthesis of the designed units can be achieved by adopting a similar procedure to that used for the synthesis of **42** (**Chapter 2**). In addition, the reduction reaction of the carbonyl group in the isoquinoline units was proposed as follows.

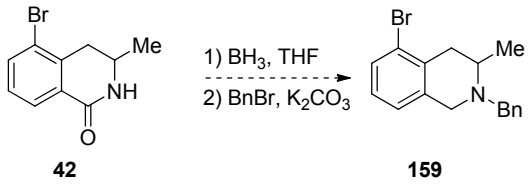

42 **159**

Scheme 6.1 The proposed synthesis of the 1,2,3,4-tetrahydroisoquinoline derivatives *via* reduction of compound **42**.

6.2 Preparation of michellamine B analogues

6.2.1 Synthesis of monomeric naphthylisoquinoline alkaloid *via* Suzuki cross-coupling

Three monomeric naphthylisoquinolines (**96-98**) with an ethyl ester substituent in the naphthyl ring were prepared in 44%-58% yields from the naphthylboronic ester (**38**)

and halogenated isoquinolines (**39**-**42**) *via* Pd-catalyzed Suzuki cross-coupling, while three monomeric naphthylisoquinolines (**43**, **99**-**100**) with methyl substituent in the naphthyl ring were prepared in 51%-75% yields from the naphthyl boronic acid (**37**) and halogenated isoquinolines (**39**-**42**). Iodo isoquinoline **41** proved to be more reactive in the Suzuki reaction comparing to the brominated isoquinoline **40**.

6.2.2 Synthesis of michellamine B analogues *via* oxidative dimerization

In order to activate the ArC3 position for the subsequent dimerization, three phenolic monomeric naphthylisoquinolines (**44**, **107** and **109**) were obtained *via* debenzylation reactions using Pd/C/H_2 reduction system in 92%-95% yields, though the double bond between C and N in the isoquinoline unit of **109** was reduced. Two dimeric naphthylisoquinolines (**112** and **113**), as michellamine B analogues, were synthesized in 31%-35% from the phenolic monomeric naphthylisoquinolines (**44** and **107**) *via* a Ag_2O-induced oxidative dimerization strategy, while this oxidative coupling of naphthylisoquinoline **109** with free amine was unsuccessful for the corresponding dimer.

6.2.3 Biological activities of the naphthylisoquinolines

The synthesised monomeric and dimeric naphthylisoquinolines were tested *in vitro* against the HIV-1 RT enzyme showing weak to mild inhibitory activities. The monomeric naphthylisoquinolines exhibited better anti-HIV activity than korupensamines with % inhibition ranging from 1.1% to 71.2%. Compound **107**, bearing a phenol and carbonyl group demonstrated best activity with an IC_{50} value of 61.3 μM, while **43** with benzyl protecting group obtained the highest inhibition (71.2%) at the concentration of 100 μM among all the testing compounds. Weak inhibitory

activity was observed for the dimeric naphthylisoquinolines (**112** and **113**) with a maximum inhibition of only 8.1% at the concentration of 10 μM.

Five monomeric naphthylisoquinolines (**99**, **43**, **97**, **109** and **44**) exhibited weak activity against *Plasmodium falciparum* (2.66-4.34 μg/mL). Compound **97**, featuring two methoxy groups in the isoquinoline unit and an ester group in naphthyl ring, obtained best anti-malaria activity with an IC_{50} value of 5.76 μM. All the tested compounds showed high cytotoxicity (1.95-30.09 μg/mL).

All the monomeric naphthylisoquinolines exhibited moderate to low activities against the three cell lines KB (oral cavity cancer), MCF-7 (breast cancer) and NCI-H187 (small cell lung cancer). Moderate activity against small cell lung cancer was obtained for **99** (IC_{50} = 5.71 μg/mL), whereas compound **43** with two methoxy groups in the isoquinoline unit showed best activity against breast cancer among all the testing compounds with an IC_{50} value of 6.41 μg/mL.

All the monomeric naphthylisoquinolines showed no activities against *Escherichia coli*, *Klebsiella pneumoniae*, *Acinetobacter baumannii* and *Pseudomonas aeruginosa*, while three compounds (**99**, **43** and **109**) exhibited low activity against *Staphylococcus aureus* with MIC values from 16 μg/mL to 32 μg/mL.

6.2.4 Suggested synthesis of michellamine B analogues *via* binaphthyl core units

In order to obtain HIV RT inhibitors with a potentially better inhibitory activity, a range of novel isoquinoline substituted dimeric naphthylisoquinoline targets can be synthesized to obtain more data in terms of structure-activity relationship. In this manner, the importance of the isoquinoline substitutes for HIV-RT activity could be further investigated. Since the final dimerization step from the monomeric

naphthylisoquinolines obtained low yields, a new strategy applying di-coupling method in the last step can be adopted to increase the overall yield of the synthesis. From the dinaphthyl intermediate **111**, diboronic acid **160** can be synthesized over 5 steps by following a similar synthetic route of boronic acid **37**. A subsequent di-Suzuki cross-coupling with halogenated isoquinlines can afford the target michellamine B analogues.

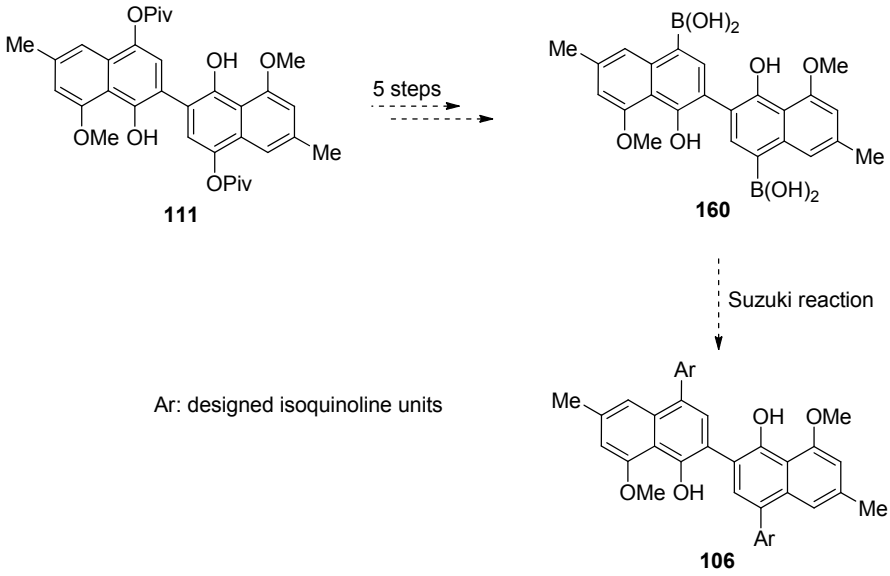

Scheme 6.2 Proposed alternative synthesis of the novel isoquinoline substituted dimeric naphthylisoquinoline *via* di-coupling strategy.

6.3 Synthesis of analogues of marine bioluminescent substrate coelenterazine

6.3.1 Synthesis of coelenterazine analogues

A highly convergent and adaptable synthesis of the coelenterazine-like imidazo[1,2-*a*]pyridines was achieved. This simple synthesis involves 11 steps in total with only six linear steps, proceeding in respectable 33-44% overall yields from commercially available 2-aminonicotinic acid. Four new coelenterazine analogues (**121**, **153-155**) based on the 3-hydroxyimidazo[1,2-*a*]pyridine scaffold were prepared and

tested for their antioxidant ability – three compounds showed moderate activities with IC_{50} values from 58.7 μM to 72.8 μM. Their optical properties, including UV absorption, fluorescent emission, Stocks shift and quantum yields, were also studied.

6.3.2 Potential study of luciferase's enzymatic kinetics

The crystal structural information of coelenterazine binding with the luciferase (Michaelis complex) in transition state is very important for characterization of the luciferase bioluminescent mechanism. Because of the instability of coelenterazine and the rapid catalytic rate of this bioluminescence reaction, it is extremely difficult to observe and characterize the Michaelis complex. Due to the structural similarity, the synthesized inhibitor **121**, which closely resembles coelenterazine and is chemically stable, can bind to the enzyme to form a pseudo-Michaelis complex without transforming to the product, thus allowing the "trapped" transition state to be characterized. The development of the crystals of luciferase binding with **121** for the study of the luciferase's enzymatic kinetics can be achieved in near future.

Chapter 7: Experimental

7.1 Synthesis

7.1.1 General procedure

7.1.1.1 Reagents and Solvents

Dry THF, Et_2O and CH_2Cl_2 were obtained from a Pure Solv MD-5 solvent purification system. Alternatively, THF was distilled from Na/benzophenone under N_2. Anhydrous DMF and DMSO were purchased and used without further purification. HPLC grade CH_2Cl_2 was used for extractions and column chromatography. H_2O was obtained from a Millipore purification system. N_2 was dried by passing through a $CaCl_2$ tube. Grignard reagents were prepared with Mg turnings that were washed with 2 M HCl and Et_2O before being dried under high vacuum. Na was purchased as lumps in oil and was washed with hexanes before use. NaH was weighed and used as a 60% suspension in mineral oil. LiBr were dried in a 110 ^oC oven for at least 24 h and cooled under N_2 before use. All other reagents and solvents were purchased reagent grade and used without further purification or drying unless otherwise stated. All aqueous solutions stated with a percentage are dissolved in H_2O and refer to g/100 mL (eg: 10% Na_2SO_3 = 10 g/100 mL). All organic solvent mixtures stated are in v/v proportions.

7.1.1.2 Reactions and Purifications

All reactions were performed in acetone washed and oven dried glassware with magnetic stirring under a positive pressure of N_2 unless specified that the reaction was carried out in air. Anhydrous and/or air sensitive liquids were introduced into the reaction vessel through a rubber septum with a syringe. The majority of other liquid

reagents were weighed analytically and mixed with the appropriate solvent before being added to the reaction vessel. Air sensitive and/or hygroscopic solid reagents were handled under N_2 and weighed either directly into the reaction vessel or transferred as a solution in the appropriate solvent.

All reactions performed at −40 and −78 ^{o}C used liquid N_2/CH_3CN and liquid N_2/EtOAc slush baths, respectively. Thermal heating of reactions was carried out with paraffin oil bath or sand bath. Microwave reactions were performed using a Discover CEM Focused Microwave Synthesis System in 10 mL closed vessels under N_2 (unless stated otherwise) with a power setting of 100 W.

Reactions heated either thermally or under microwave irradiation were cooled to rt before quenching and work-up, or crystallisation/precipitation at lower temperatures than ambient. All organic extracts were dried with anhydrous $MgSO_4$ or Na_2SO_4 and gravity filtered. All solvents were evaporated under reduced pressure on a rotary evaporator and products dried under high vacuum (~1 mbar) at rt unless otherwise stated.

Purification by column chromatography was performed using Flash Merck Silica Gel 60 (63-200 mesh) under a positive pressure of air. In cases where deactivated silica required, silica was deactivated by addition of specific amount of Et_3N to the eluting solvent. Preparative Thin Layer Chromatography (PTLC) was performed using pre-coated glass plates (20 × 20 cm) with a layer thickness of 500 or 2000 microns.

7.1.1.3 Analysis and Characterisation

Thin Layer Chromatography (TLC) was performed using Merck Silica Gel F_{254} pre-coated aluminium plates. Visualisation was accomplished using UV light and/or an iodine/silica stain. Melting points (Mp.) were determined using a Gallenkamp (Griffin) melting point apparatus or Büchi melting point M-560 apparatus. Temperatures are expressed in degrees Celsius (^{o}C).

Infrared (IR) spectra were recorded with neat liquid or solid samples using a Shimadzu IR Affinity-1 FTIR spectrometer in combination with the Single Reflection Horizontal Attenuated Total Reflectance (HATR) accessory MIRacle 10, fitted with a 1.5 mm round diamond crystal. IR data was recorded as number of wavelength per unit distance (υ_{max}) in cm^{-1} with peak intensity assigned as weak (w), medium (m) or strong (s).

Proton (^{1}H) and carbon (^{13}C) nuclear magnetic resonance (NMR) spectra were recorded at 500 and 126 MHz respectively on a Varian Inova 500 MHz spectrometer or a VNMRS PS54 500 MHz spectrometer. Alternatively, ^{1}H and ^{13}C NMR spectra were recorded at 300 and 75 MHz respectively on a Varian Mercury 300 MHz spectrometer. NMR spectra were acquired in $CDCl_3$ with chemical shifts (δ) reported in parts per million (ppm) relative to TMS (^{1}H: δ = 0 ppm) and $CDCl_3$ (^{13}C: δ = 77.16 ppm). Alternatively, where stated, spectra were acquired in $(CD_3)_2SO$ with δ values reported relative to $(CH_3)_2SO$ (^{1}H: δ = 2.50 ppm) and $(CD_3)_2SO$ (^{13}C: δ = 39.52), or in CD_3OD with δ values relative to $(C\underline{H}_3)OH$ (^{1}H: δ = 3.31 ppm) and $(CD_3)OD$ (^{13}C: δ = 49.00 ppm). Coupling constants (*J*) are reported in Hertz (Hz). *J* values listed in ^{1}H NMR spectral data refer to coupling between hydrogen nuclei. Multiplicities are reported as

singlet (s), broad singlet (bs), doublet (d), doublet of doublets (dd), triplet (t), quartet (q), triplet of doublet (td) or multiplet (m).

Low resolution mass spectra were obtained by electrospray ionisation (ESI) mass spectrometry on a Micromass Platform LCZ spectrometer or a Shimadzu LC-2010EV spectrometer by injecting the samples as a solution in MeOH. In some cases 1% formic acid was added to suppress dimerization and or aid in protonation. Alternatively, electron impact (EI) mass spectra were performed using a Shimadzu QP-5050 spectrometer with compounds dissolved in CH_2Cl_2. High resolution mass spectrometry (HRMS) was performed using either electrospray ionisation (ESI) technique on a Waters QTOF Xevo spectrometer or electron impact technique (EI) on a Micromass Autospec Premier spectrometer. Ion mass charge (*m/z*) values of molecular ions (M), fragment peaks and adducts are stated with their relative abundances in parentheses. For compounds with more than one major isotope all significant isotopic peaks are reported.

X-ray diffraction data sets were collected on a Nonius Kappa-CCD area-detector diffractometer equipped with IFG capillary X-ray focusing collimators and an Oxford Cryosystems crystal cooling device. Calculations were performed using maXus, Crystals and Reals software packages.

7.1.1.4 Other Considerations

All compounds prepared as racemic mixtures are drawn flat without showing the stereogenic atoms/axis.

Where a known compound was prepared according to literature procedures or by a new or modified method, notation and reference appeared in the text. The ^{1}H and ^{13}C NMR spectral data of known compounds is included within and is in agreement with that

previously reported unless otherwise noted. Some manuscripts however did not contain complete (or any) physical and spectral data and/or were published before modern characterisation techniques were available. Therefore, the additional data is included herein and noted where appropriate.

7.1.2 Synthesis of michellamine B analogues

7.1.2.1 Preparation of naphthyl boronic acid

Methyl 3-methylbut-2-enoate (**62**)

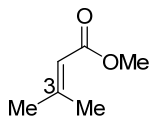

This is a known compound and it was prepared according to the known procedure.[56] A solution of methanol (130 mL), 3,3-dimethylacrylic acid (35.0 g) and concentrated sulphuric acid (2 mL) were heated at reflux for 16 h. H_2O (50 mL) was added and the reaction mixture extracted with Et_2O (3 × 150 mL). The combined organic layers were washed with saturated aqueous Na_2CO_3 solution, dried ($MgSO_4$) and concentrated. Distillation gave the ester **62** (33.4 g, 83%) as a colourless oil. ^{1}H NMR (500 MHz, $CDCl_3$) δ 5.68 (s, 1H, H2), 3.68 (s, 3H, OCH_3), 2.17 (s, 3H, H4a), 1.90 (s, 3H, H4b). ^{13}C NMR (126 MHz, $CDCl_3$) δ 167.2 (C=O), 156.8 (C3), 115.9 (C2), 50.8 (OCH_3), 27.4 (C4a), 20.3 (C4b). MS (EI): *m/z* 149 (M^+, 20%), 83 (100%).

((1-Methoxy-3-methylbuta-1,3-dien-1-yl)oxy)trimethylsilane (**51**)

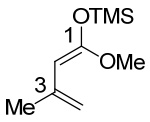

This is a known compound and it was prepared according to the known procedure.[56] To a stirring solution of diisopropylamine (2.00 mL, 14.5 mmol) in THF (10 mL) was added *n*-BuLi (7.30 mL, 14.5 mmol) dropwise at −78 °C over 1 h. The mixture was warmed to rt over 1 h, then cooled to −78 °C. A solution of **62** (1.50 g, 13.2 mmol) in THF (5 mL) was added dropwise to the mixture over 30 min.

After being stirred for 1 h at −78 °C, TMSCl (2.00 mL, 15.8 mmol) was added slowly over 1 h and the mixture was stirred at −78 °C for 30 min, and then allowed to warm to rt over 1 h. The solvent was removed under reduced pressure and the slurry was suspended with hexane (20 mL), filtered and concentrated to afford the crude product **51** as a light yellow liquid (2.43 g, 98%) and used without further purification. ^{1}H NMR (500 MHz, $CDCl_3$) δ 4.78 (s, 1H, H4a), 4.54 (s, 1H, H4b), 4.26 (s, 1H, H2), 3.57 (s, 3H, OCH_3), 1.93 (s, 3H, CH_3), 0.23 (s, 9H, Si-CH_3). ^{13}C NMR (126 MHz, $CDCl_3$) δ 157.8 (C1), 140.5 (C3), 107.6 (C4), 80.9 (C2), 55.2 (OCH_3), 23.8 (CH_3), 0.5 (Si-CH_3).

5-Methoxy-7-methylnaphthalene-1,4-dione (**52**)

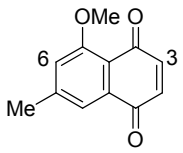

This is a known compound and it was prepared according to the known procedure.[56] To a solution of **51** (2.40 g, 12.9 mmol) in CH_2Cl_2 (120 mL) was added slowly benzoquinone (2.80 g, 25.8 mmol) at rt. After stirred for 20 h, AcOH (1.60 mL, 28.4 mmol) was added to the above solution, the mixture was stirred at rt for 30 min. The mixture was concentrated and the residue was recrystallized from MeOH to afford **52** (2.44 g, 84%) as yellow crystals. ^{1}H NMR (500 MHz, $CDCl_3$) δ 7.54 (s, 1H, H8), 7.10 (s, 1H, H6), 6.83 (s, 2H, H2, H3), 3.99 (s, 3H, OCH_3), 2.48 (s, 3H, CH_3). ^{13}C NMR (126 MHz, $CDCl_3$) δ 185.6 (C1), 184.2 (C4), 160.0 (C5), 146.5 (C7), 141.1 (C2), 136.2 (C3), 134.0 (C8a), 120.2 (C8), 118.5 (C6), 117.8 (C4a), 56.5 (OCH_3), 22.4 (CH_3). MS (EI): *m/z* 202 (M^+, 100%).

4-Hydroxy-5-methoxy-7-methylnaphthalen-1-yl pivalate (**63**)

This is a known compound and it was prepared according to the known procedure.[56] To a mixture of **52** (589 mg, 2.91 mmol) and $Na_2S_2O_4.2H_2O$ (5.00 g, 23.8 mmol) at rt was added CH_2Cl_2 (20 mL) and H_2O (20 mL) under N_2. The mixture was stirred at rt for 1 h

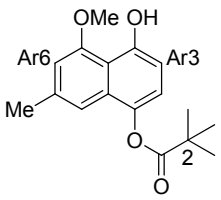

before the two phases were separated. The aqueous layers were further extracted with CH_2Cl_2 (3 × 50 mL). The combined CH_2Cl_2 layer was dried ($MgSO_4$) and concentrated to provide the crude reduction product (582 mg, 2.90 mmol) which was used directly without further purification. To a solution of the aforementioned crude product (582 mg, 2.90 mmol) in CH_2Cl_2 (20 mL) at 0 ^oC under N_2 was added Et_3N (0.44 mL, 3.20 mmol) and pivaloyl chloride (0.39 mL, 3.17 mmol). After stirred at rt for 2.5 h, the mixture was concentrated and subjected to flash silica gel column chromatography (hexanes/EtOAc: 20/1) to afford **63** (731 mg, 87% over two steps) as a white solid. ^1H NMR (500 MHz, $CDCl_3$) δ 9.17 (s, 1H, OH), 7.11 (s, 1H, ArH8), 7.01 (d, *J* = 8.3 Hz, 1H, ArH2), 6.75 (d, *J* = 8.3 Hz, 1H, ArH3), 6.61 (s, 1H, ArH6), 4.01 (s, 3H, OCH_3), 2.43 (s, 3H, Ar-CH_3), 1.46 (s, 9H, 3×CH_3). ^{13}C NMR (126 MHz, $CDCl_3$) δ 177.5 (C=O), 156.4 (ArC5), 152.5 (ArC4), 138.6 (ArC1), 136.5 (ArC7), 129.7 (ArC8a), 120.1 (ArC2), 114.1 (ArC8), 114.0 (ArC4a), 108.7 (ArC3), 106.9 (ArC6), 56.3 (OCH_3), 39.5 (C2), 27.5 (3×CH_3), 22.5 (Ar-CH_3). MS (EI): *m/z* 288 (M^+, 40%), 204 (100%).

4-(Benzyloxy)-5-methoxy-7-methylnaphthalen-1-yl pivalate (**64**)

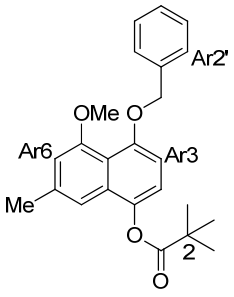

This is a known compound and it was prepared according to the known procedure.[56] To a solution of **63** (2.00 g, 6.94 mmol) in DMF (15 mL) at 0 ^oC was charged NaH (60%, 0.330 g, 8.32 mmol). The mixture was stirred at 0 ^oC under N_2 for 10 min before BnBr (0.86 mL, 7.30 mmol) was added. The resulting mixture was allowed to warm to rt over 1 h and then filtered, then washed with H_2O (5 mL) and Et_2O (1 mL) to afford **64** (2.58 g, 93%) as a white solid. ^1H NMR (500 MHz, $CDCl_3$) δ 7.28 (d, 2H, *J* = 7.5 Hz, ArH2′, ArH6′), 7.40 (t, 2H, *J* = 7.5 Hz, ArH3′, ArH5′), 7.32 (t, 1H,

J = 7.5 Hz, ArH4′), 7.15 (s, 1H, ArH8), 7.03 (d, 1H, *J* = 8.0 Hz, ArH2), 6.81 (d, 1H, *J* = 8.0 Hz, ArH3), 6.71 (s, 1H, ArH6), 5.12 (s, 2H, Ar′-CH_2), 3.93 (s, 3H, OCH_3), 2.46 (s, 3H, Ar-CH_3), 1.48 (s, 9H, 3×CH_3). ^{13}C NMR (126 MHz, $CDCl_3$) δ 177.5 (C=O), 157.4 (ArC5), 154.1 (ArC4), 140.4 (ArC1), 137.8 (ArC7), 137.2 (ArC1′), 130.6 (ArC8a), 128.5 (ArC3′), 127.7 (ArC4′), 127.2 (ArC2′), 118.5 (ArC2), 117.3 (ArC4a), 112.8 (ArC8), 109.0 (ArC6), 107.3 (ArC3), 72.1 (Ar′-CH_2), 56.4 (OCH_3), 39.5 (C2), 27.5 (3×CH_3), 22.5 (Ar-CH_3). MS (EI): *m/z* 378 (M^+, 60%), 203 (100%).

4-(Benzyloxy)-5-methoxy-7-methylnaphthalen-1-yl trifluoromethanesulfonate (**65**)[d]

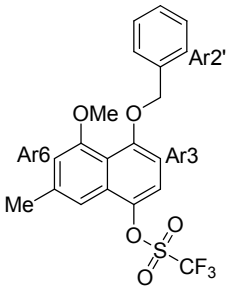

This is a known compound and it was prepared according to the known procedure.[56] A solution of **64** (10.0 g, 26.4 mmol) and KOH (5.93 g, 106 mmol) in MeOH (300 mL) and H_2O (100 mL) was stirred at 50 °C under N_2 for 3 h. After the mixture cooled to rt, H_2O (150 mL) and CH_2Cl_2 (200 mL) was added. HCl (1 M) aqueous solution was added to acidify the mixture until the pH of the aqueous layer reached 5~6. The organic layer was separated and the aqueous layer was further extracted with CH_2Cl_2 (2 × 50 mL). The combined organic layers were dried (Na_2SO_4) and concentrated and the residue was re-dissolved in CH_2Cl_2 (200 mL). To this solution at −78 °C under N_2 was charged Et_3N (18.40 mL, 132 mmol) and Tf_2O (5.00 mL, 29.00 mmol). The mixture was stirred at −78 °C for 0.5 h and then concentrated. The residue was subjected to flash silica gel column chromatography (hexanes/EtOAc: 20/1) to provide **65** (10.1 g, 89%) as a white solid. ^{1}H NMR (300 MHz, $CDCl_3$) δ 7.57 (d, *J* = 7.4 Hz, 2H, ArH2′, ArH6′), 7.42 (t, *J* = 7.3 Hz, 2H, ArH3′, ArH5′), 7.36 (s, 1H, ArH8), 7.31-7.35 (m, 1H, ArH4′), 7.30 (d, *J* = 8.6 Hz, 1H, ArH2), 6.77 (s, 1H, ArH6),

[d] *CF_3 didn't show any signal in ^{13}C NMR spectrum.*

6.75 (d, *J* = 8.8 Hz, 1H, ArH3), 5.18 (s, 1H, Ar′-CH_2), 3.94 (s, 2H, OCH_3), 2.52 (s, 2H, CH_3). ^{13}C NMR (75 MHz, $CDCl_3$) δ 157.5 (ArC5), 156.2 (ArC4), 139.2 (ArC1), 139.1 (ArC1′), 137.1 (ArC8), 130.2 (ArC8a), 128.6 (ArC3′), 127.9 (ArC4′), 127.0 (ArC2′), 121.0 (CF_3), 118.7 (ArC2), 117.2 (ArC4a), 112.3 (ArC8), 109.6 (ArC6), 105.3 (ArC3), 71.5 (Ar-CH_2), 56.3 (OCH_3), 22.5 (CH_3). MS (EI): *m/z* 426 (M^+, 50%), 293 (100%).

2-(4-(Benzyloxy)-5-methoxy-7-methylnaphthalen-1-yl)-4,4,5,5-tetramethyl-1,3,2-dioxaborolane (**66**)[e]

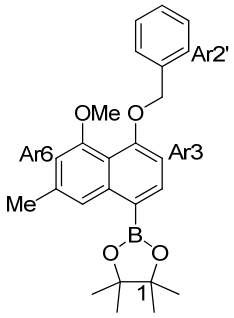

This is a known compound and it was prepared according to the known procedure.[56] A mixture of **65** (7.00 g, 16.4 mmol), KOAc (4.83 g, 49.2 mmol), bispinacolatodiboron (6.25 g, 24.6 mmol), Pd(dppf)Cl_2 (401 mg, 3 mol%), and 1,1'-bis(diphenylphosphino)ferrocene (dppf, 273 mg, 3 mol%) in dioxane (100 mL) was stirred in a sealed tube at 100 ^{o}C under N_2 for 7 h. H_2O (100 mL) and EtOAc (50 mL) was added to quench the reaction. The organic layer was separated, washed with water (3 × 50 mL), brine (50 mL), dried (Na_2SO_4), concentrated, and the residue was subjected to flash silica gel column chromatography (hexanes/EtOAc: 100/1) to provide **66** (6.10 g, 15.1 mmol, 92%) as a white solid. ^{1}H NMR (500 MHz, $CDCl_3$) δ 8.16 (s, 1H, ArH8), 7.95 (d, *J* = 7.7 Hz, 1H, ArH2), 7.59 (d, *J* = 7.4 Hz, 2H, ArH2′, ArH6′), 7.39 (t, *J* = 7.3 Hz, 2H, ArH3′, ArH5′), 7.31 (t, *J* = 7.2 Hz, 1H, ArH4′), 6.84 (d, *J* = 7.8 Hz, 1H, ArH3), 6.70 (s, 1H, ArH6), 5.22 (s, 2H, Ar′-CH_2), 3.92 (s, 3H, OCH_3), 2.49 (s, 3H, Ar-CH_3), 1.40 (s, 12H, 4×CH_3). ^{13}C NMR (126 MHz, $CDCl_3$) δ 159.1 (ArC5), 157.3 (ArC4), 141.5 (ArC7), 137.6 (ArC1′), 137.4 (ArC2), 136.8 (ArC8a), 128.5 (ArC3′), 127.6 (ArC4′), 127.0 (ArC2′), 120.6 (ArC8), 116.1 (ArC4a),

[e] *ArC1 didn't show any signal in ^{13}C NMR spectrum.*

108.5 (ArC6), 106.4 (ArC3), 83.5 (C1), 70.9 (Ar′-CH_2), 56.4 (OCH_3), 25.1 (4×CH_3), 22.5 (Ar-CH_3). MS (EI): *m/z* 404 (M^+, 100%).

(4-(Benzyloxy)-5-methoxy-7-methylnaphthalen-1-yl)boronic acid (**37**)[f]

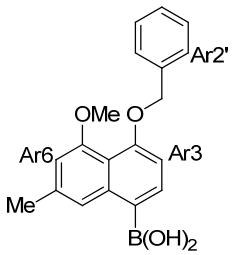

This is a known compound and it was prepared according to the known procedure.[56] To a solution of **66** (2.00 g, 4.95 mmol) in THF/H_2O (40 mL/10 mL) was added $NaIO_4$ (3.18 g, 14.9 mmol). The mixture was stirred at rt for 30 min and then HCl solution (1 M, 2.5 mL) was added. The resulting mixture was stirred at rt for 12 h, then H_2O (50 mL) was added to the mixture and extracted with EtOAc (2 × 30 mL). The combined organic phases were washed sequentially with water (40 mL) and brine (20 mL), dried (Na_2SO_4), concentrated, and recrystallized from EtOAc/hexane to afford **37** (1.32 g, 82%) as a gray solid. ^{1}H NMR (300 MHz, CD_3OD) δ 7.61 (d, *J* = 7.4 Hz, 2H, ArH2′, ArH6′), 7.47-7.26 (m, 4H, ArH2, ArH3′, ArH4′, ArH5′), 7.08 (s, 1H, ArH8,), 6.95 (d, *J* = 7.7 Hz, 1H, ArH3), 6.80 (s, 1H, ArH6), 5.19 (s, 2H, Ar′-CH_2), 3.92 (s, 3H, OCH_3), 2.46 (s, 3H, CH_3). ^{13}C NMR (126 MHz, CD_3OD) δ 158.7 (ArC5), 158.1 (ArC4), 140.6 (ArC7), 139.1 (ArC1′), 137.8 (ArC8a), 132.2 (ArC2), 129.3 (ArC3′), 128.5 (ArC4′), 128.1 (ArC2′), 121.1 (ArC8), 117.3 (ArC4a), 109.5 (ArC6), 108.4 (ArC3), 72.2 (Ar′-CH_2), 56.7 (OCH_3), 22.0 (CH_3). MS (EI): *m/z* 322 (M^+, 40%), 278 (100%).

Ethyl 8-bromo-5-isopropoxy-4-methoxy-2-naphthoate (**49**)

This is a known compound and it was prepared according to the known procedure.[49,60,140] Iodomethane (0.16 mL, 0.37 g, 2.61 mmol) was added to a suspension of **56** (0.23 g, 0.653 mmol) and potassium carbonate (0.37 g, 2.66 mmol) in acetone and

[f] *ArC1 didn't show any signal in ^{13}C NMR spectrum.*

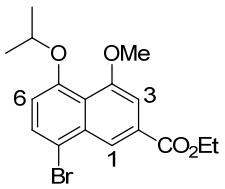

heated at reflux for 18 h. The reaction mixture was concentrated under reduced pressure, diluted with H_2O (10 mL) and extracted with chloroform (3 × 10 mL). The combined organic layers were washed with 2 M NaOH (10 mL), brine (25 mL), dried (Na_2SO_4), filtered, evaporated and recrystallized from CH_2Cl_2/hexane to give **49** (0.220 g, 92%) as a light yellow solid. ^{1}H NMR (500 MHz, $CDCl_3$) δ 8.56 (d, *J* = 1.6 Hz, 1H, ArH1), 7.70 (d, *J* = 8.2 Hz, 1H, ArH7), 7.46 (bs, 1H, ArH3), 6.87 (d, *J* = 8.2 Hz, 1H, ArH6), 4.57-4.49 (m, 1H, C<u>H</u>$(CH_3)_2$), 4.45 (q, *J* = 7.1 Hz, 2H, C<u>H</u>$_2$CH$_3$), 4.01 (s, 3H, OCH_3), 1.46 (t, *J* = 7.1 Hz, 3H, $CH_2C\underline{H}_3$), 1.40 (d, *J* = 5.9 Hz, 6H, CH(C<u>H</u>$_3$)$_2$). ^{13}C NMR (126 MHz, $CDCl_3$) δ 166.5 (C=O), 157.6 (ArC4), 155.0 (ArC5), 134.4 (ArC8a), 131.1 (ArC2), 129.2 (ArC7), 122.7 (ArC1), 122.6 (ArC4a), 115.5 (ArC8), 114.9 (ArC3), 105.8 (ArC6), 73.4 (<u>C</u>$(CH_3)_2$), 61.3 (<u>C</u>H_2CH_3), 56.4 (OCH_3), 21.9 (CH(<u>C</u>H$_3$)$_2$), 14.4 ($CH_2\underline{C}H_3$). MS (EI): *m/z* 369 (M^+, ^{81}Br, 100%), 367 (M^+, ^{79}Br, 100%).

Ethyl 5-isopropoxy-4-methoxy-8-(4,4,5,5-tetramethyl-1,3,2-dioxaborolan-2-yl)-2-naphthoae (**38**)

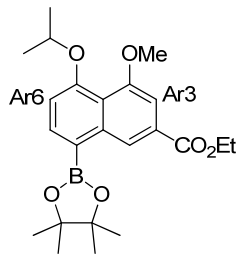

This is a known compound and it was prepared according to the known procedure.[70] A mixture of **49** (0.350 g, 1.36 mmol), KOAc (0.270 g, 2.73 mmol), and $PdCl_2$(dppf) (0.060 g, 10 mol%) in dry THF (5 mL) was heated at reflux in a sealed tube overnight. The reaction mixture was concentrated under reduced pressure, diluted with H_2O and extracted with chloroform (3 × 10 mL). The combined organic layers were washed with brine (25 mL), dried (Na_2SO_4), filtered, evaporated and the residue was subjected to flash silica gel column chromatography (hexane/EtOAc: 5/95) to give the boronic ester **38** (0.26 g, 91%) as a white solid. ^{1}H NMR (500 MHz, $CDCl_3$) δ 9.20 (d, *J* = 0.8 Hz, 1H,

ArH1), 7.99 (d, *J* = 7.8 Hz, 1H, ArH7), 7.39 (bs, 1H, ArH3), 6.98 (d, *J* = 7.9 Hz, 1H, ArH6), 4.69-4.60 (m, 1H, $CH(CH_3)_2$), 4.42 (q, *J* = 7.1 Hz, 2H, $C\underline{H}_2CH_3$), 3.98 (s, 3H, OCH_3), 1.46 (t, *J* = 7.1 Hz, 3H, $CH_2C\underline{H}_3$), 1.42 (d, *J* = 3.6 Hz, 6H, $CH(C\underline{H}_3)_2$), 1.26 (s, 12H, $2\times C(CH_3)_2$). ^{13}C NMR (126 MHz, $CDCl_3$) δ 167.3 (C=O), 158.1 (ArC4), 157.7 (ArC5), 140.6 (ArC8a), 137.3 (ArC7), 128.2 (ArC4a), 124.6 (ArC1), 121.2 (ArC8), 112.5 (ArC6), 105.2 (ArC3), 83.7 ($\underline{C}(CH_3)_2$), 83.6 ($\underline{C}(CH_3)_2$), 72.4 ($\underline{C}H(CH_3)_2$), 61.0 ($\underline{C}H_2CH_3$), 56.5 (OCH_3), 25.1 ($C(\underline{C}H_3)_2$), 25.0 ($C(\underline{C}H_3)_2$), 22.1 ($CH(\underline{C}H_3)_2$), 14.4 ($CH_2\underline{C}H_3$). MS (EI): *m/z* 414 (M^+, 40%) 372 (100%).

7.1.2.2 Preparation of halogenated isoquinolines

General procedure 1: preparation of (2-nitrovinyl)benzene derivatives

To a solution of benzaldehyde derivative (20 mmol) in acetic acid (10 mL) was added nitromethane (12.2 g, 200 mmol) and $Al(OAc)_3$ (770 mg, 10 mmol). The reaction mixture was heated at reflux for 5 h. The resulting solution was poured into saturated $NaHCO_3$ aqueous solution (25 mL) slowly and extracted with EtOAc (3 × 30 mL). The combined organic layers were dried (Na_2SO_4), concentrated, and the residues were crystallized from MeOH to afford the nitrostyrene product.

(E)-1-Methoxy-3-(2-nitrovinyl)benzene (**79**)

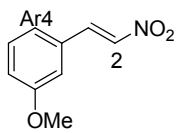

This is a known compound and it was prepared according to the known procedure.[80] Using **General procedure 1**, 3-methoxybenzaldehyde **77** (2.70 g, 20.0 mmol) gave **79** (3.20 g, 91%) as yellow crystals. ^{1}H NMR (500 MHz, CD_3Cl) δ 7.95 (d, *J* = 14.0 Hz, 1H, H2), 7.56 (d, *J* = 14.0 Hz, 1H, H1), 7.36 (dd, *J* = 8.0, 8.5 Hz, 1H, ArH5), 7.13 (d, *J* = 8.0 Hz, 1H, ArH4), 7.04 (m, 2H, ArH2, ArH6), 3.85 (s, 3H, OCH_3). ^{13}C NMR (126 MHz, CD_3Cl) δ 160.1 (ArC1), 139.0 (C1), 137.3 (C2),

131.3 (ArC3), 130.4 (ArC5), 121.7 (ArC4), 117.9 (ArC6), 113.9 (ArC2), 55.4 (CH_3). MS (EI): *m/z* 179 (M^+, 100%).

(E)-1,3-dimethoxy-5-(2-nitrovinyl)benzene (**80**)

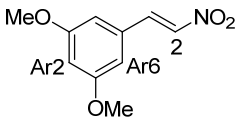

This is a known compound and it was prepared according to the known procedure.[80] Using **General procedure 1**, 3,5-dimethoxybenzaldehyde **78** (3.30 g, 20.0 mmol) gave the nitrostyrene derivative **80** (4.00 g, 96%) as yellow crystals. ^{1}H NMR (500 MHz, CD_3Cl) δ 7.90 (d, *J* = 14.0 Hz, 1H, H2), 7.54 (d, *J* =14.0 Hz, 1H, H1), 6.66 (d, *J* = 1.8 Hz, 2H, ArH4, ArH6), 6.58 (bs, 1H, ArH2), 3.82 (s, 6H, 2×OCH_3). ^{13}C NMR (126 MHz, CD_3Cl) δ 161.3 (ArC1, ArC3), 139.1 (C1), 137.5 (C2), 131.7 (ArC5), 107.0 (ArC4, ArC6), 104.1 (ArC2), 55.5 (2×OCH_3). MS (EI): *m/z* 209 (M^+, 100%).

General procedure 2: Preparation of *N*-phenethylacetamide derivatives

Step 1

A solution of the nitrostyrene derivative (15 mmol) in anhydrous THF (40 mL) was added dropwise to a stirred solution of $LiAlH_4$ (60 mmol) in THF (100 mL) at 0 ^{o}C. The reaction mixture was allowed to warm to rt and was then heated at reflux for 5 h. The resulting mixture was cooled to 0 ^{o}C and treated with an excess of 30% NaOH aqueous solution. The liquid layer was decanted and extracted with EtOAc (3 × 50 mL). The combined organic layers were dried (Na_2SO_4), and concentrated to afford the corresponding amine, which was used in **Step 2** without further purification.

Step 2

To a stirred solution of the crude amine in CH_2Cl_2 (25 mL) at 0 ^{o}C was added Et_3N

(15 mmol) and acetyl chloride (15 mmol). The mixture was allowed to warm to rt and stirred for 15 min. The resulting suspension was diluted with water (20 mL) and the layers were separated. The organic layer was washed with dilute HCl (15 mL), saturated $NaHCO_3$ (15 mL) followed by brine (15 mL), then dried (Na_2SO_4), concentrated, and the resulting residue was subjected to flash silica gel column chromatography (hexanes/EtOAc: 30/70 containing 5% Et_3N) to afford the desired acetamide derivative.

N-(3-Methoxyphenethyl)acetamide (**81**)

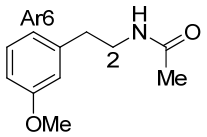

This is a known compound and it was prepared according to the known procedure.[80] Using the **General procedure 2**, (*E*)-(2-nitrovinyl)benzene **79** (2.20 g, 15.0 mmol) gave **81** (1.60 g, 56% over two steps) as a brown oil. ^{1}H NMR (500 MHz, $CDCl_3$) δ 7.20 (m, 1H ArH5), 6.73-6.78 (m, 3H, ArH2, ArH4, ArH6), 6.24 (bs, 1H, NH), 3.77 (s, 3H, OCH_3), 3.47 (td, *J* = 7.5 Hz, 6.5 Hz, 2H, H2), 2.77 (t, *J* = 7.5 Hz, 2H, H1), 1.92 (s, 3H, CH_3). ^{13}C NMR (126 MHz, $CDCl_3$) δ 170.2 (C=O), 159.7 (ArC3), 140.4 (ArC1), 129.4 (ArC5), 120.8 (ArC6), 114.2 (ArC2), 111.6 (ArC4), 54.9 (OCH_3), 40.4 (C2), 35.4 (C1), 22.9 (CH_3). MS (ESI): *m/z* 194 ($[M+H]^+$).

N-(3,5-Dimethoxyphenethyl)acetamide (**82**)

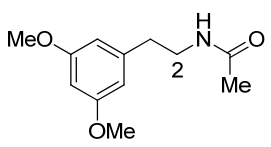

This is a known compound and it was prepared according to the known procedure.[80] Using the **General procedure 2**, (*E*)-1,3-dimethoxy-5-(2-nitrovinyl)benzene **80** (3.10 g, 15.0 mmol) gave **82** (2.10 g, 63% over two steps) as a brown oil. ^{1}H NMR (500 MHz, $CDCl_3$) δ 6.34 (s, 3H, ArH2, ArH4, ArH6), 5.64 (bs, 1H, NH), 3.78 (s, 6H, 2×OCH_3), 3.50 (td, *J* = 6.9 Hz, 6.0 Hz, 2H, H2), 2.75 (t, *J* = 6.9 Hz, 2H, H1), 1.94 (s, 3H, CH_3). ^{13}C NMR

(126 MHz, $CDCl_3$) δ 170.1 (C=O), 160.9 (ArC3, ArC5), 141.2 (ArC1), 106.7 (ArC2, ArC6), 98.3 (ArC4), 55.2 (2×OCH_3), 40.4 (C2), 35.8 (C1), 23.3 (CH_3). MS (EI): *m/z* 223 (M^+, 30%), 164 (100%).

General procedure 3: Bromination of *N*-phenethylacetamide derivatives

To a solution of the acetamide derivative (5.20 mmol) in CH_2Cl_2 (20 mL) was added bromine solution (0.900 g, 5.7 mmol) in CH_2Cl_2 (10 mL) dropwise at 0 ºC. The reaction mixture was allowed to warm up to rt and stirred for 2 h. The resulting mixture was diluted with H_2O (20 mL) and the layers were separated. The organic layer was washed successively with $NaHCO_3$ (15 mL), 10% $Na_2S_2O_5$ solution (15 mL) and brine (15 mL), then dried (Na_2SO_4), concentrated, and the resulting residue was subjected to flash silica gel column chromatography (hexanes/EtOAc: 30/70 containing 5% Et_3N) to afford the corresponding bromo derivative.

N-(2-Bromo-5-methoxyphenethyl)acetamide (**83**)

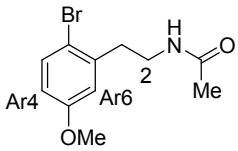

This is a known compound and it was prepared according to the known procedure.[80] Using **General procedure 3**, *N*-(3-methoxyphenethyl)acetamide **81** (1.00 g, 5.20 mmol) and bromine (0.900 g, 5.70 mmol) gave **83** (1.20 g, 87%) as a light brown solid. ^{1}H NMR (500 MHz, $CDCl_3$) δ 7.40 (d, *J* = 8.5 Hz, 1H, ArH3), 6.78 (d, *J* = 3.0 Hz, 1H, ArH6), 6.64-6.67 (dd, *J* = 8.7, 2.9 Hz, 1H, ArH4), 5.96 (bs, 1H, NH), 3.77 (s, 3H, OCH_3), 3.50 (td, *J* = 7.0 Hz, 6.5 Hz, 2H, H2), 2.92 (t, *J* = 7.0 Hz, 2H, H1), 1.95 (s, 3H, CH_3). ^{13}C NMR (126 MHz, $CDCl_3$) δ 170.2 (C=O), 158.9 (ArC5), 139.2 (ArC1), 133.3 (ArC3), 116.3 (ArC4), 114.8 (ArC2), 113.9 (ArC6), 55.4 (OCH_3), 39.2 (C2), 35.8 (C1), 23.2 (CH_3). MS (ESI): *m/z* 272 ($[M+H]^+$, ^{79}Br, 100%), 274 ($[M+H]^+$, ^{81}Br, 100%).

N-(2-Bromo-3,5-dimethoxyphenethyl)acetamide (**84**)

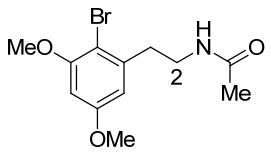

This is a known compound and it was prepared according to the known procedure.[80] Using **General procedure 3**, *N*-(3,5-dimethoxyphenethyl) acetamide **82** (1.20 g, 5.20 mmol) and bromine (0.900 g, 5.70 mmol) gave the **84** (1.40 g, 89%) as a light brown solid. ^{1}H NMR (500 MHz, $CDCl_3$) δ 6.40 (d, *J* = 2.5 Hz, 1H, ArH6), 6.36 (d, *J* = 2.5 Hz, 1H, ArH4), 5.71 (bs, 1H, NH), 3.84 (s, 3H, OCH_3), 3.77 (s, 3H, OCH_3), 3.52 (td, *J* = 7.0 Hz, 6.5 Hz, 2H, H2), 2.95 (t, *J* = 7.0 Hz, 2H, H1), 1.94 (s, 3H, CH_3). ^{13}C NMR (126 MHz, $CDCl_3$) δ 170.1 (C=O), 159.6 (ArC5), 156.8 (ArC3), 140.2 (ArC1), 106.9 (ArC6), 104.8 (ArC2), 98.1 (ArC4), 56.3 (OCH_3), 55.5 (OCH_3), 39.3 (C2), 36.1 (C1), 23.3 (CH_3). MS (EI): *m/z* 303 (M+, 20%, ^{81}Br), 301 (M+, 20%, ^{79}Br), 222 (100%).

N-(2-Iodo-3,5-dimethoxyphenethyl)acetamide (**90**)

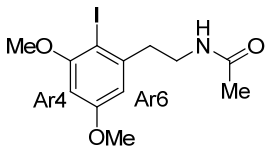

To a solution of *N*-(3,5-dimethoxyphenethyl)acetamide **89** (1.00 g, 4.48 mmol) was added Ag_2SO_4 (4.21g, 13.5 mmol), and then a solution of iodine (1.14 g, 4.48 mmol) in ethanol (20 mL) was added dropwise. After stirring for 30 min, the inorganic salts were removed by filtration, and the residue was subjected to flash silica gel column chromatography (CH_2Cl_2/EtOAc: 1/2 containing 5% Et_3N) to afford **90** (1.36g, 87%) as a white solid. Mp. 118-119 ^{o}C. IR (neat) υ_{max} 3338 (w), 2933 (w), 1640 (m), 1579 (m), 1547 (m), 1453 (w), 1407 (w), 1332 (w), 1319 (w), 1293 (w), 1280 (w), 1204 (s), 1161 (s), 1101 (w), 1049 (w), 1009 (w), 847 (w), 820 (w), 701 (w), 603 (w). ^{1}H NMR (500 MHz, $CDCl_3$) δ 6.46 (d, *J* = 2.5 Hz, 1H, ArH6), 6.33 (d, *J* = 2.5 Hz, 1H, ArH4), 5.58 (bs, 1H, NH), 3.86 (s, 3H, Ar3-OCH_3), 3.80 (s, 3H, Ar5-OCH_3), 3.51 (td, *J* = 7.0, 6.5 Hz, 2H,

N-CH_2), 3.00 (t, J = 7.0 Hz, 2H, Ar-CH_2), 1.96 (s, 3H, CH_3). ^{13}C NMR (126 MHz, $CDCl_3$) δ 170.3 (C=O), 161.2 (ArC3), 159.2 (ArC5), 143.8 (ArC1), 107.1 (ArC6), 97.4 (ArC4), 82.0 (ArC2), 56.6 (Ar3-OCH_3), 55.7 (Ar5-OCH_3), 40.7 (N-CH_2), 39.7 (Ar-CH_2), 23.5 (CH_3). MS (EI): *m/z* 349 (M^+, 20%), 222 (100%). HRMS (ESI) calcd for $C_{12}H_{17}INO_3$: 350.0253, found 350.0258.

General procedure 4: Preparation of isoquinolines by cyclization reaction.

To a solution of the acetamide derivative (2.50 mmol) in CH_3CN (20 mL) was added $POCl_3$ (32.0 mmol) and P_2O_5 (2.50 mmol) and the resulting mixture was heated at reflux for 6 h. The solvent was evaporated under reduced pressure and the resulting residue was diluted with CH_2Cl_2 (10 mL) followed by stirring in aqueous KOH (30 mL, 1 M) for 10 min. The layers were separated and the aqueous layer was extracted with EtOAc (3 × 10 mL). The combined organic layers were washed with brine (25 mL), dried (Na_2SO_4), concentrated, and the residue subjected to flash silica gel column chromatography (hexane/ethyl acetate: 60/40 containing 5% Et_3N) to give the isoquinoline.

5-Bromo-8-methoxy-1-methyl-3,4-dihydroisoquinoline (**39**)

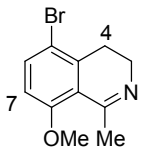

This is a known compound and it was prepared according to the known procedure.[80] Using **General procedure 4**, *N*-(2-bromo-5-methoxyphenethyl)acetamide **83** (548 mg, 2.00 mmol) gave **39** (447 mg, 88%) as a brown solid. ^{1}H NMR (300 MHz, $CDCl_3$) δ 7.87 (d, J = 9.1 Hz, 1H, H6), 7.00 (d, J = 9.1 Hz, 1H, H7), 4.01 (s, 3H, OCH_3), 3.85 (t, J = 7.2 Hz, 2H, H3), 3.13 (t, J = 7.5 Hz, 2H, H4), 3.02 (s, 3H, CH_3). ^{13}C NMR (75 MHz, $CDCl_3$) δ 175.2 (C1), 160.9 (C8), 141.5 (C6), 138.9 (C4a), 116.9 (C8a), 114.6 (C5), 113.2 (C7), 56.6

(OCH_3), 40.1 (C3), 26.8 (C4), 24.2 (CH_3). MS (EI): *m/z* 253 (M^+, ^{79}Br, 100%) 255 (M^+, ^{81}Br, 97%).

5-Bromo-6,8-dimethoxy-1-methyl-3,4-dihydroisoquinoline (**40**)

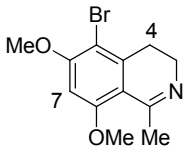

This is a known compound and it was prepared according to the known procedure.[80] Using **General procedure 4**, *N*-(2-bromo-3,5-dimethoxyphenethyl)acetamide **84** (1.51g, 5.00 mmol) gave **40** (1.30 g, 90%) as a brown solid. ^1H NMR (500 MHz, CD_3OD) δ 6.81 (s, 1H, H7), 4.09 (s, 6H, OCH_3), 3.73 (t, *J* = 7.3 Hz, 2H, H3), 3.20 (t, *J* = 7.5 Hz, 2H, H4), 2.77 (s, 3H, CH_3). ^{13}C NMR (126 MHz, CD_3OD) δ 176.3 (C1), 165.7 (C8), 165.6 (C6), 142.1 (C4a), 110.7 (C8a), 106.0 (C5), 96.9 (C7), 57.9 (8-OCH_3), 57.3 (6-OCH_3), 41.3 (C4), 28.3 (C3), 24.7 (CH_3). MS (EI): *m/z* 283 (M^+, ^{79}Br, 100%) 285 (M^+, ^{81}Br, 97%).

5-Iodo-6,8-dimethoxy-1-methyl-3,4-dihydroisoquinoline (**41**)

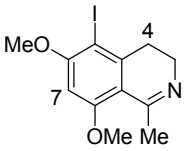

Using **General procedure 4**, **90** (1.05g, 3.00 mmol) gave **41** (0.850 g, 86%) as a yellow solid. Mp. 205-206 ^oC. IR (neat) υ_{max} 2651 (m), 1632 (m), 1566 (s), 1425 (w), 1354 (w), 1317 (w), 1280 (s), 1224 (s), 1123 (w), 1084 (w), 1016 (w), 916 (w), 840 (w), 739 (w). ^1H NMR (500 MHz, CD_3OD) δ 6.76 (s, 1H, H7), 4.09 (s, 6H, OCH_3), 3.71 (t, *J* = 7.1 Hz, 2H, H3), 3.19 (t, *J* = 7.4 Hz, 2H, H4), 2.76 (s, 3H, CH_3). ^{13}C NMR (126 MHz, CD_3OD) δ 176.1 (C1), 167.7 (C8), 166.7 (C6), 146.0 (C4a), 111.1 (C8a), 96.0 (C7), 83.3 (C5), 58.0 (8-OCH_3), 57.1 (6-OCH_3), 41.8 (C4), 34.0 (C3), 24.4 (CH_3). MS (EI): *m/z* 331 (M^+, 100%). HRMS (ESI) calcd for $C_{12}H_{14}INO_2$: 332.0148, found 332.0164.

5-Bromo-3-methyl-3,4-dihydroisoquinolin-1(2H)-one (**42**)

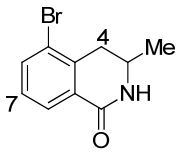

This is a known compound and it was prepared according to the known procedure.[82] To a solution of 1-bromo-2-(2-isocyanatopropyl)benzene (**76**) (1.93 g, 8.01 mmol) in tetrachloroethylene (20 mL) in a flask equipped with a reflux condenser was added aluminium chloride (2.24 g, 16.8 mmol) and the reaction mixture was heated at 80 °C for 3 h. Upon heating, the reaction mixture turned black. The reaction mixture was quenched with 3 M aq. HCl (2.92 mL), diluted with CH_2Cl_2 (100 mL) and filtered. The filter cake was washed with CH_2Cl_2 (100 mL), the filtrate dried ($MgSO_4$), filtered, evaporated and the residue was subjected to flash silica gel column chromatography (CH_2Cl_2/ethyl acetate: 8/2) yielded the desired 3,4-dihydroisoquinolinone **42** as a yellowish solid (612 mg, 31%). ^{1}H NMR (500 MHz, $CDCl_3$) δ 8.00 (1H, d, *J* = 8.0 Hz, H8), 7.72 (1H, d, *J* = 8.5 Hz, H6), 7.68 (1H, bs, NH), 7.28 (1H, t, *J* = 8.0 Hz, H7), 3.80- 3.87 (1H, m, H3), 3.18 (1H, dd, *J* = 16.0, 4.5 Hz, H4b), 2.69 (1H, dd, *J* = 16.8, 10.5 Hz, H4a), 1.37 (3H, d, *J* = 6.6 Hz, CH3). ^{13}C NMR (126 MHz, $CDCl_3$) δ 164.6 (C1), 138.3 (C4a), 135.9 (C6), 131.5 (C5), 128.4 (C7), 127.3 (C8), 123.0 (C8a), 46.3 (C3), 36.1 (C4), 20.9 (CH3). MS (EI): *m/z* 241 (M^+, ^{81}Br, 30%), 239 (M^+, ^{79}Br, 32%).

7.1.2.3 Preparation of naphthylisoquinoline alkaloids by Suzuki coupling

General Procedure 5: **Suzuki coupling of naphthyl boronic acid and halogenated isoquinolines**

A mixture of **37** (1.10 mmol), halogenated isoquinoline (1.00 mmol), Pd $(PPh_3)_4$ (5 mol%) and 2 M Na_2CO_3 aqueous solution (8.00 mmol) in dioxane (20 mL) in a sealed tube under N_2 was heated and stirred at reflux for 18 h. The mixture was cooled to rt, diluted with H_2O (10 mL) and extracted with EtOAc (3 × 20 mL). The combined

organic layers were washed with brine (25 mL), dried (Na_2SO_4), filtered, evaporated and the residue was subjected to flash silica gel column chromatography (hexane/ethyl acetate: 60/40 containing 5% Et_3N) to give the target monomer.

5-(4-(Benzyloxy)-5-methoxy-7-methylnaphthalen-1-yl)-8-methoxy-1-methyl-3,4-dihydroisoquinoline (**99**)

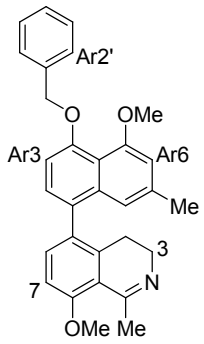

Using the **General Procedure 5**, **37** (142 mg, 0.440 mmol) and **39** (101 mg, 0.400 mmol) gave **99** (102 mg, 57%) as a light brown solid. Mp. 148 ^{o}C. IR (neat) υ_{max} 3741 (w), 2940 (w), 2839 (w), 2360 (m), 1618 (w), 1574 (s), 1455 (w), 1369 (w), 1321 (w), 1274 (s), 1181 (w), 1143 (w), 1081 (s), 972 (w), 836 (m), 738 (m), 691 (m). ^{1}H NMR (500 MHz, $CDCl_3$) δ 7.62 (d, *J* = 7.5 Hz, 2H, ArH2′, ArH6′), 7.42 (t, *J* = 7.6 Hz, 2H, ArH3′, ArH5′), 7.33 (t, *J* = 7.3 Hz, 1H, ArH4′), 7.27 (d, *J* = 8.5 Hz, 1H, H6), 7.14 (d, *J* = 7.8 Hz, 1H, ArH2), 6.95 (d, *J* = 8.5 Hz, 1H, H7), 6.89 (d, *J* = 7.9 Hz, 1H, ArH3), 6.76 (s, 1H, ArH8), 6.71 (s, 1H, ArH6), 5.23 (s, 2H, Ar′-CH_2), 3.95 (s, 3H, Ar-OCH_3), 3.94 (s, 3H, 8-OCH_3), 3.32-3.36 (m, 2H, H3), 2.55 (s, 3H, 1-CH_3), 2.34 (s, 3H, Ar-CH_3), 2.18 (t, *J* = 7.0 Hz, 2H, H4). ^{13}C NMR (126 MHz, $CDCl_3$) δ 164.8 (C1), 157.5 (ArC5), 156.7 (C8), 155.9 (ArC4), 140.3 (ArC4a), 137.8 (ArC1′), 136.6 (ArC8a), 136.2 (ArC7), 133.6 (C6), 131.8 (C5), 130.6 (ArC1), 128.5 (ArC3′, ArC5′), 128.2 (ArC2), 127.6 (ArC4′), 127.1 (ArC2′, ArC6′), 119.4 (C8a), 117.9 (ArC8), 116.4 (ArC4a), 109.8 (C7), 108.6 (ArC6), 107.2 (ArC3), 71.5 (Ar′-CH_2), 56.4 (Ar′-OCH_3), 55.5 (8-OCH_3), 46.8 (C3), 27.9 (1-CH_3), 25.0 (C4), 22.2 (Ar-CH_3). MS (EI): *m/z* 451 (M^+, 80%), 360 (100%). HRMS (ESI) calcd for $C_{30}H_{30}NO_3$: 452.2226, found 452.2234.

5-(4-(Benzyloxy)-5-methoxy-7-methylnaphthalen-1-yl)-6,8-dimethoxy-1-methyl-3,4-dihydroisoquinoline (**43**)

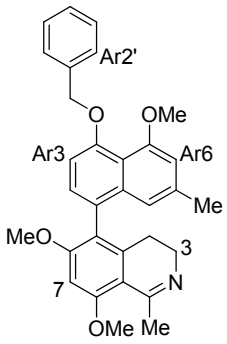

Using the **General Procedure 5**, **37** (256 mg, 0.790 mmol) and **41** (238 mg, 0.720 mmol) gave **43** (175 mg, 51%) as a light brown solid. Mp. 149-150 ^{o}C. IR (neat) υ_{max} 2935 (w), 2835 (w), 2361 (w), 1615 (w), 1578 (s), 1452 (w), 1433 (w), 1370 (w), 1347 (w), 1304 (w), 1269 (m), 1233 (w), 1207 (m), 1180 (w), 1145 (w), 1088 (s), 1023 (w), 826 (w), 737 (m), 697 (m). ^{1}H NMR (500 MHz, $CDCl_3$) δ 7.62 (d, *J* = 7.5 Hz, 2H, ArH2′, ArH6′), 7.42 (t, *J* = 7.6 Hz, 2H, ArH3′, ArH5′), 7.32 (t, *J* = 7.3 Hz, 1H, ArH4′), 7.10 (d, *J* = 7.9 Hz, 1H, ArH2), 6.91 (d, *J* = 7.9 Hz, 1H, ArH3), 6.69 (s, 1H, ArH8), 6.68 (s, 1H, ArH6), 6.52 (s, 1H, H7), 5.22 (s, 2H, Ar′-CH_2), 3.97 (s, 3H, 8-OCH_3), 3.94 (s, 3H, Ar-OCH_3), 3.69 (s, 3H, 6-OCH_3), 3.40-3.17 (m, 2H, H3), 2.51 (s, 3H, 1-CH_3), 2.33 (s, 3H, Ar-CH_3), 2.19-1.96 (m, 2H, H4). ^{13}C NMR (126 MHz, $CDCl_3$) δ 164.4 (C1), 160.1 (C6), 158.6 (C8), 157.5 (ArC5), 155.9 (ArC4), 142.1 (C4a), 138.0 (ArC1′), 136.5 (ArC8a), 136.4 (ArC7), 128.8 (ArC2), 128.4 (ArC3′, ArC5′), 127.6 (ArC4′), 127.1 (ArC2′, ArC6′), 126.4 (ArC1), 120.3 (C5), 117.5 (ArC8), 116.6 (ArC4a), 113.1 (C8a), 108.7 (ArC6), 107.4 (ArC3), 93.9 (C7), 71.4 (Ar′-CH_2), 56.4 (Ar-OCH_3), 55.9 (6-OCH_3), 55.6 (8-OCH_3), 46.7 (C3), 27.9 (1-CH_3), 25.2 (C4), 22.2 (Ar-CH_3). MS (EI): *m/z* 481 (M^+, 90%), 390 (100%). HRMS (ESI) calcd for $C_{31}H_{32}NO_4$: 482.2331, found 482.2329.

5-(4-(Benzyloxy)-5-methoxy-7-methylnaphthalen-1-yl)-3-methyl-3,4-dihydroisoquinolin-1(2H)-one (**100**)

Using the **General Procedure 5**, **37** (71 mg, 0.22 mmol) and **42** (48 mg, 0.20 mmol)

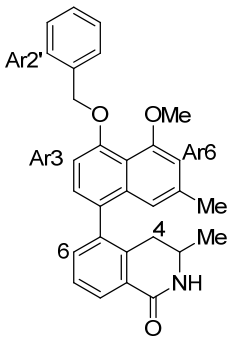

gave **100** (66 mg, 75%) as a light brown solid. Mp. 221 °C. IR (neat) υ_{max} 3190 (w), 3063 (w), 2925 (w), 2362 (w), 1668 (m), 1621 (w), 1578 (s), 1452 (w), 1396 (w), 1370 (m), 1322 (m), 1268 (m), 1240 (w), 1182 (w), 1147 (w), 1111 (w), 1086 (m), 1030 (w), 964 (w), 827 (m), 733 (s), 693 (w), 635 (w), 615 (w). ^{1}H NMR (500 MHz, $CDCl_3$) δ 8.17 (d, *J* = 6.9 Hz, 1H, H8), 7.63 (d, *J* = 7.4 Hz, 2H, ArH2′, ArH6′), 7.47-7.38 (m, 4H, ArH3′, ArH5′, H6, H7), 7.38-7.32 (m, 1H, ArH4′), 7.19 (d, *J* = 7.8 Hz, 1/2H, ArH2), 7.12 (d, *J* = 7.8 Hz, 1/2H, ArH2), 6.92 (d, *J* = 7.8 Hz, 1H, ArH3), 6.77 (s, 1/2H, ArH8), 6.73 (d, *J* = 4.5 Hz, 1H, ArH6), 6.60 (s, 1/2H, ArH8), 6.04 (d, *J* = 4.5 Hz, 1H, NH), 5.25 (s, 2H, $ArCH_2$), 3.97 (s, 3H, OCH_3), 3.73-3.63 (m, 1H, H3), 2.58-2.38 (m, 2H, H4), 2.35 (s, 3/2H, Ar7-CH_3), 2.33 (s, 3/2H, Ar7-CH_3), 1.15 (d, *J* = 3.0 Hz, 3/2H, 3-CH_3), 1.13 (d, *J* = 3.0 Hz, 3/2H, 3-CH_3). ^{13}C NMR (126 MHz, $CDCl_3$) δ 166.7 (C=O), 157.5 (ArC5), 156.2 (ArC4), 140.1 (C5), 137.7 (ArC8a), 137.0 (ArC7), 135.9 (C4a), 134.8 (C6), 134.6 (ArC1′), 130.4 (ArC3′, ArC5′), 128.8 (ArC2′, ArC6′), 128.7 (ArC4′), 128.5 (ArC2), 127.7 (C8a), 127.3 (ArC1), 127.1 (C7), 126.8 (C8), 117.9 (ArC8), 116.2 (ArC4a), 108.7 (ArC6), 107.0 (ArC3), 71.5 (Ar′CH_2), 56.4 (OCH_3), 46.9 (C3), 33.7 (C4), 22.2 (Ar7-CH_3), 21.4 (3-CH_3). MS (EI): *m/z* 437 (M^+, 90%), 91 (100%). HRMS (ESI) calcd for $C_{29}H_{28}NO_3$: 438.2069, found 438.2066.

General procedure 6: Debenzylation of naphthylisoquinoline alkaloids

Benzyl protected naphthylisoquinoline alkaloid (0.10 mmol) was dissolved in MeOH/CH_2Cl_2 (10 mL/5 mL), followed by addition of Pd/C (10 mol%, 5 mg). The resulting mixture was stirred at rt under 1 atm of H_2 for 2 h and then filtered. The filtrate was concentrated and the residue was subjected to flash silica gel column chromatography (hexane/ethyl acetate: 70/30 containing 5% Et_3N) to afford the target

compound as a light brown solid.

8-Methoxy-4-(8-methoxy-1-methyl-1,2,3,4-tetrahydroisoquinolin-5-yl)-6-methylnaphtha len-1-ol (**109**)

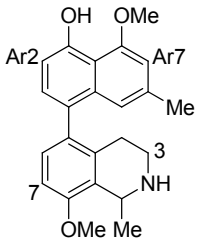

Using the **General procedure 6**, **99** (93 mg, 0.20 mmol) gave **109** (67 mg, 92%) as a brown solid. Mp. 184 ^{o}C (decomp.). IR (neat) υ_{max} 3401 (w), 2944 (w), 2362 (m), 1669 (w), 1615 (w), 1583 (s), 1453 (w), 1436 (w), 1397 (m), 1262 (s), 1126 (w), 1110 (w), 1083 (w), 1034 (w), 957 (w), 820 (m), 733 (w), 637 (w), 613 (w). ^{1}H NMR (500 MHz, CD_3OD) δ 7.19-6.99 (m, 3H, H6, ArH3, H7), 6.82-6.71 (m, 2H, ArH5, ArH2), 6.63 (s, 1H, ArH7), 4.90-4.86 (m, 1H, H1), 4.07 (s, 3H, Ar8-OCH_3), 3.95 (s, 3H, 8-OCH_3), 3.43-3.21 (m, 2H, H3), 2.82-2.55 (m, 2H, H4), 2.31 (s, 3H, Ar6-CH_3), 1.68 (m, 3H, 1-CH_3). ^{13}C NMR (126 MHz, CD_3OD) δ 157.9 (ArC8), 156.6 (C8), 155.6 (ArC1), 137.7 (C4a), 136.5 (ArC4a), 134.7 (ArC6), 132.4 (C5), 132.2 (C6), 130.3 (ArC3), 129.2 (C8a), 123.4 (ArC4), 119.4 (ArC5), 114.6 (ArC8a), 110.0 (ArC2), 109.8 (C7), 107.6 (ArC7), 56.8 (Ar8-OCH_3), 56.2 (8-OCH_3), 48.3 (C1), 37.2 (C3), 24.5 (C4), 22.2 (Ar6-CH_3), 18.1 (1-CH_3). MS (EI): *m/z* 363 (M^+, 30%), 348 (100%). HRMS (ESI) calcd for $C_{23}H_{26}NO_3$: 364.1913, found 364.1926.

4-(6,8-Dimethoxy-1-methyl-3,4-dihydroisoquinolin-5-yl)-8-methoxy-6-methylnaphthale n-1-ol (**44**)

Using the **General procedure 6**, **43** (48 mg, 0.10 mmol) gave **44** (37 mg, 95%) as a brown solid. Mp. 179 ^{o}C (decomp.). IR (neat) υ_{max} 3739 (w), 3396 (w), 2571 (w), 2363 (w), 1644 (w), 1621 (w), 1580 (s), 1430 (m), 1360 (m),1321 (m), 1284 (m), 1257 (m), 1221 (s), 1124 (m), 1085 (s), 1036 (w), 953 (w), 828 (m), 724 (w), 617 (w). ^{1}H NMR

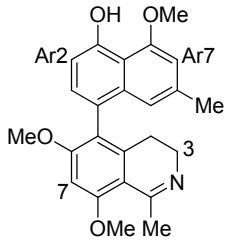

(300 MHz, $CDCl_3$) δ 9.48 (s, 1H, OH), 7.04 (d, *J* = 7.8 Hz, 1H, ArH3), 6.86 (d, *J* = 7.8 Hz, 1H, ArH2), 6.66 (s, 1H, ArH5), 6.57 (s, 1H, ArH7), 6.54 (s, 1H, H7), 4.10 (s, 3H, Ar8-OCH_3), 4.08 (s, 3H, 8-OCH_3), 3.81 (s, 3H, 6-OCH_3), 3.64-3.40 (m, 2H, H3), 3.01 (s, 3H, 1-CH_3), 2.60-2.39 (m, 2H, H4), 2.35 (s, 3H, Ar6-CH_3). ^{13}C NMR (75 MHz, $CDCl_3$) δ 173.9 (C1), 166.1 (C6), 163.8 (ArC8), 156.5 (C8), 154.9 (ArC1), 140.7 (ArC4a), 136.7 (ArC6), 135.0 (C4a), 129.9 (ArC3), 121.9 (ArC4), 121.4 (C8a), 117.3 (ArC7), 113.5 (C5), 109.4 (ArC2), 108.4 (C8a), 106.6 (ArC5), 94.0 (ArC7), 56.26 (OCH_3), 56.23 (OCH_3), 56.15 (OCH_3), 39.9 (C3), 24.5 (C4), 24.2 (1-CH_3), 22.3 (Ar-CH_3). MS (EI): *m/z* 391 (M^+, 100%). HRMS (ESI) calcd for $C_{24}H_{26}NO_4$: 392.1862, found 392.1870.

5-(4-Hydroxy-5-methoxy-7-methylnaphthalen-1-yl)-3-methyl-3,4-dihydroisoquinolin-1(2H)-one (**107**)

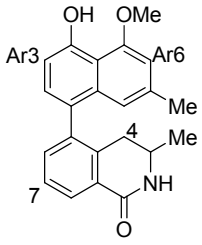

Using the **General procedure 6**, **100** (88 mg, 0.20 mmol) gave **107** (76 mg, 94%) as a brown solid. Mp. 210-211 °C. IR (neat) υ_{max} 3421 (w), 3200 (w), 2962 (w), 1671 (s), 1616 (w), 1588 (w), 1433 (m), 1397 (m), 1258 (s), 1175 (w), 1130 (m), 1097 (w), 1032 (w), 957 (w), 824 (m), 755 (w), 614 (m). ^{1}H NMR (500 MHz, $CDCl_3$) δ 9.44 (s, 1H, OH), 8.15 (d, *J* = 6.6 Hz, 1H, H8), 7.51-7.34 (m, 2H, H7, H6), 7.18 (d, *J* = 7.8 Hz, 1/2H, ArH2), 7.11 (d, *J* = 7.8 Hz, 1/2H, ArH2), 6.86 (d, *J* = 7.6 Hz, 1H, ArH3), 6.79 (s, 1/2H, ArH8), 6.71 (bs, 1H, NH), 6.66 (s, 1H, ArH6), 6.62 (s, 1/2H, ArH8), 4.08 (s, 3H, OCH_3), 3.73-3.61 (m, 1H, CH), 2.56-2.39 (m, 2H, H4), 2.34 (s, 3/2H, Ar7-CH_3), 2.33 (s, 3/2H, Ar7-CH_3), 1.15 (d, *J* = 5.4 Hz, 3H, 3-CH_3). ^{13}C NMR (126 MHz, CDCl3) δ 156.5 (C=O), 154.61 (ArC5), 154.57 (ArC4), 139.7 (C5), 137.6 (ArC8a), 136.4 (ArC7), 135.2 (C4a), 134.8

(C6), 128.9 (ArC2), 128.2 (C8a), 127.8 (ArC1), 127.3 (C8), 126.6 (C7), 118.7 (ArC8), 113.4 (ArC4a), 109.3 (ArC3), 106.7 (ArC6), 56.4 (OCH_3), 46.8 (C3), 33.7 (C4), 22.2 (Ar7-CH_3), 21.3 (3-CH_3). MS (ESI): *m/z* 348 ($[M+H]^+$, 100%). HRMS (ESI) calcd for $C_{22}H_{22}NO_3$: 348.1600, found 348.1594.

General procedure 7: Suzuki coupling of naphthyl boronic ester and halogenated isoquinolines

A mixture of boronic ester **38** (0.10 mmL), halogenated isoquinoline (0.10 mmol), K_2CO_3 (0.40 mmol) and $PdCl_2$(dppf) (5 mol%) in dry dioxane (30 mL) was heated at reflux in a sealed tube under N_2 for 24 h. The mixture was cooled to rt, diluted with H_2O (10 mL) and extracted with EtOAc (3 × 20 mL). The combined organic layers were washed with brine (25 mL), dried (Na_2SO_4), filtered, evaporated and the residue subjected to flash silica gel column chromatography (hexane/ethyl acetate: 50/50 containing 5% Et_3N) to give the target naphthylisoquinoline alkaloids.

Ethyl 5-isopropoxy-4-methoxy-8-(8-methoxy-1-methyl-3,4-dihydroisoquinolin-5-yl)-2-naphthoate (**96**)

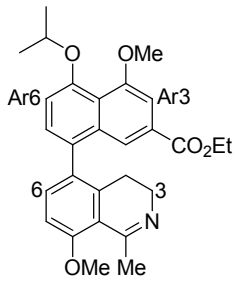

Using the **General procedure 7**, **38** (62 mg, 0.15 mmol) and **39** (38 mg, 0.15 mmol) gave **96** (40 mg, 58%) as a brown semi-solid. IR (neat) υ_{max} 2934 (w), 2858 (w), 1713 (s), 1617 (w), 1585 (m), 1460 (w), 1369 (m), 1275 (s), 1224 (m), 1195 (s), 1030 (m), 949 (w), 916 (w), 835 (w), 762 (m), 692 (w). ^{1}H NMR (500 MHz, $CDCl_3$) δ 7.78 (d, *J* = 1.0 Hz, 1H, ArH1), 7.39 (bs, 1H, ArH3), 7.28 (d, *J* = 8.5 Hz, 1H, H6), 7.25 (d, *J* = 7.9 Hz, 1H, ArH7), 7.06 (d, *J* = 7.9 Hz, 1H, ArH6), 6.97 (d, *J* = 8.5 Hz, 1H, H7), 4.66-4.54 (m, 1H, C<u>H</u>$(CH_3)_2$), 4.38-4.27 (m, 2H, C<u>H</u>$_2$$CH_3$), 4.02 (s, 3H, Ar4-$OCH_3$), 3.95 (s, 3H,

8-OCH_3), 3.40-3.29 (m, 2H, H3), 2.54 (s, 3H, 1-CH_3), 2.16 (t, J = 7.0 Hz, 2H, H4), 1.45 (d, J = 1.4 Hz, 6H, CH($C\underline{H}_3$)$_2$), 1.33 (t, J = 7.1 Hz, 3H, $CH_2C\underline{H}_3$). ^{13}C NMR (75 MHz, $CDCl_3$) δ 166.8 (C=O), 164.9 (C1), 157.8 (ArC4), 156.9 (C8), 154.7 (ArC5), 140.2 (C4a), 135.3 (ArC8a), 133.7 (C6), 132.8 (ArC8), 130.8 (C5), 128.9 (ArC7), 128.1 (ArC2), 121.8 (ArC1), 121.4 (ArC4a), 119.4 (C8a), 114.2 (ArC6), 109.9 (C7), 105.1 (ArC3), 73.3 ($\underline{C}H(CH_3)_2$), 61.2 ($\underline{C}H_2CH_3$), 56.5 (Ar4-OCH_3), 55.6 (8-OCH_3), 46.5 (C3), 27.8 (1-CH_3), 25.2 (C4), 24.9 ($CH_2\underline{C}H_3$), 22.3 (CH($\underline{C}H_3$)$_2$), 22.2 (CH($\underline{C}H_3$)$_2$). MS (EI): *m/z* 461 (M^+, 70%), 404 (100%). HRMS (ESI) calcd for $C_{28}H_{32}NO_5$ 462.2280, found 462.2290.

Ethyl 8-(6,8-dimethoxy-1-methyl-3,4-dihydroisoquinolin-5-yl)-5-isopropoxy-4-methoxy-2-naphthoate (**97**)

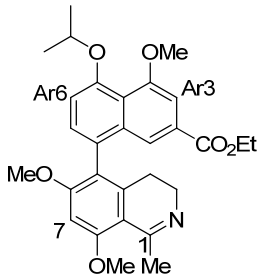

Using the **General procedure 7**, **38** (133 mg, 0.40 mmol) and **41** (132 mg, 0.40 mmol) gave **97** (87 mg, 44%) as a brown solid. Mp. 57-58 °C. IR (neat) υ_{max} 3743 (w), 2974 (w), 1713 (m), 1616 (w), 1579 (s), 1515 (w), 1455 (m), 1373 (w), 1345 (w), 1304 (w), 1275 (m), 1230 (s), 1116 (s), 1086 (s), 1024 (m), 927 (w), 817 (w), 766 (w), 721 (w). ^{1}H NMR (500 MHz, $CDCl_3$) δ 7.71 (s, 1H, ArH1), 7.37 (s, 1H, ArH3), 7.20 (d, J = 7.7 Hz, 1H, ArH7), 7.06 (d, J = 7.8 Hz, 1H, ArH6), 6.52 (s, 1H, H7), 4.65-4.56 (m, 1H, CH), 4.37-4.28 (m, 2H, $C\underline{H}_2CH_3$), 4.01 (s, 3H, Ar4-OCH_3), 3.97 (s, 3H, 8-OCH_3), 3.68 (s, 3H, 6-OCH_3), 3.41-3.17 (m, 2H, H3), 2.51 (s, 3H, 1-CH_3), 2.19-1.94 (m, 2H, H4), 1.45 (d, J = 5.5 Hz, 6H, CH($C\underline{H}_3$)$_2$), 1.33 (t, J = 6.8 Hz, 3H, $CH_2C\underline{H}_3$). ^{13}C NMR (126 MHz, $CDCl_3$) δ 166.8 (C=O), 164.4 (C1), 160.0 (C8), 158.9 (ArC4), 157.8 (C6), 154.7 (ArC5), 141.9 (ArC8a), 135.6 (C4a), 129.6 (ArC7), 128.6 (ArC8), 128.0 (ArC2), 121.74 (ArC1), 121.70 (ArC4a), 119.4 (C5), 114.1 (ArC6), 113.2 (C8a), 105.2 (ArC3), 94.1 (C7), 73.0

(<u>C</u>H), 61.0 (<u>C</u>H_2CH_3), 56.6 (Ar4-OCH_3), 55.8 (8-OCH_3), 55.6 (6-OCH_3), 46.6 (C3), 27.8 (1-CH_3), 25.3 (C4), 22.3 (2 × CH_3), 14.4 (CH_2<u>C</u>H_3). MS (EI): *m/z* 491 (M^+, 90%), 434 (100%). HRMS (ESI) calcd for $C_{29}H_{34}NO_6$: 492.2386, found 492.2403.

Ethyl 5-isopropoxy-4-methoxy-8-(3-methyl-1-oxo-1,2,3,4-tetrahydroisoquinolin-5-yl)-2-naphthoate (**98**)

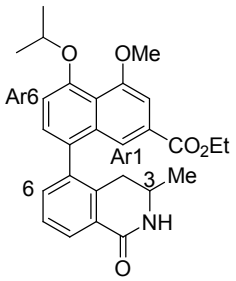

Using the **General procedure 7**, **38** (104 mg, 0.25 mmol) and **42** (60 mg, 0.25 mmol) gave **98** (60 mg, 54%) as a brown solid. Mp. 203-204 ^oC. IR (neat) υ_{max} 2975 (w), 1715 (m), 1669 (s), 1583 (s), 1444 (w), 1372 (s), 1331 (w), 1275 (s), 1227 (s), 1191 (w), 1119 (s), 1018 (m), 918 (w), 817 (w), 762 (m), 727 (m), 687 (w). ^1H NMR (500 MHz, $CDCl_3$) δ 8.19 (t, *J* = 6.5 Hz, 1H, H8), 7.78 (s, 1/2H, ArH1), 7.60 (s, 1/2H, ArH1), 7.49-7.39 (m, 3H, H6, H7, ArH3), 7.28 (d, *J* = 8.1 Hz, 1/2H, ArH7), 7.23 (d, *J* = 7.9 Hz, 1/2H, ArH7), 7.07 (dd, *J* = 7.9, 2.7 Hz, 1H, ArH6), 6.26 (s, 1/2H, NH), 6.20 (s, 1/2H, NH), 4.64 (m, 1H, C<u>H</u>$(CH_3)_2$), 4.38-4.27 (m, 2H, C<u>H</u>$_2CH_3$), 4.03 (s, 3H, OCH_3), 3.79-3.63 (m, 1H, H3), 2.54-2.30 (m, 2H, H4), 1.47 (d, *J* = 5.9 Hz, 6H, CH(C<u>H</u>$_3)_2$), 1.30 (m, 3H, CH_2C<u>H</u>$_3$), 1.15 (t, *J* = 5.9 Hz, 3H, 3-CH_3). ^{13}C NMR (126 MHz, $CDCl_3$) δ 166.7 (C=O), 166.5 (C1), 158.0 (ArC4), 155.2 (ArC5), 139.3 (ArC8a), 137.4 (C5), 135.1 (C4a), 134.6 (C6), 132.4 (ArC8), 129.1 (C8a), 128.6 (ArC7), 128.4 (ArC2), 127.7 (C8), 126.9 (C7), 121.5 (ArC4a), 121.3 (ArC1), 113.7 (ArC6), 105.4 (ArC3), 73.1 (<u>C</u>H$(CH_3)_2$), 61.2 (<u>C</u>H_2CH_3), 56.5 (OCH_3), 46.8 (C3), 34.3 (C4), 22.3 (2×CH_3), 21.4 (CH_2<u>C</u>H_3), 14.4 (3-CH_3). MS (EI): *m/z* 447 (M^+, 70%), 390 (100%). HRMS (ESI) calcd for $C_{27}H_{30}NO_5$: 448.2124, found 448.2135.

7.1.2.4 Preparation of michellamine B analogues by oxidative dimerization

General procedure 8: Oxidative dimerization of the naphthylisoquinoline alkaloids

A solution of naphthylisoquinoline (0.010 mmol) in dry CH_2Cl_2 (10 mL) containing 0.2% NEt_3 was treated with Ag_2O (116 mg, 0.50 mmol). After 18 h stirring at rt in air, the solvent was removed and the residue was subjected to a short flash silica gel column chromatography (CH_2Cl_2/methanol: 50:1) to afford the deep-violet coloured intermediate. The intermediate was hydrogenated using a hydrogen balloon in ethanol (3 mL) in the presence of Pd/C 10% (5 mg) for 1 h. After evaporation of the solvent, the residue subjected to a flash silica gel column chromatography (CH_2Cl_2/methanol: 10/1) to afford the target michellamine analogues as a brown solid.

1,1'-Dihydroxy-8,8'-dimethoxy-6,6'-dimethyl-[2,2'-binaphthalene]-4,4'-diyl bis(2,2-dimethylpropanoate) (**111**)

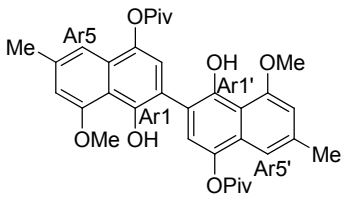

Using the **General procedure 8**, **63** (29 mg, 0.10 mmol) gave the **111** (12 mg, 42%) as a brown solid. Mp. 246-247 ^{o}C. IR (neat) υ_{max} 3744 (w), 3363 (w), 2967 (w), 1748 (m), 1625 (w), 1459 (m), 1403 (m), 1354 (w), 1280 (w), 1250 (w), 1112 (s), 1039 (m), 958 (w), 902 (w), 830 (w), 762 (w), 620 (w). ^{1}H NMR (500 MHz, $CDCl_3$) δ 9.59 (s, 2H, 2 × OH), 7.21 (s, 2H, ArH3, ArH3′), 7.13 (s, 2H, ArH5, ArH5′), 6.64 (s, 2H, ArH7, ArH7′), 4.01 (s, 6H, 2×OCH_3), 2.46 (s, 6H, 2×CH_3), 1.46 (s, 18H, 3×CH_3). ^{13}C NMR (126 MHz, $CDCl_3$) δ 177.5 (2×C=O), 156.5 (ArC8, ArC8′), 149.4 (ArC1, ArC1′), 138.1 (ArC4, ArC4′), 136.3 (ArC6, ArC6′), 129.4 (ArC4a, ArC4a′), 123.1 (ArC3, ArC3′), 118.1 (ArC2, ArC2′), 114.11 (ArC5, ArC5′), 114.08 (ArC8a, ArC8a′), 107.1 (ArC7, ArC7′), 56.3 (OCH_3), 39.4 ($\underline{C}CH_3$), 27.6 (3×CH_3), 22.5

(CH_3). MS (EI): *m/z* 574 (M^+, 100%). HRMS (ESI) calcd for $C_{34}H_{39}O_8$: 575.2645, found 575.2647.

5,5'-(1,1'-Dihydroxy-8,8'-dimethoxy-6,6'-dimethyl-[2,2'-binaphthalene]-4,4'-diyl)bis(3-methyl-3,4-dihydroisoquinolin-1(2H)-one) (**113**)

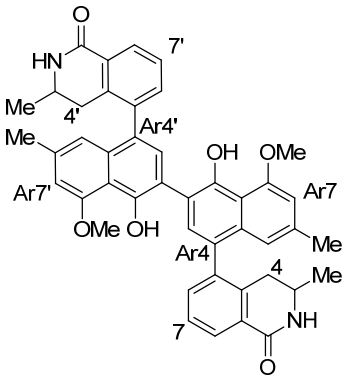

Using the **General procedure 8**, **107** (11 mg, 0.030 mmol) gave the **113** (3.6 mg, 35%) as a brown solid. Mp. 236-237 ^oC. IR (neat) υ_{max} 3744 (w), 3363 (w), 2967 (w), 1748 (m), 1625 (w), 1459 (w), 1403 (m), 1354 (m), 1280 (w), 1250 (w), 1112 (s), 1039 (m), 958 (w), 902 (w), 830 (w), 762 (w), 620 (w). ^1H NMR (500 MHz, CD_3OD) δ 7.98 (bs, 2H, H8, H8′), 7.39-7.17 (m, 6H, H6, H6′, H7, H7′, ArH3, ArH3′), 6.79 (s, 2H, ArH5, ArH5′), 6.72 (s, 1H, ArH7, ArH7′), 6.60 (s, 1H, ArH7, ArH7′), 4.04 (s, 3H, Ar8-OCH_3), 4.03 (s, 3H, Ar8′-OCH_3), 3.63-3.46 (m, 2H, H3, H3′), 2.64-2.34 (m, 4H, H4, H4′), 2.30 (s, 6H, Ar6-CH_3, Ar6′-CH_3), 1.08-1.02 (m, 6H, 3-CH_3, 3′-CH_3). ^{13}C NMR (126 MHz, CD3OD) δ 158.0 (C=O), 152.4 (ArC8, ArC8′), 152.3 (ArC1, ArC1′), 141.5 (C5, C5′), 139.0 (ArC4a, ArC4a′), 137.7 (C4a, C4a′), 136.1 (C6, C6′), 135.6 (ArC6, ArC6′), 133.8 (ArC3, ArC3′), 129.9 (C8a, C8a′), 128.2 (ArC4, ArC4′), 127.7 (C7, C7′), 127.5 (C8, C8′), 119.6 (ArC2, ArC2′), 119.1 (ArC7, ArC7′), 114.7 (ArC8a, ArC8a′), 107.9 (ArC5, ArC5′), 56.9 (OCH_3), 47.6 (C3, C3′), 34.7 (C4, C4′), 21.08 (Ar7-CH_3, Ar7′-CH_3), 20.97 (3-CH_3, 3′-CH_3). MS (ESI): *m/z* 693 ($[M+H]^+$, 80%). HRMS (ESI) calcd for $C_{44}H_{41}N_2O_6$: 693.2965, found 693.2996.

4,4′-Bis(6,8-dimethoxy-1-methyl-3,4-dihydroisoquinolin-5-yl)-8,8′-dimethoxy-6,6′-dimethyl-[2,2′-binaphthalene]-1,1′-diol (**112**)

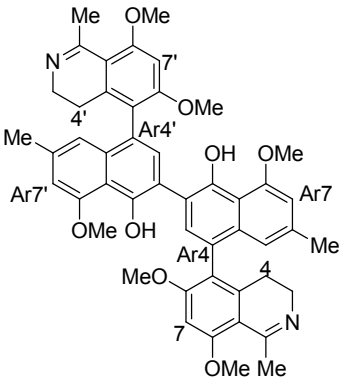

Using the **General procedure 8**, **44** (10 mg, 0.025 mmol) gave the **112** (3.0 mg, 31%) as a brown solid. Mp. 215 ^{o}C (decomp.). IR (neat) υ_{max} 3743 (w), 3364 (w), 2967 (w), 1750 (w), 1654 (s), 1585 (s), 1455 (w), 1402 (s), 1358 (m), 1262 (m), 1158 (m), 1100 (s), 1023 (m), 959 (w), 902 (w), 830 (m), 757 (m), 612 (w). ^{1}H NMR (500 MHz, CD_3OD) δ 7.26 (s, 1H, ArH3 or ArH3′), 7.25 (s, 1H, ArH3 or ArH3′), 6.84 (s, 2H, ArH7 or ArH7′ or H7 or H7′), 6.83 (s, 2H, ArH7 or ArH7′ or H7 or H7′), 6.65 (s, 2H, ArH5 or ArH5′), 4.14 (s, 6H, Ar8-OCH_3, Ar8′-OCH_3), 4.09 (s, 6H, 8-OCH_3, 8′-OCH_3), 3.85 (s, 3H, 6-OCH_3 or 6′-OCH_3), 3.84 (s, 3H, 6-OCH_3 or 6′-OCH_3), 3.61-3.43 (m, 4H, H3, H3′), 2.81 (s, 3H, 1-CH_3 or 1′-CH_3), 2.80 (s, 3H, 1-CH_3 or 1′-CH_3), 2.55-2.42 (m, 4H, H4, H4′), 2.33 (s, 6H, Ar6-CH_3, Ar6′-CH_3). ^{13}C NMR (126 MHz, CD_3OD) δ 176.0 (C1, C1′), 168.2 (C6, C6′), 166.0 (ArC8, ArC8′), 158.1 (C8, C8′), 152.6 (ArC1, ArC1′), 142.2 (C4a, C4a′), 137.8 (ArC6, ArC6′), 136.0 (ArC4a, ArC4a′), 134.5 (ArC3, ArC3′), 123.0 (ArC4, ArC4′), 122.7 (ArC2, ArC2′), 119.9 (C5, C5′), 118.7 (ArC5, ArC5′), 114.9 (ArC8a, ArC8a′), 109.6 (C8a, C8a′), 108.0 (ArC7, ArC7′), 95.8 (C7, C7′), 57.1 (Ar8-OCH_3, Ar8′-OCH_3 or 8-OCH_3, 8′-OCH_3), 57.0 (Ar8-OCH_3, Ar8′-OCH_3 or 8-OCH_3, 8′-OCH_3), 56.9 (6-OCH_3, 6′-OCH_3), 41.7 (C3, C3′), 25.74 (C4, C4′ or 1-CH_3, 1′-CH_3), 25.72 (C4, C4′ or 1-CH_3, 1′-CH_3), 22.1 (Ar6-CH_3, Ar6′-CH_3). MS (ESI): *m/z* 781 ($[M+H]^+$, 40%). HRMS (ESI) calcd for $C_{48}H_{48}N_2O_8$: 781.3489, found 781.3528.

7.1.3 Preparation of coelenterazine analogues

7.1.3.1 Synthesis of substituted 2-aminopyridine

2-Amino-5-bromonicotinic acid (**130**)

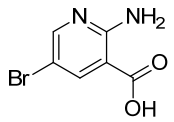

This is a known compound but not fully characterized, and it was prepared according to the known procedure.[141] To a suspension of 2-aminonicotinic acid **124** (7.50 g, 54 mmol) in glacial acetic acid (30 mL) was added a solution of bromine (3.60 mL, 69 mmol) in glacial acetic acid (5 mL) and the mixture stirred at rt for 20 h. The resulting precipitate was filtered and washed with glacial acetic acid until the filtrate remained colourless. The remaining solid was air dried and then recrystallized from boiling methanol to afford **130** (11.3 g, 97%) as a white crystalline needle. Mp. 247-249 ^{o}C. IR (neat) υ_{max} 3301 (m), 2942 (w), 2871 (w), 2013 (w), 1704 (s), 1635 (m), 1522 (m), 1451 (m), 1361 (m), 1305 (s), 1239 (m), 1036 (s), 879 (m), 796 (m), 703 (s) cm^{-1}. ^{1}H NMR (500 MHz, DMSO) δ 8.44 (d, *J* = 2.5 Hz, 1H, ArH4), 8.33 (d, *J* = 2.5 Hz, 1H, ArH6), 7.67 (bs, 2H, NH_2). ^{13}C NMR (126 MHz, DMSO) δ 166.1 (C=O), 155.2 (ArC2), 147.3 (ArC6), 145.5 (ArC4), 110.9 (ArC3), 103.6 (ArC5). MS (EI): *m/z* 216 (M^+, ^{79}Br, 100%) 218 (M^+, ^{81}Br, 100%). HRMS (ESI): calcd for $C_6H_6N_2O_2{}^{79}Br$ 216.9613, found 216.9612.

2-Amino-5-bromo-N-methoxy-N-methylnicotinamide (**131**)

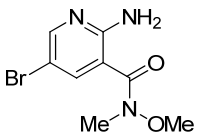

This is a known compound but not fully characterized, and it was prepared by a new procedure.[142] To a solution of 2-amino-6-chloronicotinic acid **130** (4.99 g, 29.0 mmol) in anhydrous DMF (50 mL) was added 1-hydroxybenzotriazole hydrate (HOBt) (6.21 g, 40.6 mmol) and *N*,*N*,*N*′,*N*′-tetramethyl-*O*-(1*H*-benzotriazol-1-yl)uronium hexafluorophosphate (HBTU)

(15.4 g, 40.6 mmol). A solution of *N,O*-dimethylhydroxylamine hydrochloride (306 mg, 3.15 mmol) in anhydrous DMF (15 mL) was treated with *N,N*-diisopropylethylamine (8.28 g, 64.1 mmol) and immediately added to the reaction. The mixture was stirred at 0 ^{o}C for 10 min and then at rt for 5 h. The reaction was diluted with EtOAc (150 mL) and H_2O (100 mL) and the aqueous layer was then extracted with EtOAc (3 x 150 mL). The combined organic layers were washed with H_2O, brine, then concentrated and the residue subjected to flash silica gel column chromatography (hexane/ethyl acetate: 80/20) to give **131** (4.72 g, 74%) as a light yellow solid. Mp. 82-83 ^{o}C. IR (neat) υ_{max} 3420 (m), 3275 (w), 3140 (m), 1626 (s), 1557 (s), 1448 (m), 1376 (s), 1240 (m), 1199 (m), 1164 (w), 1131 (w), 1052 (m), 977 (s), 908 (m), 838 (m), 781 (m), 738 (m), 677 (m), 627 (m) cm^{-1}. ^{1}H NMR (500 MHz, $CDCl_3$) δ 8.15 (s, 1H, ArH4), 7.89 (s, 1H, ArH6), 5.78 (s, 2H, NH_2), 3.57 (s, 3H, OCH_3), 3.35 (s, 3H, NCH_3). ^{13}C NMR (126 MHz, $CDCl_3$) δ 167.1 (C=O), 156.7 (ArC2), 151.3 (ArC6), 140.0 (ArC4), 111.8 (ArC3), 106.1 (ArC5), 61.5 (OCH_3), 33.4 (NCH_3). MS (EI): *m/z* 259 (M^+, ^{79}Br, 20%), 261 (M^+, ^{81}Br, 20%), 199 (100%), 201 (100%). HRMS (ESI): calcd for $C_8H_{11}N_3O_2{}^{79}Br$ 260.0035, found 260.0025.

(2-Amino-5-bromopyridin-3-yl)(phenyl)methanone (**125**)

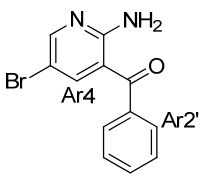

This is a known compound but not fully characterized, and it was prepared according to the known procedure.[143] A suspension of 2-amino-5-bromo-*N*-methoxy-*N*-methyl-nicotinamide **131** (1.00 g, 3.38 mmol) in anhydrous THF (50 mL) was cooled to −50 °C under N_2 and a 1.0 M solution of phenylmagnesium bromide in ether (13.50 mL, 13.50 mmol) was added rapidly affording an orange solution. The mixture was stirred and slowly warmed to rt over 1 h. The resulting yellow-orange solution was diluted with a 10% (w/w) aqueous

citric acid solution (75 mL) and EtOAc (200 mL). The organic phase was separated and washed with a 10% (w/w) aqueous citric acid solution (75 mL) and saturated aqueous $NaHCO_3$ (75 mL). The organic phase was then dried (Na_2SO_4) and concentrated to afford **125** (936 mg, 95%) as a yellow crystalline solid without any further purification required. Mp. 145-146 ^oC. IR (neat) υ_{max} 3417 (m), 3272 (w), 3126 (m), 1631 (s), 1569 (w), 1537 (m), 1448 (m), 1390 (m), 1347 (w), 1293 (m), 1222 (s), 1148 (m), 1072 (w), 1031 (w), 1002 (w), 946 (m), 917 (w), 844 (m), 803 (w), 769 (m), 746 (w), 700 (s), 650 (s) cm^{-1}. ^1H NMR (500 MHz, $CDCl_3$) δ 8.28 (d, J = 2.0 Hz, 1H, ArH4), 7.85 (d, J = 1.9 Hz, 1H, ArH6), 7.64-7.55 (m, 3H, ArH2′, ArH4′, ArH6′), 7.51 (t, J = 7.5 Hz, 2H, ArH3′, ArH5′), 6.79 (bs, 2H, NH_2). ^{13}C NMR (126 MHz, $CDCl_3$) δ 196.8 (C=O), 158.3 (ArC2), 154.6 (ArC6), 144.3 (ArC4), 138.5 (ArC1′), 132.1 (ArC4′), 129.1 (ArC2′, ArC6′), 128.7 (ArC3′, ArC5′), 114.1 (ArC3), 105.4 (ArC5). MS (EI): *m/z* 276 (M^+, ^{79}Br, 100%), 278 (M^+, ^{81}Br, 100%). HRMS (ESI): calcd for $C_{12}H_{10}N_2O^{79}Br$ 276.9976, found 276.9975.

(2-Amino-5-(4-methoxyphenyl)pyridin-3-yl)(phenyl)methanone (**132**)

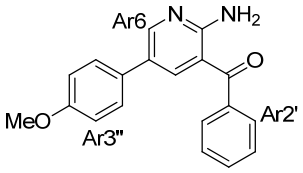

A mixture of (2-amino-5-bromopyridin-3-yl)(phenyl) -methanone **125** (200 mg, 0.72 mmol), 4-methoxyphenyl -boronic acid (164 mg, 1.1 mmol), $Pd(dppf)Cl_2$ (26 mg, 0.036 mmol) and $NaHCO_3$ (185 mg, 2.2 mmol) in toluene (20 mL) was heated at reflux for 12 h under N_2. The mixture was cooled to rt, diluted with H_2O (10 mL) and extracted with EtOAc (3 × 20 mL). The combined organic layers were dried ($MgSO_4$) and concentrated, and the residue subjected to flash silica gel column chromatography (hexane/ethyl acetate: 60/40) to give **132** (187 mg, 85%) as a yellow solid. Mp. 156-157 ^oC. IR (neat) υ_{max} 3388 (m), 3145 (w), 1619 (m), 1546 (m), 1511 (m), 1456 (m), 1442 (m), 1387 (w), 1328 (w), 1303 (w), 1227 (s), 1178 (m), 1142 (w), 1029 (m), 956 (m),

926 (m), 854 (m), 823 (m), 807 (m), 772 (m), 702 (m), 657 (m) cm^{-1}. ^1H NMR (500 MHz, $CDCl_3$) δ 8.48 (s, 1H, ArH6), 7.93 (s, 1H, ArH4), 7.67 (d, *J* = 8.0 Hz, 2H, ArH2′, ArH6′), 7.57 (t, *J* = 7.0 Hz, 1H, ArH4′), 7.49 (t, *J* = 7.5 Hz, 2H, ArH3′, ArH5′), 7.34 (d, *J* = 9.0 Hz, 2H, ArH2″, ArH6″), 6.94 (d, *J* = 8.5 Hz, 2H, ArH3″, ArH5″), 6.82 (bs, 2H, NH_2), 3.82 (s, 3H, OCH_3). ^{13}C NMR (126 MHz, $CDCl_3$) δ 196.0 (C=O), 159.3 (ArC4″), 158.6 (ArC2), 152.1 (ArC6), 140.8 (ArC4), 139.3 (ArC1′), 131.9 (ArC4′), 130.1 (ArC1″), 129.3 (ArC2′, ArC6′), 128.7 (ArC3′, ArC5′), 127.5 (ArC2″, ArC6″), 125.7 (ArC5), 114.7 (ArC3″, ArC5″), 112.9 (ArC3), 55.6 (OCH_3). MS (EI): *m/z* 304 (M^+, 100%). HRMS (ESI): calcd for $C_{19}H_{17}N_2O_2$ 305.1290, found 305.1286.

(2-Amino-5-(4-hydroxyphenyl)pyridin-3-yl)(phenyl)methanone (**133**)

Strategy 1

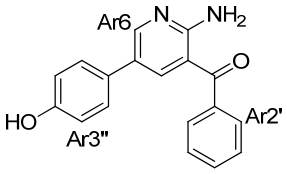

A mixture of (2-amino-5-(4-methoxyphenyl)pyridin-3-yl) -(phenyl)methanone **132** (304 mg, 1.0 mmol) and sodium ethanethiolate (494 mg, 5 mmol) in DMF (5 mL) was heated at 100 °C for 20 h under N_2 atmosphere. The resulting mixture was then quenched with a saturated aqueous NH_4Cl solution (20 mL), extracted with EtOAc (5 × 50 mL) and the combined organic layers were washed with brine (25 mL), dried (Na_2SO_4), filtered, evaporated and the residue subjected to flash silica gel column chromatography (hexane/ethyl acetate: 60/40) to give **133** (238 mg, 82%) as a pale yellow solid. Mp. 215-216 ^oC. IR (neat) υ_{max} 3489 (w), 3343 (m), 1640 (m), 1612 (w), 1600 (w), 1576 (m), 1550 (w), 1512 (m), 1441 (m), 1349 (w), 1325 (w), 1265 (m), 1231 (s), 1173 (m), 956 (m), 833 (m), 773 (m), 708 (m), 694 (m) cm^{-1}. ^1H NMR (500 MHz, DMSO) δ 9.46 (s, 1H, OH), 8.50 (s, 1H, ArH4), 7.60 (s, 1H, ArH6), 7.61-7.66 (m, 3H, ArH2′, ArH4′,

ArH6′), 7.54-7.57 (m, 4H, ArH3′, ArH5′, NH_2), 7.30 (d, *J* = 8.0 Hz, 2H, ArH2″, ArH6″), 6.79 (d, *J* = 8.5 Hz, 2H, ArH3″, ArH5″). ^{13}C NMR (126 MHz, DMSO) δ 197.1 (C=O), 158.3 (ArC4″), 156.7 (ArC2), 151.7 (ArC6), 139.2 (ArC4), 138.9 (ArC1′), 131.6 (ArC4′), 128.8 (ArC2′, ArC6′), 128.5 (ArC2″, ArC6″), 127.7 (ArC1″), 126.8 (ArC3′, ArC5′), 123.9 (ArC5), 115.8 (ArC3″, ArC5″), 111.3 (ArC3). MS (EI): *m/z* 290 (M^+, 100%). HRMS (ESI): calcd for $C_{18}H_{15}N_2O_2$ 291.1134, found 291.1135.

Strategy 2

A mixture of (2-amino-5-bromopyridin-3-yl)(phenyl)methanone **125** (1.50 g, 5.40 mmol), 4-hydroxylphenylboronic acid (1.12 g, 8.10 mmol), $PdCl_2(PPh_3)_2$ (190 mg, 0.270 mmol) and Na_2CO_3 (1.72 g, 16.2 mmol) in dioxane (40 mL) under N_2 was heated and stirred at reflux for 18 h. The mixture was cooled to rt, diluted with H_2O (10 mL) and extracted with EtOAc (3 × 20 mL). The combined organic layers were washed with brine (25 mL), dried (Na_2SO_4), filtered, evaporated and the residue subjected to flash silica gel column chromatography (hexane/ethyl acetate: 60/40) to give **133** (1.43 g, 91%) as a yellow solid.

4-(6-Amino-5-benzylpyridin-3-yl)phenol (**126**)

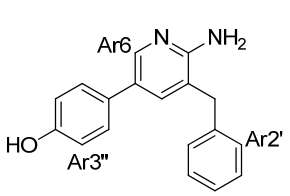

A stirred mixture of (2-amino-5-(4-hydroxyphenyl) -pyridin-3-yl)(phenyl)methanone **133** (290 mg, 1.0 mmol), ethylene glycol (2 mL) and hydrazine hydrate (0.5 mL) was heated at 100 °C for 1 h and then allowed to cool to rt. KOH pellets (500 mg) were added and the resulting mixture was heated in a sand bath at 240 °C for 1 h. After cooling to rt, the reaction mixture was diluted with H_2O (20 mL) and extracted with EtOAc (5 × 50 mL). The combined organic layers were washed with dilute aqueous

HCl solution (30 mL), dried ($MgSO_4$), concentrated and the residue subjected to flash silica gel column chromatography (hexane/ethyl acetate: 50/50) to give **126** (237 mg, 86%) as a white solid. Mp. 195-196 ^oC. IR (neat) υ_{max} 3241 (w), 3194 (w), 1653 (s), 1614 (s), 1574 (m), 1519 (m), 1451 (m), 1342 (m), 1269 (m), 1230 (m), 1177 (m), 823 (s), 741 (s), 697 (m), 627 (m) cm^{-1}. ^1H NMR (500 MHz, DMSO) δ 9.73 (s, 1H, OH), 8.14 (s, 1H, ArH6), 8.03 (s, 1H, ArH4), 7.80 (s, 2H, NH_2), 7.42 (d, *J* = 8.4 Hz, 2H, ArH2″, ArH6″), 7.38-7.29 (m, 4H, ArH2′, ArH3′, ArH5′, ArH6′), 7.28-7.19 (m, 1H, ArH4′), 6.85 (d, *J* = 8.3 Hz, 2H, ArH3″, ArH5″), 4.02 (s, 2H, $ArCH_2$). ^{13}C NMR (126 MHz, DMSO) δ 157.7 (ArC4″), 151.7 (ArC2), 141.2 (ArC6), 137.5 (ArC1′), 130.9 (ArC4), 128.8 (ArC2′, ArC6′), 128.6 (ArC3′, ArC5′), 127.2 (ArC2″, ArC6″), 126.7 (ArC4′), 125.3 (ArC1″), 125.2 (ArC5), 125.1 (ArC3), 116.0 (ArC3″, ArC5″), 34.5 ($ArCH_2$). MS (EI): *m/z* 276 (M^+, 100%). HRMS (ESI): calcd for $C_{18}H_{17}N_2O$ 277.1341, found 277.1349.

7.1.3.2 Preparation of benzylglyoxals

General Procedure 9: **The preparation of chlorohydrins**

To a mixture of Mg (35 mmol) and a catalytic amount of I_2 in dry THF (30 mL) was added bromobenzene (30 mmol) dropwise under N_2, maintaining a gentle reflux. Once the magnesium had been consumed, the reagent was transferred to a dry flask with CuI (2.5 mmol) in dry THF (2.5 mmL). The solution was cooled to −60 ^oC and epichlorohydrin (30 mmol) in THF (10 mL) was added dropwise. The reaction mixture was then warmed to 0 ^oC and stirred for 1 h. The reaction mixture was quenched by saturated NH_4Cl (50 mL) and extracted with EtOAc (3 × 25 mL). The combined organic layers were washed with H_2O (3 × 25 mL), brine (25 mL), dried ($MgSO_4$), concentrated and the residue subjected to flash silica gel column chromatography (hexane/ethyl

acetate: 90/10) to yield the chlorohydrin.

1-Chloro-3-phenylpropan-2-ol (**144**)

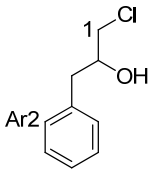

This is a known compound and it was prepared according to the known procedure.[144] Using the **General Procedure 9**, bromobenzene (4.71 g, 30 mmol) and epichlorohydrin (2.78 g, 30.0 mmol) gave **144** (4.60 g, 90%) as a colourless oil. ^{1}H NMR (500 MHz, $CDCl_3$) δ 7.32 (t, *J* = 7.5 Hz, 2H, ArH3, ArH5), 7.23-7.27 (m, 3H, ArH2, ArH4, ArH6), 4.09-4.02 (m, 1H, H2), 3.62 (dd, 1H, *J* = 4.0, 11.1 Hz, $H1_a$), 3.50 (dd, *J* = 4.0, 11.1 Hz, 1H, $H1_b$), 2.89 (d, *J* = 7.0 Hz, 2H, H3), 2.19 (d, *J* = 5.0 Hz, 1H, OH). ^{13}C NMR (75 MHz, $CDCl_3$) δ 137.1 (ArC1), 129.5 (ArC3, ArC5), 128.9 (ArC2, ArC6), 127.0 (ArC4), 72.4 (C2), 49.4 (C1), 40.8 (C3). MS (EI): *m/z* 170 (M^+, 40%), 84 (100%).

1-(4-((Tert-butyldimethylsilyl)oxy)phenyl)-3-chloropropan-2-ol (**143**)

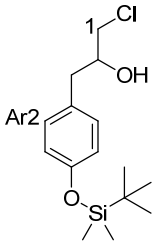

Using the **General Procedure 9**, (4-bromophenoxy)(*tert*-butyl)-dimethylsilane (6.31 g, 22 mmol) and epichlorohydrin (2.04 g, 22.0 mmol) gave **143** (5.20 g, 80%) as a colourless oil. IR (neat) υ_{max} 2933 (w), 2859 (w), 1609 (w), 1509 (m), 1467 (w), 1256 (s), 1171 (w), 1045 (w), 912 (s), 836 (s), 780 (m), 693 (m) cm^{-1}. ^{1}H NMR (500 MHz, $CDCl_3$) δ 7.08 (d, *J* = 8.3 Hz, 2H, ArH3, ArH5), 6.79 (d, *J* = 8.3 Hz, 2H, ArH2, ArH6), 3.97-4.04 (m, 1H, H2), 3.60 (dd, *J* = 4.0, 11.1 Hz, 1H, $H1_a$), 3.49 (dd, *J* = 6.0, 11.1 Hz, 1H, $H1_b$), 2.82 (d, *J* = 6.6 Hz, 2H, H3), 2.18 (d, *J* = 5.1 Hz, 1H, OH), 0.98 (s, 9H, CCH_3), 0.19 (s, 6H, $SiCH_3$). ^{13}C NMR (126 MHz, $CDCl_3$) δ 154.6 (ArC1), 130.3 (ArC4), 129.5 (ArC3, ArC5), 120.5 (ArC2, ArC6), 72.3 (C2), 49.1 (C1), 39.8 (C3), 25.7 (SiC), 18.2 (CH_3), -4.4 ($SiCH_3$). MS (EI): *m/z* 300 (M^+, 60%), 199 (100%).

HRMS (ESI): calcd for $C_{15}H_{26}O_2SiCl$ 301.1391, found 301.1387.

General Procedure 10: The preparation of chloropropanones

1-Chloro-3-phenylpropan-2-ol (1.0 mmol) was dissolved in CH_2Cl_2 (40 mL) at 0 ^oC and treated with Dess-Martin periodinane (1.0 mmol). The reaction was allowed to warm to rt and stirred for 4 h. The reaction mixture was concentrated and the residue subjected to flash silica gel column chromatography (hexane/ethyl acetate: 90/10) to yield the target compound.

1-Chloro-3-phenylpropan-2-one (**146**)

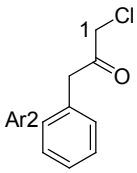

This is a known compound and it was prepared according to the known procedure.[145] Using the **General Procedure 10**, 1-chloro-3-phenylpropan-2-ol **144** (170 mg, 1.00 mmol) and Dess-Martin periodinane (424 mg, 1.00 mmol) gave **146** (148 mg, 88%) as a yellowish oil. ^1H NMR (300 MHz, $CDCl_3$) δ 7.22-7.42 (m, 5H, ArH), 4.12 (s, 2H, H1), 3.89 (s, 2H, H3). ^{13}C NMR (75 MHz, $CDCl_3$) δ 200.1 (C=O), 133.0 (ArC1), 129.6 (ArC2, ArC6), 129.0 (ArC3, ArC5), 127.5 (ArC4), 47.7 (C1), 46.9 (C3). MS (EI): *m/z* 168 (M^+, 40%), 91 (100%).

1-(4-((Tert-butyldimethylsilyl)oxy)phenyl)-3-chloropropan-2-one (**145**)

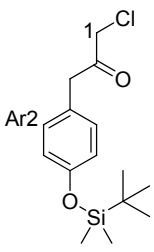

Using the **General Procedure 10**, 1-(4-((*tert*-butyldimethylsilyl)oxy) -phenyl)-3-chloropropan-2-ol **143** (4.80 g, 16.0 mmol) and Dess-Martin periodinane (6.78 g, 16.0 mmol) gave **145** (3.50 g, 91%) as a yellow oil. IR (neat) υ_{max} 2955 (w), 2932 (w), 2859 (w), 1733 (m), 1609 (m), 1509 (s), 1469 (m), 1395 (m), 1257 (s), 1171 (w), 1104 (w), 1053 (w), 911 (s), 836 (s), 780

(s), 692 (m) cm^{-1}. ^{1}H NMR (500 MHz, $CDCl_3$) δ 7.08 (d, *J* = 8.2 Hz, 2H, ArH2, ArH6), 6.80 (d, *J* = 8.3 Hz, 2H, ArH3, ArH5), 4.10 (s, 2H, H1), 3.80 (s, 2H, H3), 0.98 (s, 12H, CCH_3), 0.19 (s, 6H, $SiCH_3$). ^{13}C NMR (126 MHz, $CDCl_3$) δ 200.2 (C=O), 155.1 (ArC4), 130.4 (ArC2, ArC6), 125.4 (ArC1), 120.5 (ArC3, ArC5), 47.6 (C1), 46.1 (C3), 25.7 (CH_3), 18.2 (SiC), -4.4 ($SiCH_3$). MS (EI): *m/z* 298 (M^+, 40%), 205 (100%). HRMS (ESI): calcd for $C_{15}H_{24}O_2SiCl$ 299.1234, found 299.1228.

General Procedure 11: The preparation of bromopropanones

A solution of 1-chloro-3-phenylpropan-2-one (1.0 mmol) was dissolved in acetone (15 mL) and treated with lithium bromide (8.0 mmol). The mixture was stirred at rt overnight. The solvent was evaporated and the resulting solid was dissolved in EtOAc, washed with H_2O (2 × 25 mL) and brine, dried ($MgSO_4$) and evaporated to dryness.

1-Bromo-3-phenylpropan-2-one (**147**)

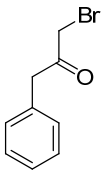

This is a known compound and it was prepared according to the known procedure.[146] Using the **General Procedure 11**, 1-chloro-3-phenylpropan-2-one **146** (168 mg, 1.00 mmol) and lithium bromide (696 mg, 8.00 mmol) gave **147** (185 mg, 88%) as a yellow-brown oil. ^{1}H NMR (500 MHz, $CDCl_3$) δ 7.22-7.36 (m, 5H), 3.94 (s, 2H), 3.91 (s, 2H). ^{13}C NMR (126 MHz, $CDCl_3$) δ 199.5 (C=O), 133.3 (ArC1), 129.6 (ArC2, ArC6), 129.1 (ArC3, ArC5), 127.6 (ArC4), 46.9 (C3), 33.6 (C1). MS (EI): *m/z* 212 (M^+, ^{79}Br, 40%), 214 (M^+, ^{81}Br, 40%), 91 (100%).

1-Bromo-3-(4-((tert-butyldimethylsilyl)oxy)phenyl)propan-2-one (**137**)

Using the **General Procedure 11**, 1-(4-((*tert*-butyldimethylsilyl)oxy)

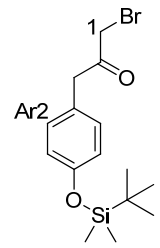

-phenyl)-3-chloropropan-2-one **145** (298 mg, 1.00 mmol) and lithium bromide (696 mg, 8.00 mmol) gave **137** (294 mg, 85%) as a yellow-brown oil. IR (neat) υ_{max} 2933 (w), 2858 (w), 1723 (m), 1608 (m), 1508 (s), 1466 (w), 1395 (w), 1257 (s), 1170 (w), 1103 (w), 1047 (w), 911 (s), 835 (s), 781 (s), 694 (m) cm^{-1}. ^{1}H NMR (500 MHz, $CDCl_3$) δ 7.08 (d, J = 8.2 Hz, 2H, ArH2, ArH6), 6.81 (d, J = 8.2 Hz, 2H, ArH3, ArH5), 3.90 (s, 2H, H1), 3.86 (s, 2H, H3), 0.98 (s, 12H, CCH_3), 0.19 (s, 6H, $SiCH_3$). ^{13}C NMR (126 MHz, $CDCl_3$) δ 199.9 (C=O), 155.3 (ArC4), 130.6 (ArC2, ArC6), 125.8 (ArC1), 120.7 (ArC3, ArC5), 46.2 (C3), 33.6 (C1), 25.8 (CH_3), 18.3 (SiC), -4.3 ($SiCH_3$). MS (EI): *m/z* 342 (M^+, ^{79}Br, 40%), 344 (M^+, ^{81}Br, 40%), 205 (100%). HRMS (ESI): calcd for $C_{15}H_{24}O_2Si^{79}Br$ 343.0729, found 343.0718.

General Procedure 12: The preparation of phenylpropyl nitrate

$AgNO_3$ (2.3 mmol) was added to a solution of 1-bromo-3-phenylpropan-2-one (1.0 mmol) in dry acetonitrile (2 mL) at rt and the mixture was stirred for 40 h. The mixture was filtered through a flash silica pad and concentrated under vacuum to obtain the target compound.

2-Oxo-3-phenylpropyl nitrate (**149**)

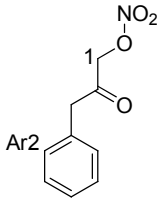

This is a known compound and it was prepared according to the known procedure.[147] Using the **General Procedure 12**, 1-bromo-3-phenylpropan-2-one **147** (213 mg, 1.00 mmol) and $AgNO_3$ (391 mg, 2.30 mmol) gave **149** (186 mg, 95%) as a yellow oil. IR (neat) υ_{max} 2934 (w), 1736 (m), 1642 (s), 1404 (m), 1282 (s), 1024 (m), 977 (m), 844 (s), 753 (m), 701 (s), 638 (m) cm^{-1}. ^{1}H NMR (500 MHz, $CDCl_3$) δ 7.22-7.38 (m, 5H, ArH), 4.95

(s, 2H, H1), 3.78 (s, 2H, H3). ^{13}C NMR (126 MHz, $CDCl_3$) δ 198.8 (C=O), 131.8 (ArC1), 129.4 (ArC2, ArC6), 129.2 (ArC3, ArC5), 127.8 (ArC4), 73.3 (C1), 46.6 (C3). MS (EI): *m/z* 195 (M^+, 40%), 91 (100%). HRMS (ESI): calcd for $C_9H_{10}NO_4$ 196.0610, found 196.0619.

3-(4-((Tert-butyldimethylsilyl)oxy)phenyl)-2-oxopropyl nitrate (**148**)

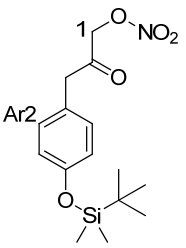

Using the **General Procedure 12**, 1-bromo-3-(4-((*tert*-butyldimethylsilyl)oxy)phenyl)propan-2-one **137** (343 mg, 1.00 mmol) and $AgNO_3$ (391 mg, 2.30 mmol) gave **148** as a yellow oil (186 mg, 89%). IR (neat) υ_{max} 2943 (m), 2861 (w), 1735 (m), 1649 (m), 1509 (m), 1262 (s), 910 (s), 836 (s), 786 (s), 693 (m), 626 (m) cm^{-1}. ^{1}H NMR (500 MHz, $CDCl_3$) δ 7.08 (d, *J* = 8.0 Hz, 2H, ArH2, ArH6), 6.82 (d, *J* = 8.1 Hz, 2H, ArH3, ArH5), 4.94 (s, 2H, H1), 3.70 (s, 2H, H3), 0.98 (s, 12H, CCH_3), 0.20 (s, 6H, $SiCH_3$). ^{13}C NMR (126 MHz, $CDCl_3$) δ 199.3 (C=O), 155.5 (ArC4), 130.5 (ArC2, ArC6), 124.5 (ArC1), 120.9 (ArC3, ArC5), 73.4 (C1), 46.1 (C3), 25.8 (CH_3), 18.4 (SiC), -4.3 ($SiCH_3$). MS (EI): *m/z* 325 (M^+, 40%), 221 (100%). HRMS (ESI): calcd for $C_{15}H_{24}NO_5Si$ 326.1424, found 326.1426.

General Procedure 13: The preparation of benzylglyoxals

$NaOAc{\cdot}3H_2O$ (0.80 mmol) was slowly added to a solution of 2-oxo-3-phenylpropyl nitrate (0.80 mmol) in DMSO (5 mL). The reaction mixture was stirred at 25 °C for 1 h and then poured into ice-water. The resulting mixture was saturated with NaCl and then extracted with EtOAc (3 × 25 mL). The organic phase was washed with H_2O (25 mL), aqueous $NaHCO_3$ (25 mL) and then again with H_2O. Removal of the solvent by distillation under reduced pressure followed by drying in vacuum afforded the target

compound as a colourless solid.

2-Oxo-3-phenylpropanal (**150**)

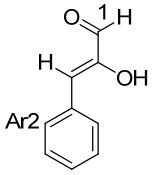

This is a known compound and it was prepared according to the known procedure.[147] Using the **General Procedure 13**, 2-oxo-3-phenylpropyl nitrate **149** (156 mg, 0.80 mmol) and NaOAc·3H_2O (109 mg, 0.80 mmol) gave **150** as a colourless solid (105 mg, 89%). Mp. 98-99 ^oC. IR (neat) υ_{max} 3207 (m), 1658 (m), 1631 (m), 1411 (m), 1376 (m), 1328 (w), 1308 (w), 1280 (w), 1207 (m), 1161 (m), 922 (s), 843 (m), 756 (w), 712 (m), 684 (s) cm^{-1}. ^1H NMR (500 MHz, $CDCl_3$) δ 9.26 (s, 1H, H1), 7.42 (d, *J* = 8.0 Hz, 2H, ArH2, ArH6), 7.42 (t, *J* = 7.5 Hz, 2H, ArH3, ArH5), 7.34 (t, *J* = 8.0 Hz, 1H, ArH4), 6.63 (s, 1H, OH), 6.17 (s, 1H, H3). ^{13}C NMR (126 MHz, $CDCl_3$) δ 188.3 (C=O), 148.7 (C2), 133.6 (ArC1), 130.5 (ArC2, ArC6), 129.4 (ArC3, ArC5), 128.7 (ArC4), 122.8 (C3). MS (EI): *m/z* 148 (M^+, 45%), 91 (100%). HRMS (ESI): calcd for $C_9H_9O_2$ 149.0603, found 149.0597.

3-(4-Hydroxyphenyl)-2-oxopropanal (**129**)

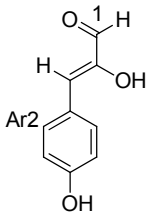

Using the **General Procedure 13**, 3-(4-((*tert*-butyldimethylsilyl)oxy) -phenyl)-2-oxopropyl nitrate **148** (782 mg, 2.40 mmol) and NaOAc·3H_2O (327 mg, 2.40 mmol) gave **129** (342 mg, 87%) as a colourless solid. Mp. 160-161 ^oC. IR (neat) υ_{max} 3396 (m), 3139 (m), 1615 (m), 1569 (s), 1506 (m), 1456 (w), 1376 (m), 1302 (w), 1292 (w), 1240 (m), 1164 (m), 913 (m), 854 (s), 754 (m), 703 (s) cm^{-1}. ^1H NMR (300 MHz, DMSO) δ 9.87 (bs, 1H, ArOH), 9.45 (bs, 1H, OH), 9.18 (s, 1H, H1), 7.70 (d, *J* = 8.5 Hz, 2H, ArH2, ArH6), 6.81 (d, *J* = 8.5 Hz, 2H, ArH3, ArH5), 6.26 (s, 1H, H3). ^{13}C NMR (75 MHz, DMSO) δ 189.2 (C=O), 158.2 (ArC4), 149.2 (C2), 131.8 (ArC2, ArC6), 125.7 (ArC1), 124.4 (C3), 115.6 (ArC3,

ArC5). MS (ESI): 163 ([M-H]$^-$). HRMS (ESI): calcd for $C_9H_9O_3$ 165.0552, found 165.0552.

7.1.3.3 Preparation of imidazo[1,2-*a*]pyridin-3-ol analogues

General Procedure 14: The preparation of imidazo[1,2-*a*]pyridin-3-ol analogues

To a degassed solution of pyridin-2-amine (1.0 mmol) and keto aldehyde (1.5 mmol) in 20% water/dioxane (5 mL) was added 10% (w/w) aqueous HCl solution (1.5 mL) and the mixture was stirred under a N_2 atmosphere at rt for 5 min, and then heated at reflux for 16 h. After cooling, H_2O (10 mL) was added at 0 ^oC. The resulting precipitate was filtered and recrystallized from methanol/ether to provide a yellow solid.

8-Benzyl-2-(4-hydroxybenzyl)-6-(4-hydroxyphenyl)imidazo[1,2-a]pyridin-3-ol (**121**)

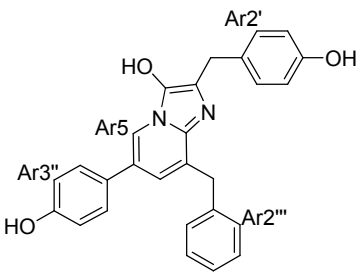

Using the **General Procedure 14**, 4-(6-amino-5-benzylpyridin-3-yl)phenol **126** (83 mg, 0.30 mmol) and 3-(4-hydroxyphenyl)-2 -oxopropanal **129** (74 mg, 0.45 mmol) gave **121** as a yellow solid (78 mg, 62%). Mp. 150 ^oC (decomp.). IR (neat) υ_{max} 3123 (w), 3116 (w), 1645 (m), 1606 (m), 1565 (m), 1507 (s), 1452 (m), 1375 (m), 1270 (m), 1235 (s), 1172 (m), 1147 (m), 1098 (m), 830 (s), 792 (m), 784 (m), 756 (m), 729 (m), 700 (m), 671 (m), 653 (w) cm^{-1}. ^1H NMR (500 MHz, CD_3OD) δ 8.31 (s, 1H, ArH5), 7.40 (d, *J* = 7.7 Hz, 2H, ArH2″, ArH6″), 7.34-7.20 (m, 6H, ArH7, ArH2‴, ArH3‴, ArH4‴, ArH5‴, ArH6‴), 7.07 (d, *J* = 8.1 Hz, 2H, ArH2′, ArH6′), 6.86 (d, *J* = 8.1 Hz, 2H, ArH3″, ArH5″), 6.69 (d, *J* = 8.0 Hz, 2H, ArH3′, ArH5′), 4.21 (s, 2H, ArC8CH_2), 4.02 (s, 2H, ArC2CH_2). MS (ESI): *m/z* 423 ([M+H]$^+$, 100%). HRMS (ESI): calcd for $C_{27}H_{23}N_2O_3$ 423.1709, found 423.1706.

2,8-Dibenzyl-6-(4-hydroxyphenyl)imidazo[1,2-a]pyridin-3-ol (**153**)

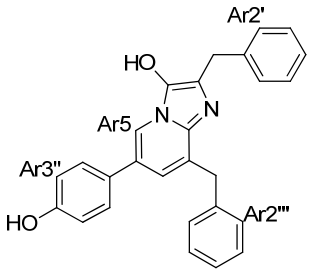

Using the **General procedure 14**, 4-(6-amino-5-benzylpyridin-3-yl)phenol **126** (55 mg, 0.20 mmol) and 3-phenyl-2-oxopropanal **150** (44 mg, 0.30 mmol) gave **153** (55 mg, 67%) as a yellow solid. Mp. > 200 ^{o}C. IR (neat) υ_{max} 3316 (w), 1649 (w), 1609 (m), 1572 (m), 1493 (m), 1454 (m), 1393 (m), 1270 (m), 1242 (w), 1177 (m), 1108 (m), 1033 (w), 918 (m), 832 (m), 735 (m), 700 (m), 669 (w) cm^{-1}. ^{1}H NMR (500 MHz, CD_3OD) δ 8.38 (s, 1H, ArH5), 7.57 (s, 1H, ArH7), 7.42 (d, *J* = 7.9 Hz, 2H, ArH2″, ArH6″), 7.35-7.15 (m, 10H, ArH2′, ArH3′, ArH4′, ArH5′, ArH6′, ArH2‴, ArH3‴, ArH4‴, ArH5‴, ArH6‴), 6.88 (d, *J* = 8.0 Hz, 2H, ArH3″, ArH5″), 4.28 (s, 2H, ArC2CH_2), 4.22 (s, 2H, ArC8CH_2). MS (ESI): *m/z* 407 ($[M+H]^+$, 100%). HRMS (ESI): calcd for $C_{27}H_{23}N_2O_2$ 407.1760, found 407.1766.

4,4′-(8-Benzyl-3-hydroxyimidazo[1,2-a]pyridine-2,6-diyl)diphenol (**154**)

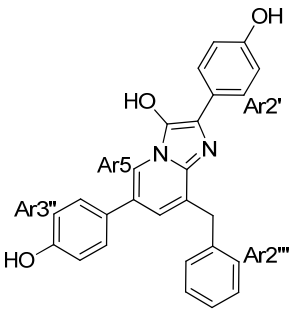

Using the **General procedure 14**, 4-(6-amino-5-benzylpyridin-3-yl)phenol **126** (55 mg, 0.20 mmol) and 4-hydroxyphenylglyoxal **151** (60 mg, 0.30 mmol) gave **154** (64 mg, 79%) as a yellow solid. Mp. 191-192 ^{o}C. IR (neat) υ_{max} 3138 (w), 1651 (m), 1601 (w), 1569 (m), 1504 (s), 1443 (m), 1372 (m), 1228 (s), 1169 (s), 1105 (m), 909 (w), 827 (s), 782 (w), 739 (m), 697 (m), 669 (w), 626 (w), 613 (w) cm^{-1}. ^{1}H NMR (300 MHz, DMSO) δ 9.62 (bs, 3H, OH), 8.24 (s, 1H, ArH5), 7.94 (s, 1H, ArH7), 7.57-7.13 (m, 9H, ArH3′, ArH5′, ArH3″, ArH5″, ArH2‴, ArH3‴, ArH4‴, ArH5‴, ArH6‴), 6.95-6.73 (m, 4H, ArH2′, ArH2″, ArH6″), 4.35 (s, 2H,

$ArCH_2$). MS (ESI): *m/z* 409 ($[M+H]^+$, 100%). HRMS (ESI): calcd for $C_{26}H_{21}N_2O_3$ 409.1552, found 409.1572.

8-Benzyl-6-(4-hydroxyphenyl)-2-phenylimidazo[1,2-a]pyridin-3-ol (**155**)

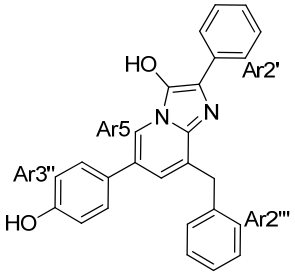

Using the **General procedure 14**, 4-(6-amino-5 -benzylpyridin-3-yl)phenol **126** (55 mg, 0.20 mmol) and phenylglyoxal **152** (45 mg, 0.30 mmol) gave **155** (65 mg, 83%) as a yellow solid. Mp. > 200 ^oC. IR (neat) υ_{max} 3261 (m), 3074 (w), 3033 (w), 2819 (w), 2572 (w), 2163 (w), 1658 (m), 1614 (m), 1506 (m), 1443 (m), 1364 (m), 1263 (m), 1222 (m), 1170 (m), 1102 (w), 1087 (w), 919 (w), 822 (m), 757 (m), 696 (s), 644 (s) cm^{-1}. ^1H NMR (500 MHz, DMSO) δ 9.80 (bs, 2H, OH), 8.42 (s, 1H, ArH5), 8.07 (d, *J* = 7.1 Hz, 2H, ArH2′, ArH6′), 7.64 (s, 1H, ArH7), 7.51 (d, *J* = 7.6 Hz, 2H, ArH2″, ArH6″), 7.40-7.45 (m, 4H, ArH3′, ArH4′, ArH5′, ArH4‴), 7.33 (t, *J* = 7.1 Hz, 2H, ArH2‴, ArH6‴), 7.27-7.16 (m, 2H, ArH3‴, ArH5‴), 6.89 (d, *J* = 7.9 Hz, 2H, ArH3″, ArH5″), 4.43 (s, 2H, $ArCH_2$). MS (ESI): *m/z* 391 ($[M-H]^-$, 100%). HRMS (ESI): calcd for $C_{26}H_{19}N_2O_2$ 391.1447, found 391.1437.

7.2 Biological activity testing

7.2.1 HIV RT testing

Preparations of working solutions

Reverse Transcriptase: The lyophilized reverse transcriptase (500 ng) was dissolved in autoclaved redistilled water (250 μL) to obtain a final concentration of 2 ng/μL.

Reaction mixture for using poly (A) × oligo (dT)$_{15}$: The template was dissolved in autoclaved redistilled water (430 μL) and 100 μL of this solution was added to each of three vials containing the nucleotides which were each previously diluted with

incubation buffer (1 mL). The final concentration of the reaction mixture is 46 mM Tris-HCl, 266 mM potassium chloride, 27.5 mM magnesium chloride, 9.2 mM DDT, 10 μM dUTP/dTTP, template/primer hybrid, 750 $mA_{260\ nm}$/mL.

Anti-DIG-POD: The lyophilizate anti-DIG-POD was dissolved in autoclaved redistilled water (0.5 mL) and conjugate dilution buffer was added to a concentration of 200 mU/mL. (50 μL antibody solution and 4.95 mL of conjugate dilution buffer).

Washing buffer: Autoclaved redistilled water (225 mL) was added to the provided washing buffer per bottle and the mixture was mixed thoroughly before use.

ABTS substrate solution: An ATBS tablet was dissolved in substrate buffer and mixed thoroughly.

Prepare testing samples in 1 mL DMSO solutions in the concentrations of 5 mM as a stock solution. Then dilute them to 500 μM (10 times using DMSO) and 100 μM. 6 μL of each sample added to a PCR plate.A reaction mixture (54 μL) of RT (0.5 ng, supplied by adding 0.25 μL of the 2 ng/μL stock solution), lysis buffer (33.75 μL) and the reaction mixture for using poly (A) × oligo $(dT)_{15}$ (20 μL) was added to each sample and the PCR plate. Incubated at 37 °C for 1 h and then frozen at −40 °C in the freezer for 5 min. The PCR plate was allowed to taw and the samples were added to the Streptavidin plate provided by the RT kit, and incubated at 37 °C for 1 h. The solvent was discharged and the Streptavidin plate was washed with washing buffer (5 × 200 μL for each sample). Anti-DIG-POD (diluted 1 in 100 in conjugate dilution buffer to a concentration of 200 mU/mL, 200 μL for each sample) was added and the Streptavidin plate was incubated at 37 °C for 1 h. The Streptavidin plate was washed with washing buffer (5 × 200 μL for each sample). The ABTS substrate solution (200 μL for each

sample) was added and the Streptavidin plate was incubated at room temperature for 10-30 min until a dark green colour was visible. The absorbance at 405 nm was read using a Microplate reader.

A negative and positive control have been added in the Streptavidin plate. The negative control consists of 54 μL of reaction mixture without the RT enzyme. The positive control consists of 54 μL of reaction mixture with RT enzyme and without RT inhibitor.

7.2.2 Testing method of the anti-plasmodial assay

The compounds were tested *in vitro* against *Plasmodium falciparum*, K1CB1 (K1), which is a multidrug resistant (chloroquine and antifolate resistant) strain, a generous gifts from Professor Sodsri Thaithong, Chulalongkorn University, Bangkok, Thailand. The parasites were maintained in human red-blood cells in RPMI 1640 medium supplemented with 25 mM HEPES, 0.2% sodium bicarbonate and 8% human serum, at 37 ºC in a 3% CO_2 incubator.[148] Samples were dissolved in DMSO and the *in vitro* anti-malarial activity testing was carried out using the microdilution radioisotope technique. The test sample (25 μL, in the culture medium) was placed in triplicate in a 96-well plate where parasitized erythrocytes (200 μL) with a cell suspension (1.5%) of parasitemia (0.5-1%) were then added to the wells. The ranges of the final concentrations of the samples were varied from 2×10^{-5} to 1×10^{-7} M with 0.1% of solvent. The plates were then cultured under standard conditions for 24 h after which 3H-hypoxanthine (25 μL, 0.5 mCi) was added. The culture was incubated for 18-20 h after which the DNA from the parasite was harvested from the culture onto glass fiber filters and a liquid scintillation counter used to determine the amount of 3H-hypoxanthine incorporation.[149,150] The inhibitory concentration of the sample was

determined from its dose-response curves or by calculation. The assay was performed in at least three replicates. Dihydroartemisinine and mefloquine were used as positive controls.

7.2.3 Testing method of the anti-cancer assay

The cancer growth inhibition assays of the three human-cell lines KB (epidermoid carcinoma of oral cavity, ATCC CCL-17), MCF-7 (breast adenocarcinoma, ATCC HTB-22) and NCI-H187 (small cell lung carcinoma, ATCC CRL-5804) and the Vero cell assay were performed using the Resazurin Microplate Assay (REMA) method.[151] In brief, cells at a logarithmic growth phase were harvested and diluted (*e.g.* to 2.2 × 104 cells/mL for KB and to 3.3 × 104 cells/mL for NCI-H187) in fresh medium. Successively, 5 µl of test sample diluted in 5% DMSO, and 45 µL of cell suspension were added to 384-well plates, incubated at 37 °C in a 5% CO_2 incubator. After the incubation period (*e.g.* three days for KB, and five days for NCI-H187), 12.5 µL of 62.5 µg/mL resazurin solution was added to each well and the plates were then incubated at 37 °C for 4 hours. The fluorescence signal was measured using a SpectraMax M5 multi-detection microplate reader (Molecular Devices, USA) at the excitation and emission wavelengths of 530 nm and 590 nm. The % inhibition of cell growth was calculated by the following equation:

$$\% \text{ inhibition} = [1-(FU_T / FU_C)] \times 100\%$$

FU_T and FU_C are the mean fluorescent unit from treated and untreated conditions, respectively. Dose response curves were plotted from 6 concentrations of 3-fold serially diluted test compounds and the sample concentrations that inhibit cell growth by 50% (IC_{50}) been derived using the SOFTMax Pro software (Molecular Devices, USA).

Ellipticine, doxorubicin and tamoxifen were used as a positive control, and 0.5% DMSO and water were used as a negative control.[151]

7.2.4 Testing method of the anti-microbial assay

7.2.4.1 Purpose

Tested for bacterial growth inhibition activity against a primary panel including *Escherichia coli*, *Klebsiella pneumoniae, Acinetobacter baumannii, Pseudomonas aeruginosa* and *Staphylococcus aureus* (MRSA)

7.2.4.2 Compound preparation

Dry weights of the testing compounds were supplied. Namfon Pantarat prepared stock solutions at 10 mg/mL in DMSO, according to the weight reported for each compound. Gentle heating and sonication was required to solubilise the compounds. The highest concentration tested for each compound was 32 μg/mL.

7.2.4.3 Single point bacterial inhibition assay

The primary bacteria panel, including *Escherichia coli* ATCC 25922 (GN_001), *Klebsiella pneumoniae* ATCC 700603 (GN_003), *Acinetobacter baumannii* ATCC 19606 (GN_034), *Pseudomonas aeruginosa* ATCC 27853 (GN_042) and *Staphylococcus aureus* ATCC 43300 (MRSA) (GP_020) were cultured in Muller Hinton broth (**MHB**) at 37 °C overnight. A sample of each culture was then diluted 40-fold in fresh MHB broth and incubated at 37 °C for 1.5-3 hrs. The compounds were plated at a single test concentration of 64 μg/mL. Colistin, Polymyxin B, Vancomycin and Daptomycin were serially diluted two-fold across the wells, with compound concentrations ranging from 0.5 to 64 μg/mL, as controls of bacterial inhibitors. The

resultant mid-log phase cultures were diluted to the final concentration of 5×105 CFU/mL, then 50 µL was added to each well of the compound containing 96-well plates (Corning; Cat. No 3641, NBS), giving a final compound concentration range of 0.25 µg/mL to 32 µg/mL for control inhibitors and 32 µg/mL for test compounds. All the plates were covered and incubated at 37 °C for 24 h.

Inhibition of bacterial growth was determined visually and was recorded at 32 µg/mL were 100% inhibition was identified.

7.2.4.4 MIC (Minimum Inhibitory Concentration) assay

The primary bacteria panel, including *Escherichia coli* ATCC 25922 (GN_001) and *Staphylococcus aureus* ATCC 43300 (MRSA) (GP_020) were cultured in Muller Hinton broth (MHB) at 37°C overnight. A sample of each culture was then diluted 40-fold in fresh MHB broth and incubated at 37 °C for 1.5-3 h. The compounds were serially diluted two-fold across the wells of non-binding surface 96-well plates (Corning; Cat. No 3641, NBS), with compound concentrations ranging from 0.03 µg/mL to 64 µg/mL, plated in duplicate. The resultant mid-log phase cultures were diluted to the final concentration of 5×105 CFU/mL, then 50 µL was added to each well of the compound-containing 96-well plates, giving a final compound concentration range of 0.015 µg/mL to 32 µg/mL. All the plates were covered and incubated at 37 °C for 24 h.

Inhibition of bacterial growth was determined visually after 24 h**,** where the MIC is recorded as the lowest compound concentration with no visible growth.

7.2.4.5 Tested Bacteria Strains

ID	Organism	Strain	Description	Type
GN_001:02	Escherichia coli	ATCC 25922	control strain	G-ve
GN_003:02	Klebsiella pneumoniae	ATCC 700603	MDR	G-ve
GN_034:02	Acinetobacter baumannii	ATCC 19606	type strain	G-ve
GN_042:02	Pseudomonas aeruginosa	ATCC 27853	type strain	G-ve
GN_020:02	Staphylococcus aureus	ATCC 43300	MRSA	G+ve

7.2.5 Testing method of the DPPH testing

DPPH assays were conducted to test the free radical scavenging ability of the compounds **132**, **126**, **121** and **153-155**. The protocol developed was adapted to 96-well plates based on the Brand-Williams method.[139] 2,2-Diphenyl-1-picrylhydrazyl (DPPH, 20 mg) was dissolved in MeOH (100 mL), stored at −20 °C, and employed as a stock solution. A working DPPH solution was prepared by diluting the stock solution with MeOH. Stock solutions of the pure compounds being tested were diluted to concentrations in the range 0-100 μM (0, 12.50, 18.75, 25.00, 37.50, 50.00, 75.00, and 100.00 μM) on 96-well plates. Substrates (50 μL/well) with the above concentrations in triplicate were mixed with freshly prepared DPPH solution (150 μL/well). The lowest concentration in one of the triplicates was left blank (50 μL of MeOH without sample)

as a negative in order to obtain the initial DPPH absorbance at 515 nm. The absorbance of the reaction mixtures at 515 nm in the 96-well plates were monitored at 5, 10, 15, 30, 45, 60 and 120 min. Absorbance changes at different concentrations of each compound tested were plotted as a standard curve. The inhibition percentage was calculated as follows:

$$Inhibition\% = (Abs_{negtive} - Abs_{sample})/Abs_{negative} \times 100\%$$

References

(1) Weiss, R. A. *Science* **1993**, *260*, 1273.

(2) Douek, D. C.; Roederer, M.; Koup, R. A. *Annu. Rev. Med.* **2009**, *60*, 471.

(3) Cunningham, A. L.; Donaghy, H.; Harman, A. N.; Kim, M.; Turville, S. G. *Curr. Opin. Microbiol.* **2010**, *13*, 524.

(4) Bofill, M.; Janossy, G.; Lee, C. A.; Macdonaldburns, D.; Phillips, A. N.; Sabin, C.; Timms, A.; Johnson, M. A.; Kernoff, P. B. A. *Clin. Exp. Immunol.* **1992**, *88*, 243.

(5) Gottlieb, M. S.; Schroff, R.; Schanker, H. M.; Weisman, J. D.; Fan, P. T.; Wolf, R. A.; Saxon, A. *N. Engl. J. Med.* **1981**, *305*, 1425.

(6) Quagliarello, V. *Yale J. Biol. Med.* **1982**, *55*, 443.

(7) UNAIDS Global Report 2014.
http://apps.who.int/iris/bitstream/10665/128494/1/9789241507585_eng.pdf?ua=1
Accessed by 15.03.2015

(8) Gilbert, P. B.; McKeague, I. W.; Eisen, G.; Mullins, C.; Gueye, N. A.; Mboup, S.; Kanki, P. J. *Stat.Med.* **2003**, *22*, 573.

(9) Smith, J. A.; Daniel, R. *ACS Chem. Biol.* **2006**, *1*, 217.

(10) De Bethune, M. P. *Antiviral Res.* **2010**, *85*, 75.

(11) Balzarini, J., De Clercq, E. *Textbook of AIDS Medicine*; 2nd ed.; Williams &Wilkins: Baltimore, 1998.

(12) Balzarini, J.; DeClercq, E. *Method Enzymol* **1996**, *275*, 472.

(13) Cihlar, T.; Ray, A. S. *Antiviral Res.* **2010**, *85*, 39.

(14) Balzarini, J. *Curr. Top. Med. Chem.* **2004**, *4*, 1825.

(15) Sluis-Cremer, N.; Temiz, N. A.; Bahar, I. *Curr. HIV Res.* **2004**, *2*, 323.

(16) Tronchet, J. M.; Seman, M. *Curr. Top. Med. Chem.* **2003**, *3*, 1496.

(17) Tarby, C. M. *Curr. Top. Med. Chem.* **2004**, *4*, 1045.

(18) Sluis-Cremer, N.; Temiz, N. A.; Bahar, I. *Curr. HIV Res.* **2004**, *2*, 323.

(19) Onafuwa-Nuga, A.; Telesnitsky, A. *Microbiol. Mol. Biol. R.* **2009**, *73*, 451.

(20) Hirschel, B.; Francioli, P. *N. Engl. J. Med.* **1998**, *338*, 906.

(21) Baba, M.; Tanaka, H.; De Clercq, E.; Pauwels, R.; Balzarini, J.; Schols, D.; Nakashima, H.; Perno, C. F.; Walker, R. T.; Miyasaka, T. *Biochem. Biophys. Res. Commun.* **1989**, *165*, 1375.

(22) Miyasaka, T.; Tanaka, H.; Baba, M.; Hayakawa, H.; Walker, R. T.; Balzarini, J.; De Clercq, E. *J. Med. Chem.* **1989**, *32*, 2507.

(23) Pauwels, R.; Andries, K.; Desmyter, J.; Schols, D.; Kukla, M. J.; Breslin, H. J.; Raeymaeckers, A.; Van Gelder, J.; Woestenborghs, R.; Heykants, J.; Schellekens, K.; Janssen, M. A. C.; De Clercq, E.; Janssen, P. A. J. *Nature* **1990**, *343*, 470.

(24) Debyser, Z.; Pauwels, R.; Andries, K.; Desmyter, J.; Kukla, M.; Janssen, P. A.; De Clercq, E. *Proc. Natl. Acad. Sci. U. S. A.* **1991**, *88*, 1451.

(25) Grob, P. M.; Wu, J. C.; Cohen, K. A.; Ingraham, R. H.; Shih, C. K.; Hargrave, K. D.; Mctague, T. L.; Merluzzi, V. J. *Aids Res. Hum. Retrov.* **1992**, *8*, 145.

(26) Romero, D. L.; Morge, R. A.; Genin, M. J.; Biles, C.; Busso, M.; Resnick, L.; Althaus, I. W.; Reusser, F.; Thomas, R. C.; Tarpley, W. G. *J. Med. Chem.* **1993**, *36*, 1505.

(27) Young, S. D.; Britcher, S. F.; Tran, L. O.; Payne, L. S.; Lumma, W. C.; Lyle, T. A.; Huff, J. R.; Anderson, P. S.; Olsen, D. B.; Carroll, S. S.; Pettibone, D. J.;

Obrien, J. A.; Ball, R. G.; Balani, S. K.; Lin, J. H.; Chen, I. W.; Schleif, W. A.; Sardana, V. V.; Long, W. J.; Byrnes, V. W.; Emini, E. A. *Antimicrob. Agents Chemother.* **1995**, *39*, 2602.

(28) Das, K.; Clark, A. D.; Lewi, P. J.; Heeres, J.; de Jonge, M. R.; Koymans, L. M. H.; Vinkers, H. M.; Daeyaert, F.; Ludovici, D. W.; Kukla, M. J.; De Corte, B.; Kavash, R. W.; Ho, C. Y.; Ye, H.; Lichtenstein, M. A.; Andries, K.; Pauwels, R.; de Béthune, M.-P.; Boyer, P. L.; Clark, P.; Hughes, S. H.; Janssen, P. A. J.; Arnold, E. *J. Med. Chem.* **2004**, *47*, 2550.

(29) Janssen, P. A. J.; Lewi, P. J.; Arnold, E.; Daeyaert, F.; de Jonge, M.; Heeres, J.; Koymans, L.; Vinkers, M.; Guillemont, J.; Pasquier, E.; Kukla, M.; Ludovici, D.; Andries, K.; de Béthune, M.-P.; Pauwels, R.; Das, K.; Clark, A. D.; Frenkel, Y. V.; Hughes, S. H.; Medaer, B.; De Knaep, F.; Bohets, H.; De Clerck, F.; Lampo, A.; Williams, P.; Stoffels, P. *J. Med. Chem.* **2004**, *48*, 1901.

(30) Best, B. M.; Goicoechea, M. *Expert Opin. Drug Metab. Toxicol.* **2008**, *4*, 965.

(31) Podzamczer, D.; Fumero, E. *Exp. Opin. Pharmacother.* **2001**, *2*, 2065.

(32) Mowbray, C. E.; Burt, C.; Corbau, R.; Gayton, S.; Hawes, M.; Perros, M.; Tran, I.; Price, D. A.; Quinton, F. J.; Selby, M. D.; Stupple, P. A.; Webster, R.; Wood, A. *Bioorg. Med. Chem. Lett.* **2009**, *19*, 5857.

(33) Zala, C.; St Clair, M.; Dudas, K.; Kim, J.; Lou, Y.; White, S.; Piscitelli, S.; Dumont, E.; Pietropaolo, K.; Zhou, X. J.; Mayers, D. *Antimicrob. Agents Chemother.* **2012**, *56*, 2570.

(34) Hamatake, R., Z. Zhang, W. Xu, D. Bellows, A. Raney, J.-L. Girardet, and B. Quart. In *47th Intersci. Conf. Antimicrob. Agents Chemother. American Society for Microbiology* Washington, DC, 2007.

(35) Boone, L. R. *Curr. Opin. Invest. Drugs* **2006**, *7*, 128.

(36) Creagh, T.; Ruckle, J. L.; Tolbert, D. T.; Giltner, J.; Eiznhamer, D. A.; Dutta, B.; Flavin, M. T.; Xu, Z. Q. *Antimicrob. Agents Chemother.* **2001**, *45*, 1379.

(37) Lai, M. T.; Munshi, V.; Touch, S.; Tynebor, R. M.; Tucker, T. J.; McKenna, P. M.; Williams, T. M.; DiStefano, D. J.; Hazuda, D. J.; Miller, M. D. *Antimicrob. Agents Chemother.* **2009**, *53*, 2424.

(38) Lu, M. Q.; Felock, P. J.; Munshi, V.; Hrin, R. C.; Wang, Y. J.; Yan, Y. W.; Munshi, S.; McGaughey, G. B.; Gomez, R.; Anthony, N. J.; Williams, T. M.; Grobler, J. A.; Hazuda, D. J.; McKenna, P. M.; Miller, M. D.; Lai, M. T. *Antimicrob. Agents Chemother.* **2012**, *56*, 3324.

(39) Lai, M. T.; Feng, M. Z.; Falgueyret, J. P.; Tawa, P.; Witmer, M.; DiStefano, D.; Li, Y.; Burch, J.; Sachs, N.; Lu, M. Q.; Cauchon, E.; Campeau, L. C.; Grobler, J.; Yan, Y. W.; Ducharme, Y.; Cote, B.; Asante-Appiah, E.; Hazuda, D. J.; Miller, M. D. *Antimicrob. Agents Chemother.* **2014**, *58*, 1652.

(40) Usach, I.; Melis, V.; Peris, J. E. *J. Int. AIDS Soc.* **2013**, *16*, 1.

(41) Manfredi, K. P.; Blunt, J. W.; Cardellina, J. H., 2nd; McMahon, J. B.; Pannell, L. L.; Cragg, G. M.; Boyd, M. R. *J. Med. Chem.* **1991**, *34*, 3402.

(42) Boyd, M. R.; Hallock, Y. F.; Cardellina, J. H., 2nd; Manfredi, K. P.; Blunt, J. W.; McMahon, J. B.; Buckheit, R. W., Jr.; Bringmann, G.; Schaffer, M.; Cragg, G. M.; et al. *J. Med. Chem.* **1994**, *37*, 1740.

(43) McMahon, J. B.; Currens, M. J.; Gulakowski, R. J.; Buckheit, R. W., Jr.; Lackman-Smith, C.; Hallock, Y. F.; Boyd, M. R. *Antimicrob. Agents Chemother.* **1995**, *39*, 484.

(44) Hallock, Y. F.; Manfredi, K. P.; Blunt, J. W.; Cardellina, J. H.; Schaeffer, M.; Gulden, K.-P.; Bringmann, G.; Lee, A. Y.; Clardy, J. *J. Org. Chem.* **1994**, *59*, 6349.

(45) Bringmann, G.; Harmsen, S.; Holenz, J.; Geuder, T.; Götz, R.; A. Keller, P.; Walter, R.; F. Hallock, Y.; H. Cardellina Ii, J.; R. Boyd, M. *Tetrahedron* **1994**, *50*, 9643.

(46) Kelly, T. R.; Garcia, A.; Lang, F.; Walsh, J. J.; Bhaskar, K. V.; Boyd, M. R.; Götz, R.; Keller, P. A.; Walter, R.; Bringmann, G. *Tetrahedron Lett.* **1994**, *35*, 7621.

(47) Hoye, T. R.; Chen, M.; Mi, L.; Priest, O. P. *Tetrahedron Lett.* **1994**, *35*, 8747.

(48) Hobbs, P. D.; Upender, V.; Liu, J.; Pollart, D. J.; Thomas, D. W.; Dawson, M. I. *Chem. Commun.* **1996**, 923.

(49) Bringmann, G.; Götz, R.; Harmsen, S.; Holenz, J.; Walter, R. *Liebigs Annalen* **1996**, 2045.

(50) Hobbs, P. D.; Upender, V.; Dawson, M. I. *Synlett* **1997**, 965.

(51) Bringmann, G.; Gotz, R.; Keller, P. A.; Walter, R.; Boyd, M. R.; Lang, F. R.; Garcia, A.; Walsh, J. J.; Tellitu, I.; Bhaskar, K. V.; Kelly, T. R. *J. Org. Chem.* **1998**, *63*, 1090.

(52) Bringmann, G.; Breuning, M.; Tasler, S. *Synthesis* **1999**, *1999*, 525.

(53) Bringmann, G.; Ochse, M.; Gotz, R. *J. Org. Chem.* **2000**, *65*, 2069.

(54) Bringmann, G.; Ortmann, T.; Feineis, D.; Peters, E. M.; Peters, K. *Synthesis-Stuttgart* **2000**, 383.

(55) Thasana, N.; Pisutjaroenpong, S.; Ruchirawat, S. *Synlett* **2006**, *2006*, 1080.

(56) Xu, G.; Fu, W.; Liu, G.; Senanayake, C. H.; Tang, W. *J. Am. Chem. Soc.* **2013**, *136*, 570.

(57) Upender, V.; Pollart, D. J.; Liu, J.; Hobbs, P. D.; Olsen, C.; Chao, W. R.; Bowden, B.; Crase, J. L.; Thomas, D. W.; Pandey, A.; Lawson, J. A.; Dawson, M. I. *J. Heterocycl. Chem.* **1996**, *33*, 1371.

(58) Zhang, H.; Zembower, D. E.; Chen, Z. *Bioorg. Med. Chem. Lett.* **1997**, *7*, 2687.

(59) Buckheit, R. W.; Fliakasboltz, V.; Decker, W. D.; Roberson, J. L.; Pyle, C. A.; White, E. L.; Bowden, B. J.; Mcmahon, J. B.; Boyd, M. R.; Bader, J. P.; Nickell, D. G.; Barth, H.; Antonucci, T. K. *Antiviral Res.* **1994**, *25*, 43.

(60) Woodfield, S. The design and synthesis of anti-HIV agents: expanding the SAR data of michellamine B analogues. PhD dissertation, University of Wollongong, 2005.

(61) Keller, P. A.; Birch, C.; Leach, S. P.; Tyssen, D.; Griffith, R. *J. Mol. Graphics Modell.* **2003**, *21*, 365.

(62) Bringmann, G.; Saeb, W.; Koppler, D.; François, G. *Tetrahedron* **1996**, *52*, 13409.

(63) Bringmann, G.; Gotz, R.; Francois, G. *Tetrahedron* **1996**, *52*, 13419.

(64) Bringmann, G.; Holenz, J.; Weirich, R.; Rübenacker, M.; Funke, C.; Boyd, M. R.; Gulakowski, R. J.; François, G. *Tetrahedron* **1998**, *54*, 497.

(65) Bringmann, G.; Saeb, W.; Wohlfarth, M.; Messer, K.; Brun, R. *Tetrahedron* **2000**, *56*, 5871.

(66) Bringmann, G.; Wohlfarth, M.; Rischer, H.; Schlauer, J.; Brun, R. *Phytochemistry* **2002**, *61*, 195.

(67) Xu, M. J.; Bruhn, T.; Hertlein, B.; Brun, R.; Stich, A.; Wu, J.; Bringmann, G. *Chem. Eur. J.* **2010**, *16*, 4206.

(68) Bringmann, G.; Zhang, G. L.; Buttner, T.; Bauckmann, G.; Kupfer, T.; Braunschweig, H.; Brun, R.; Mudogo, V. *Chem. Eur. J.* **2013**, *19*, 916.

(69) Bringmann, G.; Lombe, B. K.; Steinert, C.; Ioset, K. N.; Brun, R.; Turini, F.; Heubl, G.; Mudogo, V. *Org. Lett.* **2013**, *15*, 2590.

(70) Luu, T. T. T. Studies in reverse transcriptase: synthesis of inhibitors,

conformational analysis, and integration of drug design. PhD dissertation, University of Wollongong, 2000.

(71) Bringmann, G.; Götz, R.; Keller, P. A.; Walter, R.; Henschel, P.; Schäffer, M.; Stäblein, M.; Kelly, T. R.; Boyd, M. R. *Heterocycles* **1994**, *39*, 503.

(72) Ishiyama, T.; Murata, M.; Miyaura, N. *J. Org. Chem.* **1995**, *60*, 7508.

(73) Ishiyama, T.; Miyaura, N. *Chem. Rec.* **2004**, *3*, 271.

(74) Miyaura, N.; Suzuki, A. *Chem. Rev.* **1995**, *95*, 2457.

(75) Lam, K. C.; Marder, T. B.; Lin, Z. Y. *Organometallics* **2010**, *29*, 1849.

(76) Burke, A. J.; Maycock, C. D.; Ventura, M. R. *Org. Biomol. Chem.* **2006**, *4*, 2361.

(77) Weinbach, E. C.; Hartung, W. H. *J. Org. Chem.* **1950**, *15*, 676.

(78) Mollov, N. M.; Venkov, A. P. *Synthesis-Stuttgart* **1978**, 62.

(79) Cho, S. D.; Song, S. Y.; Hur, E. J.; Chen, M.; Joo, W. H.; Falck, J. R.; Yoon, Y. J.; Shin, D. S. *Tetrahedron Lett.* **2001**, *42*, 6251.

(80) Abdel-Hamid, M. K. The Development of New Anti-HIV Therapeutics Targeting the Reverse Transcriptase Enzyme. PhD dissertation, University of Wollongong, 2011.

(81) Fodor, G.; Nagubandi, S. *Tetrahedron* **1980**, *36*, 1279.

(82) Sele, A. M. The Design, Synthesis and HIV-1 Reverse Transcriptase Inhibitory Activity of Michellamine B Inspired Substituted Biheteroaryls. PhD dissertation, University of Wollongong, 2013.

(83) Jana, R.; Pathak, T. P.; Sigman, M. S. *Chem. Rev.* **2011**, *111*, 1417.

(84) Nakamura, I.; Yamamoto, Y. *Chem. Rev.* **2004**, *104*, 2127.

(85) Miyaura, N.; Yamada, K.; Suzuki, A. *Tetrahedron Lett.* **1979**, *20*, 3437.

(86) Li, C.-J. *Angew. Chem. Int. Ed.* **2003**, *42*, 4856.

(87) Colacot, T. J. *Platinum Met. Rev.* **2011**, *55*, 84.

(88) Suzuki, A. *Angew. Chem. Int. Ed.* **2011**, *50*, 6722.

(89) Negishi, E.-i. *Angew. Chem. Int. Ed.* **2011**, *50*, 6738.

(90) Kotha, S.; Lahiri, K.; Kashinath, D. *Tetrahedron* **2002**, *58*, 9633.

(91) Martin, R.; Buchwald, S. L. *Acc. Chem. Res.* **2008**, *41*, 1461.

(92) Billingsley, K.; Buchwald, S. L. *J. Am. Chem. Soc.* **2007**, *129*, 3358.

(93) Billingsley, K. L.; Anderson, K. W.; Buchwald, S. L. *Angew. Chem. Int. Ed.* **2006**, *45*, 3484.

(94) Kotha, S.; Lahiri, K.; Kashinath, D. *Tetrahedron* **2002**, *58*, 9633.

(95) Bringmann, G.; Hamm, A.; Schraut, M. *Org. Lett.* **2003**, *5*, 2805.

(96) Huang, S.; Petersen, T. B.; Lipshutz, B. H. *J. Am. Chem. Soc.* **2010**, *132*, 14021.

(97) Hassan, J.; Sévignon, M.; Gozzi, C.; Schulz, E.; Lemaire, M. *Chem. Rev.* **2002**, *102*, 1359.

(98) Bringmann, G.; Price Mortimer, A. J.; Keller, P. A.; Gresser, M. J.; Garner, J.; Breuning, M. *Angew. Chem. Int. Ed.* **2005**, *44*, 5384.

(99) Keller, P. A.; Yepuri, N. R.; Kelso, M. J.; Mariani, M.; Skelton, B. W.; White, A. H. *Tetrahedron* **2008**, *64*, 7787.

(100) Bringmann, G.; Pabst, T.; Busemann, S.; Peters, K.; Peters, E.-M. *Tetrahedron* **1998**, *54*, 1425.

(101) Bringmann, G.; Saeb, W.; Mies, J.; Messer, K.; Wohlfarth, M.; Brun, R. *Synthesis-Stuttgart* **2000**, 1843.

(102) Bringmann, G.; Saeb, W.; Mies, J.; Messer, K.; Wohlfarth, M.; Brun, R. *Synthesis* **2000**, *2000*, 1843.

(103) Roche Life Science

http://lifescience.roche.com/shop/products/reverse-transcriptase-assay-colorimetric

Accessed 15.03.2015

(104) Shimomura, O.; Johnson, F. H.; Saiga, Y. *J. Cell. Comp. Physiol.* **1962**, *59*, 223.

(105) Shimomura, O.; Johnson, F. H. *Tetrahedron Lett.* **1973**, *14*, 2963.

(106) Shimomura, O.; Johnson, F. H.; Morise, H. *Biochemistry* **1974**, *13*, 3278.

(107) Knight, M. R.; Campbell, A. K.; Smith, S. M.; Trewavas, A. J. *Nature* **1991**, *352*, 524.

(108) Contag, C. H.; Spilman, S. D.; Contag, P. R.; Oshiro, M.; Eames, B.; Dennery, P.; Stevenson, D. K.; Benaron, D. A. *Photochem. Photobiol.* **1997**, *66*, 523.

(109) Dubuisson, M. L. N.; Rees, J. F.; Marchand-Brynaert, J. *Drug Dev. Ind. Pharm.* **2005**, *31*, 827.

(110) Rees, J. F.; De Wergifosse, B.; Noiset, O.; Dubuisson, M.; Janssens, B.; Thompson, E. M. *J. Exp. Biol.* **1998**, *201*, 1211.

(111) Saleh, L.; Plieth, C. *Nat. Protoc.* **2010**, *5*, 1635.

(112) De Wergifosse, B.; Dubuisson, M.; Marchand-Brynaert, J.; Trouet, A.; Rees, J. F. *Free Radical Biol. Med.* **2004**, *36*, 278.

(113) Burton, M.; De Tollenaere, C.; Cavalier, J. F.; Marchand, C.; Dussart, F.; Marchand-Brynaert, J.; Rees, J. F. *Free Radical Res.* **2003**, *37*, 145.

(114) Devillers, I.; Dive, G.; De Tollenaere, C.; Falmagne, B.; De Wergifosse, B.; Rees, J. F.; Marchand-Brynaert, J. *Bioorg. Med. Chem. Lett.* **2001**, *11*, 2305.

(115) Cavalier, J. F.; Burton, M.; De Tollenaere, C.; Dussart, F.; Marchand, C.; Rees, J. F.; Marchand-Brynaert, J. *Synthesis* **2001**, 768.

(116) Dubuisson, M. L. N.; Rees, J. F.; Marchand-Brynaert, J. *Mini-Rev. Med. Chem.*

2004, *4*, 421.

(117) De Wael, F.; Jeanjot, P.; Moens, C.; Verbeuren, T.; Cordi, A.; Bouskela, E.; Rees, J. F.; Marchand-Brynaert, J. *Bioorg. Med. Chem.* **2009**, *17*, 4336.

(118) Shimomura, O.; Musicki, B.; Kishi, Y. *Biochem. J* **1989**, *261*, 913.

(119) Jones, K.; Keenan, M.; Hibbert, F. *Synlett* **1996**, *1996*, 509.

(120) Keenan, M.; Jones, K.; Hibbert, F. *Chem. Commun.* **1997**, 323.

(121) Jones, K.; Hibbert, F.; Keenan, M. *Trends Biotechnol.* **1999**, *17*, 477.

(122) Mosrin, M.; Bresser, T.; Knochel, P. *Org. Lett.* **2009**, *11*, 3406.

(123) Kondo, N.; Kuse, M.; Mutarapat, T.; Thasana, N.; Isobe, M. *Heterocycles* **2005**, *65*, 843.

(124) Devillers, I.; Arrault, A.; Olive, G.; Marchand-Brynaert, J. *Tetrahedron Lett.* **2002**, *43*, 3161.

(125) Shimomura, O.; Johnson, F. H. *Proc. Natl. Acad. Sci.* **1978**, *75*, 2611.

(126) Moran, L. A.; Horton, R. A.; Scrimgeour, G.; Perry, M. *Principles of Biochemistry*; 4th ed.; Pearson Education: New Jersey, 2006.

(127) Stepanyuk, G. A.; Liu, Z. J.; Markova, S. S.; Frank, L. A.; Lee, J.; Vysotski, E. S.; Wang, B. C. *Photochem. Photobiol. Sci.* **2008**, *7*, 442.

(128) Tschitschibabin, A. E. *Ber. Dtsch. Chem. Ges.* **1925**, *58*, 1704.

(129) Enguehard-Gueiffier, C.; Gueiffier, A. *Mini Rev. Med. Chem.* **2007**, *7*, 888.

(130) Deady, L. W.; Stanborough, M. S. *Aust. J. Chem.* **1981**, *34*, 1295.

(131) Kaminski, J. J.; Hilbert, J. M.; Pramanik, B. N.; Solomon, D. M.; Conn, D. J.; Rizvi, R. K.; Elliott, A. J.; Guzik, H.; Lovey, R. G.; et, a. *J. Med. Chem.* **1987**, *30*, 2031.

(132) Alcaide, B.; Plumet, J.; Sierra, M. A.; Vicent, C. *J. Org. Chem.* **1989**, *54*, 5763.

(133) Doise, M.; Blondeau, D.; Sliwa, H. *Heterocycles* **1992**, *34*, 2065.

(134) Arnold, W. D.; Bounaud, P.; Chen, C.; Eastman, B.; Gosberg, A.; Gradl, S. N.; Hopkins, S.; Li, Z.; McDonald, I.; Sprengeler, P. A.; Steensma, R. W.; Wilson, M. E. U.S. Patent 20090143352, **2009**, CAN 150: 563810.

(135) Choi, H. Y.; Chi, D. Y. *Org. Lett.* **2003**, *5*, 411.

(136) Cao, J. J.; Kopajtic, T.; Katz, J. L.; Newman, A. H. *Bioorg. Med. Chem. Lett.* **2008**, *18*, 5238.

(137) Weinstein, D. S.; Gong, H.; Duan, J.; Dhar, T. G. M.; Yang, B. V.; Chen, P.; Jiang, B. Patent WO 2008021926 (A2), **2008**, CAN 148: 285174.

(138) Steinhagen, H.; Scheiper, B.; Matter, H.; McCort, G.; Begis, G.; Goberville, P.; Thiers, B. Patent WO 2011012538 (A1), **2011**, CAN 154: 207650.

(139) Brand-Williams, W.; Cuvelier, M. E.; Berset, C. *Lebenson. Wiss. Technol.* **1995**, *28*, 25.

(140) Bringmann, G.; Goetz, R.; Keller, P. A.; Walter, R.; Henschel, P.; Schaeffer, M.; Staeblein, M.; Kelly, T. R.; Boyd, M. R. *Heterocycles* **1994**, *39*, 503.

(141) Zhang, D.; Ai, J.; Liang, Z.; Li, C.; Peng, X.; Ji, Y.; Jiang, H.; Geng, M.; Luo, C.; Liu, H. *Bioorg. Med. Chem.* **2012**, *20*, 5169.

(142) Maltais, F.; Bemis, G.; Wang, T.; Jimenez, J.-M.; Knegtel, R.; Davis, C.; Fraysse, D. Patent US 20090124602 (A1), **2009**, CAN150:539572.

(143) Jimenez, J.-M.; Bemis, G.; Maltais, F.; Wang, T.; Knegtel, R.; Davis, C.; Fraysse, D.; Boyall, D.; Settimo, L.; Young, S.; Mortimore, M. Patent WO 2008094992 (A2), **2008**, CAN149:224106.

(144) Poessl, T. M.; Kosjek, B.; Ellmer, U.; Gruber, C. C.; Edegger, K.; Faber, K.; Hildebrandt, P.; Bornscheuer, U. T.; Kroutil, W. *Adv. Synth. Catal.* **2005**, *347*, 1827.

(145) Benneche, T.; Christiansen, M. L.; Undheim, K. *Acta Chem. Scand., Ser. B* **1986**,

B40, 700.

(146) Perner, R. J.; Koenig, J. R.; Di, D. S.; Gomtsyan, A.; Schmidt, R. G.; Lee, C.-H.; Hsu, M. C.; McDonald, H. A.; Gauvin, D. M.; Joshi, S.; Turner, T. M.; Reilly, R. M.; Kym, P. R.; Kort, M. E. *Bioorg. Med. Chem.* **2010**, *18*, 4821.

(147) Inoue, S.; Sugiura, S.; Kakoi, H.; Hasizume, K.; Goto, T.; Iio, H. *Chem. Lett.* **1975**, 141.

(148) Trager, W.; Jensen, J. B. *Science* **1976**, *193*, 673.

(149) Desjardins, R. E.; Canfield, C. J.; Haynes, J. D.; Chulay, J. D. *Antimicrob. Agents Chemother.* **1979**, *16*, 710.

(150) Tarnchompoo, B.; Sirichaiwat, C.; Phupong, W.; Intaraudom, C.; Sirawaraporn, W.; Kamchonwongpaison, S.; Vanichtanankul, J.; Thebtaranonth, Y.; Yuthavong, Y. *J. Med. Chem.* **2002**, *45*, 1244.

(151) O'Brien, J.; Wilson, I.; Orton, T.; Pognan, F. *Eur. J. Biochem.* **2000**, *267*, 5421.

Appendix 1: Chemical Structures of the Dimeric Naphthylisoquinoline Alkaloids

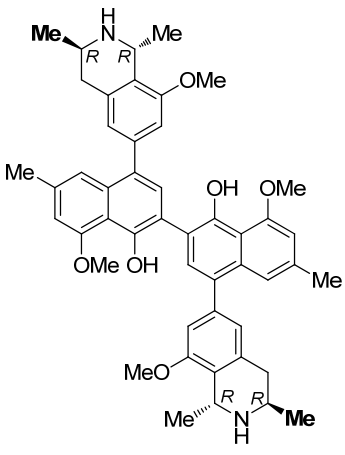

Pindikamine A (**I**)

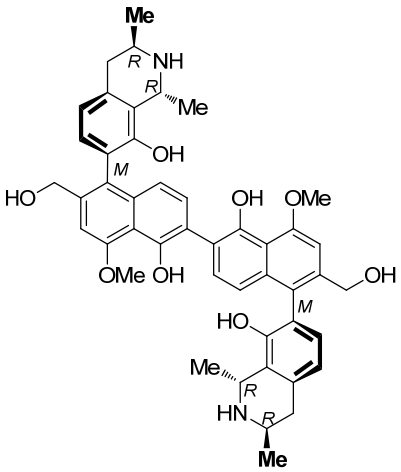

Jozipeltine A (**II**)

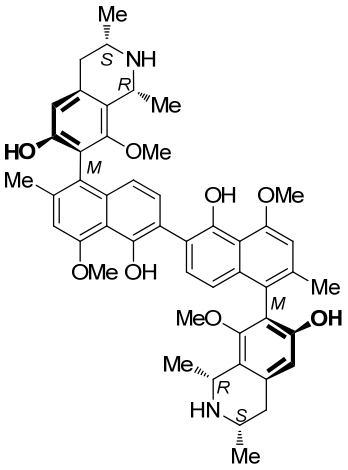

Ancistrogriffithine A (**III**)

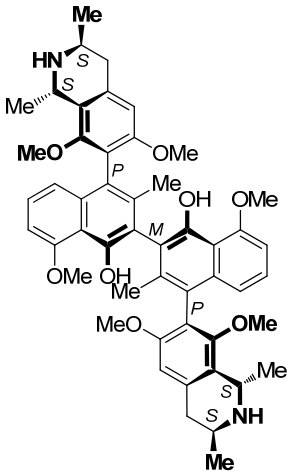

Shuangancistrotectorine A (**IV**)

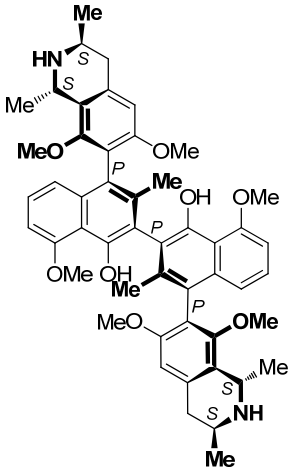

Shuangancistrotectorine B (**V**)

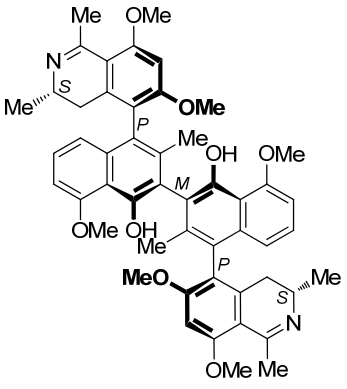

Shuangancistrotectorine C (**VI**)

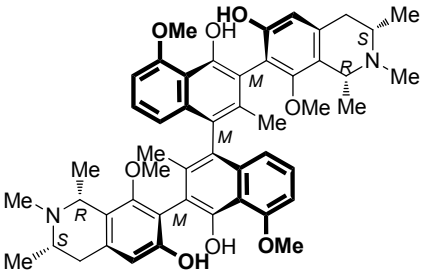

Shuangancistrotectorine D (**VII**)

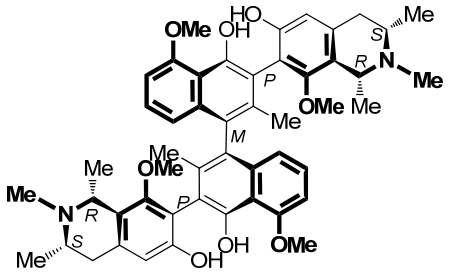

Shuangancistrotectorine E (**VIII**)

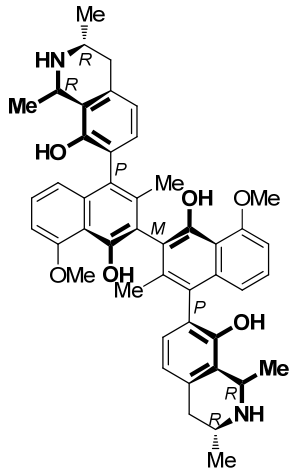

Jozimine A_2 (**IX**)

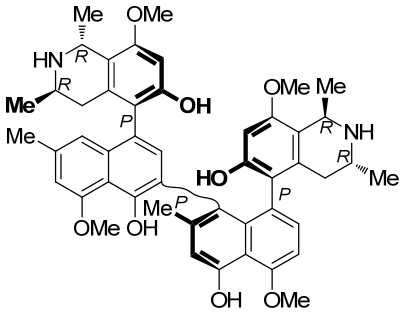

Mbandakamine A (**X**)

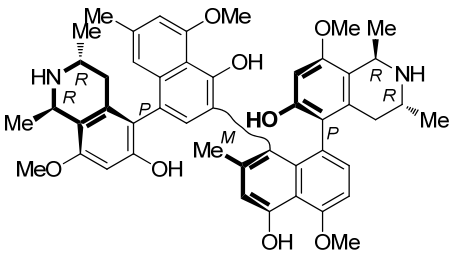

Mbandakamine B (**XI**)

Appendix 2: X-Ray Crystallographic Data

Appendix 2.1: compound 98

Crystal data

$C_{27}H_{29}NO_5$
$M_r = 447.53$
Monoclinic, $P2_1/a$
$a = 8.8697$ (1) Å
$b = 14.4698$ (3) Å
$c = 19.4107$ (4) Å
$\beta = 102.2617$ (11)°
$V = 2434.39$ (8) Å^3
$Z = 4$

$F(000) = 952$
$D_x = 1.221$ Mg m^{-3}
Mo $K\alpha$ radiation, $\lambda = 0.71073$ Å
Cell parameters from 29885 reflections
$\theta = 3\ \ 27.5°$
$\mu = 0.08$ mm^{-1}
$T = 200$ K
Block, Colourless
0.43 × 0.19 × 0.10 mm

Data collection

Nonius KappaCCD diffractometer
Graphite monochromator
φ & ω scans
Absorption correction: Integration via Gaussian method (Coppens, 1970) implemented in *maXus* (2000)
$T_{min} = 0.975$, $T_{max} = 0.992$

49210 measured reflections
5584 independent reflections
3762 reflections with $I > 2.0\sigma(I)$
$R_{int} = 0.036$
$\theta_{max} = 27.5°$, $\theta_{min} = 2.6°$
$h = -11 \rightarrow 11$
$k = -18 \rightarrow 18$
$l = -25 \rightarrow 25$

Refinement

Refinement on F^2
Least-squares matrix: Full
$R[F^2 > 2\sigma(F^2)] = 0.056$
$wR(F^2) = 0.156$
$S = 0.96$
5584 reflections
342 parameters
39 restraints
Primary atom site location: Structure-invariant direct methods

Hydrogen site location: Inferred from neighbouring sites
H atoms treated by a mixture of independent and constrained refinement
Method = Modified Sheldrick $w = 1/[\sigma^2(F^2) + (0.08P)^2 + 0.67P]$, where $P = (\max(F_o^2,0) + 2F_c^2)/3$
$(\Delta/\sigma)_{max} = 0.012$
$\Delta\rho_{max} = 0.28$ e Å^{-3}
$\Delta\rho_{min} = -0.29$ e Å^{-3}

Special details

Refinement. Direct methods gave the locations of most atoms, but it quickly became apparent that C14 was disordered over two sites, corresponding to disorder of packing of molecules with an inversion of configuration at this atom. Two sites (C14 and C141) were therefore used for this atom, and subsequent for each of two more (C32 and C321; O33 and O331). Restraints were applied so corresponding bond distances and displacement parameters would tend to be similar, and the relative occupancies of the two images were refined.

A difference map at this stage revealed peaks that suggested there was a small degree of disorder in the —COOEt chain too. C27 was assumed to be common to both images, and new sites O281, O291, C301 and C311 were introduced. In view of their low occupancy, these sites were assigned isotropic displacement parameters set equal to U_{eq} of the corresponding site of the major image. Restraints were applied to the low-occupancy sites so distances and angles would match values of the major sites. The relative occupancies were refined.

H atoms attached to C were included at calculated positions and ride on the atoms to which they are respectively bonded. The H atom attached to N was included at the position indicated by a difference electron density map and was refined positionally. Note that, although it has been treated as one site here, it is possibly the average of two sites, arising from the disorder in this section of the molecule, which are close together.

The largest peaks in the final difference map are located within the disorder.

Fractional atomic coordinates and isotropic or equivalent isotropic displacement parameters (Å²)

	x	*y*	*z*	U_{iso}*/U_{eq}	Occ. (<1)
O21	0.26381 (13)	0.39501 (9)	0.36057 (6)	0.0585	
O25	0.52356 (12)	0.41069 (9)	0.44130 (6)	0.0530	

O28	1.0072 (4)	0.5929 (4)	0.42524 (18)	0.0929	0.818 (4)
O29	0.97077 (18)	0.62318 (17)	0.31083 (8)	0.0606	0.818 (4)
O33	0.8906 (9)	0.5913 (5)	0.0044 (4)	0.0929	0.529 (10)
N15	0.8643 (2)	0.45904 (17)	0.05810 (9)	0.0790	
C1	0.2936 (2)	0.48024 (15)	0.18545 (9)	0.0628	
C2	0.23425 (19)	0.43844 (14)	0.23897 (9)	0.0593	
C3	0.31883 (17)	0.43214 (12)	0.30662 (8)	0.0469	
C4	0.47330 (16)	0.46806 (11)	0.32360 (8)	0.0414	
C5	0.57524 (17)	0.46058 (11)	0.39171 (8)	0.0438	
C6	0.71891 (18)	0.50028 (12)	0.40441 (8)	0.0490	
C7	0.76974 (17)	0.54808 (12)	0.35049 (8)	0.0485	
C8	0.67906 (17)	0.55347 (12)	0.28434 (8)	0.0464	
C9	0.53002 (16)	0.51320 (11)	0.26883 (8)	0.0435	
C10	0.43832 (18)	0.51804 (13)	0.19872 (8)	0.0525	
C11	0.4982 (2)	0.56525 (15)	0.14165 (8)	0.0593	
C12	0.6177 (2)	0.52791 (15)	0.11375 (9)	0.0627	
C13	0.6864 (3)	0.43446 (17)	0.13518 (13)	0.0900	
C14	0.7804 (6)	0.3866 (4)	0.0894 (3)	0.0703	0.529 (10)
C16	0.8085 (3)	0.5418 (2)	0.03548 (11)	0.0823	
C17	0.6766 (2)	0.57787 (17)	0.06387 (9)	0.0692	
C18	0.6163 (2)	0.6632 (2)	0.04145 (10)	0.0843	
C19	0.4951 (2)	0.6989 (2)	0.06625 (12)	0.0888	
C20	0.4368 (2)	0.64974 (18)	0.11635 (10)	0.0757	
C22	0.11744 (19)	0.34744 (14)	0.34743 (10)	0.0587	
C23	0.1312 (3)	0.25555 (15)	0.31320 (13)	0.0801	
C24	0.0786 (2)	0.33851 (18)	0.41916 (11)	0.0804	
C26	0.6272 (2)	0.39666 (14)	0.50772 (9)	0.0606	
C27	0.92549 (19)	0.59125 (15)	0.36803 (9)	0.0607	
C30	1.1216 (3)	0.6655 (2)	0.32312 (15)	0.0762	0.818 (4)
C31	1.1485 (4)	0.6955 (2)	0.25450 (18)	0.0882	0.818 (4)
C32	0.883 (2)	0.3057 (11)	0.1214 (11)	0.0831	0.529 (10)
C141	0.8289 (6)	0.4240 (4)	0.1217 (3)	0.0633	0.471 (10)
O291	0.9302 (9)	0.6677 (6)	0.3234 (4)	0.0610*	0.182 (4)
C301	1.0698 (13)	0.7283 (9)	0.3350 (7)	0.0760*	0.182 (4)
C311	1.1858 (18)	0.6759 (11)	0.3063 (9)	0.0880*	0.182 (4)
O331	0.8359 (9)	0.5856 (7)	−0.0177 (3)	0.0887	0.471 (10)
O281	1.013 (2)	0.5831 (16)	0.4256 (10)	0.0940*	0.182 (4)
C321	0.874 (3)	0.3231 (11)	0.1228 (13)	0.0865	0.471 (10)
H151	0.948 (3)	0.4408 (17)	0.0414 (13)	0.0900*	
H11	0.2323	0.4824	0.1390	0.0753*	
H21	0.1327	0.4138	0.2282	0.0712*	
H61	0.7844	0.4955	0.4499	0.0587*	
H81	0.7163	0.5846	0.2482	0.0556*	
H181	0.6592	0.6976	0.0086	0.1012*	
H191	0.4513	0.7566	0.0494	0.1065*	
H201	0.3529	0.6747	0.1336	0.0908*	
H221	0.0414	0.3840	0.3177	0.0704*	
H231	0.0342	0.2249	0.3048	0.0960*	
H232	0.2061	0.2188	0.3434	0.0960*	
H233	0.1619	0.2648	0.2697	0.0960*	
H241	−0.0174	0.3075	0.4148	0.0965*	
H242	0.0717	0.3983	0.4385	0.0965*	
H243	0.1571	0.3041	0.4494	0.0965*	
H261	0.5775	0.3610	0.5375	0.0727*	

O28	1.0072 (4)	0.5929 (4)	0.42524 (18)	0.0929	0.818 (4)
O29	0.97077 (18)	0.62318 (17)	0.31083 (8)	0.0606	0.818 (4)
O33	0.8906 (9)	0.5913 (5)	0.0044 (4)	0.0929	0.529 (10)
N15	0.8643 (2)	0.45904 (17)	0.05810 (9)	0.0790	
C1	0.2936 (2)	0.48024 (15)	0.18545 (9)	0.0628	
C2	0.23425 (19)	0.43844 (14)	0.23897 (9)	0.0593	
C3	0.31883 (17)	0.43214 (12)	0.30662 (8)	0.0469	
C4	0.47330 (16)	0.46806 (11)	0.32360 (8)	0.0414	
C5	0.57524 (17)	0.46058 (11)	0.39171 (8)	0.0438	
C6	0.71891 (18)	0.50028 (12)	0.40441 (8)	0.0490	
C7	0.76974 (17)	0.54808 (12)	0.35049 (8)	0.0485	
C8	0.67906 (17)	0.55347 (12)	0.28434 (8)	0.0464	
C9	0.53002 (16)	0.51320 (11)	0.26883 (8)	0.0435	
C10	0.43832 (18)	0.51804 (13)	0.19872 (8)	0.0525	
C11	0.4982 (2)	0.56525 (15)	0.14165 (8)	0.0593	
C12	0.6177 (2)	0.52791 (15)	0.11375 (9)	0.0627	
C13	0.6864 (3)	0.43446 (17)	0.13518 (13)	0.0900	
C14	0.7804 (6)	0.3866 (4)	0.0894 (3)	0.0703	0.529 (10)
C16	0.8085 (3)	0.5418 (2)	0.03548 (11)	0.0823	
C17	0.6766 (2)	0.57787 (17)	0.06387 (9)	0.0692	
C18	0.6163 (2)	0.6632 (2)	0.04145 (10)	0.0843	
C19	0.4951 (2)	0.6989 (2)	0.06625 (12)	0.0888	
C20	0.4368 (2)	0.64974 (18)	0.11635 (10)	0.0757	
C22	0.11744 (19)	0.34744 (14)	0.34743 (10)	0.0587	
C23	0.1312 (3)	0.25555 (15)	0.31320 (13)	0.0801	
C24	0.0786 (2)	0.33851 (18)	0.41916 (11)	0.0804	
C26	0.6272 (2)	0.39666 (14)	0.50772 (9)	0.0606	
C27	0.92549 (19)	0.59125 (15)	0.36803 (9)	0.0607	
C30	1.1216 (3)	0.6655 (2)	0.32312 (15)	0.0762	0.818 (4)
C31	1.1485 (4)	0.6955 (2)	0.25450 (18)	0.0882	0.818 (4)
C32	0.883 (2)	0.3057 (11)	0.1214 (11)	0.0831	0.529 (10)
C141	0.8289 (6)	0.4240 (4)	0.1217 (3)	0.0633	0.471 (10)
O291	0.9302 (9)	0.6677 (6)	0.3234 (4)	0.0610*	0.182 (4)
C301	1.0698 (13)	0.7283 (9)	0.3350 (7)	0.0760*	0.182 (4)
C311	1.1858 (18)	0.6759 (11)	0.3063 (9)	0.0880*	0.182 (4)
O331	0.8359 (9)	0.5856 (7)	−0.0177 (3)	0.0887	0.471 (10)
O281	1.013 (2)	0.5831 (16)	0.4256 (10)	0.0940*	0.182 (4)
C321	0.874 (3)	0.3231 (11)	0.1228 (13)	0.0865	0.471 (10)
H151	0.948 (3)	0.4408 (17)	0.0414 (13)	0.0900*	
H11	0.2323	0.4824	0.1390	0.0753*	
H21	0.1327	0.4138	0.2282	0.0712*	
H61	0.7844	0.4955	0.4499	0.0587*	
H81	0.7163	0.5846	0.2482	0.0556*	
H181	0.6592	0.6976	0.0086	0.1012*	
H191	0.4513	0.7566	0.0494	0.1065*	
H201	0.3529	0.6747	0.1336	0.0908*	
H221	0.0414	0.3840	0.3177	0.0704*	
H231	0.0342	0.2249	0.3048	0.0960*	
H232	0.2061	0.2188	0.3434	0.0960*	
H233	0.1619	0.2648	0.2697	0.0960*	
H241	−0.0174	0.3075	0.4148	0.0965*	
H242	0.0717	0.3983	0.4385	0.0965*	
H243	0.1571	0.3041	0.4494	0.0965*	
H261	0.5775	0.3610	0.5375	0.0727*	

H262	0.6566	0.4548	0.5292	0.0727*	
H263	0.7164	0.3649	0.5006	0.0727*	
H301	1.1249	0.7173	0.3535	0.0914*	0.818
H302	1.1981	0.6220	0.3439	0.0914*	0.818
H311	1.2472	0.7238	0.2608	0.1058*	0.818
H312	1.0713	0.7387	0.2340	0.1058*	0.818
H313	1.1445	0.6435	0.2243	0.1058*	0.818
H131	0.7514	0.4414	0.1805	0.1080*	0.529
H132	0.6032	0.3944	0.1383	0.1080*	0.529
H133	0.6929	0.4266	0.1843	0.1080*	0.471
H134	0.6206	0.3884	0.1100	0.1080*	0.471
H141	0.7081	0.3603	0.0513	0.0841*	0.529
H1411	0.8998	0.4514	0.1599	0.0761*	0.471
H321	0.9358	0.2810	0.0880	0.0967*	0.529
H322	0.9553	0.3280	0.1611	0.0967*	0.529
H323	0.8214	0.2587	0.1360	0.0967*	0.529
H3211	0.9746	0.3171	0.1133	0.1079*	0.471
H3212	0.8726	0.2960	0.1672	0.1079*	0.471
H3213	0.8017	0.2926	0.0870	0.1079*	0.471
H3011	1.1061	0.7400	0.3839	0.0912*	0.182
H3012	1.0468	0.7852	0.3107	0.0912*	0.182
H3111	1.2781	0.7110	0.3122	0.1056*	0.182
H3112	1.2066	0.6190	0.3308	0.1056*	0.182
H3113	1.1473	0.6642	0.2576	0.1056*	0.182

Atomic displacement parameters (Å²)

	U^{11}	U^{22}	U^{33}	U^{12}	U^{13}	U^{23}
O21	0.0430 (6)	0.0799 (9)	0.0520 (7)	−0.0207 (6)	0.0086 (5)	0.0061 (6)
O25	0.0431 (6)	0.0709 (8)	0.0443 (6)	−0.0076 (5)	0.0072 (5)	0.0091 (5)
O28	0.0508 (10)	0.172 (3)	0.0486 (9)	−0.0526 (14)	−0.0044 (8)	0.0142 (12)
O29	0.0397 (8)	0.0907 (15)	0.0521 (9)	−0.0193 (8)	0.0114 (6)	0.0040 (8)
O33	0.098 (4)	0.115 (3)	0.081 (4)	−0.033 (3)	0.053 (3)	−0.009 (3)
N15	0.0732 (11)	0.1160 (17)	0.0552 (10)	−0.0294 (11)	0.0302 (9)	−0.0183 (10)
C1	0.0512 (10)	0.0897 (14)	0.0443 (9)	−0.0209 (9)	0.0032 (7)	0.0003 (9)
C2	0.0433 (8)	0.0791 (13)	0.0533 (10)	−0.0207 (8)	0.0052 (7)	−0.0022 (9)
C3	0.0421 (8)	0.0522 (9)	0.0476 (9)	−0.0084 (7)	0.0119 (7)	−0.0025 (7)
C4	0.0369 (7)	0.0453 (8)	0.0427 (8)	−0.0027 (6)	0.0100 (6)	−0.0058 (6)
C5	0.0403 (7)	0.0507 (9)	0.0417 (8)	−0.0012 (7)	0.0117 (6)	−0.0019 (7)
C6	0.0393 (8)	0.0647 (11)	0.0421 (8)	−0.0052 (7)	0.0070 (6)	−0.0019 (7)
C7	0.0378 (7)	0.0622 (10)	0.0455 (8)	−0.0069 (7)	0.0087 (6)	−0.0037 (7)
C8	0.0406 (8)	0.0573 (10)	0.0431 (8)	−0.0073 (7)	0.0131 (6)	−0.0036 (7)
C9	0.0397 (7)	0.0507 (9)	0.0408 (8)	−0.0044 (6)	0.0102 (6)	−0.0058 (7)
C10	0.0462 (8)	0.0702 (12)	0.0409 (8)	−0.0117 (8)	0.0089 (7)	−0.0023 (8)
C11	0.0484 (9)	0.0897 (14)	0.0374 (8)	−0.0204 (9)	0.0038 (7)	0.0013 (8)
C12	0.0593 (10)	0.0906 (14)	0.0388 (9)	−0.0249 (10)	0.0120 (7)	−0.0075 (9)
C13	0.1176 (19)	0.0842 (16)	0.0881 (16)	−0.0155 (14)	0.0665 (15)	−0.0117 (13)
C14	0.065 (3)	0.099 (4)	0.050 (3)	−0.030 (2)	0.018 (2)	−0.022 (2)
C16	0.0841 (15)	0.120 (2)	0.0503 (11)	−0.0375 (15)	0.0304 (11)	−0.0152 (12)
C17	0.0603 (11)	0.1100 (17)	0.0362 (8)	−0.0266 (11)	0.0082 (8)	0.0017 (10)
C18	0.0601 (12)	0.139 (2)	0.0512 (11)	−0.0243 (13)	0.0069 (9)	0.0289 (13)
C19	0.0593 (12)	0.129 (2)	0.0735 (14)	−0.0074 (12)	0.0039 (10)	0.0437 (14)
C20	0.0508 (10)	0.1151 (18)	0.0585 (11)	−0.0079 (11)	0.0055 (9)	0.0242 (12)
C22	0.0396 (8)	0.0696 (12)	0.0654 (11)	−0.0145 (8)	0.0080 (7)	0.0117 (9)

C23	0.0721 (13)	0.0689 (14)	0.0951 (16)	−0.0182 (11)	0.0086 (11)	0.0101 (12)
C24	0.0539 (11)	0.1136 (19)	0.0756 (14)	−0.0225 (11)	0.0178 (10)	0.0175 (12)
C26	0.0525 (9)	0.0825 (13)	0.0444 (9)	−0.0049 (9)	0.0046 (7)	0.0102 (9)
C27	0.0435 (9)	0.0896 (14)	0.0485 (10)	−0.0159 (9)	0.0085 (8)	0.0036 (9)
C30	0.0436 (12)	0.109 (2)	0.0781 (17)	−0.0241 (14)	0.0172 (12)	0.0093 (15)
C31	0.0787 (18)	0.093 (2)	0.102 (2)	−0.0211 (15)	0.0387 (17)	0.0154 (17)
C32	0.086 (5)	0.093 (5)	0.075 (4)	−0.003 (4)	0.029 (3)	−0.018 (4)
C141	0.058 (3)	0.092 (4)	0.042 (3)	−0.011 (2)	0.016 (2)	−0.017 (2)
O331	0.078 (4)	0.150 (4)	0.043 (2)	−0.038 (3)	0.026 (2)	−0.004 (3)
C321	0.083 (5)	0.103 (6)	0.083 (5)	−0.007 (5)	0.039 (4)	−0.025 (5)

Geometric parameters (Å, º)

O21 C3	1.3566 (19)	C16 O331	1.277 (6)
O21 C22	1.4435 (19)	C17 C18	1.379 (3)
O25 C5	1.3584 (18)	C18 C19	1.369 (3)
O25 C26	1.4301 (19)	C18 H181	0.950
O28 C27	1.191 (4)	C19 C20	1.390 (3)
O29 C27	1.341 (2)	C19 H191	0.950
O29 C30	1.445 (3)	C20 H201	0.950
O33 C16	1.262 (5)	C22 C23	1.503 (3)
N15 C14	1.488 (5)	C22 C24	1.509 (3)
N15 C16	1.334 (3)	C22 H221	0.950
N15 C141	1.431 (4)	C23 H231	0.950
N15 H151	0.91 (2)	C23 H232	0.950
C1 C2	1.398 (2)	C23 H233	0.950
C1 C10	1.368 (2)	C24 H241	0.950
C1 H11	0.950	C24 H242	0.950
C2 C3	1.370 (2)	C24 H243	0.950
C2 H21	0.950	C26 H261	0.950
C3 C4	1.437 (2)	C26 H262	0.950
C4 C5	1.438 (2)	C26 H263	0.950
C4 C9	1.427 (2)	C27 O291	1.412 (8)
C5 C6	1.372 (2)	C27 O281	1.223 (17)
C6 C7	1.406 (2)	C30 C31	1.468 (4)
C6 H61	0.950	C30 H301	0.950
C7 C8	1.365 (2)	C30 H302	0.950
C7 C27	1.488 (2)	C31 H311	0.950
C8 C9	1.417 (2)	C31 H312	0.950
C8 H81	0.950	C31 H313	0.950
C9 C10	1.431 (2)	C32 H321	0.950
C10 C11	1.492 (2)	C32 H322	0.950
C11 C12	1.397 (3)	C32 H323	0.950
C11 C20	1.385 (3)	C141 C321	1.514 (14)
C12 C13	1.505 (3)	C141 H1411	0.950
C12 C17	1.396 (3)	O291 C301	1.495 (12)
C13 C14	1.509 (5)	C301 C311	1.479 (14)
C13 C141	1.352 (5)	C301 H3011	0.950
C13 H131	0.950	C301 H3012	0.950
C13 H132	0.950	C311 H3111	0.950
C13 H133	0.950	C311 H3112	0.950
C13 H134	0.950	C311 H3113	0.950
C14 C32	1.530 (13)	C321 H3211	0.950
C14 H141	0.950	C321 H3212	0.950

C16 C17	1.489 (3)	C321 H3213	0.950
O25···C26^{i}	3.332 (2)	O281···C24^{v}	3.59 (2)
O25···O25^{i}	3.529 (2)	O291···C311^{vi}	3.10 (2)
O28···C26^{ii}	3.231 (4)	O291···C31^{vi}	3.245 (8)
O28···C24^{i}	3.415 (4)	O291···C301^{vi}	3.58 (1)
O33···N15^{iii}	2.802 (9)	O331···N15^{iii}	2.998 (9)
O33···O33^{iii}	3.30 (2)	O331···C1^{vii}	3.353 (6)
O33···C19^{iv}	3.323 (8)	C4···C23^{viii}	3.548 (3)
O33···O331^{iii}	3.50 (1)	C5···C23^{viii}	3.559 (3)
O33···C16^{iii}	3.508 (9)	C5···C26^{i}	3.576 (3)
O281···C26^{ii}	3.19 (2)	C8···C301^{vi}	3.50 (1)
O281···C24^{i}	3.47 (2)		
C3 O21 C22	120.66 (13)	C19 C20 C11	121.5 (2)
C5 O25 C26	117.72 (12)	C19 C20 H201	119.2
C27 O29 C30	116.06 (17)	C11 C20 H201	119.3
C14 N15 C16	125.7 (3)	O21 C22 C23	110.22 (15)
C16 N15 C141	117.9 (3)	O21 C22 C24	104.53 (14)
C14 N15 H151	117.3 (16)	C23 C22 C24	112.82 (18)
C16 N15 H151	114.7 (16)	O21 C22 H221	109.7
C141 N15 H151	123.3 (16)	C23 C22 H221	109.7
C2 C1 C10	121.28 (16)	C24 C22 H221	109.7
C2 C1 H11	119.4	C22 C23 H231	109.5
C10 C1 H11	119.4	C22 C23 H232	109.5
C1 C2 C3	121.67 (15)	H231 C23 H232	109.5
C1 C2 H21	119.2	C22 C23 H233	109.5
C3 C2 H21	119.2	H231 C23 H233	109.5
C2 C3 O21	123.55 (14)	H232 C23 H233	109.5
C2 C3 C4	119.81 (14)	C22 C24 H241	109.5
O21 C3 C4	116.62 (13)	C22 C24 H242	109.5
C3 C4 C5	124.49 (14)	H241 C24 H242	109.5
C3 C4 C9	117.67 (13)	C22 C24 H243	109.5
C5 C4 C9	117.83 (13)	H241 C24 H243	109.5
C4 C5 O25	116.77 (13)	H242 C24 H243	109.5
C4 C5 C6	120.82 (14)	O25 C26 H261	109.5
O25 C5 C6	122.39 (14)	O25 C26 H262	109.5
C5 C6 C7	120.31 (14)	H261 C26 H262	109.5
C5 C6 H61	119.8	O25 C26 H263	109.5
C7 C6 H61	119.8	H261 C26 H263	109.5
C6 C7 C8	120.68 (14)	H262 C26 H263	109.5
C6 C7 C27	117.70 (14)	C7 C27 O29	112.46 (15)
C8 C7 C27	121.61 (15)	C7 C27 O28	125.0 (2)
C7 C8 C9	120.86 (14)	O29 C27 O28	122.4 (2)
C7 C8 H81	119.6	C7 C27 O291	109.6 (3)
C9 C8 H81	119.6	C7 C27 O281	123.1 (10)
C4 C9 C8	119.36 (13)	O291 C27 O281	122.8 (10)
C4 C9 C10	120.78 (13)	O29 C30 C31	107.4 (2)
C8 C9 C10	119.86 (14)	O29 C30 H301	110.0
C9 C10 C1	118.71 (15)	C31 C30 H301	110.0
C9 C10 C11	120.55 (14)	O29 C30 H302	110.0
C1 C10 C11	120.72 (15)	C31 C30 H302	110.0
C10 C11 C12	121.99 (19)	H301 C30 H302	109.5
C10 C11 C20	119.48 (17)	C30 C31 H311	109.5

C12 C11 C20	118.51 (17)	C30 C31 H312	109.5
C11 C12 C13	122.42 (17)	H311 C31 H312	109.5
C11 C12 C17	119.7 (2)	C30 C31 H313	109.5
C13 C12 C17	117.90 (19)	H311 C31 H313	109.5
C12 C13 C14	119.4 (2)	H312 C31 H313	109.5
C12 C13 C141	112.8 (3)	C14 C32 H321	110.3
C12 C13 H131	106.9	C14 C32 H322	108.1
C14 C13 H131	107.0	H321 C32 H322	109.5
C12 C13 H132	106.9	C14 C32 H323	110.0
C14 C13 H132	106.9	H321 C32 H323	109.5
H131 C13 H132	109.5	H322 C32 H323	109.5
C12 C13 H133	108.6	N15 C141 C13	120.8 (4)
C141 C13 H133	108.7	N15 C141 C321	104.3 (10)
C12 C13 H134	108.6	C13 C141 C321	111.3 (10)
C141 C13 H134	108.6	N15 C141 H1411	107.1
H133 C13 H134	109.5	C13 C141 H1411	107.1
C13 C14 N15	107.7 (4)	C321 C141 H1411	105.2
C13 C14 C32	117.8 (9)	C27 O291 C301	119.9 (7)
N15 C14 C32	113.6 (9)	O291 C301 C311	105.2 (10)
C13 C14 H141	106.1	O291 C301 H3011	110.5
N15 C14 H141	106.1	O291 C301 H3012	110.5
C32 C14 H141	104.7	C311 C301 H3012	110.5
N15 C16 O33	117.1 (4)	H3011 C301 H3012	109.5
N15 C16 C17	117.29 (19)	C301 C311 H3111	109.4
O33 C16 C17	123.8 (5)	C301 C311 H3112	109.5
N15 C16 O331	126.1 (5)	H3111 C311 H3112	109.5
C17 C16 O331	115.1 (5)	C301 C311 H3113	109.6
C16 C17 C12	121.0 (2)	H3111 C311 H3113	109.5
C16 C17 C18	118.64 (19)	H3112 C311 H3113	109.5
C12 C17 C18	120.4 (2)	C141 C321 H3211	110.0
C17 C18 C19	120.49 (19)	C141 C321 H3212	110.8
C17 C18 H181	119.8	C141 C321 H3213	107.5
C19 C18 H181	119.8	H3211 C321 H3212	109.5
C18 C19 C20	119.4 (2)	H3211 C321 H3213	109.5
C18 C19 H191	120.3	H3212 C321 H3213	109.5
C20 C19 H191	120.3		

O21 C3 C2 C1	177.7 (2)	C4 C5 C6 C7	−0.9 (3)
O21 C3 C4 C5	5.1 (2)	C4 C9 C8 C7	1.2 (2)
O21 C3 C4 C9	−175.8 (1)	C4 C9 C10 C11	−180.0 (2)
O25 C5 C4 C3	4.5 (2)	C5 C4 C9 C8	−3.8 (2)
O25 C5 C4 C9	−174.7 (1)	C5 C4 C9 C10	176.1 (2)
O25 C5 C6 C7	177.4 (2)	C5 C6 C7 C8	−1.9 (3)
O28 C27 O29 C30	−3.9 (5)	C5 C6 C7 C27	178.8 (2)
O28 C27 C7 C6	−4.4 (4)	C6 C5 O25 C26	−2.7 (2)
O28 C27 C7 C8	176.3 (4)	C6 C5 C4 C9	3.7 (2)
O29 C27 C7 C6	171.0 (2)	C6 C7 C8 C9	1.7 (3)
O29 C27 C7 C8	−8.3 (3)	C7 C8 C9 C10	−178.7 (2)
O33 C16 N15 C14	−173.6 (5)	C7 C27 O29 C30	−179.5 (2)
O33 C16 C17 C12	−162.1 (4)	C7 C27 O291 C301	174.2 (8)
O33 C16 C17 C18	16.0 (5)	C8 C9 C10 C11	0.0 (3)
O281 C27 O291 C301	18 (2)	C9 C8 C7 C27	−179.0 (2)
O281 C27 C7 C6	4 (1)	C9 C10 C11 C12	70.5 (2)
O281 C27 C7 C8	−176 (1)	C9 C10 C11 C20	−108.0 (2)

O291 C27 C7 C6	−152.9 (4)	C10 C11 C12 C13	4.7 (3)
O291 C27 C7 C8	27.8 (4)	C10 C11 C12 C17	−175.6 (2)
O331 O33 C16 N15	117 (1)	C10 C11 C20 C19	176.1 (2)
O331 O33 C16 C17	−79 (1)	C11 C12 C13 C14	162.5 (3)
O331 C16 N15 C141	175.7 (5)	C11 C12 C13 C141	−159.2 (3)
O331 C16 C17 C12	169.1 (4)	C11 C12 C17 C16	177.3 (2)
O331 C16 C17 C18	−12.8 (5)	C11 C12 C17 C18	−0.8 (3)
N15 C14 C13 C12	34.1 (4)	C11 C20 C19 C18	−0.2 (3)
N15 C16 C17 C12	1.9 (3)	C12 C11 C20 C19	−2.4 (3)
N15 C16 C17 C18	−180.0 (2)	C12 C13 C14 C32	164.0 (7)
N15 C141 C13 C12	−40.1 (5)	C12 C13 C141 C321	−163 (1)
C1 C2 C3 C4	−0.8 (3)	C12 C17 C18 C19	−1.9 (3)
C1 C10 C9 C4	1.4 (3)	C13 C12 C11 C20	−176.9 (2)
C1 C10 C9 C8	−178.7 (2)	C13 C12 C17 C16	−3.0 (3)
C1 C10 C11 C12	−110.9 (2)	C13 C12 C17 C18	178.9 (2)
C1 C10 C11 C20	70.7 (2)	C13 C14 N15 C16	−38.1 (4)
C2 C1 C10 C9	0.7 (3)	C13 C141 N15 C16	40.9 (6)
C2 C1 C10 C11	−177.9 (2)	C14 N15 C16 C17	21.3 (4)
C2 C3 O21 C22	8.9 (3)	C14 C13 C12 C17	−17.2 (3)
C2 C3 C4 C5	−176.4 (2)	C16 N15 C14 C32	−170.4 (8)
C2 C3 C4 C9	2.8 (2)	C16 N15 C141 C321	167 (1)
C3 O21 C22 C23	72.5 (2)	C16 C17 C18 C19	−180.0 (2)
C3 O21 C22 C24	−166.0 (2)	C17 C12 C11 C20	2.8 (3)
C3 C2 C1 C10	−1.0 (3)	C17 C12 C13 C141	21.1 (4)
C3 C4 C5 C6	−177.2 (2)	C17 C16 N15 C141	−18.7 (4)
C3 C4 C9 C8	177.0 (2)	C17 C18 C19 C20	2.3 (3)
C3 C4 C9 C10	−3.1 (2)	C27 O29 C30 C31	−180.0 (2)
C4 C3 O21 C22	−172.6 (2)	C27 O291 C301 C311	77 (1)
C4 C5 O25 C26	175.5 (1)		

Symmetry codes: (i) −*x*+1, −*y*+1, −*z*+1; (ii) −*x*+2, −*y*+1, −*z*+1; (iii) −*x*+2, −*y*+1, −*z*; (iv) *x*+1/2, −*y*+3/2, *z*; (v) *x*+1, *y*, *z*; (vi) *x*−1/2, −*y*+3/2, *z*; (vii) −*x*+1, −*y*+1, −*z*; (viii) *x*+1/2, −*y*+1/2, *z*.

Hydrogen-bond geometry (Å, º)

D H···*A*	*D* H	H···*A*	*D*···*A*	*D* H···*A*
N15 H151···O33^{iii}	0.91 (2)	1.89 (3)	2.802 (6)	173 (2)
N15 H151···O331^{iii}	0.91 (2)	2.10 (3)	2.998 (6)	169 (2)

Symmetry code: (iii) −*x*+2, −*y*+1, −*z*.

Appendix 2.2: compound 99

Crystal data

$C_{30}H_{29}NO_3$
$M_r = 451.56$
Triclinic, $P\bar{1}$
Hall symbol: -P 1
$a = 10.7708$ (3) Å
$b = 11.2749$ (5) Å
$c = 12.2367$ (4) Å
$\alpha = 62.920$ (4)°
$\beta = 73.089$ (3)°
$\gamma = 61.658$ (4)°
$V = 1159.20$ (9) Å^3
$Z = 2$
$F(000) = 480$
$D_x = 1.294$ Mg m^{-3}
Mo $K\alpha$ radiation, $\lambda = 0.71070$ Å
Cell parameters from 10608 reflections
$\theta = 2$ 30°
$\mu = 0.08$ mm^{-1}

$T = 150$ K
Block, pale yellow
0.49 × 0.29 × 0.17 mm

Data collection

Oxford Diffraction SuperNova diffractometer
Graphite monochromator
ω scans
Absorption correction: multi-scan
CrysAlis PRO, Agilent Technologies, Version 1.171.37.21t (release 24-10-2013 CrysAlis171 .NET) (compiled Oct 24 2013,16:12:21) Empirical absorption correction using spherical harmonics, implemented in SCALE3 ABSPACK scaling algorithm.
$T_{min} = 0.96$, $T_{max} = 0.99$
28954 measured reflections
6472 independent reflections
4961 reflections with $I > 2.0\sigma(I)$
$R_{int} = 0.033$
$\theta_{max} = 30.9°$, $\theta_{min} = 2.2°$
$h = -15 \rightarrow 15$
$k = -15 \rightarrow 16$
$l = -17 \rightarrow 16$

Refinement

Refinement on F^2
Least-squares matrix: full
$R[F^2 > 2\sigma(F^2)] = 0.050$
$wR(F^2) = 0.133$
$S = 0.99$
6472 reflections
307 parameters
0 restraints
Primary atom site location: structure-invariant direct methods
Hydrogen site location: difference Fourier map
H-atom parameters constrained
Method = Modified Sheldrick $w = 1/[\sigma^2(F^2) + ($ $0.06P)^2 + 0.58P]$, where $P = (\max(F_o^2,0) + 2F_c^2)/3$
$(\Delta/\sigma)_{max} = 0.001$
$\Delta\rho_{max} = 0.56$ e Å^{-3}
$\Delta\rho_{min} = -0.35$ e Å^{-3}

Special details

Refinement

Most of the hydrogen atoms were observed in a difference electron density map synthesized prior to their inclusion. H atoms were included at calculated positions and were initially refined with soft restraints on the bond lengths and angles to regularize their geometry (C H in the range 0.93 0.98 Å) and with U_{iso}(H) in the range 1.2 1.5 times U_{eq} of the parent atom, after which the positions were refined with riding constraints.

The largest features in the final difference electron density map are generally located midway between bonded atoms.

Fractional atomic coordinates and isotropic or equivalent isotropic displacement parameters (Å²)

	x	*y*	*z*	U_{iso}*/U_{eq}
O1	1.08178 (10)	0.56252 (11)	0.12696 (10)	0.0269
O2	0.29527 (10)	0.24792 (12)	0.49497 (9)	0.0268
O3	0.36422 (11)	0.11744 (11)	0.35340 (9)	0.0264
N1	0.67681 (13)	0.83243 (13)	0.02690 (11)	0.0270
C1	0.74057 (13)	0.53553 (14)	0.19442 (12)	0.0190
C2	0.59603 (14)	0.63232 (15)	0.14775 (13)	0.0236
C3	0.56740 (15)	0.78899 (15)	0.11663 (13)	0.0257
C4	0.80579 (15)	0.73918 (15)	0.03925 (13)	0.0224
C5	0.84591 (13)	0.59138 (14)	0.13981 (12)	0.0193
C6	0.98143 (14)	0.50638 (15)	0.18311 (12)	0.0206
C7	1.00774 (14)	0.37283 (15)	0.28179 (13)	0.0228
C8	0.90219 (14)	0.32055 (15)	0.33343 (13)	0.0222
C9	0.76890 (14)	0.39791 (14)	0.28981 (12)	0.0198
C10	0.65515 (14)	0.34165 (14)	0.34900 (12)	0.0196
C11	0.58186 (15)	0.35729 (15)	0.45687 (13)	0.0231
C12	0.46130 (14)	0.32466 (15)	0.50927 (13)	0.0229
C13	0.41778 (14)	0.26923 (14)	0.45521 (12)	0.0204
C14	0.50023 (13)	0.23450 (14)	0.34976 (12)	0.0191
C15	0.47398 (14)	0.15918 (15)	0.29659 (12)	0.0213

C16	0.55664 (15)	0.13206 (16)	0.19433 (13)	0.0248
C17	0.66912 (15)	0.17780 (17)	0.13784 (13)	0.0259
C18	0.69645 (14)	0.25002 (15)	0.18646 (12)	0.0228
C19	0.61660 (13)	0.27730 (14)	0.29388 (12)	0.0196
C20	0.91619 (16)	0.78645 (18)	−0.05407 (14)	0.0309
C21	1.22556 (14)	0.46631 (17)	0.15087 (15)	0.0302
C22	0.21243 (15)	0.27948 (17)	0.60117 (13)	0.0257
C23	0.08454 (15)	0.24762 (16)	0.62475 (12)	0.0237
C24	−0.05050 (15)	0.35048 (17)	0.63923 (14)	0.0278
C25	−0.16845 (16)	0.31794 (18)	0.66765 (15)	0.0315
C26	−0.15159 (17)	0.18276 (18)	0.68165 (14)	0.0320
C27	−0.01714 (18)	0.08035 (17)	0.66485 (15)	0.0327
C28	0.10044 (16)	0.11264 (16)	0.63611 (14)	0.0287
C29	0.33640 (16)	0.03935 (17)	0.30572 (15)	0.0288
C30	0.75932 (19)	0.1415 (2)	0.02859 (17)	0.0430
H21	0.5236	0.6046	0.2099	0.0277*
H22	0.5912	0.6209	0.0739	0.0292*
H31	0.5666	0.8017	0.1925	0.0318*
H32	0.4760	0.8546	0.0840	0.0311*
H71	1.0967	0.3190	0.3146	0.0272*
H81	0.9212	0.2299	0.4016	0.0266*
H111	0.6106	0.3954	0.4960	0.0270*
H121	0.4085	0.3441	0.5816	0.0278*
H161	0.5368	0.0823	0.1597	0.0300*
H181	0.7741	0.2792	0.1494	0.0270*
H201	0.8695	0.8732	−0.1218	0.0460*
H202	0.9698	0.8080	−0.0175	0.0454*
H203	0.9850	0.7108	−0.0856	0.0459*
H211	1.2833	0.5211	0.0953	0.0440*
H212	1.2404	0.4357	0.2368	0.0434*
H213	1.2520	0.3805	0.1321	0.0426*
H221	0.2693	0.2171	0.6726	0.0308*
H222	0.1843	0.3825	0.5850	0.0308*
H241	−0.0618	0.4447	0.6285	0.0331*
H251	−0.2614	0.3891	0.6774	0.0390*
H261	−0.2311	0.1602	0.7017	0.0382*
H271	−0.0047	−0.0116	0.6729	0.0398*
H281	0.1947	0.0415	0.6249	0.0347*
H291	0.2541	0.0219	0.3574	0.0418*
H292	0.4153	−0.0535	0.3148	0.0413*
H293	0.3159	0.0962	0.2196	0.0420*
H301	0.8222	0.1909	−0.0116	0.0652*
H302	0.8158	0.0427	0.0543	0.0679*
H303	0.7063	0.1602	−0.0306	0.0674*

Atomic displacement parameters (Å²)

	U^{11}	U^{22}	U^{33}	U^{12}	U^{13}	U^{23}
O1	0.0178 (5)	0.0267 (5)	0.0345 (6)	−0.0113 (4)	−0.0024 (4)	−0.0077 (4)
O2	0.0243 (5)	0.0393 (6)	0.0279 (5)	−0.0197 (4)	0.0082 (4)	−0.0204 (5)
O3	0.0264 (5)	0.0331 (6)	0.0317 (5)	−0.0188 (4)	0.0044 (4)	−0.0187 (4)
N1	0.0253 (6)	0.0243 (6)	0.0289 (6)	−0.0105 (5)	−0.0048 (5)	−0.0062 (5)
C1	0.0178 (6)	0.0211 (6)	0.0208 (6)	−0.0080 (5)	−0.0004 (5)	−0.0107 (5)
C2	0.0174 (6)	0.0271 (7)	0.0255 (7)	−0.0098 (5)	−0.0020 (5)	−0.0085 (5)

C3	0.0202 (6)	0.0243 (7)	0.0266 (7)	−0.0057 (5)	−0.0025 (5)	−0.0082 (6)
C4	0.0248 (7)	0.0240 (7)	0.0226 (6)	−0.0130 (6)	−0.0024 (5)	−0.0087 (5)
C5	0.0190 (6)	0.0204 (6)	0.0209 (6)	−0.0085 (5)	0.0000 (5)	−0.0100 (5)
C6	0.0186 (6)	0.0227 (6)	0.0240 (7)	−0.0096 (5)	0.0010 (5)	−0.0119 (5)
C7	0.0183 (6)	0.0229 (6)	0.0272 (7)	−0.0061 (5)	−0.0033 (5)	−0.0112 (5)
C8	0.0230 (6)	0.0195 (6)	0.0225 (6)	−0.0078 (5)	−0.0024 (5)	−0.0072 (5)
C9	0.0197 (6)	0.0210 (6)	0.0215 (6)	−0.0095 (5)	0.0015 (5)	−0.0111 (5)
C10	0.0191 (6)	0.0187 (6)	0.0214 (6)	−0.0082 (5)	−0.0013 (5)	−0.0077 (5)
C11	0.0246 (7)	0.0261 (7)	0.0247 (7)	−0.0132 (6)	−0.0003 (5)	−0.0124 (6)
C12	0.0244 (7)	0.0264 (7)	0.0214 (6)	−0.0126 (6)	0.0024 (5)	−0.0121 (5)
C13	0.0197 (6)	0.0209 (6)	0.0209 (6)	−0.0098 (5)	0.0003 (5)	−0.0077 (5)
C14	0.0183 (6)	0.0190 (6)	0.0203 (6)	−0.0076 (5)	−0.0023 (5)	−0.0074 (5)
C15	0.0201 (6)	0.0217 (6)	0.0247 (7)	−0.0098 (5)	−0.0019 (5)	−0.0093 (5)
C16	0.0239 (7)	0.0294 (7)	0.0286 (7)	−0.0121 (6)	−0.0005 (5)	−0.0166 (6)
C17	0.0237 (7)	0.0330 (8)	0.0258 (7)	−0.0123 (6)	0.0015 (5)	−0.0163 (6)
C18	0.0210 (6)	0.0275 (7)	0.0228 (7)	−0.0118 (5)	0.0018 (5)	−0.0119 (5)
C19	0.0190 (6)	0.0182 (6)	0.0208 (6)	−0.0066 (5)	−0.0021 (5)	−0.0074 (5)
C20	0.0287 (7)	0.0337 (8)	0.0278 (7)	−0.0183 (6)	−0.0026 (6)	−0.0036 (6)
C21	0.0173 (6)	0.0320 (8)	0.0388 (8)	−0.0091 (6)	−0.0001 (6)	−0.0137 (7)
C22	0.0258 (7)	0.0330 (8)	0.0245 (7)	−0.0162 (6)	0.0054 (5)	−0.0157 (6)
C23	0.0254 (7)	0.0293 (7)	0.0192 (6)	−0.0151 (6)	0.0024 (5)	−0.0098 (5)
C24	0.0273 (7)	0.0307 (7)	0.0302 (8)	−0.0142 (6)	0.0036 (6)	−0.0163 (6)
C25	0.0242 (7)	0.0388 (9)	0.0352 (8)	−0.0147 (7)	0.0038 (6)	−0.0187 (7)
C26	0.0315 (8)	0.0421 (9)	0.0301 (8)	−0.0243 (7)	0.0028 (6)	−0.0131 (7)
C27	0.0400 (9)	0.0287 (8)	0.0336 (8)	−0.0216 (7)	0.0011 (7)	−0.0096 (6)
C28	0.0279 (7)	0.0264 (7)	0.0285 (7)	−0.0118 (6)	0.0005 (6)	−0.0085 (6)
C29	0.0303 (7)	0.0301 (7)	0.0365 (8)	−0.0168 (6)	−0.0005 (6)	−0.0175 (6)
C30	0.0407 (9)	0.0702 (13)	0.0440 (10)	−0.0350 (9)	0.0174 (8)	−0.0415 (10)

Geometric parameters (Å, º)

O1	C6	1.3647 (16)	C15	C16	1.3761 (19)
O1	C21	1.4283 (17)	C16	C17	1.412 (2)
O2	C13	1.3625 (16)	C16	H161	0.960
O2	C22	1.4340 (16)	C17	C18	1.3692 (19)
O3	C15	1.3618 (16)	C17	C30	1.505 (2)
O3	C29	1.4231 (17)	C18	C19	1.4217 (18)
N1	C3	1.4628 (18)	C18	H181	0.958
N1	C4	1.2841 (18)	C20	H201	0.966
C1	C2	1.5091 (18)	C20	H202	0.987
C1	C5	1.4087 (18)	C20	H203	0.980
C1	C9	1.4042 (19)	C21	H211	0.984
C2	C3	1.516 (2)	C21	H212	0.982
C2	H21	0.977	C21	H213	0.986
C2	H22	0.988	C22	C23	1.5013 (19)
C3	H31	0.999	C22	H221	0.988
C3	H32	0.972	C22	H222	0.986
C4	C5	1.4956 (19)	C23	C24	1.388 (2)
C4	C20	1.503 (2)	C23	C28	1.392 (2)
C5	C6	1.4104 (18)	C24	C25	1.392 (2)
C6	C7	1.3944 (19)	C24	H241	0.960
C7	C8	1.3851 (19)	C25	C26	1.380 (2)
C7	H71	0.948	C25	H251	0.957
C8	C9	1.3927 (19)	C26	C27	1.388 (2)

C8 H81	0.952	C26 H261	0.941
C9 C10	1.4938 (18)	C27 C28	1.386 (2)
C10 C11	1.3675 (18)	C27 H271	0.941
C10 C19	1.4312 (18)	C28 H281	0.969
C11 C12	1.4096 (19)	C29 H291	0.974
C11 H111	0.954	C29 H292	0.967
C12 C13	1.3722 (19)	C29 H293	0.978
C12 H121	0.959	C30 H301	0.962
C13 C14	1.4388 (18)	C30 H302	0.927
C14 C15	1.4362 (18)	C30 H303	0.939
C14 C19	1.4306 (18)		

O1···C20	2.719 (2)	C18···C28^{iii}	3.522 (2)
O1···C24^{i}	3.308 (2)	C18···C1	3.516 (2)
O2···O3	2.5003 (16)	C19···C2	3.484 (2)
O3···C21^{ii}	3.398 (2)	C20···O1	2.719 (2)
O3···O2	2.5003 (16)	C21···C15^{iv}	3.269 (2)
C1···C18	3.516 (2)	C21···C24^{i}	3.569 (2)
C2···C19	3.484 (2)	C21···O3^{iv}	3.398 (2)
C11···C11^{i}	3.347 (2)	C21···C14^{iv}	3.544 (2)
C11···C12^{i}	3.592 (2)	C24···C21^{i}	3.569 (2)
C12···C29^{iii}	3.555 (2)	C24···O1^{i}	3.308 (2)
C12···C11^{i}	3.592 (2)	C28···C18^{iii}	3.522 (2)
C14···C21^{ii}	3.544 (2)	C28···C17^{iii}	3.545 (2)
C15···C21^{ii}	3.269 (2)	C29···C12^{iii}	3.555 (2)
C17···C28^{iii}	3.545 (2)		

C6 O1 C21	117.53 (11)	C16 C17 C18	119.09 (13)
C13 O2 C22	117.91 (11)	C16 C17 C30	119.35 (13)
C15 O3 C29	118.02 (11)	C18 C17 C30	121.53 (13)
C3 N1 C4	117.19 (12)	C17 C18 C19	121.74 (13)
C2 C1 C5	116.74 (12)	C17 C18 H181	119.2
C2 C1 C9	122.10 (12)	C19 C18 H181	119.0
C5 C1 C9	121.14 (12)	C10 C19 C14	119.94 (11)
C1 C2 C3	108.74 (11)	C10 C19 C18	120.59 (12)
C1 C2 H21	110.2	C14 C19 C18	119.42 (12)
C3 C2 H21	110.8	C4 C20 H201	108.7
C1 C2 H22	110.7	C4 C20 H202	111.1
C3 C2 H22	109.9	H201 C20 H202	109.0
H21 C2 H22	106.5	C4 C20 H203	111.7
C2 C3 N1	112.16 (11)	H201 C20 H203	109.2
C2 C3 H31	109.8	H202 C20 H203	107.2
N1 C3 H31	106.9	O1 C21 H211	106.2
C2 C3 H32	110.8	O1 C21 H212	111.6
N1 C3 H32	108.7	H211 C21 H212	109.5
H31 C3 H32	108.3	O1 C21 H213	109.5
N1 C4 C5	122.66 (12)	H211 C21 H213	109.9
N1 C4 C20	116.16 (13)	H212 C21 H213	110.1
C5 C4 C20	121.18 (12)	O2 C22 C23	107.14 (11)
C4 C5 C1	117.35 (11)	O2 C22 H221	109.4
C4 C5 C6	123.97 (12)	C23 C22 H221	110.4
C1 C5 C6	118.67 (12)	O2 C22 H222	109.6
C5 C6 O1	117.25 (12)	C23 C22 H222	110.9
C5 C6 C7	120.24 (12)	H221 C22 H222	109.3

O1 C6 C7	122.48 (12)	C22 C23 C24	120.51 (13)
C6 C7 C8	119.72 (12)	C22 C23 C28	120.25 (13)
C6 C7 H71	120.2	C24 C23 C28	119.22 (13)
C8 C7 H71	120.1	C23 C24 C25	120.44 (14)
C7 C8 C9	121.86 (13)	C23 C24 H241	119.2
C7 C8 H81	118.8	C25 C24 H241	120.3
C9 C8 H81	119.3	C24 C25 C26	120.01 (14)
C1 C9 C8	118.23 (12)	C24 C25 H251	120.3
C1 C9 C10	120.55 (12)	C26 C25 H251	119.7
C8 C9 C10	121.06 (12)	C25 C26 C27	119.88 (14)
C9 C10 C11	118.88 (12)	C25 C26 H261	120.1
C9 C10 C19	122.10 (11)	C27 C26 H261	120.0
C11 C10 C19	118.98 (12)	C26 C27 C28	120.22 (15)
C10 C11 C12	121.95 (13)	C26 C27 H271	120.5
C10 C11 H111	119.1	C28 C27 H271	119.3
C12 C11 H111	118.9	C23 C28 C27	120.21 (14)
C11 C12 C13	120.18 (12)	C23 C28 H281	119.0
C11 C12 H121	119.5	C27 C28 H281	120.8
C13 C12 H121	120.3	O3 C29 H291	105.1
C12 C13 O2	122.82 (12)	O3 C29 H292	110.2
C12 C13 C14	120.28 (12)	H291 C29 H292	108.5
O2 C13 C14	116.88 (12)	O3 C29 H293	111.0
C13 C14 C15	124.43 (12)	H291 C29 H293	110.6
C13 C14 C19	118.06 (12)	H292 C29 H293	111.1
C15 C14 C19	117.51 (11)	C17 C30 H301	112.9
C14 C15 O3	116.04 (11)	C17 C30 H302	109.5
C14 C15 C16	120.83 (12)	H301 C30 H302	106.7
O3 C15 C16	123.13 (12)	C17 C30 H303	113.3
C15 C16 C17	121.35 (13)	H301 C30 H303	108.6
C15 C16 H161	119.5	H302 C30 H303	105.3
C17 C16 H161	119.1		

C21 O1 C6 C5	−166.78 (13)	C19 C10 C11 C12	−6.1 (2)
C21 O1 C6 C7	15.1 (2)	C9 C10 C19 C14	−175.55 (14)
C22 O2 C13 C12	−2.7 (2)	C9 C10 C19 C18	7.0 (2)
C22 O2 C13 C14	178.99 (13)	C11 C10 C19 C14	1.9 (2)
C13 O2 C22 C23	179.80 (12)	C11 C10 C19 C18	−175.63 (14)
C29 O3 C15 C14	−178.51 (13)	C10 C11 C12 C13	3.0 (2)
C29 O3 C15 C16	1.4 (2)	C11 C12 C13 O2	−173.91 (14)
C4 N1 C3 C2	−40.3 (2)	C11 C12 C13 C14	4.3 (2)
C3 N1 C4 C5	0.2 (2)	O2 C13 C14 C15	−10.0 (2)
C3 N1 C4 C20	−180.00 (16)	O2 C13 C14 C19	170.13 (13)
C5 C1 C2 C3	−35.38 (17)	C12 C13 C14 C15	171.62 (14)
C9 C1 C2 C3	142.98 (14)	C12 C13 C14 C19	−8.2 (2)
C2 C1 C5 C4	−1.35 (19)	C13 C14 C15 O3	−1.1 (2)
C2 C1 C5 C6	178.15 (13)	C13 C14 C15 C16	179.00 (15)
C9 C1 C5 C4	−179.73 (13)	C19 C14 C15 O3	178.75 (13)
C9 C1 C5 C6	−0.2 (2)	C19 C14 C15 C16	−1.2 (2)
C2 C1 C9 C8	−175.22 (13)	C13 C14 C19 C10	5.1 (2)
C2 C1 C9 C10	0.2 (2)	C13 C14 C19 C18	−177.38 (13)
C5 C1 C9 C8	3.1 (2)	C15 C14 C19 C10	−174.74 (13)
C5 C1 C9 C10	178.46 (13)	C15 C14 C19 C18	2.8 (2)
C1 C2 C3 N1	56.69 (16)	O3 C15 C16 C17	179.71 (15)
N1 C4 C5 C1	22.1 (2)	C14 C15 C16 C17	−0.4 (2)

N1	C4	C5	C6	−157.41 (16)	C15	C16	C17	C18	0.3 (2)
C20	C4	C5	C1	−157.73 (15)	C15	C16	C17	C30	178.11 (16)
C20	C4	C5	C6	22.8 (2)	C16	C17	C18	C19	1.4 (2)
C1	C5	C6	O1	178.96 (13)	C30	C17	C18	C19	−176.36 (16)
C1	C5	C6	C7	−2.9 (2)	C17	C18	C19	C10	174.52 (15)
C4	C5	C6	O1	−1.6 (2)	C17	C18	C19	C14	−3.0 (2)
C4	C5	C6	C7	176.58 (14)	O2	C22	C23	C24	−128.70 (14)
O1	C6	C7	C8	−178.85 (14)	O2	C22	C23	C28	53.28 (17)
C5	C6	C7	C8	3.1 (2)	C22	C23	C24	C25	−176.54 (14)
C6	C7	C8	C9	−0.2 (2)	C28	C23	C24	C25	1.5 (2)
C7	C8	C9	C1	−2.9 (2)	C22	C23	C28	C27	176.31 (14)
C7	C8	C9	C10	−178.27 (14)	C24	C23	C28	C27	−1.7 (2)
C1	C9	C10	C11	−96.83 (17)	C23	C24	C25	C26	0.0 (2)
C1	C9	C10	C19	80.58 (19)	C24	C25	C26	C27	−1.3 (2)
C8	C9	C10	C11	78.43 (19)	C25	C26	C27	C28	1.1 (2)
C8	C9	C10	C19	−104.17 (17)	C26	C27	C28	C23	0.5 (2)
C9	C10	C11	C12	171.43 (14)					

Symmetry codes: (i) −*x*+1, −*y*+1, −*z*+1; (ii) *x*−1, *y*, *z*; (iii) −*x*+1, −*y*, −*z*+1; (iv) *x*+1, *y*, *z*.

Appendix 2.3: compound 100

Crystal data

$C_{29}H_{27}NO_3$
$M_r = 437.54$
Triclinic, $P\bar{1}$
Hall symbol: -P 1
$a = 8.6668$ (3) Å
$b = 11.5627$ (4) Å
$c = 13.1493$ (4) Å
$\alpha = 100.702$ (3)°
$\beta = 95.417$ (2)°
$\gamma = 93.082$ (2)°
$V = 1285.58$ (8) Å^3
$Z = 2$
$F(000) = 464.001$
$D_x = 1.130$ Mg m^{-3}

Mo $K\alpha$ radiation, $\lambda = 0.71070$ Å
Cell parameters from 11286 reflections
$\theta = 3\ 30°$
$\mu = 0.07$ mm^{-1}
$T = 150$ K
Block, colourless
0.47 × 0.26 × 0.18 mm

Data collection

New Xcalibur, Atlas diffractometer
Radiation source: Enhance (Mo) X-ray Source
Graphite monochromator
ω scans

Absorption correction: multi-scan *CrysAlis PRO*, Agilent Technologies, Version 1.171.37.21t (release 24-10-2013 CrysAlis171 .NET) (compiled Oct 24 2013,16:12:21) Empirical absorption correction using spherical harmonics, implemented in SCALE3 ABSPACK scaling algorithm.
$T_{min} = 0.97$, $T_{max} = 0.99$
27657 measured reflections
7065 independent reflections
5581 reflections with $I > 2.0\sigma(I)$
$R_{int} = 0.021$
$\theta_{max} = 30.8°$, $\theta_{min} = 2.2°$
$h = -12 \rightarrow 11$
$k = -16 \rightarrow 16$
$l = -18 \rightarrow 17$

Refinement

Refinement on F^2
Least-squares matrix: full
$R[F^2 > 2\sigma(F^2)] = 0.056$
$wR(F^2) = 0.168$
$S = 0.99$
7065 reflections
308 parameters
4 restraints
Primary atom site location: structure-invariant direct methods

Hydrogen site location: difference Fourier map
H atoms treated by a mixture of independent and constrained refinement
Method = Modified Sheldrick $w = 1/[\sigma^2(F^2) + (0.09P)^2 + 0.6P]$, where $P = (\max(F_o^2,0) + 2F_c^2)/3$
$(\Delta/\sigma)_{max} = 0.001$
$\Delta\rho_{max} = 0.42$ e Å^{-3}
$\Delta\rho_{min} = -0.32$ e Å^{-3}

Special details

Refinement

After identification of the $C_{29}H_{27}NO_3$ molecule, a difference electron density map revealed a number of peaks centred about the inversion centre at (0,0,0). They indicate the presence of a solvate molecule, possibly hexane and/or dichloromethane, disordered over many sites. No sensible disordered model could be formulated which would match the observed electron density, so the computer program SQUEEZE within *PLATON* was used to account for the electron density in this region of the unit cell. [Sluis and Spek (1990)] The program identified solvent accessible voids totalling 217 Å^3 and 46 electrons per unit cell were recovered. The formula weight, density *etc.* listed in the Tables do not include any correction for the missing solvate.

There is a small degree of disorder in the $C_{29}H_{27}NO_3$ molecule. Alternative sites were found for C3 and O1 which indicate disorder of packing of molecules with differing conformations at C3. The relative occupancies were refined. The minor sites were refined with isotropic displacement parameters set equal to the U_{eq} value of the corresponding major site, and restraints were applied to bonded distances involving the minor sites.

Most of the hydrogen atoms were observed in a difference electron density map synthesized prior to their inclusion. H atoms were included at calculated positions and were initially refined with soft restraints on the bond lengths and angles to regularize their geometry (C—H in the range 0.93–0.98 Å, N—H = 0.87 Å) and with U_{iso}(H) in the range 1.2–1.5 times U_{eq} of the parent atom, after which the positions were refined with riding constraints, except for H1 on N1 which was allowed to refine freely. H atoms within the disorder were simply included at calculated positions and ride on the atom to which they are respectively bonded.

The largest features in the final difference electron density map are generally located midway between bonded atoms.

Fractional atomic coordinates and isotropic or equivalent isotropic displacement parameters (Å^2)

	x	*y*	*z*	U_{iso}*/U_{eq}	Occ. (<1)
O1	0.93147 (17)	0.63929 (16)	−0.03127 (13)	0.0332	0.871 (4)

O2	0.10391 (11)	0.71371 (10)	0.45641 (8)	0.0284	
O3	0.33044 (12)	0.80541 (10)	0.58795 (8)	0.0330	
O101	0.8936 (13)	0.6025 (11)	−0.0586 (7)	0.0330*	0.129 (4)
N1	0.82638 (15)	0.52049 (12)	0.06877 (10)	0.0302	
C1	0.59511 (16)	0.67812 (13)	0.11295 (11)	0.0261	
C2	0.6268 (2)	0.58690 (15)	0.17829 (13)	0.0357	
C3	0.69347 (19)	0.48124 (15)	0.11693 (14)	0.0278	0.871 (4)
C4	0.82397 (17)	0.61195 (14)	0.01925 (11)	0.0295	
C5	0.68942 (16)	0.68669 (13)	0.03331 (11)	0.0259	
C6	0.66148 (18)	0.76669 (14)	−0.03244 (12)	0.0317	
C7	0.5379 (2)	0.83720 (16)	−0.01970 (13)	0.0369	
C8	0.44690 (18)	0.83135 (15)	0.06112 (13)	0.0343	
C9	0.47470 (16)	0.75393 (13)	0.12906 (11)	0.0267	
C10	0.37590 (16)	0.74932 (13)	0.21569 (11)	0.0256	
C11	0.22394 (16)	0.70634 (14)	0.19401 (11)	0.0296	
C12	0.13043 (16)	0.69569 (14)	0.27396 (11)	0.0297	
C13	0.18946 (15)	0.72798 (13)	0.37686 (11)	0.0246	
C14	0.34675 (15)	0.77755 (12)	0.40453 (11)	0.0237	
C15	0.41941 (16)	0.81620 (13)	0.50929 (11)	0.0260	
C16	0.57082 (17)	0.86294 (13)	0.52781 (12)	0.0298	
C17	0.66000 (16)	0.87576 (13)	0.44608 (12)	0.0293	
C18	0.59529 (16)	0.83864 (13)	0.34576 (12)	0.0274	
C19	0.43986 (15)	0.78828 (12)	0.32206 (11)	0.0241	
C20	0.7424 (2)	0.39299 (15)	0.18395 (14)	0.0391	
C21	−0.04163 (16)	0.64753 (14)	0.42870 (11)	0.0278	
C22	−0.11324 (16)	0.63112 (13)	0.52537 (11)	0.0272	
C23	−0.24671 (18)	0.55530 (15)	0.51415 (13)	0.0351	
C24	−0.31900 (19)	0.53765 (16)	0.60038 (14)	0.0397	
C25	−0.2578 (2)	0.59548 (16)	0.69876 (14)	0.0390	
C26	−0.1247 (2)	0.66999 (17)	0.71053 (13)	0.0399	
C27	−0.05238 (18)	0.68809 (15)	0.62394 (12)	0.0335	
C28	0.4018 (2)	0.84549 (16)	0.69156 (12)	0.0371	
C29	0.82315 (18)	0.93299 (16)	0.47126 (14)	0.0381	
C103	0.7549 (12)	0.5148 (7)	0.1651 (8)	0.0280*	0.129 (4)
H1	0.906 (2)	0.4752 (18)	0.0636 (15)	0.0374*	
H21	0.6989	0.6207	0.2366	0.0430*	0.871
H22	0.5324	0.5621	0.2017	0.0430*	0.871
H23	0.6405	0.6277	0.2486	0.0430*	0.129
H24	0.5360	0.5345	0.1674	0.0430*	0.129
H31	0.6104	0.4414	0.0576	0.0431*	0.871
H61	0.7292	0.7727	−0.0846	0.0377*	
H71	0.5162	0.8891	−0.0653	0.0450*	
H81	0.3642	0.8819	0.0711	0.0416*	
H111	0.1793	0.6830	0.1235	0.0351*	
H121	0.0274	0.6642	0.2557	0.0355*	
H161	0.6169	0.8862	0.5970	0.0360*	
H181	0.6543	0.8462	0.2901	0.0337*	
H201	0.6555	0.3676	0.2152	0.0471*	0.871
H202	0.8219	0.4293	0.2367	0.0471*	0.871
H203	0.7804	0.3269	0.1419	0.0471*	0.871
H204	0.6961	0.3920	0.2465	0.0471*	0.129
H205	0.8431	0.3646	0.1901	0.0471*	0.129
H206	0.6799	0.3439	0.1274	0.0471*	0.129
H211	−0.1119	0.6906	0.3884	0.0326*	

H212	−0.0241	0.5708	0.3873	0.0322*	
H231	−0.2861	0.5135	0.4479	0.0429*	
H241	−0.4082	0.4838	0.5925	0.0476*	
H251	−0.3043	0.5829	0.7580	0.0467*	
H261	−0.0837	0.7076	0.7781	0.0485*	
H271	0.0335	0.7418	0.6311	0.0405*	
H281	0.3240	0.8357	0.7366	0.0538*	
H282	0.4371	0.9281	0.7029	0.0541*	
H283	0.4881	0.7976	0.7057	0.0542*	
H291	0.8774	0.9197	0.4093	0.0586*	
H292	0.8217	1.0158	0.4979	0.0577*	
H293	0.8804	0.9002	0.5251	0.0575*	
H1031	0.8322	0.5536	0.2183	0.0348*	0.129

Atomic displacement parameters (Å²)

	U^{11}	U^{22}	U^{33}	U^{12}	U^{13}	U^{23}
O1	0.0270 (7)	0.0413 (9)	0.0360 (8)	0.0082 (6)	0.0148 (6)	0.0122 (6)
O2	0.0212 (5)	0.0380 (6)	0.0249 (5)	−0.0024 (4)	0.0059 (4)	0.0030 (4)
O3	0.0314 (5)	0.0438 (6)	0.0229 (5)	−0.0048 (5)	0.0016 (4)	0.0070 (4)
N1	0.0277 (6)	0.0329 (7)	0.0332 (6)	0.0104 (5)	0.0109 (5)	0.0080 (5)
C1	0.0240 (6)	0.0300 (7)	0.0259 (6)	0.0046 (5)	0.0063 (5)	0.0065 (5)
C2	0.0381 (8)	0.0400 (9)	0.0360 (8)	0.0146 (7)	0.0163 (6)	0.0155 (7)
C3	0.0232 (8)	0.0297 (9)	0.0314 (9)	0.0023 (6)	0.0052 (7)	0.0068 (7)
C4	0.0277 (7)	0.0367 (8)	0.0261 (7)	0.0081 (6)	0.0082 (5)	0.0067 (6)
C5	0.0237 (6)	0.0295 (7)	0.0253 (6)	0.0035 (5)	0.0062 (5)	0.0048 (5)
C6	0.0323 (7)	0.0363 (8)	0.0303 (7)	0.0064 (6)	0.0112 (6)	0.0106 (6)
C7	0.0399 (8)	0.0417 (9)	0.0358 (8)	0.0127 (7)	0.0114 (6)	0.0185 (7)
C8	0.0322 (7)	0.0396 (9)	0.0359 (8)	0.0139 (6)	0.0100 (6)	0.0129 (7)
C9	0.0224 (6)	0.0314 (7)	0.0270 (7)	0.0039 (5)	0.0052 (5)	0.0050 (5)
C10	0.0236 (6)	0.0294 (7)	0.0252 (6)	0.0063 (5)	0.0066 (5)	0.0057 (5)
C11	0.0239 (6)	0.0399 (8)	0.0245 (7)	0.0042 (6)	0.0026 (5)	0.0047 (6)
C12	0.0194 (6)	0.0410 (8)	0.0277 (7)	0.0004 (5)	0.0030 (5)	0.0037 (6)
C13	0.0205 (6)	0.0285 (7)	0.0254 (6)	0.0036 (5)	0.0058 (5)	0.0044 (5)
C14	0.0207 (6)	0.0250 (7)	0.0260 (6)	0.0037 (5)	0.0030 (5)	0.0055 (5)
C15	0.0260 (6)	0.0258 (7)	0.0268 (7)	0.0016 (5)	0.0028 (5)	0.0064 (5)
C16	0.0274 (7)	0.0304 (8)	0.0302 (7)	−0.0007 (6)	−0.0016 (5)	0.0051 (6)
C17	0.0225 (6)	0.0266 (7)	0.0387 (8)	0.0019 (5)	0.0020 (5)	0.0070 (6)
C18	0.0210 (6)	0.0278 (7)	0.0345 (7)	0.0023 (5)	0.0062 (5)	0.0071 (6)
C19	0.0208 (6)	0.0239 (7)	0.0287 (7)	0.0052 (5)	0.0049 (5)	0.0058 (5)
C20	0.0394 (9)	0.0352 (9)	0.0465 (9)	0.0081 (7)	0.0094 (7)	0.0137 (7)
C21	0.0204 (6)	0.0340 (8)	0.0282 (7)	−0.0009 (5)	0.0036 (5)	0.0043 (6)
C22	0.0213 (6)	0.0309 (7)	0.0309 (7)	0.0043 (5)	0.0069 (5)	0.0074 (6)
C23	0.0264 (7)	0.0407 (9)	0.0372 (8)	−0.0027 (6)	0.0049 (6)	0.0060 (7)
C24	0.0287 (7)	0.0429 (9)	0.0502 (10)	−0.0017 (7)	0.0122 (7)	0.0134 (8)
C25	0.0359 (8)	0.0482 (10)	0.0381 (8)	0.0054 (7)	0.0152 (7)	0.0152 (7)
C26	0.0357 (8)	0.0543 (11)	0.0297 (8)	0.0008 (7)	0.0088 (6)	0.0063 (7)
C27	0.0263 (7)	0.0417 (9)	0.0317 (7)	−0.0027 (6)	0.0053 (6)	0.0053 (6)
C28	0.0441 (9)	0.0423 (9)	0.0235 (7)	−0.0058 (7)	−0.0014 (6)	0.0078 (6)
C29	0.0257 (7)	0.0376 (9)	0.0491 (9)	−0.0047 (6)	0.0002 (6)	0.0071 (7)

Geometric parameters (Å, º)

O1 C4	1.2540 (19)	C14 C15	1.4391 (19)
O2 C13	1.3669 (16)	C14 C19	1.4307 (18)
O2 C21	1.4196 (16)	C15 C16	1.374 (2)
O3 C15	1.3668 (17)	C16 C17	1.406 (2)
O3 C28	1.4245 (17)	C16 H161	0.943
O101 C4	1.228 (8)	C17 C18	1.365 (2)
N1 C3	1.457 (2)	C17 C29	1.509 (2)
N1 C4	1.341 (2)	C18 C19	1.4212 (19)
N1 C103	1.472 (7)	C18 H181	0.945
N1 H1	0.89 (2)	C20 C103	1.475 (7)
C1 C2	1.500 (2)	C20 H201	0.950
C1 C5	1.4022 (18)	C20 H202	0.950
C1 C9	1.4048 (19)	C20 H203	0.950
C2 C3	1.508 (2)	C20 H204	0.950
C2 C103	1.428 (7)	C20 H205	0.950
C2 H21	0.950	C20 H206	0.950
C2 H22	0.950	C21 C22	1.5043 (19)
C2 H23	0.950	C21 H211	0.985
C2 H24	0.950	C21 H212	0.978
C3 C20	1.519 (2)	C22 C23	1.393 (2)
C3 H31	1.032	C22 C27	1.381 (2)
C4 C5	1.493 (2)	C23 C24	1.388 (2)
C5 C6	1.394 (2)	C23 H231	0.938
C6 C7	1.385 (2)	C24 C25	1.383 (3)
C6 H61	0.953	C24 H241	0.952
C7 C8	1.391 (2)	C25 C26	1.381 (2)
C7 H71	0.938	C25 H251	0.940
C8 C9	1.392 (2)	C26 C27	1.394 (2)
C8 H81	0.952	C26 H261	0.941
C9 C10	1.4951 (18)	C27 H271	0.929
C10 C11	1.367 (2)	C28 H281	0.954
C10 C19	1.4351 (19)	C28 H282	0.967
C11 C12	1.4055 (19)	C28 H283	0.978
C11 H111	0.954	C29 H291	0.971
C12 C13	1.3760 (19)	C29 H292	0.958
C12 H121	0.938	C29 H293	0.972
C13 C14	1.4368 (18)	C103 H1031	0.950
O1···N1^{i}	2.887 (2)	C13···C24^{iii}	3.381 (2)
O2···O3	2.5346 (15)	C18···C2	3.349 (2)
O3···O2	2.5346 (15)	C18···C1	3.272 (2)
O101···C25^{ii}	3.318 (10)	C19···C2	3.312 (2)
O101···C26^{ii}	3.264 (10)	C21···C29^{iv}	3.526 (2)
O101···N1^{i}	2.880 (12)	C24···C13^{iii}	3.381 (2)
N1···O101^{i}	2.880 (12)	C25···O101^{v}	3.318 (10)
N1···O1^{i}	2.887 (2)	C26···O101^{v}	3.264 (10)
C1···C18	3.272 (2)	C29···C29^{vi}	3.315 (2)
C2···C18	3.349 (2)	C29···C21^{vii}	3.526 (2)
C2···C19	3.312 (2)		
C13 O2 C21	116.81 (11)	C15 C16 C17	121.73 (14)
C15 O3 C28	116.84 (12)	C15 C16 H161	119.4
C3 N1 C4	122.58 (13)	C17 C16 H161	118.9

C4 N1 C103	125.2 (3)	C16 C17 C18	119.08 (13)
C3 N1 H1	117.9 (12)	C16 C17 C29	119.30 (14)
C4 N1 H1	118.8 (12)	C18 C17 C29	121.60 (14)
C103 N1 H1	110.4 (13)	C17 C18 C19	121.59 (13)
C2 C1 C5	118.23 (12)	C17 C18 H181	119.9
C2 C1 C9	122.14 (12)	C19 C18 H181	118.5
C5 C1 C9	119.63 (13)	C10 C19 C14	120.05 (12)
C1 C2 C3	111.15 (13)	C10 C19 C18	120.12 (12)
C1 C2 C103	121.7 (3)	C14 C19 C18	119.83 (13)
C1 C2 H21	109.1	C3 C20 H201	109.5
C3 C2 H21	109.1	C3 C20 H202	109.5
C1 C2 H22	109.0	H201 C20 H202	109.5
C3 C2 H22	109.0	C3 C20 H203	109.5
H21 C2 H22	109.5	H201 C20 H203	109.5
C1 C2 H23	106.4	H202 C20 H203	109.5
C103 C2 H23	106.3	C103 C20 H204	109.5
C1 C2 H24	106.3	C103 C20 H205	109.5
C103 C2 H24	106.4	C103 C20 H206	109.4
H23 C2 H24	109.5	H204 C20 H205	109.5
C2 C3 N1	109.40 (14)	H204 C20 H206	109.5
C2 C3 C20	112.36 (14)	H205 C20 H206	109.5
N1 C3 C20	109.65 (13)	O2 C21 C22	109.83 (11)
C2 C3 H31	108.2	O2 C21 H211	109.3
N1 C3 H31	107.2	C22 C21 H211	108.7
C20 C3 H31	109.9	O2 C21 H212	108.3
N1 C4 O1	123.14 (14)	C22 C21 H212	110.1
N1 C4 O101	116.2 (6)	H211 C21 H212	110.6
N1 C4 C5	116.13 (12)	C21 C22 C23	118.13 (13)
O1 C4 C5	120.59 (14)	C21 C22 C27	122.79 (13)
O101 C4 C5	122.2 (6)	C23 C22 C27	119.08 (14)
C4 C5 C1	120.34 (13)	C22 C23 C24	120.76 (15)
C4 C5 C6	118.93 (12)	C22 C23 H231	119.7
C1 C5 C6	120.71 (13)	C24 C23 H231	119.5
C5 C6 C7	119.52 (13)	C23 C24 C25	119.81 (15)
C5 C6 H61	119.2	C23 C24 H241	120.4
C7 C6 H61	121.3	C25 C24 H241	119.8
C6 C7 C8	119.88 (14)	C24 C25 C26	119.74 (15)
C6 C7 H71	119.9	C24 C25 H251	120.7
C8 C7 H71	120.2	C26 C25 H251	119.6
C7 C8 C9	121.55 (14)	C25 C26 C27	120.48 (16)
C7 C8 H81	119.7	C25 C26 H261	118.6
C9 C8 H81	118.7	C27 C26 H261	120.9
C1 C9 C8	118.58 (13)	C26 C27 C22	120.14 (14)
C1 C9 C10	120.67 (13)	C26 C27 H271	120.7
C8 C9 C10	120.72 (12)	C22 C27 H271	119.1
C9 C10 C11	120.06 (13)	O3 C28 H281	106.5
C9 C10 C19	120.50 (12)	O3 C28 H282	111.0
C11 C10 C19	119.44 (12)	H281 C28 H282	108.9
C10 C11 C12	121.29 (13)	O3 C28 H283	110.0
C10 C11 H111	120.1	H281 C28 H283	109.5
C12 C11 H111	118.6	H282 C28 H283	110.8
C11 C12 C13	120.87 (13)	C17 C29 H291	109.6
C11 C12 H121	118.6	C17 C29 H292	110.7
C13 C12 H121	120.5	H291 C29 H292	110.5

C12 C13 O2	122.37 (12)	C17 C29 H293	110.9
C12 C13 C14	120.37 (12)	H291 C29 H293	108.6
O2 C13 C14	117.25 (12)	H292 C29 H293	106.5
C13 C14 C15	125.06 (12)	C20 C103 N1	111.3 (5)
C13 C14 C19	117.89 (12)	C20 C103 C2	120.1 (6)
C15 C14 C19	117.04 (12)	N1 C103 C2	113.1 (5)
C14 C15 O3	116.94 (12)	C20 C103 H1031	103.4
C14 C15 C16	120.71 (13)	N1 C103 H1031	103.4
O3 C15 C16	122.34 (13)	C2 C103 H1031	103.3

C21 O2 C13 C12	9.3 (2)	C9 C10 C19 C14	−176.61 (13)
C21 O2 C13 C14	−170.03 (13)	C9 C10 C19 C18	4.0 (2)
C13 O2 C21 C22	174.88 (12)	C11 C10 C19 C14	2.5 (2)
C28 O3 C15 C14	−179.01 (13)	C11 C10 C19 C18	−176.85 (14)
C28 O3 C15 C16	0.2 (2)	C10 C11 C12 C13	−0.2 (2)
C4 N1 C3 C2	−45.3 (2)	C11 C12 C13 O2	−176.91 (14)
C4 N1 C3 C20	−168.97 (14)	C11 C12 C13 C14	2.4 (2)
C3 N1 C4 O1	−172.68 (16)	O2 C13 C14 C15	−1.8 (2)
C3 N1 C4 C5	11.5 (2)	O2 C13 C14 C19	177.34 (13)
C5 C1 C2 C3	−30.1 (2)	C12 C13 C14 C15	178.86 (15)
C9 C1 C2 C3	149.75 (15)	C12 C13 C14 C19	−2.0 (2)
C2 C1 C5 C4	−4.0 (2)	C13 C14 C15 O3	−0.6 (2)
C2 C1 C5 C6	177.48 (14)	C13 C14 C15 C16	−179.78 (14)
C9 C1 C5 C4	176.24 (13)	C19 C14 C15 O3	−179.74 (13)
C9 C1 C5 C6	−2.3 (2)	C19 C14 C15 C16	1.1 (2)
C2 C1 C9 C8	−176.18 (15)	C13 C14 C19 C10	−0.5 (2)
C2 C1 C9 C10	2.3 (2)	C13 C14 C19 C18	178.95 (13)
C5 C1 C9 C8	3.6 (2)	C15 C14 C19 C10	178.78 (13)
C5 C1 C9 C10	−177.95 (13)	C15 C14 C19 C18	−1.8 (2)
C1 C2 C3 N1	52.01 (18)	O3 C15 C16 C17	−178.66 (14)
C1 C2 C3 C20	174.06 (14)	C14 C15 C16 C17	0.5 (2)
O1 C4 C5 C1	−160.96 (16)	C15 C16 C17 C18	−1.3 (2)
O1 C4 C5 C6	17.6 (2)	C15 C16 C17 C29	177.12 (15)
N1 C4 C5 C1	15.0 (2)	C16 C17 C18 C19	0.5 (2)
N1 C4 C5 C6	−166.41 (14)	C29 C17 C18 C19	−177.90 (14)
C1 C5 C6 C7	−0.9 (2)	C17 C18 C19 C10	−179.50 (14)
C4 C5 C6 C7	−179.47 (15)	C17 C18 C19 C14	1.1 (2)
C5 C6 C7 C8	2.8 (2)	O2 C21 C22 C23	−171.72 (13)
C6 C7 C8 C9	−1.4 (3)	O2 C21 C22 C27	8.4 (2)
C7 C8 C9 C1	−1.8 (2)	C21 C22 C23 C24	−179.27 (15)
C7 C8 C9 C10	179.77 (15)	C27 C22 C23 C24	0.6 (2)
C1 C9 C10 C11	−109.88 (17)	C21 C22 C27 C26	179.50 (16)
C1 C9 C10 C19	69.3 (2)	C23 C22 C27 C26	−0.4 (2)
C8 C9 C10 C11	68.5 (2)	C22 C23 C24 C25	−0.3 (3)
C8 C9 C10 C19	−112.33 (17)	C23 C24 C25 C26	−0.3 (3)
C9 C10 C11 C12	176.91 (14)	C24 C25 C26 C27	0.5 (3)
C19 C10 C11 C12	−2.2 (2)	C25 C26 C27 C22	−0.2 (3)

Symmetry codes: (i) −*x*+2, −*y*+1, −*z*; (ii) *x*+1, *y*, *z*−1; (iii) −*x*, −*y*+1, −*z*+1; (iv) *x*−1, *y*, *z*; (v) *x*−1, *y*, *z*+1; (vi) −*x*+2, −*y*+2, −*z*+1; (vii) *x*+1, *y*, *z*.

Hydrogen-bond geometry (Å, °)

D H···*A*	*D* H	H···*A*	*D*···*A*	*D* H···*A*
N1 H1···O1^{i}	0.89 (2)	2.01 (2)	2.887 (3)	171.5 (18)
N1 H1···O101^{i}	0.89 (2)	2.00 (2)	2.879 (3)	170.6 (18)

Symmetry code: (i) −*x*+2, −*y*+1, −*z*.

Appendix 3: ^{1}H NMR, ^{13}C NMR spectra

Appendix 3.1 Michellamine B analogues synthesis

Monomeric naphthylisoquinoline 99

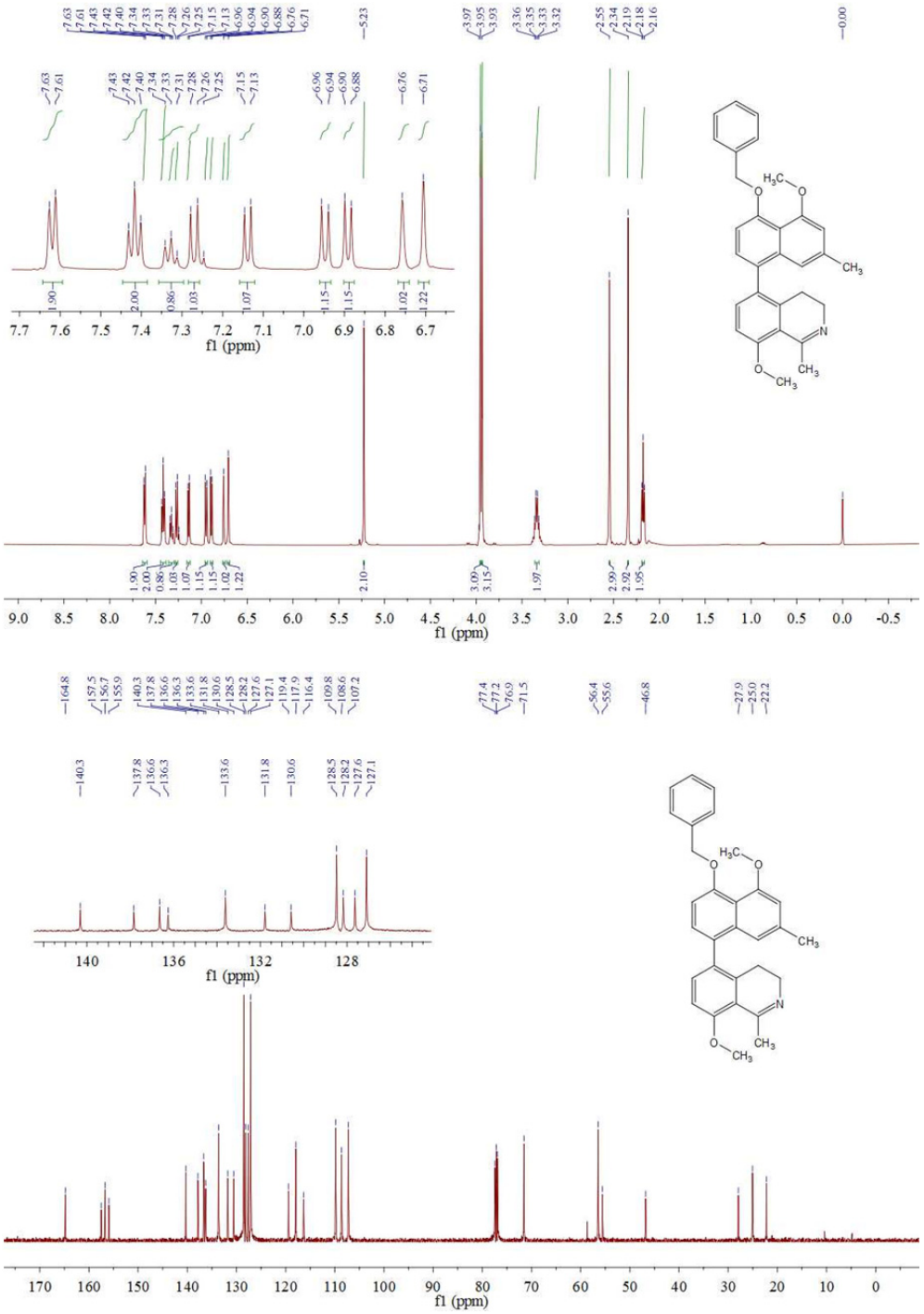

Figure A3.1.1 ^{1}H NMR (500 MHz, $CDCl_3$) and ^{13}C NMR (126 MHz, $CDCl_3$) spectra of compound **99**.

Monomeric naphthylisoquinoline 43

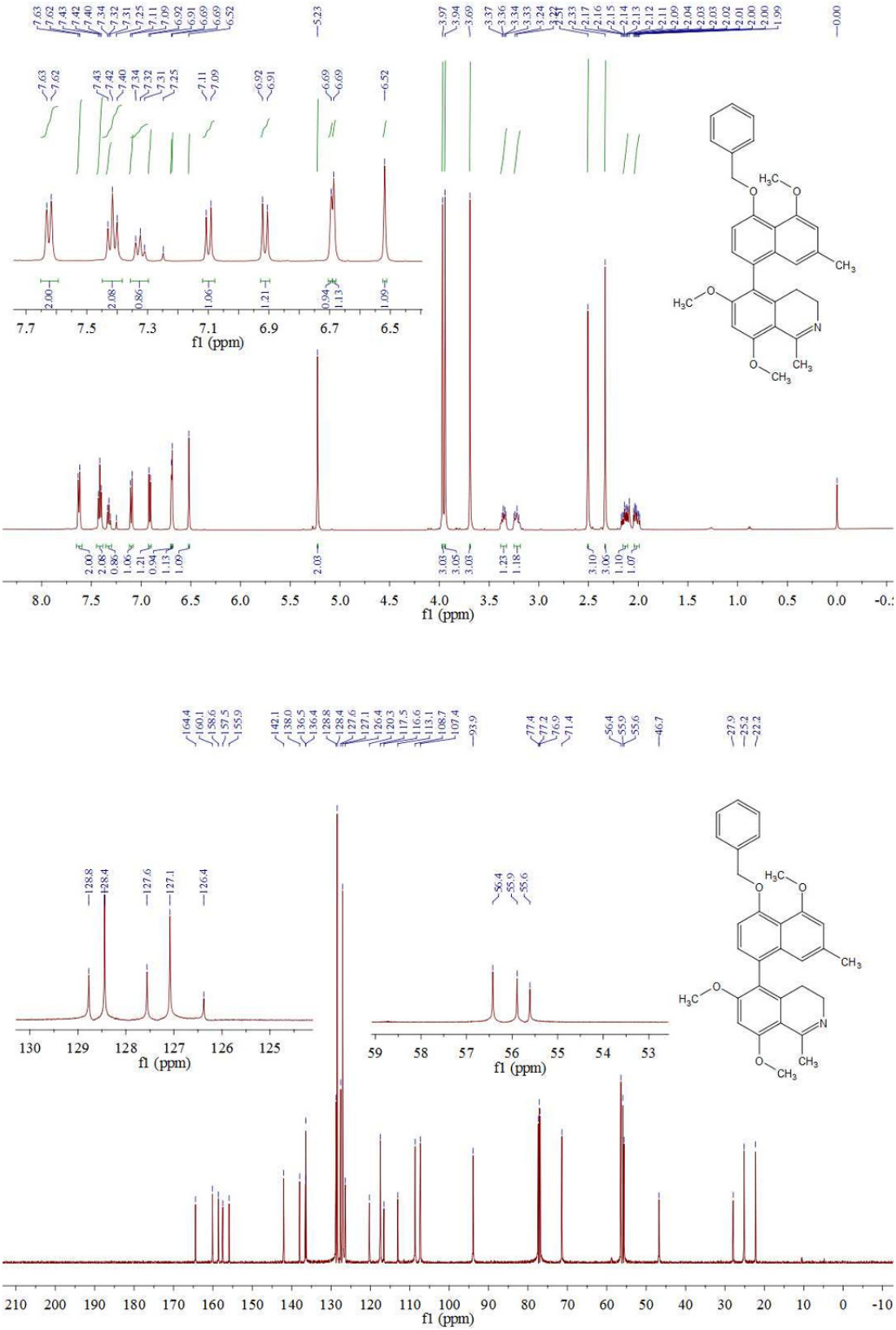

Figure 3.1.2 [1]H NMR (500 MHz, $CDCl_3$) and [13]C NMR (126 MHz, $CDCl_3$) spectra of compound **43**.

Monomeric naphthylisoquinoline 100

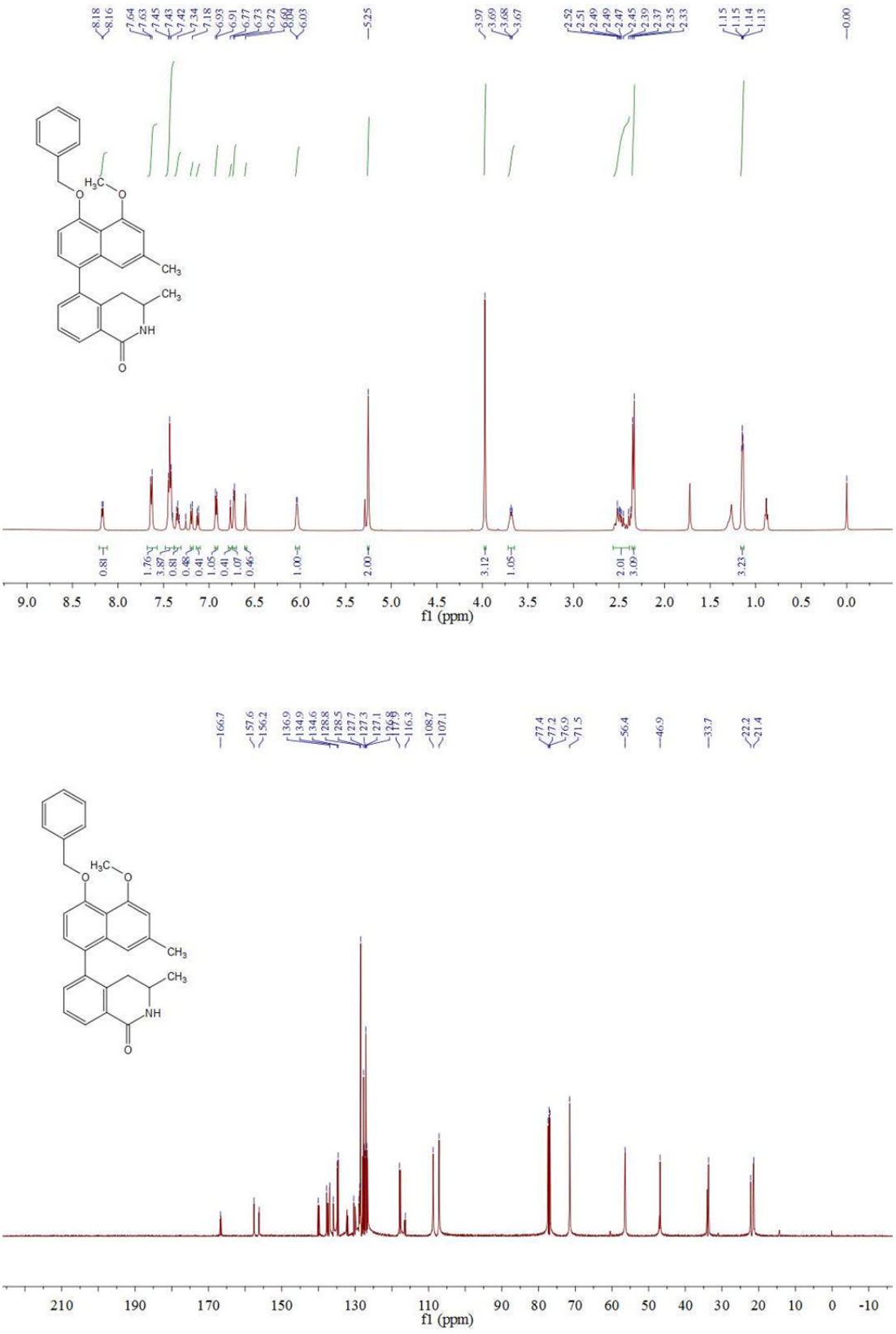

Figure 3.1.3 [1]H NMR (500 MHz, $CDCl_3$) and [13]C NMR (126 MHz, $CDCl_3$) spectra of compound **100**.

Unprotected monomeric naphthylisoquinoline 109

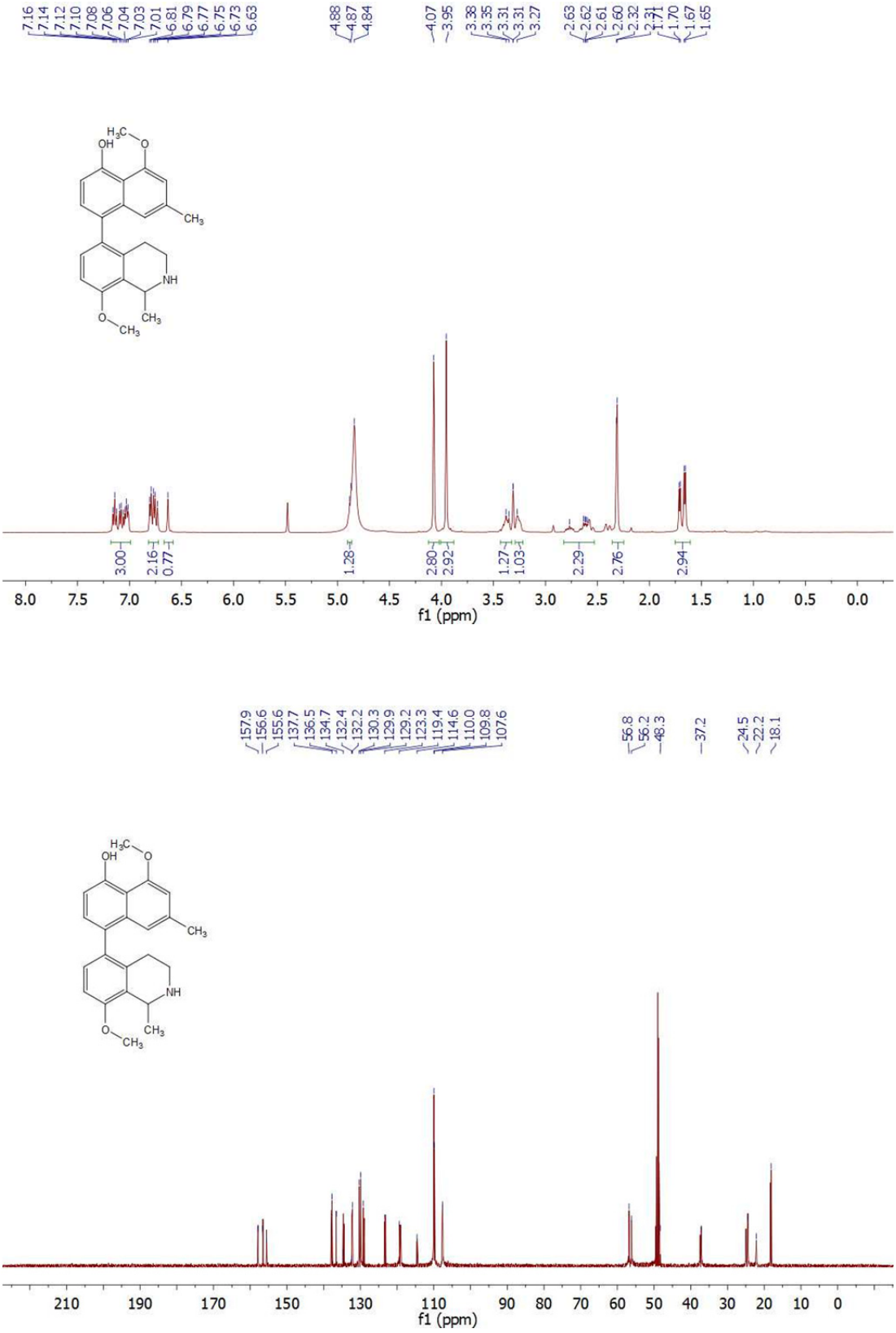

Figure 3.1.4 [1]H NMR (500 MHz, CD_3OD) and [13]C NMR (126 MHz, CD_3OD) spectra of compound **109**.

Unprotected monomeric naphthylisoquinoline 44

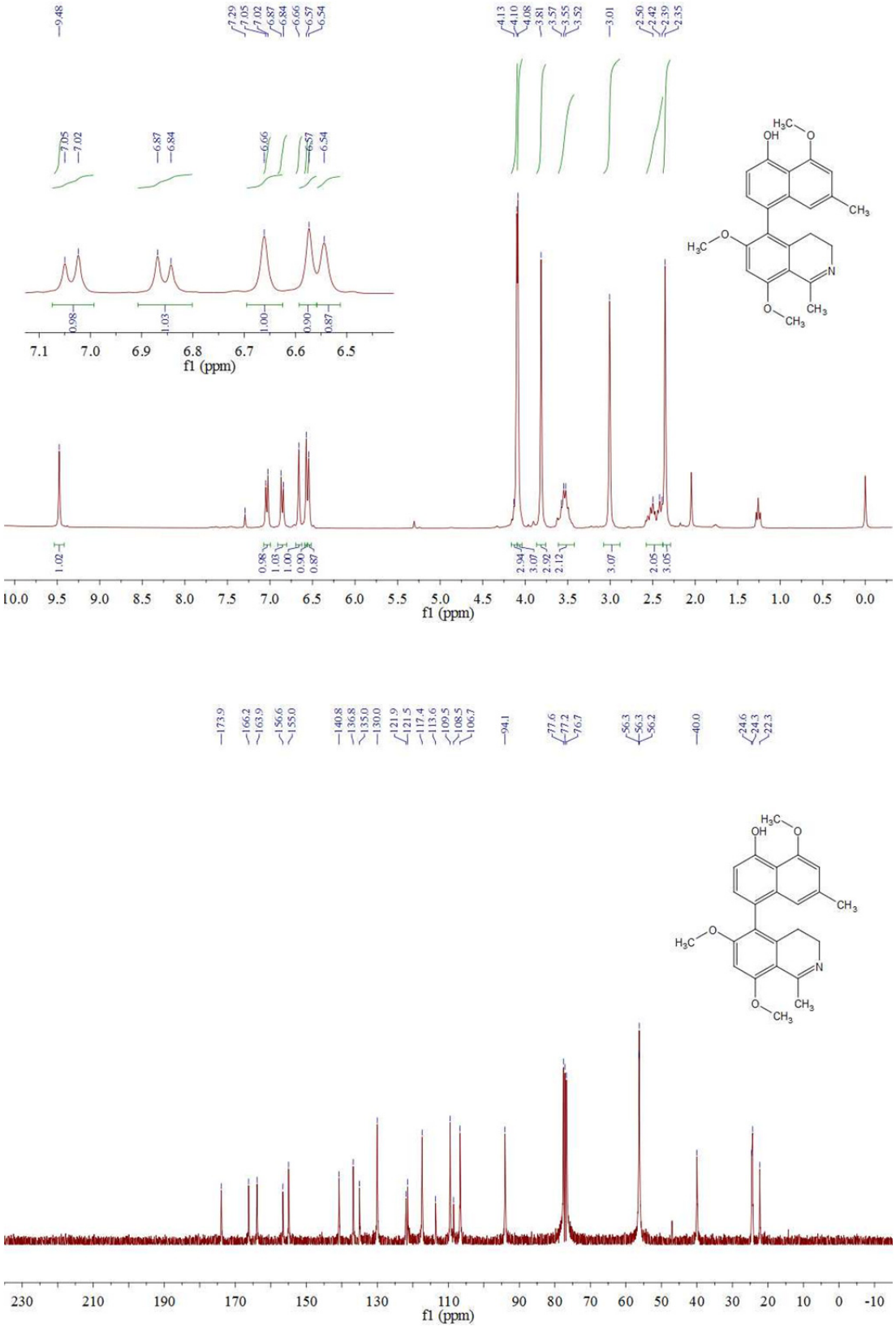

Figure 3.1.5 [1]H NMR (300 MHz, $CDCl_3$) and [13]C NMR (75 MHz, $CDCl_3$) spectra of compound **44**.

Unprotected monomeric naphthylisoquinoline 107

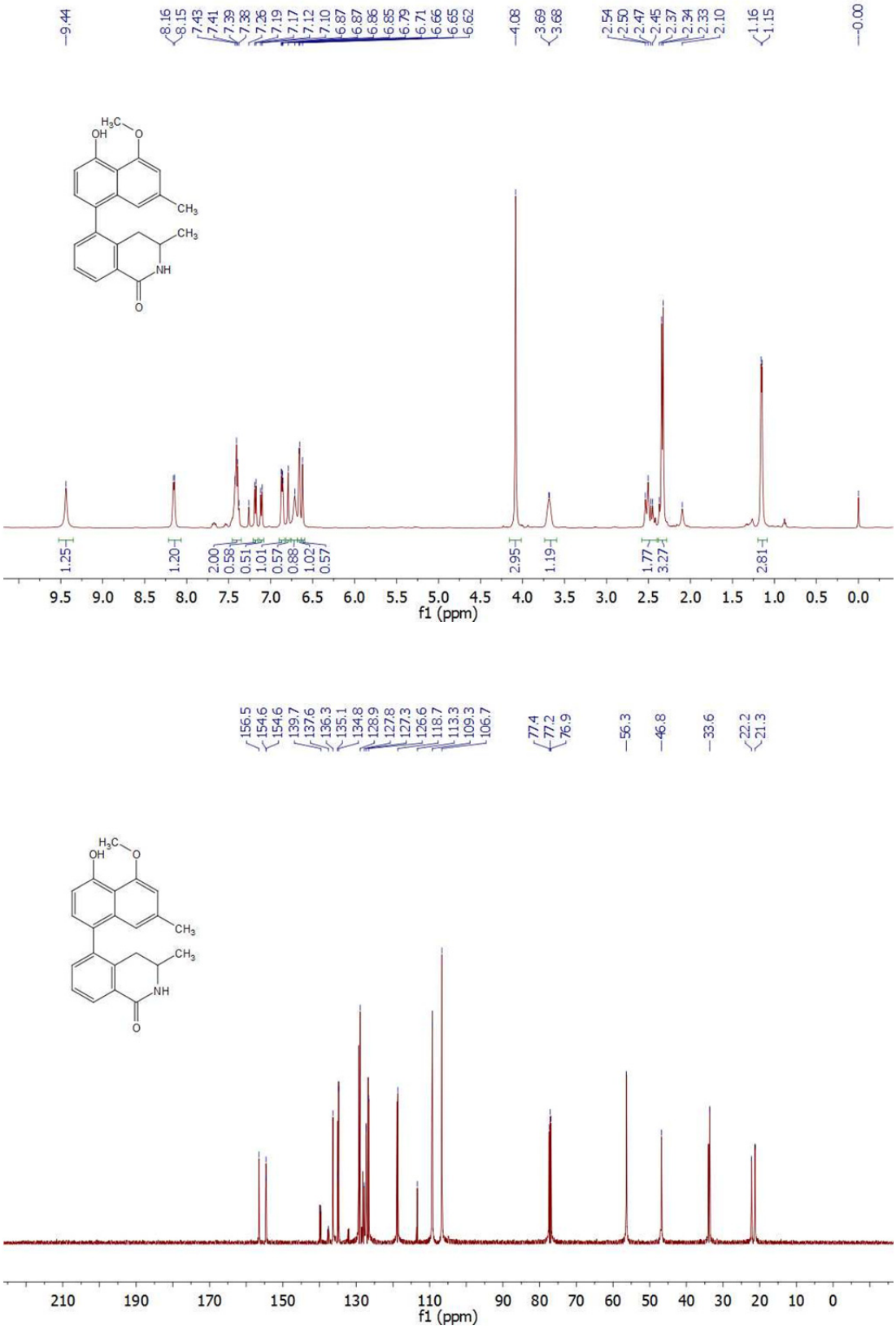

Figure 3.1.6 ^{1}H NMR (500 MHz, $CDCl_3$) and ^{13}C NMR (126 MHz, $CDCl_3$) spectra of compound **107**.

Monomeric naphthylisoquinoline with ester group 96

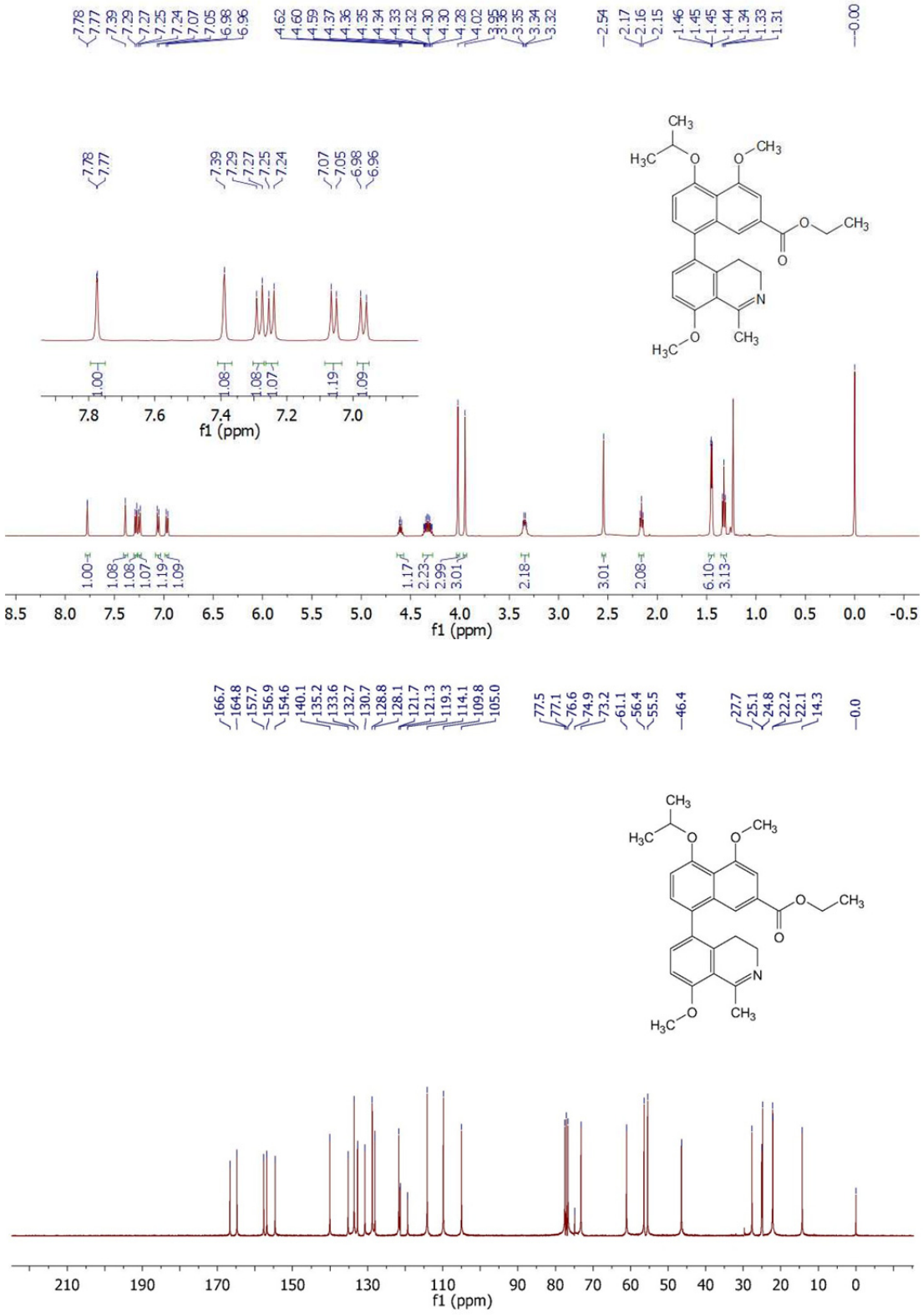

Figure 3.1.7 [1]H NMR (500 MHz, $CDCl_3$) and [13]C NMR (75 MHz, $CDCl_3$) spectra of compound **96**.

Monomeric naphthylisoquinoline with ester group 97

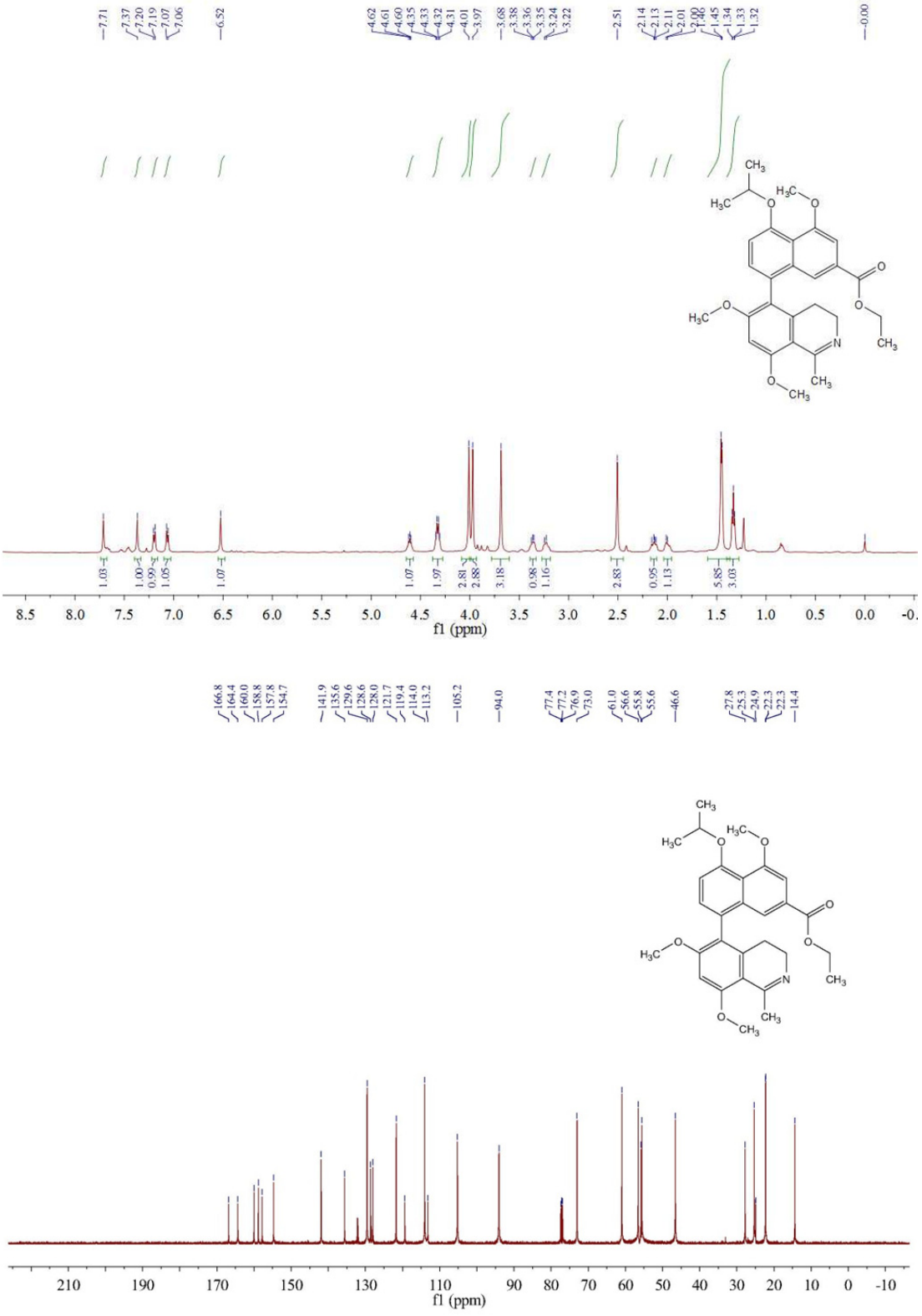

Figure 3.1.8 ^{1}H NMR (500 MHz, $CDCl_3$) and ^{13}C NMR (126 MHz, $CDCl_3$) spectra of compound **97**.

Monomeric naphthylisoquinoline with ester group 98

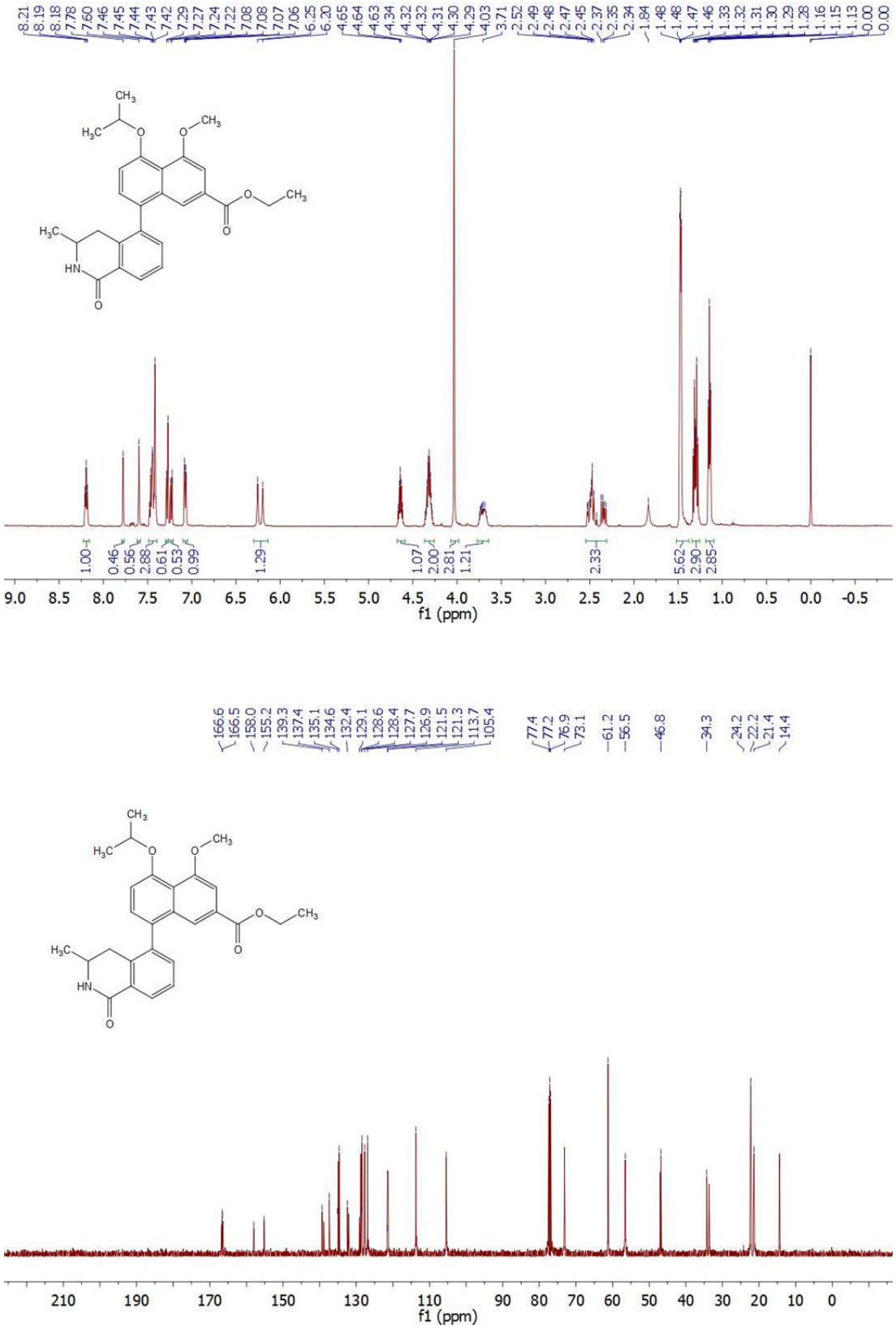

Figure 3.1.9 [1]H NMR (500 MHz, $CDCl_3$) and [13]C NMR (126 MHz, $CDCl_3$) spectra of compound **98**.

2,2'-Binaphthalene scaffold 111

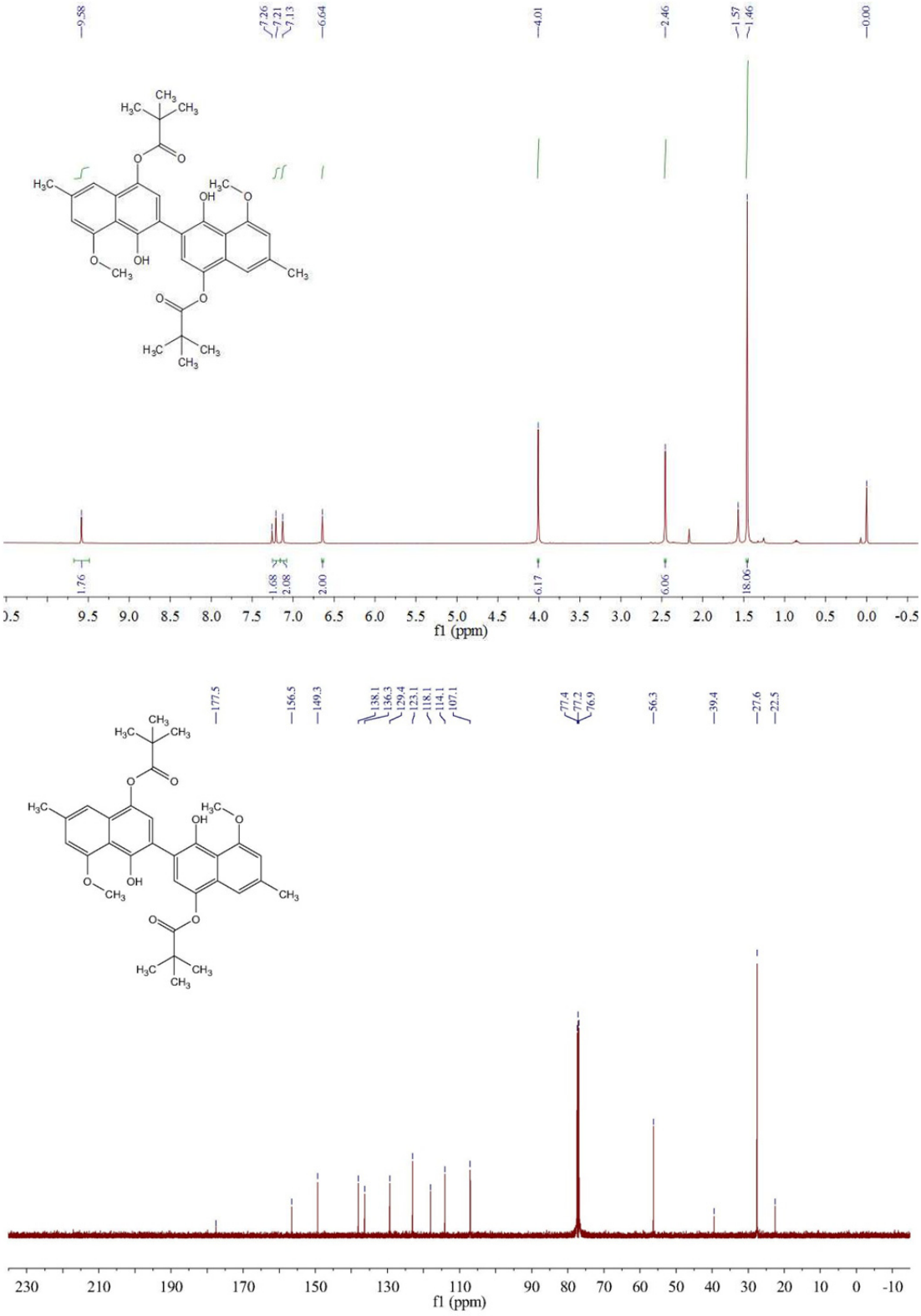

Figure 3.1.10 [1]H NMR (500 MHz, $CDCl_3$) and [13]C NMR (126 MHz, $CDCl_3$) spectra of compound **111**.

Dimeric naphthylisoquinoline 113

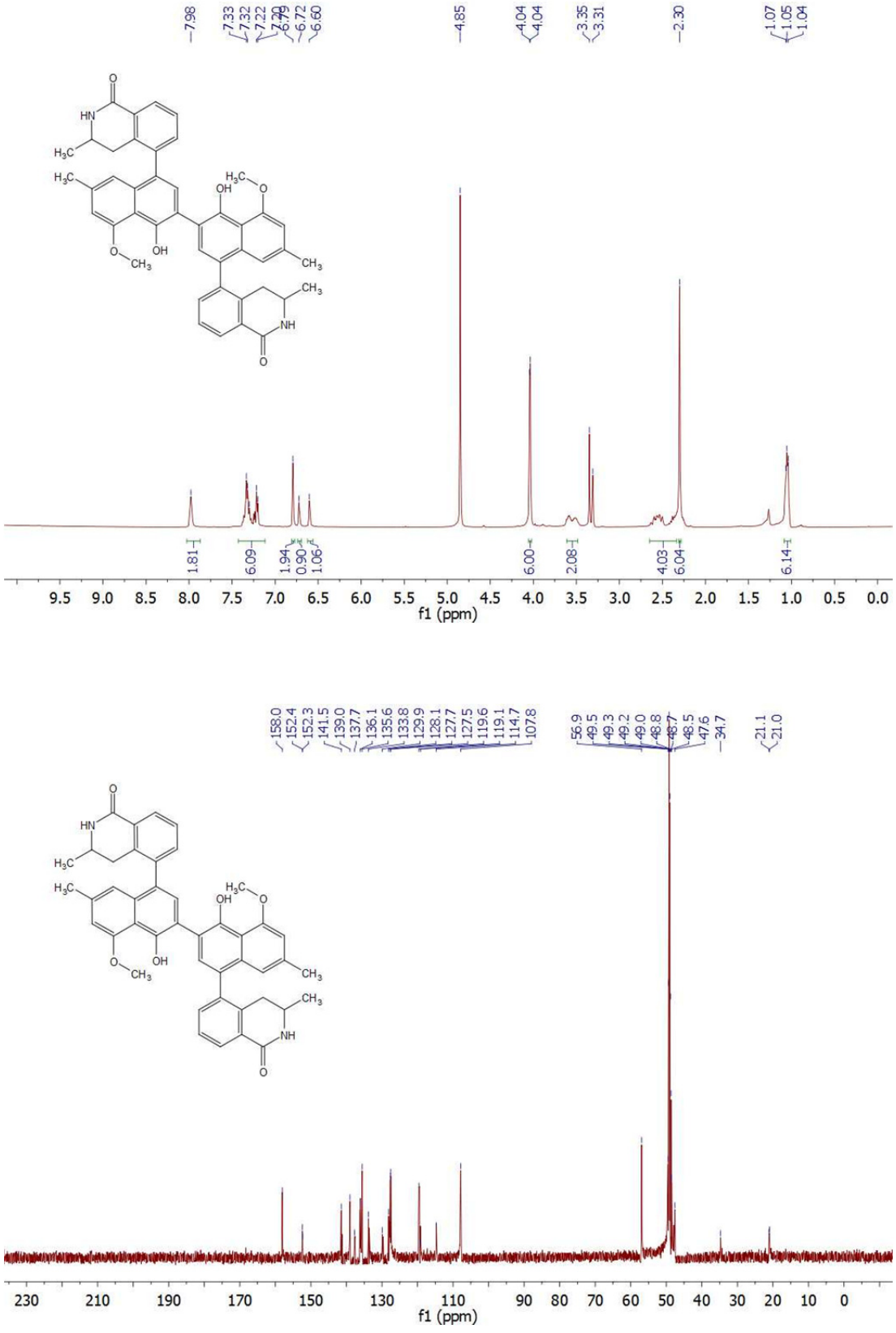

Figure 3.1.11 [1]H NMR (500 MHz, CD_3OD) and [13]C NMR (126 MHz, CD_3OD) spectra of compound **113**.

Dimeric naphthylisoquinoline 112

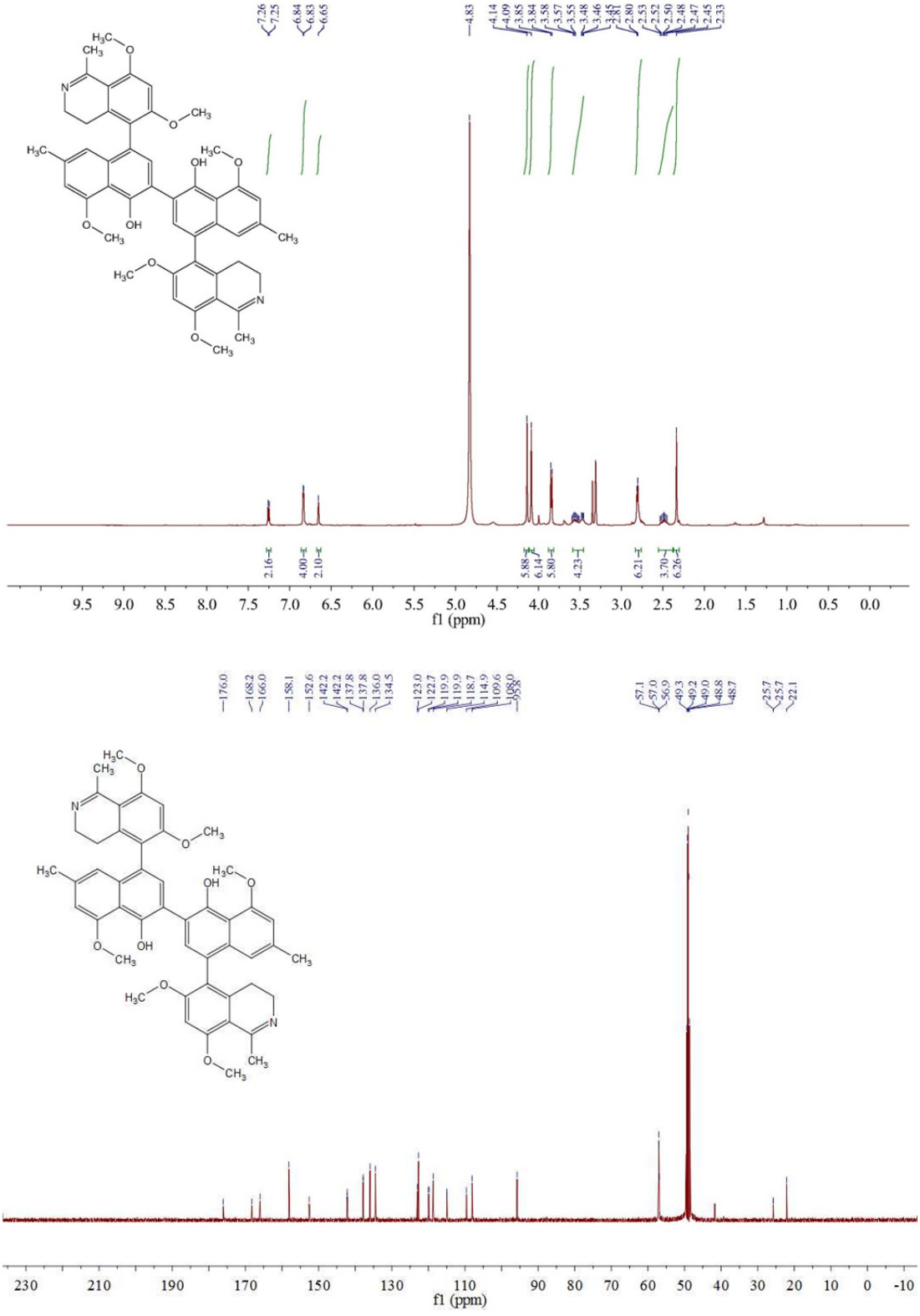

Figure 3.1.12 ^{1}H NMR (500 MHz, CD_3OD) and ^{13}C NMR (126 MHz, CD_3OD) spectra of compound **112**.

Appendix 3.2 Coelenterazine analogues synthesis

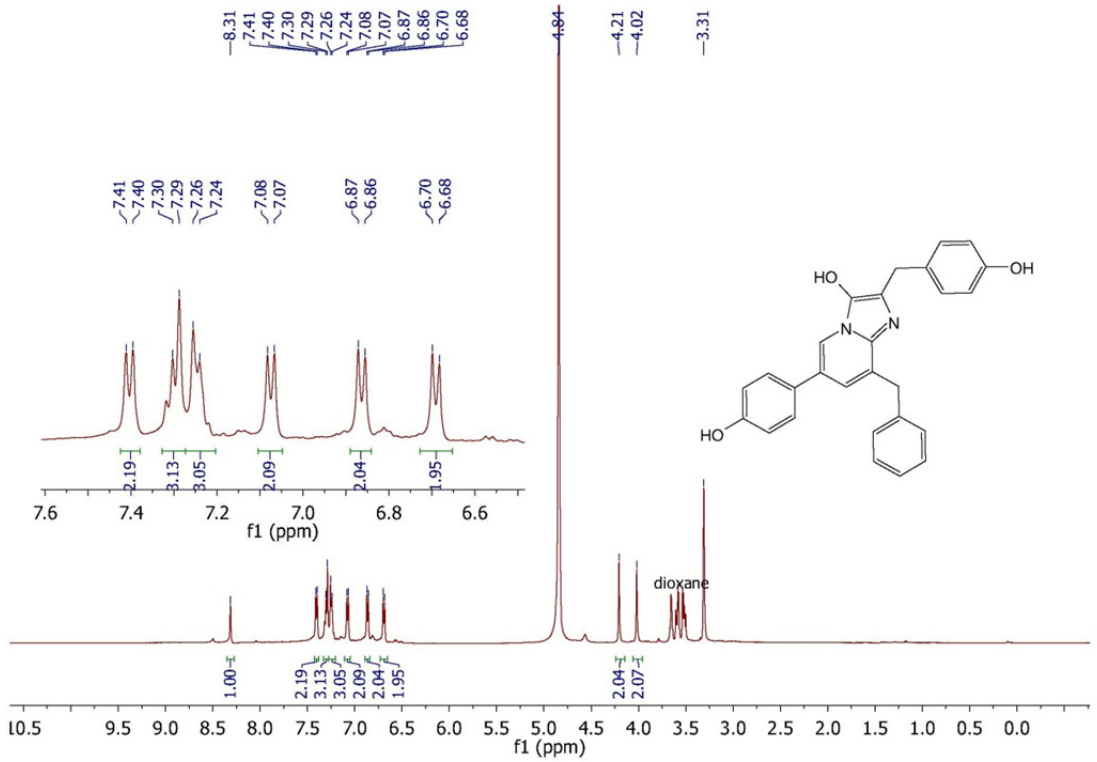

Figure 3.1.13 ^{1}H NMR (500 MHz, CD_3OD) spectrum of compound **121**.

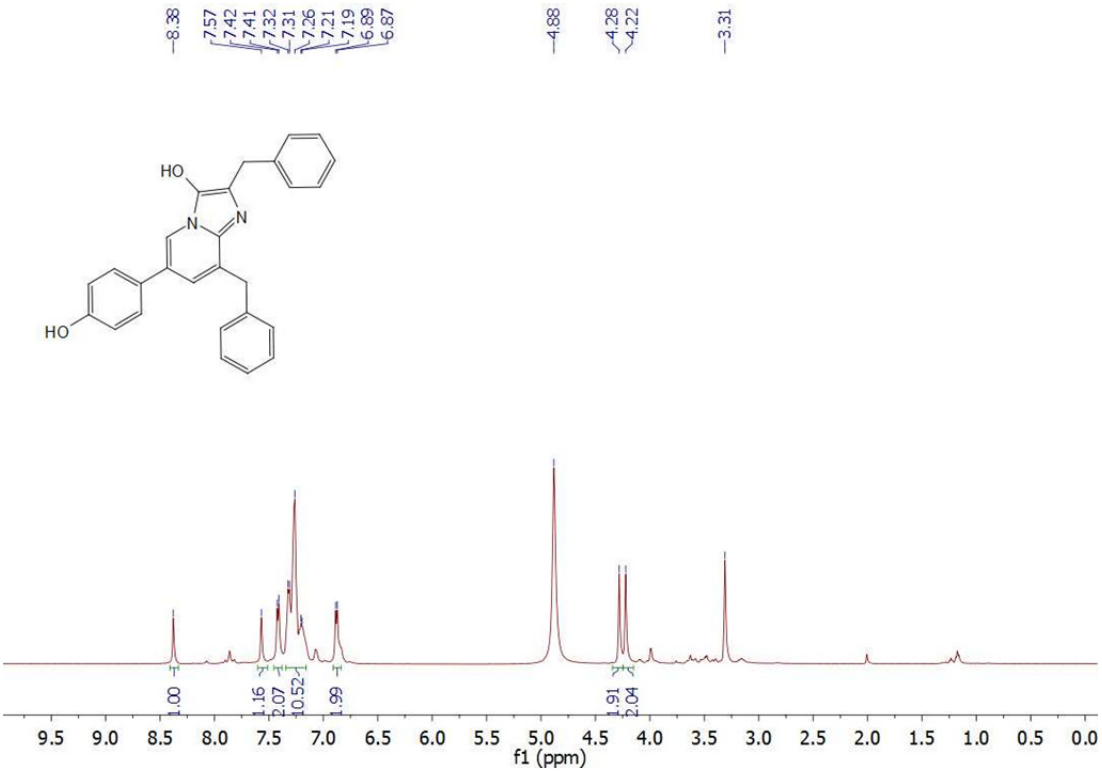

Figure 3.1.14 ^{1}H NMR (500 MHz, CD_3OD) spectrum of compound **153**.

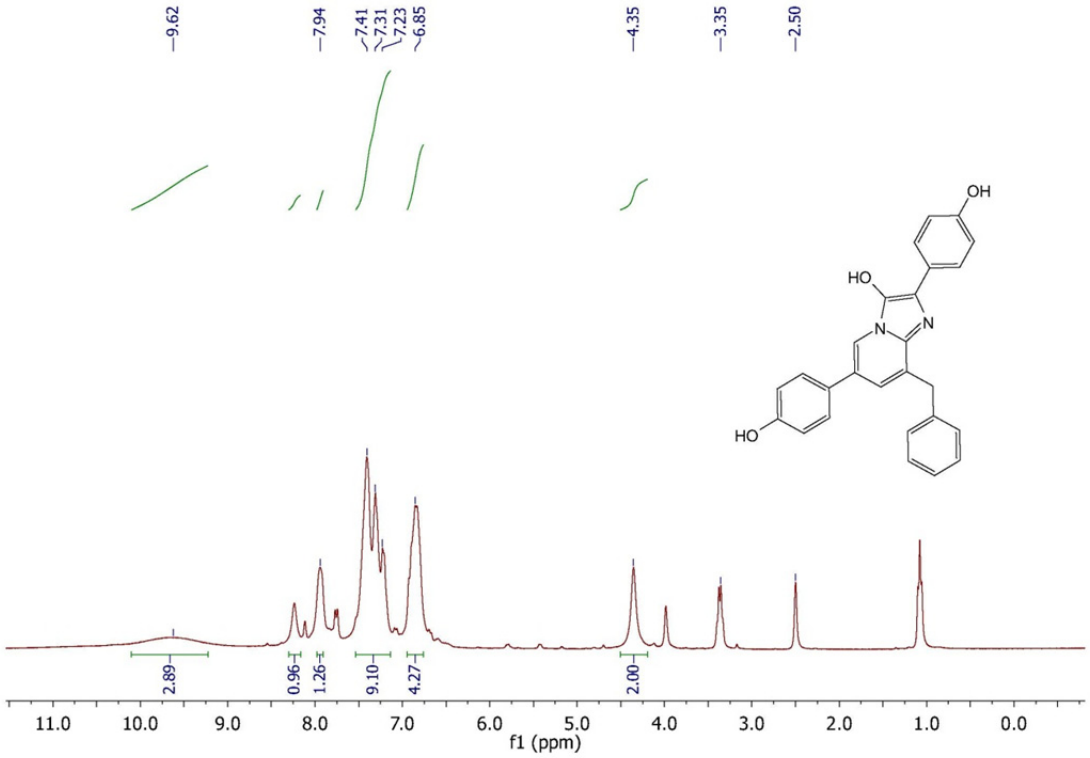

Figure 3.1.15 ^{1}H NMR (300 MHz, DMSO) spectrum of compound **154**.

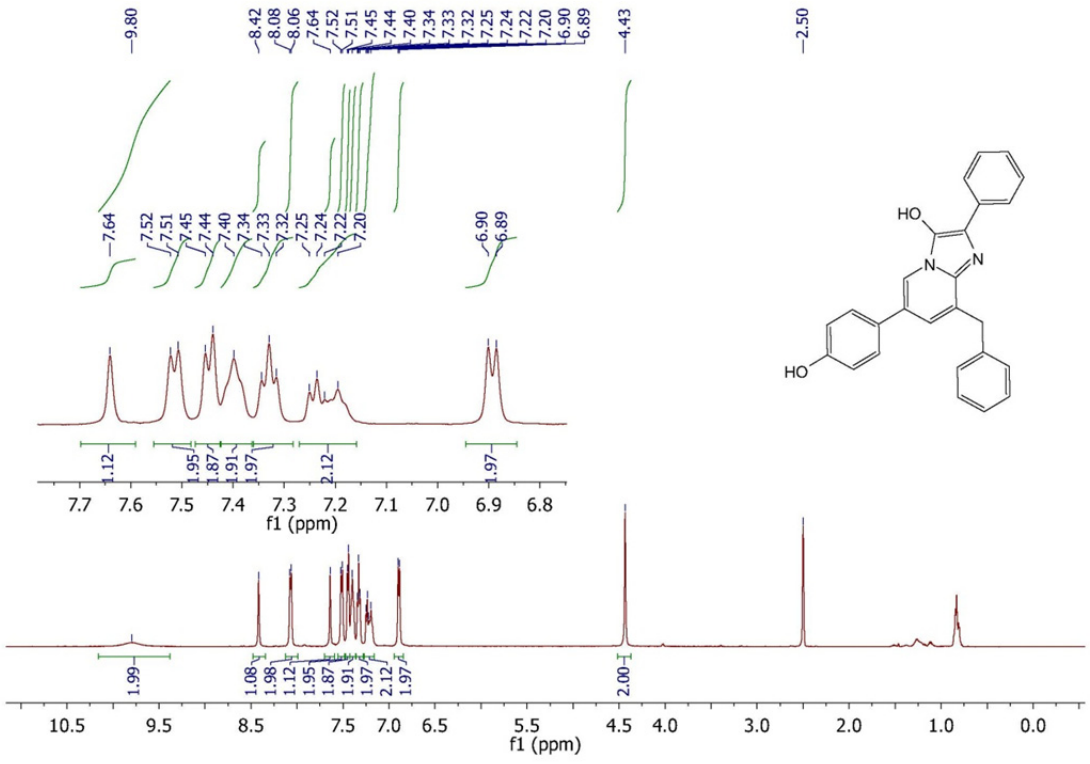

Figure 3.1.16 ^{1}H NMR (500 MHz, DMSO) spectrum of compound **155**.